



**Maynooth  
University**

National University  
of Ireland Maynooth

# **Essays on Urban Climate Model Evaluation and Application**

Paul John Alexander B.A., M.Sc., PCTL

Dissertation submitted to National University of Ireland Maynooth in partial fulfilment of the  
requirements for the degree of  
**Doctor of Philosophy**

2016

**Head of Department**  
Dr Jan Rigby

**Research Supervisors**  
Dr Rowan Fealy and Dr Gerald Mills

### **Viva Panel**

Chair.....Dr Paul Donovan  
Internal Examiner.....Professor Peter Thorne  
External Examiner.....Dr Leena Jarvi  
Date.....07 June 2016

### **Author Note**

The research presented in this thesis has been made possible through the financial support of the Doctoral Teaching Fellowship (2011-2015), Graduate Studies Department, Maynooth University, and the Department of Geography, Maynooth University.

The collection of research articles and accompanying text presented in this thesis are the authors' original preprint copies and not the version(s) accepted/printed *verbatim* by the respective publishers. The author retains the right to redistribute.

## Acknowledgements

Five years ago, in a sparsely furnished apartment some 8,010.85 kilometres from where I write from now, I sat down in room still baking from the afternoon Arizona sun, illuminated in equal parts by the early-evening sunset, a dull 40 watt energy-efficient bulb rising out of a freestanding corner lamp in the far side of the room and the white glow of my laptop screen, sitting on the kitchen table in front of me, humming audibly as it struggled to cope with the heat, to write the acknowledgments for my research masters dissertation. Having just applied for several PhD positions in various universities around the globe (in anticipation of successfully defending my masters' thesis in the coming months) I, as with my weary supervisor, who diligently wrote individual letters of support tailored for every position I applied for, had just about enough of scientific writing. At the time, I remember relishing the opportunity to dispense with formulae, convention and succinctness and return to the creative, truer form of writing. Then, as with now, I wrote my acknowledgements rising out from feelings of relief, gratitude, fear, joy, confusion, uncertainty, resolution and determination, in short, I wrote from my heart, not from my head. And amongst the fatigue, the chaotic thoughts, the memories of the whole process, the people who helped along that journey and that terrible, terrible heat, I managed (I hope) to achieve just enough clarity to articulate my thanks to all those who contributed to the work. The punishing summer sun of Arizona is now far away and long behind me, replaced by the cool crisp winds of the Irish winter, so I have one less worry, but then again... much more fatigue having endured far worse experiences than during my masters – I suppose it's a somewhat cruel take on one of my grandmothers' favourite sayings: *"When the Lord closes a door, somewhere he opens a window"*. But I also have more people to thank this time around and for this, if nothing else, I am incredibly grateful.

Naturally I will start by thanking my supervisors, Rowan and Gerald, for basically putting up with me for the past half-decade and decade (respectively) as I set out to establish my voice in an increasingly noisy field. Rarely, if ever, have I disagreed with two people with as much intensity and vigour and yet, retained the utmost admiration and respect. You are both gentlemen and scholars; and I thank you both equally for your patience, guidance and instruction (though Rowan deserves one last mention since, after all, his office was right down the hall while Gerald had the couple of kilometres buffer to save him from all the ill-timed questions).

At the lowest, darkest, most stressful times, where leaving the PhD not only seemed like the only viable option, but the best option, the ICARUS family was there to rally round and offer support and keep me in the fight. Catronia, Ciara'n, Shaun, Stephen, Simon, Irene and of course, Stephanie: you'll never know how every coffee, every laugh, every discussion (and I suppose every cigarette) got me to this point and meant just so much to me. You all have my unending gratitude. My thanks to the big brothers and sisters of the ICARUS family; Gill, Conor, Rod, Tom and Ro for the same.

Coming from three years of observational work in urban areas and moving straight into work on modelling fluxes of energy and moisture couldn't have happened so easily without help from the international urban climate community. I contacted many individuals and groups for advice and (cap in hand) asking for data, and while I won't reproduce all their names here I really have to acknowledge Sue Grimmond, Simone Kotthaus and Helen Ward for hosting my visit to King's College London, giving me a crash course in UEB models and putting up with an endless array of basic questions. My thanks also to the entire Helsinki team for fruitful

discussions on the direction of the SUEWS model during ICUC9, this really steadied my nerve towards the end of the PhD.

Completing a PhD really is a mammoth undertaking. Doing that along with a full teaching load is really the only way to prepare for academic life... but it was really challenging. I have to thank Mary Gilmartin for being in my corner and making sure the balance between teaching obligations and my research during the fellowship was kept in check. My thanks to Eilis Murray for the same (and also for giving me one or two days' extension on overdue progress reports).

If I was asked by anyone else thinking about doing a PhD through a teaching fellowship, if this was the optimum route to take, I honestly would say: "sure – if you find teaching rewarding". That ideal - teaching as a vocation - is the only thing that keeps you motivated and determined to entertain and impart knowledge to 450 students' day in, day out. I've met countless memorable individuals along the way, some who are now coming to where I was 4 year ago and have managed to retain the love for Geography despite the economic pressures and my inexperience in the beginning as a teacher. To all the students, past and present – I thank you dearly.

My thanks to the staff of Geography Department in Maynooth, there are too many staff to reproduce here (a happy complaint in such difficult times) you have my thanks for words of encouragement, support and advice. My thanks to my colleagues in IT services for the same.

To my friends, I thank you for just occasionally pulling me out of the PhD cave and into social settings and keeping me up to speed with news of the outside 9-5 world. I hope I didn't bore you all too much with my impromptu lectures about micro-climates and geography. Since I still get asked out for the odd sneaky pint, I guess it was tolerable (at least after a few glasses of wine).

To Rob, the most dedicated Geography teacher and truest friend I know. To Benjamin (Benni), for your encouragement and support as I neared the finish line – I couldn't have asked for a better colleague and friend. My deepest thanks to you both. To my family, despite everything *cognatio multum potest* as they say.

To my wife, Laura, for putting up with me during my rants about the demands of a PhD and always keeping me grounded. For your love, your friendship and your support, throughout the years. We shared in good times and truly bad times, and while this work was something I had to do alone, know that you are in every page. I know the future is bright since we will face it together.

أفتقدك وكم أحبك أنا كم يكفي ما لك أقول لا وأنا، يكفي ما على الحصول الي انظر أكن لم، العزيزة لجدتي، وأحلامنا آمالنا عن ونسمع زوجتي لتلبية أبدا تخيره لم أنت. ذلك لك وأقول أخرى مرة أراك أن على تحصل لم وأنا، والآن سلام في ترق قد. أسف أنا، أقول أن يحصل لم التي الأشياء لجميع. الأبد إلى الأسف هذا تحمل وسوف. دائما تهتم كنت

Dedicated to my Grandmother Teta  
and our little Dylan who we never got to meet

*If you were here tonight, I'd sing to you just one more time.  
A song for a heart so big: that God couldn't let it live.*

## Abstract

The field of urban climatology as a subfield of atmospheric science / physical geography has developed significantly over the past 3 decades. Major advances have occurred in the theoretical understanding of the urban effect at multiple spatial and temporal scales, as well as in empirical work seeking to observe and ultimately predict urban scale phenomenon. It is this latter development, particularly in respect to urban heat and moisture, that forms the basis of this work. Less than 5 years ago, the concept of partitioning the urban area into distinct geographic units based on the potential thermal modification of the near surface climate was proposed within the field to bring greater rigor, clarity and transferability to observations made within urban areas. The Local Climate Zone (LCZ) approach has since been applied in multiple cities globally, which has demonstrated its efficacy in understanding the urban heat island (UHI) effect through observations and transferring those results across multiple cities. However as with global scale temperature anomalies, the UHI can be viewed as symptomatic of the underlying processes rather than purely as a response i.e. while we now are capable of observing enhanced air temperatures around cities, addressing the issue requires a deeper understanding of the processes that give rise to this phenomenon, particularly if solutions are to be transferred into urban planning practices and environmental policies. To that end, urban climate models are an invaluable tool for examining urban processes in more detail. However, their application in urban areas (particularly for planning problems) remains ad hoc and unsystematic. In fact, many cities in the economically developing world lack even basic data describing (i) the underlying city, its sealed surface extent, vegetation, building materials and so forth and/or (ii) knowledge of the overlying atmosphere in and around the city, required to apply such models. In this collection of papers, a formal modelling and evaluation approach is proposed, elaborated on and applied which utilises the LCZ system. While LCZs were designed strictly for observations of the air temperature at 2m, due to its generality and resulting uptake within the urban climate community, it is argued to be an effective approach for modelling, particularly in data poor settings. The LCZ approach is linked with the Surface Urban Energy and Water Balance Scheme (SUEWS) model, a mid-complex urban energy and water balance model. Hence, the approach is referred to as the LCZ-SUEWS approach. The application of the approach primarily focuses on Dublin city (Ireland). This was done as the city houses three (2 ongoing and 1 retired) eddy-covariance flux towers used to evaluate the approach, however the results are intended to be transferrable to other domains. Three primary conclusions can be drawn from this body of work. Firstly, the LCZ-SUEWS approach performs equally well in data poor, data rich settings, meaning the approach can be applied anywhere to provide an initial assessment of the urban energy balance. Secondly, the adoption of the approach yields the additional benefit of improving communication with the urban planning community in terms of illustrating the processes that give rise to the urban effect e.g. lack of photosynthetically active vegetation, standing water bodies, and high proportion of built up coverage. This allows for more geographically and physically targeted design interventions to reduce the negative impacts of urban development such as excess heat and lack of moisture. Thirdly, there is a need for an agreed framework on model evaluation which emphasises external independent evaluation and employs novel sources of observational data, for example, remote sensing. This would improve the trustworthiness of urban climate models and further encourage their uptake.

---

# Contents

---

<b>Acknowledgements .....</b>	<b>iii</b>
<b>Abstract.....</b>	<b>v</b>
<b>List of Tables .....</b>	<b>ix</b>
<b>List of Figures.....</b>	<b>xii</b>
<b>List of Abbreviations / Symbols.....</b>	<b>xvii</b>
<b>Chapter 1 Introduction.....</b>	<b>1</b>
1.1 Introduction .....	1
1.2 Urban areas in the context of global climate change challenges .....	2
1.3 Urban Climate Models and their Application to Planning Problems .....	6
1.4 Research Aims and Objectives .....	10
1.5 Thesis Structure .....	12
1.6 Summary and Conclusion.....	13
<b>Chapter 2 Thesis Approach .....</b>	<b>15</b>
2.1 Introduction .....	15
2.2 The Local Climate Zone Approach for Modelling .....	17
2.3 Evaluation Approach.....	22
2.3.1 Model Assessment .....	23
2.3.2 Evaluation Metrics .....	24
2.4 Case Study City .....	27
2.4.1 Rationale for selecting the Greater Dublin Area .....	28
2.4.2 Geographical setting and climate .....	30
2.4.3 Demographics .....	33
2.5 Summary and Conclusion.....	35
<b>Chapter 3 Using LCZ data to run an Urban Energy Balance Model .....</b>	<b>37</b>
3.1 Preface .....	37
3.2 Abstract .....	38
3.3 Introduction .....	39
3.4 Urban energy budget (UEB) models .....	41
3.5 Methodology.....	45
3.5.1 SUEWS .....	47
3.5.2 Meteorological and energy flux data.....	48
3.5.3 Urban land-cover parameters .....	51
3.5.4 Model Experiment.....	52
3.5.5 Model Evaluation and Sensitivity .....	53
3.6 Results .....	54
3.6.1 Hourly fluxes comparison - June 2010 .....	55
3.6.2 Daily fluxes comparison .....	61
3.6.3 Impact of Meteorological Forcing Data on Performance.....	64
3.6.4 Impact of Land Cover on Performance .....	67
3.7 Discussion.....	68
3.7.1 SUEWS accuracy and measurement errors.....	68
3.7.2 Impact of non-local meteorological and LCZ data .....	70
3.8 Summary and Conclusion.....	73

<b>Chapter 4 Linking urban climate classification with an urban energy and water budget model: multi-site and multi-seasonal evaluation.....</b>	<b>74</b>
4.1 Preface .....	74
4.2 Abstract .....	74
4.3 Introduction .....	75
4.4 LCZ-SUEWS approach.....	78
4.5 Experimental outline .....	82
4.5.1 Experimental setup.....	82
4.5.2 Test locations .....	84
4.5.3 Evaluation of experiments.....	89
4.6 Results .....	91
4.6.1 Stage 1: Daily and Hourly Performance Results.....	91
4.6.2 Stage 2 and Stage 3: Performance Results .....	94
4.6.3 Seasonal and Annual Performance Results .....	95
4.7 Discussion.....	98
4.8 Conclusions .....	103
<b>Chapter 5 Spatial validation of an urban energy balance model using multi-temporal remotely sensed surface temperature.....</b>	<b>104</b>
5.1 Preface .....	104
5.2 Abstract .....	105
5.3 Introduction .....	106
5.4 Urban Energy Balance Models.....	107
5.5 Methods .....	109
5.5.1 SUEWS model .....	109
5.5.2 Forcing data and observation platforms .....	110
5.5.3 Spatial Validation.....	113
5.5.4 Spatial Evaluation .....	115
5.6 Results .....	116
5.6.1 Point Performance for turbulent fluxes .....	116
5.6.2 Spatial Correspondence of land surface temperature .....	118
5.6.3 Surface Urban Heat Island evaluation.....	120
5.7 Conclusion.....	125
<b>Chapter 6 Simulating the impact of different urban development pathways on the local climate of a mid-latitude city .....</b>	<b>126</b>
6.1 Preface .....	126
6.2 Abstract .....	127
6.3 Introduction .....	127
6.4 Integrating LCZ and SUEWS to support planning decisions.....	131
6.5 Methods .....	135
6.5.1 Case study area.....	135
6.6 Data .....	137
6.6.1 Forcing Data.....	138
6.6.2 Land cover scenarios.....	138
6.6.3 Anthropogenic Data .....	143
6.7 Results .....	144
6.7.1 Annual and seasonal flux variation .....	144
6.7.2 Spatial differences between different development pathways .....	147
6.7.3 Impact of development on seasonal diurnal fluxes .....	152
6.7.4 Design interventions for low impact development.....	153
6.8 Discussion.....	155
6.9 Conclusion.....	157

<b>Chapter 7 Discussion and Conclusions .....</b>	<b>158</b>
7.1 Discussion.....	159
7.1.1 Urban land cover data for modelling.....	159
7.1.2 Urban climate model performance .....	162
7.1.3 Interpretation of model performance: observational considerations .....	164
7.1.4 Utilising remotely sensed data for assessing model performance.....	166
7.1.5 SUEWS performance in context .....	167
7.2 Future research priorities .....	169
7.3 Final conclusions .....	170
<b>Bibliography .....</b>	<b>175</b>
<b>Appendix 1 Declarations of Co-authorship .....</b>	<b>197</b>
Paper 1 / Chapter 3 .....	197
Paper 2 / Chapter 4 .....	198
Paper 3 / Chapter 5 .....	199
Paper 4 / Chapter 6 .....	200
<b>Appendix 2 Published Words / Authors Pre-Prints.....</b>	<b>201</b>

## List of Tables

Table 1.1 A list of 10 most populous capital cities and the corresponding fraction of the national population they house. Dublin (Ireland) included as part of the study area of this thesis. Statistics drawn from World Bank (2015). .....	4
Table 2.1 Population count at the last census (2011) and projected increase for the Greater Dublin Area (GDA) between 2011-2031 (Source: CSO, 2013) .....	33
Table 3.1 Aspects of UEB models which are used for classification of model complexity. For example, in the case of criteria 1, “simple” would be associated with modelling only one or two fluxes, “complex” would be associated with modelling all fluxes .....	43
Table 3.2 Outline of Local Climate Zone Classes and their properties (modified from Stewart and Oke, 2012). Those that are asterisked are present in the Dublin study area .....	45
Table 3.3 Summary of inputs required to run SUEWS model.....	48
Table 3.4 A list of the energy budget and meteorological variables and the instruments used at each site; the height of the instruments at urban and suburban sites respectively is shown in the parentheses. The final column lists the equivalent SUEWS parameters (Table 3.3). .....	49
Table 3.5 Local climate zones (LCZ) in Dublin city with estimated plan area fractions ( $\lambda$ ). These were computed by taking the average of n randomly sampled areas (1 km <sup>2</sup> in size) within each LCZ type. The equivalent fractions calculated for the area around the urban and suburban observation sites are listed in the final two rows. ....	51
Table 3.6 Daily rainfall receipt at Dublin Airport (RA) and the difference recorded at the urban (DR <sub>A-U</sub> ) and suburban (DR <sub>A-S</sub> ) flux sites .....	56
Table 3.7 Mean hourly wind speed ( $V_A$ ), air temperature ( $T_A$ ), and shortwave radiation receipt ( $K_{\downarrow A}$ ) at Dublin Airport and the differences (D) recorded at the urban (u) and suburban (s) flux sites .....	57
Table 3.8 Root mean square error (RMSE) and Mean fractional bias (MFB) and bias direction change for each energy budget term based on hourly fluxes for June 2010. The top is urban (LCZ 2 site) bottom is suburban (LCZ 6 site). RMSE values are in W m <sup>-2</sup> . Negative values denote a reduction in RMSE (i.e. model improvement) whereas positive values denote an increase in RMSE. Negative values in MFB denote a decrease in absolute bias, positive denotes an increase in absolute bias. MFB directional changes denote if the model switches (>) from over (+) to under (-) prediction or if the direction of the bias remains the same (=).....	58
Table 3.9 Root mean square error (RMSE) values (W m <sup>-2</sup> ) for each month based on daily values of all flux terms for each Mode (N = 744 per Mode) Mode 1 uses High-Resolution land cover (HRLC) and forcing data obtained at the flux sites, Mode 2 uses HRLC and forcing data obtained off-site by a standard weather station. Mode 3 uses LCZ derived land cover fractions and off-site forcing data Finally Mode 4 uses LCZ land cover and forcing data obtained at the flux sites. ....	62
Table 3.10 Mean Fractional Bias (MFB) results for urban (LCZ2) site and suburban (LCZ6) site April-October. Mode 1 uses High-Resolution land cover (HRLC) and forcing data obtained at the flux sites, Mode 2 uses HRLC and forcing data obtained off-site by a standard weather	

station. Mode 3 uses LCZ derived land cover fractions and off-site forcing data Finally Mode 4 uses LCZ land cover and forcing data obtained at the flux sites .....65

Table 3.11 The impact of degrading meteorological forcing data (top Mode 1 versus Mode 2) and land cover (bottom, Mode 1 versus Mode 4) on daily RMSE values for the LCZ2 and LCZ6 site. Values are in  $W m^{-2}$ ; negative values denote a reduction in RMSE (i.e. model improvement) whereas positive values denote an increase in RMSE. ....66

Table 4.1 Outline of systematic experiment used to test the LCZ-SUEWS approach across multiple sites / climates / urban configurations. Each stage subsequent to stage 1 adds additional detail, hence, when interpreting results, the additional effort in providing these data should be considered. ....83

Table 4.2 Meta-data of the sites included in this study. Shown is the year in which observations were obtained, the background climate type, the location of both the flux sites and alternative synoptic stations. Shown also in meters are the instrument height of the flux towers ( $Z_m$ ) the displacement height ( $Z_0$ ) and the mean building height surrounding the site ( $Z_b$ ). ....84

Table 4.3 Land cover fractions ( $\lambda$ ) used to force the model calculated using the LCZ approach (stage 1) and traditional approach using high resolution (HR) data immediately surrounding the sites (stage 2 and 3) .....85

Table 4.4 Descriptive statistics illustrating the availability of flux data (top rows) as a percentage of the entire year considered. Note: DOY 1 = January 1<sup>st</sup>. Also given are the means ( $\mu$ ) and standard deviations ( $\sigma$ ) of wind speed (u) relative humidity (rh) air temperature ( $T_{air}$ ) air pressure (pres) and insolation (kdown) recorded at the synoptic sites. ....89

Table 4.5 Meta-data illustrating instrumentation at the four flux site along with corrections carried out on flux measurements .....90

Table 4.6 Root Mean Square Error (RMSE) statistics ( $W m^{-2}$ ) calculated for daily mean flux density and individual hourly flux densities. Also shown are mean fractional bias (MFB) calculated using the daily flux densities (-2 to +2). Also shown are the coefficient of determination ( $R^2$ ). Below presents a colour key summary for highest and lowest daily RMSE scores illustrating the best performance (lowest RMSE) to worse performance (highest RMSE): Lowest RMSE (best performance) = Green, Highest RMSE (worst performance) = Red, intermediate RMSE = Yellow .....93

Table 4.7 Seasonal RMSE values calculated for each site. Summer refers to June July and August for DUB, HAM and PHX and December January February for MEL. Winter refers to December January February for DUB, HAM and PHX and June July and August for MEL. Values are in  $Wm^{-2}$ . RMSE values are derived using daily flux densities thus are slightly more conservative than hourly RMSE values. Given also is the sum of the RMSE value across all stages, which provides an overview of seasonal performance .....97

Table 5.1 Summary meteorological conditions for the period selected for validation of SUEWS. Data is from Dublin airport station (see Figure 5.1).  $T_a$  denotes mean 2m air temperature, U denotes mean wind speed, Sun denotes the number of sunshine hours,  $Sun_{pot}$  is the fraction of the day with sunshine relative to the number of available hours,  $G_{Rad}$  denotes the mean global radiation,  $E_v$  denotes daily evaporation. Note the 11-17<sup>th</sup> are particularly clear periods. Data sourced from National Meteorological Service of Ireland (Met Eireann) ..... 114

Table 5.2 Model performance at two locations in Dublin. Shown is the hourly RMSE (Eqn. 5.4) for sensible ( $Q_H$ ) latent ( $Q_E$ ) and storage ( $\Delta Q_s$ ) heat flux for the period April 11-17, 2010. The sum of the RMSE is given in the final row, which provides a quick overview of where the model performance was best.....	116
Table 5.3 Mean monthly MODIS LST for the sub-domain used for evaluation against SUEWS. Shown are LST for each LCZ type across 2010. Values are given in °C – recall Figure 5.3 for calculation method.....	122
Table 5.4 Model performance metrics for LST, given are the RMSE and $R^2$ of SUEWS LST compared to MODIS LST.....	123
Table 6.1 Overview of a selection of Urban Climate Models (UCMs) for planning and research applications. The list below is non-exhaustive and based on non-proprietary models. The list also excludes building-scale energy models. Scale refers to the resolution of the model output, where $\mu$ = micro (1-100m) $\alpha$ = local (1-2km) $\beta$ = meso ( $> 2$ km) scale.....	130
Table 6.2 Link between urban development/features, impact on energy balance terms and resulting impact on local scale climate / urban heat island relevant for planners particularly in warm climates.....	135
Table 6.3 INPUT requirements of SUEWS model (*) indicates inputs which were used in this study.....	137
Table 6.4 Outline of the development pathway (DP) scenarios utilised in this study. Further details are provided in Brennan et al. (2009). Urban extent is defined as % of modelled grids that are classed as urban Local Climate Zones (LCZ) the % in parenthesis is the increase in urban LCZ from the 2006 base line case– see Table 6.5 and Figure 6.3.....	140
Table 6.5 MOLAND LULC classes converted into corresponding Local climate zones (LCZ) in the study area, the parenthesis in the LCZ column contains the number of grids (n) that are coded to that LCZ class for the BLC. Plan area fractions (given in % below) were obtained from Alexander et al. (2015). Population are given as persons per $km^2$ , the values in parenthesis in this column represent population in 2026. The final row illustrates % changes for 2026 for LCZ 2 DP-4 only.....	142
Table 6.6 Proportioning of $Q^*$ ( $\chi$ , $\gamma$ , $\Lambda$ ) and the Bowen ratio ( $\beta$ ) when $Q^* \geq 0$ $W m^{-2}$ . Presented are unit-less flux ratios for annual and seasonal partitioning.....	147
Table 6.7 The number of areas (as % of total model domain) with higher/lower annual values of $\chi$ , $\gamma$ and $\Lambda$ relative to BLC broken down into each DP. Note DP4 has the lowest net spatial impact meaning increases in one part of the city are offset by decreases in other parts.....	151
Table 6.8 Design interventions tested here. LCZ 6 areas in DP4 were modified as per description and the model re-run. Exemplar images in the first three rows are all existing locations for Dublin city.....	154

## List of Figures

- Figure 1.1 Overview of selected publications drawn from urban climate literature illustrating the parallel path to IPCC reports (with respect to sustainability and the role of urban climate for address global climate change) and the subsequent prioritisation of urbanisation in the most recent assessment report .....6
- Figure 1.2 Meta-analysis of papers given at international conference for urban climate (ICUC) 2003-2015. The bars show the number of studies which employ either empirical (dots) or modelling (solid) as a basis for the study. Presentations of reviews / project overviews / new methodologies are excluded from the counts. Above the bars is the % share of both methods for the total studies counted. The dashed line shows the number of UHI studies presented, either employing empirical or modelling approaches ..... 7
- Figure 1.3 The energetic basis of the urban effect (after Oke, 1987) .....8
- Figure 1.4 Overview of papers included in this collection; the bullet points show the objectives of the paper which relate to specific aim(s) which is identified below each panel ..... 12
- Figure 2.1 Above: The basis of Local Climate Zone system zones in terms of different urban/non-urban forms. Below: Examples of different urban LCZ based on components shown above i.e. LCZ 1-3 are compact highrise, midrise and lowrise respectively. .... 16
- Figure 2.2 Overview of traditional modelling approaches (first and second column) and the LCZ-Approach for modelling. The LCZ-Approach is essentially based on the principle of spatial auto-correlation which potentially reduces the number of input requirements for most UCMs..... 19
- Figure 2.3 Relationship between city size and number of input files required by SUEWS v.2013b if run at 1x1 km resolution for 1 year. Each 1x1 km grid contains 8 input files. Each data point represents the size of a real city based on data from GRUMPv1 (Balk, et al., 2006). The number of input files is used as a proxy for data requirements. The discussion in text provides a different estimate based on the rows of data contained within these 8 files, hence, this Figure is more conservative. ....20
- Figure 2.4 Land use / Land cover change illustrating urban expansion across Dublin city between 1956-1998. The areas of the map in red illustrate the urban fabric. Source: EEA (1999) .....29
- Figure 2.5 Overview of the case study city and surrounding area – referred to as the Greater Dublin Area (GDA). From Top left moving clockwise: (1) GDA in the context of the island of Ireland (2) Overview of the model domain employed in this work and the major urban areas encapsulated – areas in red are the administrative boundaries of major urban areas (defined as contiguous urban areas with a population of 1000 people or more – CSO 2012) (3) The population of the GDA based on the last census (2011) – CSO 2012 (4) Climatology of the GDA, shown is the mean annual 2m air temperature based on the climate normal (1989-2010) contours show mean annual isopleths (accumulated precipitation) – Met Éireann/Walsh (2012) (5) The physical features of the GDA, shown are major river ways and topography of the GDA - NASA, GDEM V2 and Water Body Data (SWBD) .....31

Figure 2.6 Population growth in the GDA based on national census statistics, following the 1966 census year the slope of the line increases notably indicating an increased pace of urbanisation within the region. Also shown is the trend for the GDA excluding Dublin city and County, which illustrates the shift of surrounding populations towards the city. The 2<sup>nd</sup> series (right Y-axis) shows the proportion of the total population of Ireland living within the GDA. Statistics sourced from CSO (2012) .....34

Figure 2.7 Demographic change in terms of age profile of the Greater Dublin Area (GDA) based on census statistics. The older demographic (65 and over) are plotted against the 2<sup>nd</sup> (right) Y-axis. Statistics sourced from CSO (2012) .....34

Figure 3.1 LCZ Map of Dublin also shown are flux site locations and synoptic station location with 1 km grid which represents extent of area used to calculate surface fractions (Modified from Alexander & Mills, 2014) .....45

Figure 3.2 Average hourly energy fluxes (measured and simulated) in  $W m^{-2}$  for June 2010. The graphs on the left refer to the urban site and those on the right refer to the suburban site. The rows (a–d) show simulations when SUEWS is run in different modes (a: Flux Forcing (FF) with Site Specific (SS) land cover (Mode 1), b: Synoptic Forcing (SF) with SS land cover (Mode .. ), c: SF with LCZ land cover d: FF with LCZ land cover). See text for details. X-axis is local time. ....59

Figure 3.3 Taylor Diagrams for Mode 1-4 based on daily values of  $Q_E$ ,  $Q_H$ ,  $\Delta Q_S$  and  $Q^*$  for LCZ 2 (top) and LCZ 6 (bottom) Mode 1 uses High-Resolution land cover (HRLC) and forcing data obtained at the flux sites, Mode 2 uses HRLC and forcing data obtained off-site by a standard weather station. Mode 3 uses LCZ derived land cover fractions and off-site forcing data Finally Mode 4 uses LCZ land cover and forcing data obtained at the flux sites .....63

Figure 3.4 One-Factor-A-Time (OFAT) analysis of forcing data impact on SUEWS simulation of turbulent fluxes. A based case (168 hours) was established using data derived from loess curve of required meteorological forcing (see Table 3.3). We then perturbed  $K_d$ , T and  $u \pm 10\%$  of the base case. Presented above is the % difference in the mean value (over the 168hours) of  $Q_H$   $Q_E$  and  $\Delta Q_S$ . It should be noted that RH was not modified when perturbing T, hence the apparent increase/decrease in  $Q_E$  .....66

Figure 3.5 Relative partitioning of Turbulent fluxes at each LCZ site for June (2010) the mean value of  $Q_H$   $Q_E$  and  $\Delta Q_S$  for each LCZ are subtracted from the group mean. X-Axis is  $W m^{-2}$ . LCZ images reproduced from Stewart and Oke (2012)..... 72

Figure 4.1 LCZ-SUEWS approach: At the mesoscale (10s-100s of  $Km^2$ ), model parameters are derived by integrating all LCZ across the entire domain. At the local scale (1-10s of  $Km^2$ ) specific model parameters for individual LCZ types are derived. At the microscale and building scale (10s-100s of  $m^2$ ) the approach is as yet untested, but would involve the addition of building dimensions and spacing, individual vegetative species as well as detailed material data. ....81

Figure 4.2 Location of the four sites used in this experiment (A) is Dublin, Ireland (B) is Hamburg, Germany (C) is Melbourne, Australia (D) is Phoenix, USA.. Shown are the locations of the synoptic and flux sites. Urban land cover obtained from Global Rural-Urban Mapping Project, Version 1 (GRUMPv1) .....85

Figure 4.3 – Top: LCZ description of the land cover immediately surrounding each site. Middle: Satellite imagery surrounding each of the sites. Bottom: Annual wind roses collected at the flux sites, each coloured bar represents a different wind speed ( $\text{ms}^{-1}$ ), wind direction was partitioned into 16 compass vectors. .... 88

Figure 4.4 Taylor diagrams based on all (i.e. hourly) observations for  $Q_E$  (left) and  $Q_H$  (right) ..... 98

Figure 4.5 - LCZ 6 summer time Diurnal profile for MEL, PHX and also shown is LCZ 6 site from Alexander et al. (2015) Top left panel is  $Q^*$ , followed by  $Q_H$  (top right),  $\Delta Q_S$  (bottom left) and  $Q_E$  (bottom right)..... 102

Figure 5.1 Overview of the conceptual relationship between the UWB and LST. In the dry case for Area “A” - available energy ( $Q^*$ ) will be used to heat the surface / air ( $Q_H$ ) and be stored within the urban volume ( $\Delta Q_S$ ). In the wet case, assuming all surfaces are covered in water (water bucket approach) the available energy is channelled into evaporation until the surface is dry, hence less energy is gained relative to the dry case which results in lowering of LST to compensate. SUEWS includes a ‘running’ UWB, different surfaces can transfer water to others e.g. water can runoff from roof-tops to pavements therefore SUEWS is far more physically realistic compared to a simple water bucket approach ..... 110

Figure 5.2 Above – overview of the model domain for validation and the subset used for evaluation The red boxes show the location of the flux towers and the location of the WMO site adjacent Dublin airport. The southernmost grid is the suburban flux tower (LCZ 6) the centre grid contains the urban flux site (LCZ 2) and the northernmost grid is the airport synoptic station. Below – visualisation of the relief of the evaluation subset (DEM data from NASA, GDEM V2), the callouts show the general pattern of elevation from south to north. Note the area considered is relatively consistent in terms of topography, which was done to minimise the effect of relief on LST..... 111

Figure 5.3 Conceptual summary of the evaluation of LST. Each grid above represents an LST pixel from MODIS with an observed LST value (given in  $^{\circ}\text{C}$  for convenience). The colours represent different LCZ classes, where Green is low plants (LCZ D) Blue is water (LCZ G) dark grey is compact highrise (LCZ 2) and light grey is openset lowrise (LCZ 6). LST is averaged across grids with the same LCZ class (‘i’), hence the SUHI is expressed as a difference between mean LST for LCZ classes ..... 115

Figure 5.4 Diurnal evolution of observed (dashed lines) and simulated (solid lines)  $Q_H$  (first column)  $Q_E$  (second column) and  $\Delta Q_S$  (third column) for LCZ 2 (top row) and LCZ 6 (bottom row) sites April 11-17, 2010. The corresponding RMSE values are given in Table 5.2 above ..... 117

Figure 5.5 Idealised overview of the difference between LST / SUHI as modelled by SUEWS (left) which is an integrated LST from roof tops, walls, vegetation and pavements and observed by the MODIS sensor (right) which is based on surfaces visible to the satellite. Image is adapted from Voogt & Oke (1997)..... 118

Figure 5.6 Deviation of individual LCZ from mean observed and simulated daytime LST averaged across the entire domain (recall eqn 5.5). Show are the results for April 11 which is typical of the period examined. Of interest here is whether the demarcation of LST are similar between MODIS and SUEWS for urban and non-urban LCZ ..... 119

Figure 5.7 Spatial pattern of daytime LST for the 17 April 2010 as observed by MODIS (left) and simulated by SUEWS (right). The April 17 was chosen as it was exceptionally clear period, hence, observed LST was available for the entire domain ..... 119

Figure 5.8 Top: Mean monthly SUHI intensity ( $T_{LCZ 2} - T_{LCZ D}$ ) based on observations from MODIS sensor (MOD11A2) for daytime and nighttime acquisitions. Bottom: As for panel, but LST is derived from SUEWS model. Hourly values corresponding to MODIS overpass times were used for averaging ..... 121

Figure 5.9 Taylor diagrams based on monthly LST for 2010 from MODIS and SUEWS. The left pane is daytime LST and the right is night time LST, the points represent 3 different LCZ classes, LCZ 2 (red) LCZ 6 (blue) and LCZ D (green), the purple point represents observations from MODIS, hence night time LST performance was higher than daytime,  $R^2$  and RMSE are given in Table 5.4..... 123

Figure 5.10 Scatter between observed daytime LST and simulated LST, the 1:1 line is included in order to illustrate points where the model over or underestimates LST ..... 124

Figure 6.1 Local climate zone scheme for universally describing neighbourhood morphology and thermal climate (Stewart & Oke, 2012). Each zone is defined on the basis of parameters which impact on the hydrothermal properties such as the % imperviousness, sky-view factor, building materials, waste heat, building and vegetation height and so forth..... 132

Figure 6.2 A hypothetical city comprised of different neighbourhood types (LCZ – Figure 6.1), with future land cover scenarios classified into LCZ, thus allowing for initial assessment and modelling of climatic impacts of policy / planning decisions at the neighbourhood scale (see for instance fig. 12/13 in Ching, 2013)..... 133

Figure 6.3 Study area overview. Main image shows the model domain and grids. LULC classes from CORINE were combined to show urban –v- non urban extent. The grids highlighted in blue and yellow represent the two neighbourhoods (inner city and southern suburb respectively) used to evaluate the models’ accuracy, and the red grid shows the location of the synoptic station used to force all model simulations ..... 136

Figure 6.4 Overview of present day CORINE land cover classes for study area (top left panel) with development pathway scenarios 1-4 - see text / Table 6.4 for more details ..... 139

Figure 6.5 Overview of model treatment of development pathway scenarios. Development pathways (DP-1 to DP-4) are detailed in Table 4 and in text. LCZ fractional coverages are given in Table 6.5. Each grid is coded into LCZ based on majority rule ..... 143

Figure 6.6 (a) Difference from annual mean  $Q_H$  and  $Q_E$ , this is the mean value taken across all LCZ types, positive values indicate above average annual flux magnitude, in the case of sensible heat, this indicates higher surface / air heating. Negative values indicate below average annual flux magnitude. (b) Differences as with (a) however the values are further divided into seasonal  $Q_H$  (orange shades) and  $Q_E$  (green shades). Note the width of the individual color bars indicates the value above (+) or below (-) average for example,  $Q_H$  for LCZ 101 in summer is  $-3.2 \text{ W m}^{-2}$  and  $-15.2 \text{ W m}^{-2}$  in winter. .... 146

Figure 6.7 Impact indices for BLC and DPs 1-4. Top left is the heat index ( $\gamma$ ) which is the proportion of available energy used for surface / air heating. Top right is the evaporation index

( $\gamma$ ) which is the proportion of energy used for evapotranspiration. Bottom left is the storage index ( $\Lambda$ ) which shows the proportion of available energy stored in the substrate (buildings/pavements/soils), this effectively shows the potential UHI extent. Bottom right is the Bowen ratio ( $\beta$ ) which is the relationship between the heat and evaporative index, a higher number indicates more energy is used for surface / air heating meaning less water is evaporated hence is available for runoff. .... 148

Figure 6.8 Spatial distribution of increases/decreases in impact indices compared to BLC for each DP (columns). The differences are based on annual mean values..... 150

Figure 6.9 Illustration of the domain subsets for detailed analysis of change in each DP and diurnal analysis (i.e. Section 6.7.3)..... 151

Figure 6.10 Seasonal diurnal profiles for dominant LCZ in BLC (2<sup>nd</sup> row) and DP scenarios (1<sup>st</sup> row). The first 2 columns show winter diurnal profiles; the last 2 columns show summer profiles. The 3<sup>rd</sup> row illustrates the difference in the first 2 rows in each column. Stars (\*) show  $Q^*$ , squares ( $\square$ ) show  $Q_H$ , circles ( $\circ$ ) show  $Q_E$ , triangles ( $\Delta$ ) show  $\Delta Q_S$  and crosses (+) show  $Q_F$ . The impact (final row) from left to right can be interpreted as follows: 1) increased heat storage in the inner city and higher anthropogenic heat source in winter 2) in the suburbs, increased heat storage (UHI) and surface/air heating day and night in winter 3) Increased surface/air heating during the daytime hours in the inner city during summer 4) increased heat storage and surface /air heating in summer in suburbs during summer..... 153

Figure 7.1 Illustration of the findings of Paper 1: The right-hand pane illustrates the correct circumstances in which forcing data should be provided for SUEWS i.e. based on observations made within the inertial sublayer, approximately twice the height of the surrounding roughness elements ( $Z$ ) which should be relatively homogenous (adapted from Grimmond & Oke 2002). The left-hand pane illustrates the forcing data used for specific stages of the experiment in Paper 1, based on WMO standard observations at roughly 0.5 times  $Z$ . In both cases, SUEWS performance was capable of reproducing differences in turbulent processes between an urban and suburban area ..... 164

## List of Abbreviations / Symbols

GDA	Greater Dublin Area – the geographic region encompassing Dublin City and surrounding conurbations
K↓ K↑	Incoming and Outgoing Shortwave radiation
L↓ L↑	Incoming and Outgoing Longwave radiation
LCZ	Local Climate Zone - a homogenous climate based land cover classification for urban areas
LSS	Land Surface Scheme – a specific subset of UCMs which generally employ bulk parameterisation to represent land-atmosphere exchanges
LST	Land Surface Temperature – the “skin” surface temperature of walls, pavements, and natural surfaces as observed by thermal camera or other remote sensor
Q*	Net (all-wave) Radiative flux
Q <sub>E</sub>	Latent Heat Flux
Q <sub>F</sub>	Anthropogenic Heat Flux
Q <sub>H</sub>	Sensible Heat Flux
ΔQ <sub>s</sub>	Storage Heat Flux
SEB	Surface Energy Balance - the exchange of energy between the Earth’s surface and the overlying atmosphere
SUEWS	Surface Urban Energy and Water balance Scheme – a local scale mid-complex UEB and UWB model developed in University of Helsinki / Kings College London
UBL	Urban Boundary Layer – Section of the urban atmosphere extending from the top of the roughness elements into the lowest levels of the planetary boundary layer
UCL	Urban Canopy Layer – Section of the urban atmosphere extending from the ground surface to the top of the roughness elements
UCM	Urban Climate Model – term used to describe any statistical or dynamical model applied for urban climate
UEB	Urban Energy Balance – as for SEB, though modified for urban volume and additional sources of energy associated with urban areas
UHI	Urban Heat Island – general term describing the tendency of urban air temperatures to be warmer than non-urban air temperatures, sub-type should be further identified as ‘surface’, ‘UCL’ or ‘UBL’.
UWB	Urban Water Balance – describes exchanges and flows of water in and out of a defined system or volume
β	Bowen Ratio: $\frac{Q_H}{Q_E}$
γ	Latent Heat Flux Ratio: $\frac{Q_E}{Q^*}$
Λ	Storage Heat Flux Ratio: $\frac{\Delta Q_s}{Q^*}$
λ <sub>x</sub>	Fractional coverage of surface type x
χ	Sensible Heat Flux Ratio: $\frac{Q_H}{Q^*}$

---

## Chapter 1 Introduction

---

### 1.1 Introduction

At the start of the 19<sup>th</sup> century, a mere 3% of the global population lived in urban areas with a population of 5,000 inhabitants or more. At the same time, less than 45 cities worldwide had populations over 100,000 and fewer than half of these were situated in Europe (De Vries, 2007). The majority (~66%) of large urban areas resided within Asia - cities such as Beijing, Guangzhou and Tokyo were even larger than ancient Rome at its peak (Chandler, et al., 1974). By 1950, the proportion of the global population living in such urban areas increased to 30%. As of 2007, for the first time, more than half the global population resides in cities. Based on present growth estimates, an additional 250,000 people are added to urban areas daily (Steer & Ishii, 2015). Therefore, urbanisation – that is, the replacement of natural vegetated landscapes with hard, impervious materials which are the constituents of urban areas – is continuing to accelerate and intensify as more dwellings, commercial and industrial areas as well as transport/energy infrastructure are embedded onto the landscape.

By the start of this century, a trend of populations moving away from urban centres into cheaper surrounding suburban land (i.e. suburbanisation / sprawl) had been well established, and the land area occupied by cities has grown from <0.5% to ~2% of total global land cover (Mertes, et al., 2015) during this period. While this represents a small fraction of the available land surface, urban areas are a significant nexus of human activity, consumption and waste production; combined they account for between 70-90% of global economic activity (Aston, 2012). Despite the recent evolution from industrial-production power houses into a more knowledge/service based centres, cities remain geographic areas of mass material and energy consumption, necessitating transport links which span globally and are significant emitters of greenhouse gases (GHGs). They are also areas of elevated air pollution and expanding

impervious surfaces. Thus, cities create significant environmental impacts at local, regional and global scales. As such, cities represent an important geographical scale in which to address present global environmental challenges.

However, a significant knowledge gap exists with regards to our understanding of the role of climate on cities and cities on climate (IPCC, 2014). The present work seeks to contribute to this knowledge gap through an assessment of the role of urban areas in modifying the energetics at the interface of the surface and lower atmosphere, accounting for this modification through the use of urban-scale climate models and reducing this impact through evidence based urban planning / policies. This chapter introduces the context to these topics, outlines the primary research aims, and provides an outline of the thesis. Initially, the importance of urban areas / urban climate in the context of global climate change is discussed, as this is a key rationale for undertaking this work, the role of urban climate models (UCMs) for aiding planning decisions to achieve more sustainable urban form is then discussed.

## **1.2 Urban areas in the context of global climate change challenges**

Over the past three decades, increasing emphasis has been placed on the role of sustainable development in tackling the issue of anthropogenically induced climate change. Indeed, the first assessment report (FAR) of the Intergovernmental Panel on Climate Change (IPCC) highlighted the clear need to place sustainability firmly at the centre of climate policy (IPCC, 1990). Following on from this, the second (SAR – IPCC, 1995) and third (TAR – IPCC, 2001) assessment reports highlighted the “co-benefits” of adopting sustainability as a key policy terms of economic development while highlighting the major obstacles faced by the climate challenge. The fourth report (AR4 – IPCC, 2007) shifted the focus of sustainable development as a sole duty of government actors to include non-government organisations and the wider-civil society, highlighting that ultimately sustainable development could not be

achieved at the expense of economic or social progression, both objectives would have to be met simultaneously.

In parallel, a growing body of literature was emerging surrounding research on the role of *urban* sustainable development in mitigating the negative effects of land cover change on the micro-climate in and around cities. It is well known that cities impact on the thermal and hydrological regime of the near surface climate (Oke, 1987; Whitford, et al., 2001; Wilby, 2003) as well as air quality and human health (Frumkin, 2002; Jackson, 2003; Cohen, et al., 2004). Moreover, research across multiple cities has demonstrated there is a negative relationship between green space and the urban heat island effect (Wong & Yu, 2005; Coutts, et al., 2007; Giridharan, et al., 2008; Susca, et al., 2011) while greenspace has been found to have a positive impact on human behaviour (Takano, et al., 2002; Thorsson, et al., 2004); though it has been noted the evidence linking physical and mental health well-being with urban green spaces is somewhat weak i.e. urban greenspace alone is a poor predictor in what is regarded as a multifactorial relationship (Lee & Maheswaran, 2011). Set against the grandeur of the entire planet, cities may not seem an appropriate geographic scale in which to tackle the issue of global climate change. Collectively cities currently house 54% of the global population (United Nations, 2014). Taken individually, capital cities house on average 10% of their national population – see Table 1.1. Since they house quite a large proportion of the national population, are economic and social drivers and traditionally contain the seat of national government, capital cities are a particular priority for addressing environmental, social and political issues. Therefore, there exists a strong case for the role of cities in tackling global climate change (Betsill & Bulkeley, 2006; Bulkeley, 2010) as addressing these issues often coincides with the objectives of wider sustainable development.

However, this body of work was largely carried out in parallel rather than being integrated with the IPCC. Heretofore, urban areas within the IPCC assessment reports have

tended to be viewed rather narrowly as being geographic areas that are particularly vulnerable to climate change. The notion of urban areas as possible responders to climate change or as a spatial unit to address sustainability issues is notably absent from previous IPCC reports – see Figure 1.1. A critical development emerged in the fifth assessment report whereby integrating development, urbanisation, adaptation and mitigation has been prioritised by the IPCC (IPCC, 2014). Effectively meaning that urban areas have shifted priority in the global climate change discourse.

**Table 1.1 A list of 10 most populous capital cities and the corresponding fraction of the national population they house. Dublin (Ireland) included as part of the study area of this thesis. Statistics drawn from World Bank (2015).**

<b>Country</b>	<b>Capital City</b>	<b>Population (x10<sup>6</sup>)</b>	<b>Census Year</b>	<b>as % of country</b>
China	Beijing	20.693	2012	1.5
Japan	Tokyo	13.189	2011	10.3
Russia	Moscow	11.541	2011	8.1
South Korea	Seoul	10.529	2011	21.1
Indonesia	Jakarta	10.188	2011	4.1
Mexico	Mexico City	8.851	2010	7.5
United Kingdom	London	8.630	2015	13.5
Peru	Lima	8.481	2012	28.2
Thailand	Bangkok	8.249	2010	12.4
Iran	Tehran	8.154	2010	10.9
...				
Ireland	Dublin	0.620	2011	13.5

Identifying cities as a critical geographical scale in which to achieve sustainability is arguably the first step along a much longer road. While this now focuses the research agenda on cities, several key knowledge deficits have been identified in respect to cities and how they might address climate change:

- (i) Firstly, the nature and magnitude of greenhouse gas (GHG) emissions related to urban form and function in cities is uncertain. This impacts on understanding the extent to which altering urban form can reduce GHG emissions, thus contribute effectively towards sustainable urban development. Further, there is a noted lack of consistency and comparability in terms of accounting for emissions within different urban areas,

creating an urgent need for *standardised methodologies* for local to urban scale carbon accounting (IPCC, 2014; 977) and how they relate to urban form.

- (ii) Secondly, there is a large degree of uncertainty surrounding how cities will develop in the future and the potential consequences for local scale climate interactions with global climate. There is a high agreement that urban form and function (e.g. infrastructure that aid or inhibit large commuting distances) will impact on the relationship between urban extent and emissions, though the precise extent of this is uncertain. For instance, a more intensely built city while having a high impervious fraction would likely have less per capita emissions, but may also have a lower resilience in terms of climate change impacts. Thus, creating an urban form which reduces emissions and ensures high resilience is a priority, however a strong evidence base remains elusive.
- (iii) Thirdly, the lack of evaluations on the efficacy of climate action plans which modify form and function has led to a large gap in understanding how policy responses are locally relevant. To address this, policy packages (i.e. a combination of policy measures such as carbon taxes, building regulations, incentivising renewables and so forth) which are based on characteristics of individual cities, urbanisation, forecasting development pathways and future climate should be established and evaluated on the basis of ensuring resilience and less carbon-intensive cities.

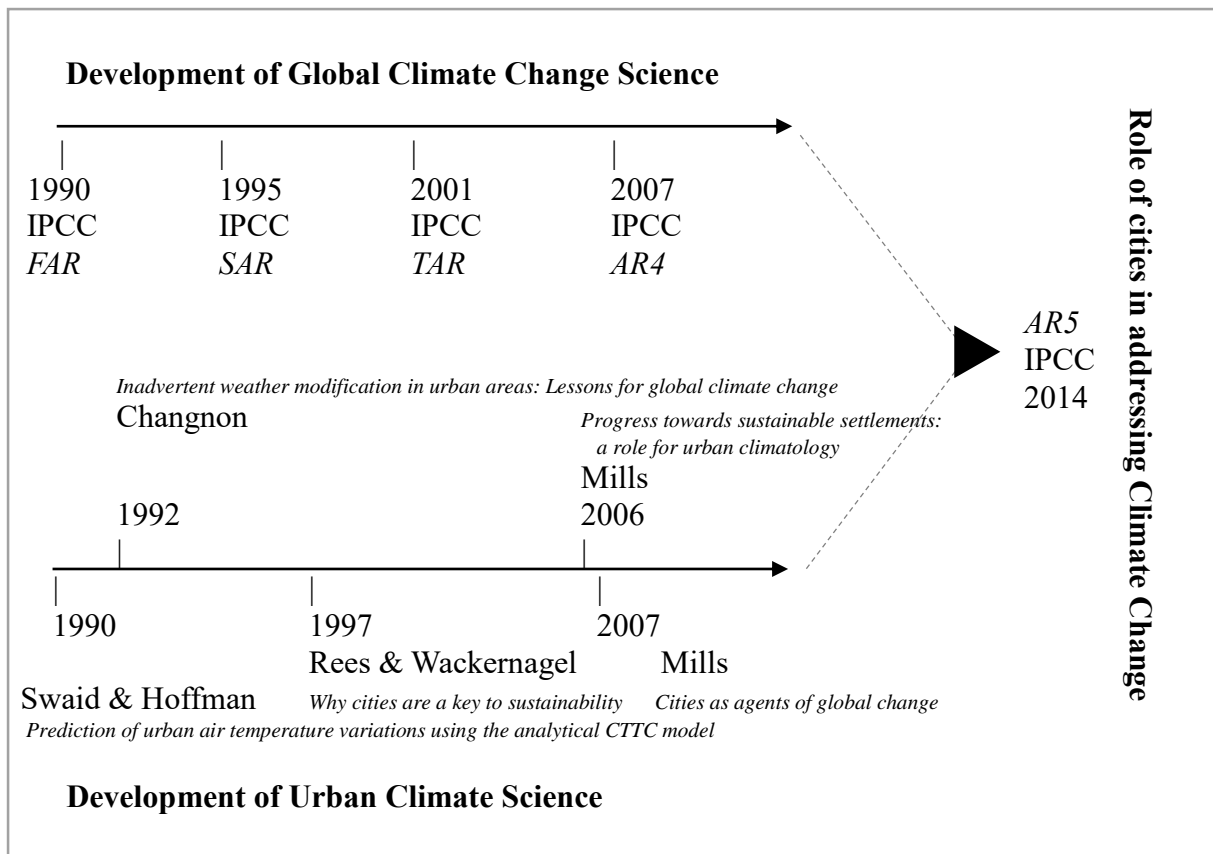


**Figure 1.1 Overview of selected publications drawn from urban climate literature illustrating the parallel path to IPCC reports (with respect to sustainability and the role of urban climate for address global climate change) and the subsequent prioritisation of urbanisation in the most recent assessment report**

### 1.3 Urban Climate Models and their Application to Planning Problems

Traditionally the urban effect has been derived through empirical means – Figure 1.2. In particular, the nocturnal urban heat island (UHI) effect has received a disproportionate amount of attention. However, despite the vast intellectual investment into the phenomenon, problems remain with its derivation and communication (Lowry, 1977; Stewart, 2011). As a consequence, there is an apparent mismatch between the urban effect arising from urban form and function and integrating this knowledge into planning practices (Hebbert & Mackillop, 2013). This is particularly unfortunate since once urban form is established, it is difficult to modify in response to inadvertent climatic consequences.

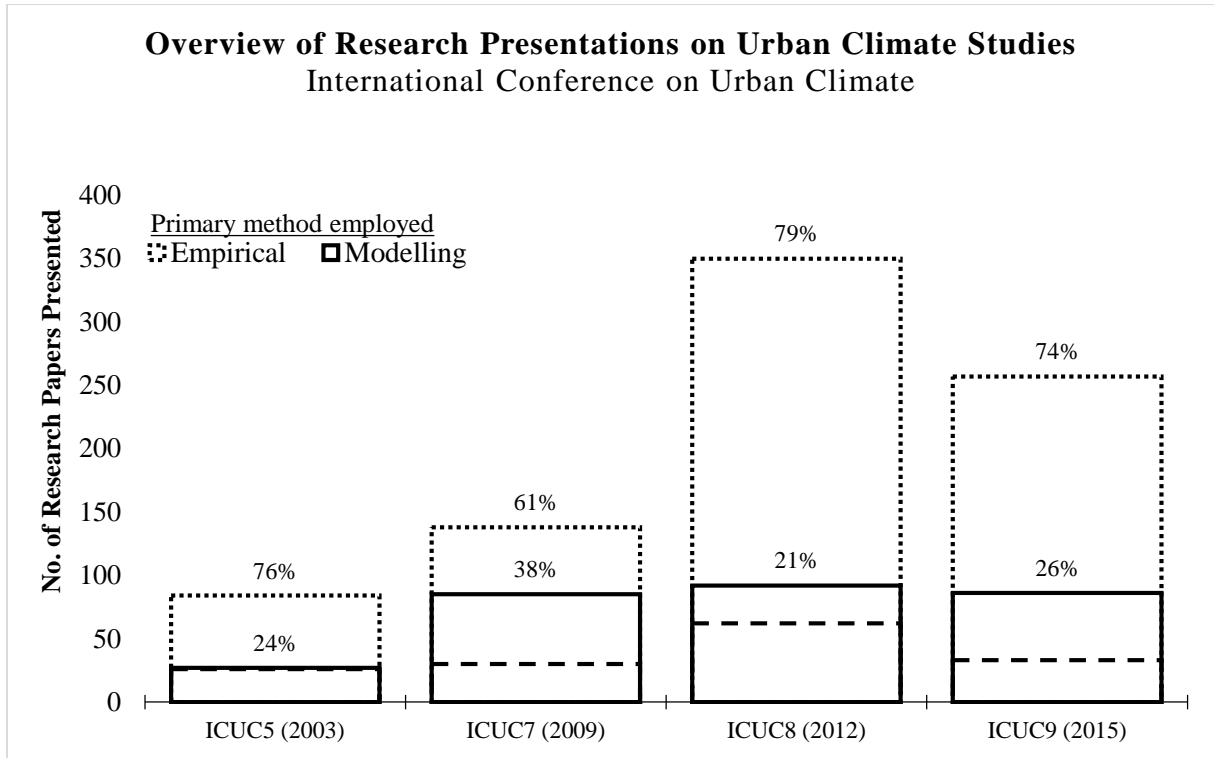


**Figure 1.2** Meta-analysis of papers given at international conference for urban climate (ICUC) 2003-2015. The bars show the number of studies which employ either empirical (dots) or modelling (solid) as a basis for the study. Presentations of reviews / project overviews / new methodologies are excluded from the counts. Above the bars is the % share of both methods for the total studies counted. The dashed line shows the number of UHI studies presented, either employing empirical or modelling approaches

The present understanding of the relationship between urban form and function and the local climate is based on the urban energy budget (UEB) – first described by Oke (1982; 1988) and later others:

$$Q^* + Q_F = Q_H + Q_E + \Delta Q_S + \Delta Q_A + e \quad \text{Eqn. 1.1}$$

where  $Q^*$  is the net radiation comprised of net shortwave and longwave radiation ( $K^*$  and  $L^*$  respectively),  $Q_F$  is the anthropogenic heat flux comprised of waste heat produced by buildings ( $Q_B$ ), vehicles ( $Q_V$ ) and human metabolism ( $Q_M$ ) (Grimmond, 1992; Sailor & Lu, 2004; Allen, et al., 2011). As per Eqn 1.1 the energy encountering an urban surface must be expended via sensible heating ( $Q_H$ ) latent heating ( $Q_E$ ) or heat storage ( $\Delta Q_S$ ) which is propagated through the urban canopy layer (UCL) and into the urban boundary layer (UBL) above the volume considered– Figure 1.3. Additionally, the energy can be lost via lateral movement i.e. advection ( $\Delta Q_A$ ), though conventionally this term is often neglected along with

any remaining sources/sinks ( $e$ ). The function of an urban area will impact on the nature and magnitude of  $Q_F$ , whereas the urban form impacts on virtually all of the right hand terms of this equation. Depending on the background climate and geographic circumstances, city planners may wish to impose a particular urban form onto the landscape that modifies the UEB in order to avoid specific issues e.g. excessive thermal loading, casting shadows on large proportions of the landscape, ventilation and so forth (Eliasson, 2000).

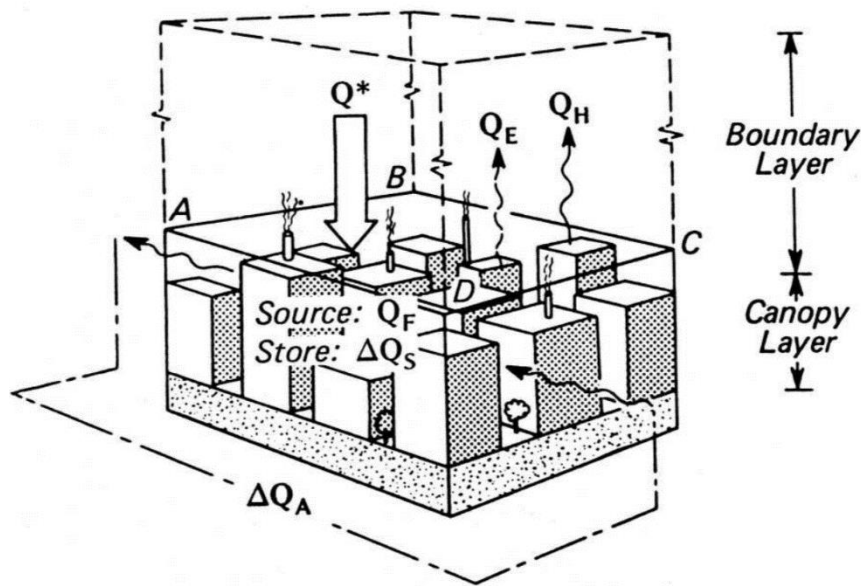


Figure 1.3 The energetic basis of the urban effect (after Oke, 1987)

Establishing the impact(s) of urban development on the local climate after urban development has been undertaken is undoubtedly critical, since it allows for assessment of consequences and reviewing of findings, effectively for lessons to be learned for future developments. Optimally, an approach which could anticipate potential consequences of one particular urban form over another in order to derive an *optimal* urban form *prior* to undertaking development. This approach can be achieved within a modelling environment, which is essentially free of risk and significant monetary investment, provided the models are adequately developed and evaluated (this is discussed further in Chapter 2). Given the fact there is little to be lost and potentially valuable information to be gained within the modelling environment, it is unsurprising that a number of urban climate models exist and have been applied in such circumstances.

For instance, Ashie *et al.* (1999) coupled a building canopy model with a computational fluid dynamics (CFD) model to examine the effects of high-albedo paint on reducing thermal loading on buildings, hence, reduce energy for cooling in Toyko. Based on their simulations, thermal loading and subsequent re-emission at night (i.e. the UHI effect) was reduced by between 0.4-1.3°C. This had a corresponding reduction of 3-25% in simulated energy used for cooling depending on the number of facades painted and whether or not buildings used HVAC systems. In other work, Ali-Toudert and Mayer (2006) applied the ENVI-MET model (after Bruse, 1999) to examine human comfort at street level in Ghardaia, Algeria. They illustrated that streets with a low height-to-width (H/W) ratio (i.e. wide streets) caused significant discomfort for pedestrians. This has direct implications for future planning within hot climate cities - requiring additional shading if wide streets are to be implemented in development plans.

Coutts *et al.* (2008) examined the effect of different urban densities on the UHI by applying The Air Pollution Model (TAPM) of Hurley (2005) in order to identify areas where further planning interventions would be needed in Melbourne, Australia, based on land cover projections for 2030. While they were able to accurately simulate the UHI in Melbourne, illustrating that high-density urban development would enhance UHI intensity by between 0.6-2.6°C under present plans, they noted the difficulty in running the TAPM model in terms of acquiring all the necessary forcing and land cover data. Based on this, they conceded that it was very unlikely that town planners would be able to directly employ such a modelling approach and would ultimately require climate impact assessment to be “outsourced” to urban climatologists.

These studies illustrate that urban form choices have consequences for micro and local-scale climate as well impacting on the urban population and building energy use, moreover, the utilisation of modelling approaches can be used to assess these impacts and thus avoid potential inadvertent consequences for the population and test design strategies to reduce building

energy requirements. However, a significant impediment to routine application of models for planning problems are the data requirements, such as detailed land cover information, required to run such models as well as the specialist knowledge required to generate and interpret their simulations. Additional impediments are robust evaluations of the model simulations, which are usually limited to the specific cases in which they are applied (Oke, 2006). Therefore, a more general modelling approach which can overcome high data requirements and specialist knowledge, alongside a greater effort to ensure consistency in the evaluation of model applications are required. Ultimately, this would allow more applications and mean that simulations could be interpreted across a wider range of urban domains. This is discussed further in Chapter 2.

#### **1.4 Research Aims and Objectives**

The key knowledge gap addressed by this thesis is the issue of data availability which inhibits the routine application of sophisticated urban climate models. Hence, the primary aim of the present work was to develop a modelling approach that has utility in data poor settings, such as rapidly developing urban areas in the economically developing world. The approach seeks to evaluate the efficacy of rapidly acquired input parameters required by a mid-complex UCM which is used for examining the urban effect on climate, which can be readily applied in locations where traditional approaches render the application of such models unfeasible. A secondary aim was to develop a means to standardise the application (and promote evaluation) of urban-scale climate models using this approach. A tertiary aim was to provide an evidentiary basis for future urban development for the main case-study city based on exchanges of heat and moisture between the surface and near surface atmosphere, though it was intended that this aim would serve more as an exemplar, thus could be extended beyond the specific case study city.

A key outcome of the present work seeks to further integrate urban climate knowledge within the wider planning communities by further demonstrating the utility of UCMs for real planning problems. This is achieved by developing a more user-friendly modelling approach which will allow for a wider number of applications. Figure 1.4 pictorially depicts the objectives of each of the papers in this collection that arise directly from these aims.

The first paper in the collection develops and evaluates the modelling approach for use in subsequent papers. A key objective of the paper was to utilise LCZ to provide parameters for use in the Surface Urban Energy and Water Balance Scheme (SUEWS) model (Järvi, et al., 2011) and evaluate the impact on model performance. The second paper builds on the first in extending the proof of concept to different cities / background climates globally. The issue of model evaluation and validation are returned to in the third paper of the collection; the use of global and freely available remotely sensed surface temperature is examined as well as the ability of the proposed LCZ-Approach for modelling to produce spatially realistic surface temperatures, an evaluation of the surface urban heat island is also presented. Finally, once the approach was evaluated in papers 1-3, it is applied to a real planning problem in paper 4. Specifically, the objective of the fourth paper was to demonstrate how the approach can be used to provide an additional evidence-base for planning decisions based on available policy options for Dublin, Ireland.

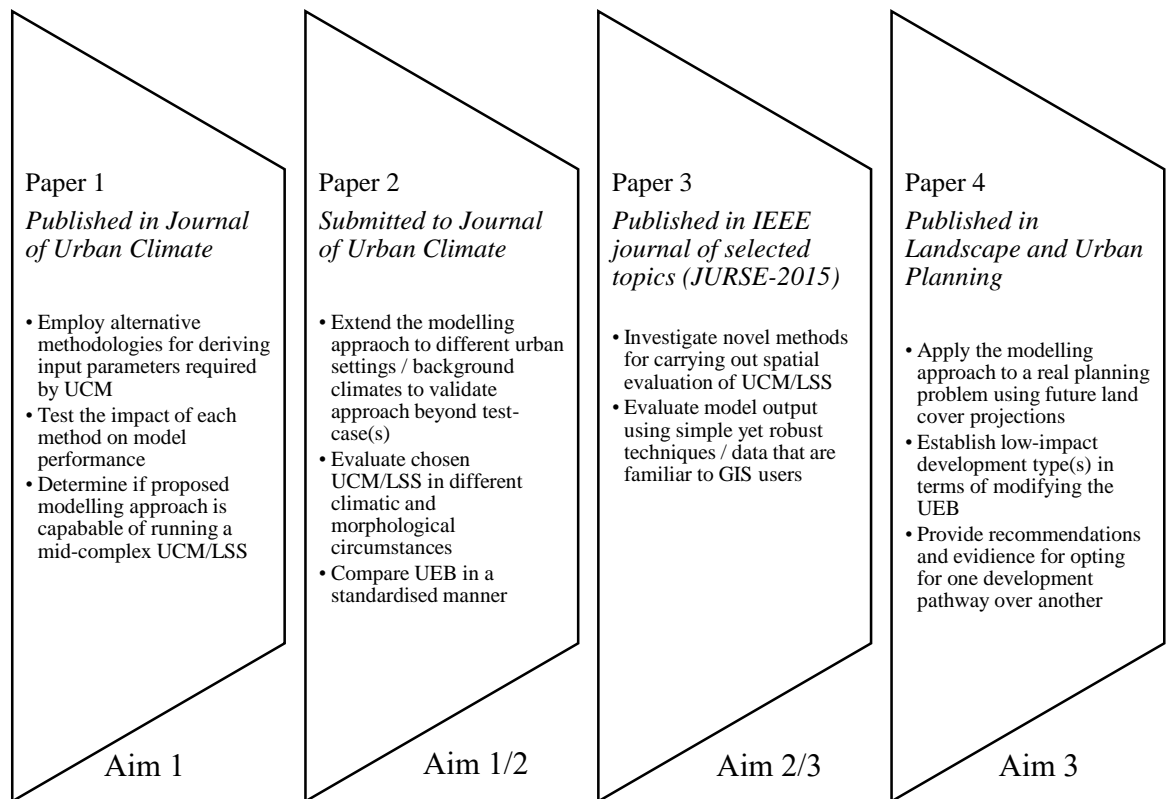


**Figure 1.4 Overview of papers included in this collection; the bullet points show the objectives of the paper which relate to specific aim(s) which is identified below each panel**

## 1.5 Thesis Structure

The collection of papers included in this thesis are contextualised by Chapter 1, Chapter 2 and Chapter 7. Having defined the primary rationale and research aims in Chapter 1, the approach taken to achieve these aims is elaborated in Chapter 2. Specifically, the principle problem identified by this thesis, the issue of data scarcity for forcing UCMs, is addressed with a modelling approach which is employed in all papers included in this thesis. Model evaluation is then discussed and the approach for evaluating model performance is set out which is subsequently employed in Papers 1-3. In the Chapters that follow, each of the papers included as part of this collection are presented, these are:

- Chapter 3 (Paper 1) Development and initial testing of the modelling approach
- Chapter 4 (Paper 2) Further evaluation of the modelling-approach and the surface urban energy and water balance scheme (SUEWS) model in multiple climates and urban settings

- Chapter 5 (Paper 3) Use of novel methods for spatial validation and an evaluation of model parameterisation of land surface temperature
- Chapter 6 (Paper 4) Application of the modelling-approach to a current planning problem
- Chapter 7 discusses the body of work contained within these papers, relates them to one another and to the research aims stated here. Additionally, this chapter presents the conclusions drawn from this thesis and recommendations for moving forward

The opening of Chapters 3-5 provides a brief statement on the papers in terms of where they were published / presented / submitted. Individual published papers are presented in the appendices, where permission was given by the relevant publishers, along with the statement of author and co-author contributions.

## **1.6 Summary and Conclusion**

In the context of global climate change, urbanisation and population growth - urban areas are a critical geographic scale of investigation when discussing sustainability. While the world has become increasingly urban in the past number of centuries it was not until very recently that the importance of urban areas has been recognised by the international scientific community. However, despite this recognition, several significant knowledge deficits exist within urban areas, particularly concerning those rapidly expanding urban areas in the economically developing world. As such, a significant knowledge-gap exists between the urban climate community and urban planner's / policy makers. Bridging this gap will aid in achieving sustainable urban development in the future.

Urban Climate Models (UCMs) represent the epitome of collective urban climate knowledge since many are empirically based and/or are based on a biophysical understanding of the modified atmosphere (the UCL / UBL) in and around cities. Yet, many require detailed information in order to be applied for planning problems. Moreover, the lack of relevant data

for many cities prohibits their use. The present work develops and applies a modelling approach that is intended to overcome many of the challenges related to the application of UCMs, while also furthering the efforts of model evaluation so as to assure the wider community of their utility. This is presented as a collection of papers published on this topic. The overall aim of the present work is to enable better communication within the urban climate community and also across other disciplines such as urban planning.

### 2.1 Introduction

UCMs have great potential to aid in planning decisions in rapidly expanding urban areas, which would further the agenda of urban sustainability / adaptation to global climate change, however, most lack the required data to be applied in a systematic way. Moreover, in order to ensure a consistent approach in model evaluation once they are applied, there is a clear need for a common approach for describing urban areas in which the model was applied to and evaluated in.

In many respects the issues of a) data availability, b) procedures and c) interoperability are analogous to the poor reporting in urban heat island studies. According to Stewart (2011) there is a serious lack of meta-data surrounding the majority of UHI studies, which traditionally reports the UHI as a difference between an urban air temperature measurement and a “rural” counterpart ( $\Delta T_{U-R}$ ). In order to address the lack of data needed to adequately judge the urban effect in different cities, ensure consistency in reporting and transferability of results between cities, Stewart and Oke (2012) developed and proposed the use of the Local Climate Zone system to address the inadequacies in describing urban-rural air temperature measurements, traditionally used in UHI studies.

The broad intention of the scheme was to aid researchers in identifying and reporting on source areas for urban temperature measurements - essentially identifying and classifying urban forms and functions that modify Eqn. 1.1 (Chapter 1) leading to observed relative thermal modification of air temperature within the urban canopy. Urban form is expressed through the LCZ systems as fractional values ( $\lambda$ ) of urban land cover e.g.  $\lambda_{\text{Building}}$ ,  $\lambda_{\text{Impervious}}$ ,  $\lambda_{\text{Pervious}}$  as well as the configuration of roughness elements and their morphological properties such as height and the packing of these features (see Figure 2.1). Urban function is defined

based on the inclusion of an estimate of land use in the area proximate to each LCZ i.e. anticipated geographical position within the urban area as well as an estimation of anthropogenic heat ( $Q_F$ ) release. The basic system comprises 10 urban classes and 7 non-urban classes which are used to describe source areas. Very shortly after the system was proposed, its utility for mapping *potential* source areas across the entirety of an urban area (rather than just patches surrounding temperature sensors) was realised, see for instance Houet and Pigeon (2011) Bechtel and Danke (2012) and Acero *et al.* (2013).

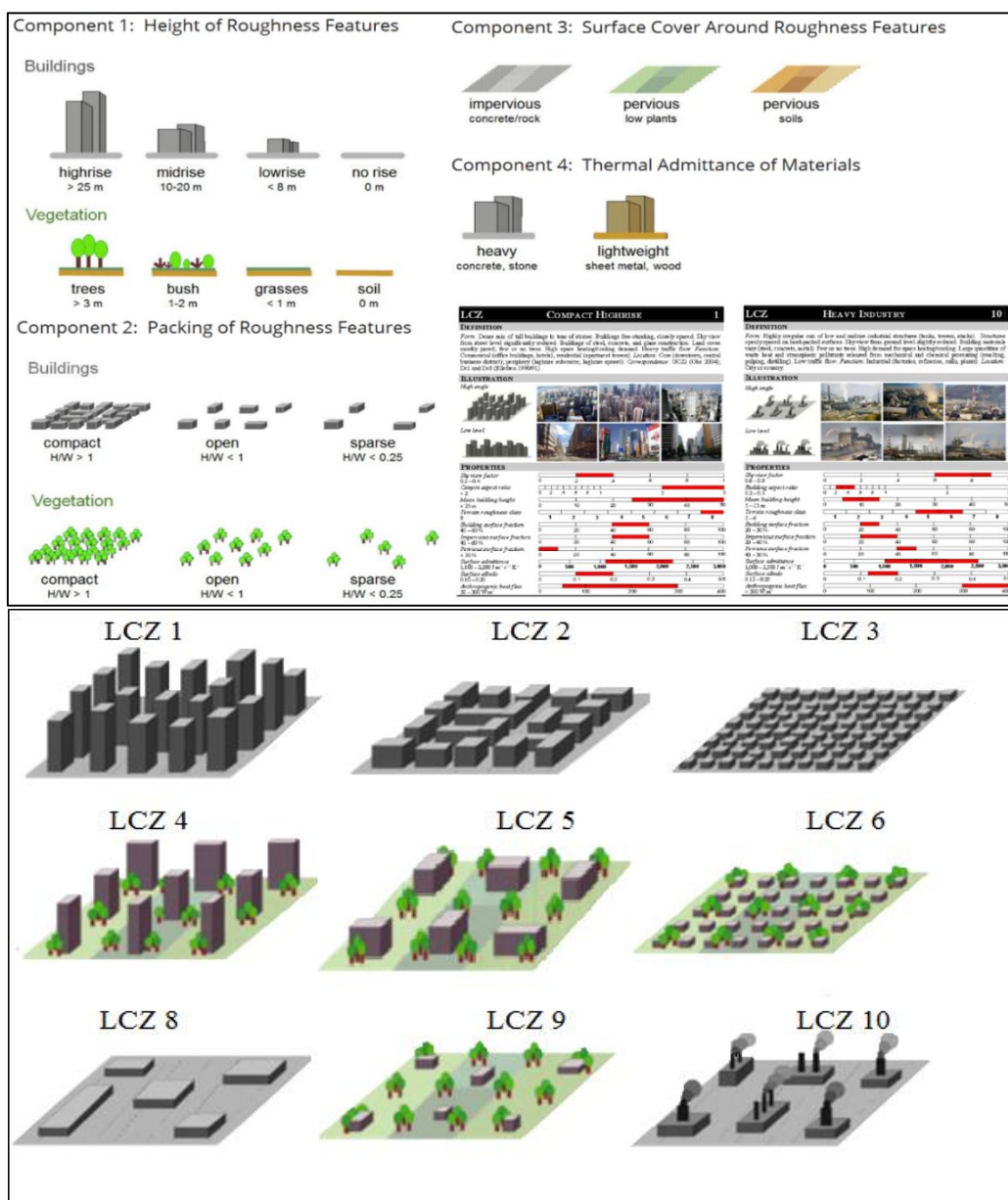


Figure 2.1 Above: The basis of Local Climate Zone system zones in terms of different urban/non-urban forms. Below: Examples of different urban LCZ based on components shown above i.e. LCZ 1-3 are compact highrise, midrise and lowrise respectively.

Mapping LCZ allows for the strategic placement of urban meteorological networks, for sampling air temperatures via traverses through the urban area as well as aiding in the communication of the urban effect to planners – this last point is similar to the objectives of urban climate maps, first proposed by Knoch around 1960 (Ren, et al., 2011) as such, the utility of LCZ for planners is evident (Ren, et al., 2013). Recently, Ching (2013) has suggested the possibility of using the parameters included in the LCZ system as a first-estimate of parameter values required by UCMs.

## **2.2 The Local Climate Zone Approach for Modelling**

The present work evaluates the proposition summarised in Ching (2013), that LCZ may be used for deriving (in a globally consistent manner) the necessary urban climate parameters required by the Weather Research and Forecasting model (WRF) but also required by most UCMs. Figure 2.2 summarises the employment of LCZ as a modelling approach in the present work, hereafter referred to as the LCZ-Approach. There are two key elements of the approach, namely, 1) as a modelling approach which reduces the derivation of input parameters and 2) as a sampling method for deriving parameter values for UCMs - both of these elements are elaborated below and employed in subsequent chapters.

To date, a common approach for modelling is to segregate the landscape into a tessellation of grids and derive the necessary parameters (land cover and meteorology) per grid – as shown in the first two columns of Figure 2.2. This represents a high data requirement cost, even for small urban settings (see Figure 2.3) and thus potentially limits model applications to small-subdomains rather than across an entire urban area. The LCZ-Approach on the other hand assumes (as per Bechtel *et al.* 2015) as its basis that contiguous areas of relatively homogenous urban form and function can be identified and classified into LCZ rather than classifying individual sites; the current work builds on this to test Ching's (2013) assertion that LCZ can provide suitable input parameters for specific urban forms / typologies for large

sections of the urban area. The fact that LCZ-mapping has proven so widespread and relatively successful in multiple cities indicates that the approach, if valid, may have relevance for developing cities where data availability is an issue. Rather than modelling individual grids, larger neighbourhood typologies are modelled and the outputs of the model applied across the relevant LCZs. In modelling neighbourhoods rather than individual grids, the LCZ-Approach assumes that the energetic response of a particular LCZs will be comparable across the domain of interest.

There are a number of limitations to this assumption; for instance, it is invalid in complex topography since elevation will impact on the depth of atmosphere radiation must travel through; hence the UEB will be modified even if neighbourhoods look similar. It is also invalid where significantly different building materials are present despite similar morphological characteristics, as the thermal properties of materials controls the partitioning of energy in terms of  $Q_H$  and  $\Delta Q_S$ . Similarly, different vegetative species will have different hydrothermal responses to radiation and water availability / stress. Land use (urban function) may also vary between neighbourhoods, for instance, one set of high-rise buildings (LCZ 1) may be used as commercial offices whereas another set of high-rise buildings (LCZ 1) may be residential apartment blocks – while the morphological characteristics could be identical, the expectation would be that the hours of occupancy, energy and water use, (in short  $Q_F$ ) are radically different.

However, despite these limitations, the LCZ-Approach for modelling may provide a first estimate of different UEB processes across a wider domain which is inexpensive compared to deriving input parameters across a much wider domain. Moreover, given the presence of planning guidelines in many domains governing the size, location and materials used in buildings coupled with the noted lack of biodiversity in many cities (Convery, 2008) these assumptions may be valid in a large number of cases.

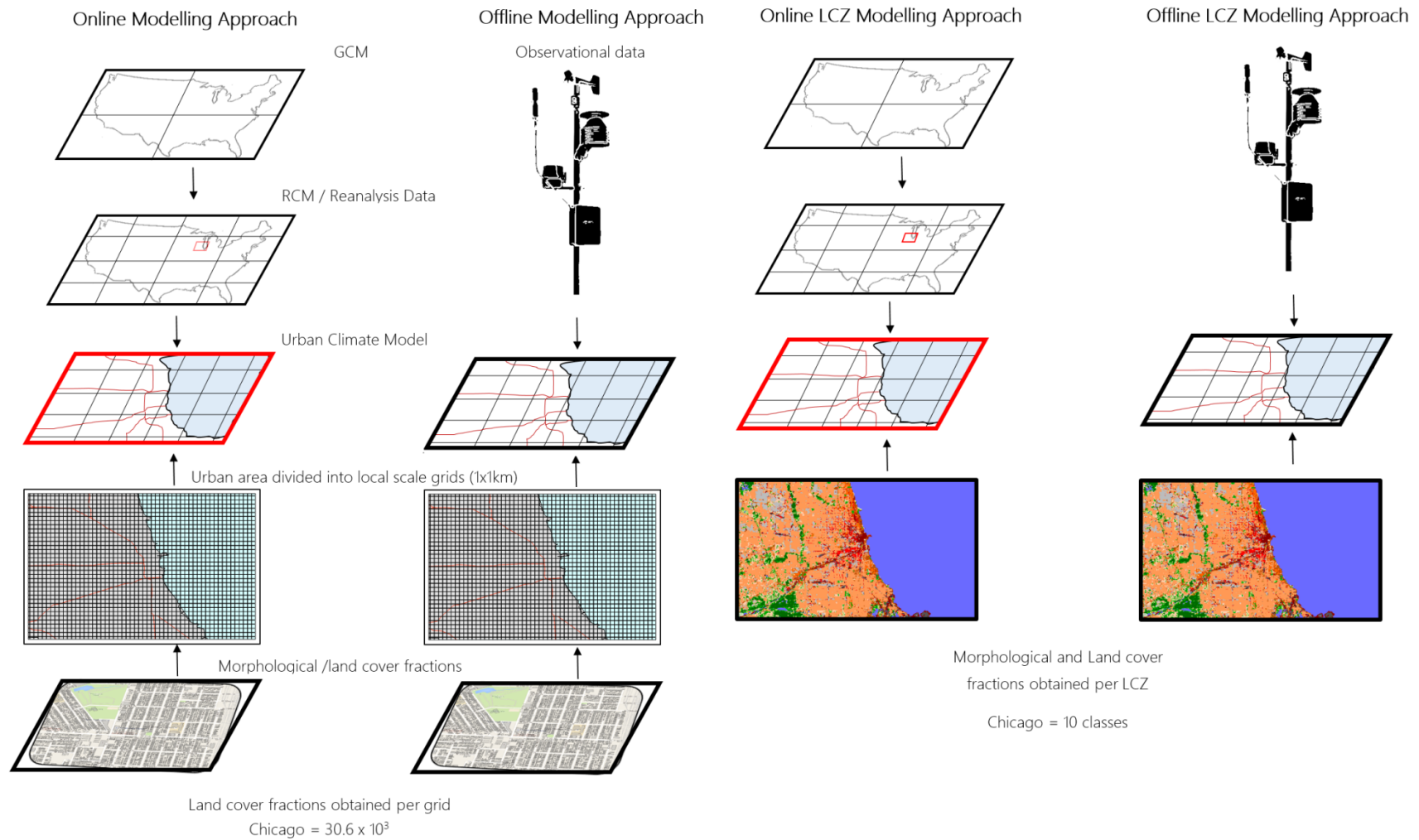


**Figure 2.2 Overview of traditional modelling approaches (first and second column) and the LCZ-Approach for modelling. The LCZ-Approach is essentially based on the principle of spatial auto-correlation which potentially reduces the number of input requirements for most UCMS**

Taking the present study domain as an example (Section 2.4 below), the domain size which would enclose Dublin city and the surrounding hinterland encompasses an area of  $\sim 1000$   $\text{Km}^2$ . If the SUEWS model were run at a  $1 \times 1$   $\text{Km}$  spatial resolution for 1 year, this would equate to  $17.5 \times 10^6$  inputs (rows of data), comprised of 365 land cover parameters, 8,760 hourly meteorological data as forcing and 8,760 phenological values for vegetation **per grid**. For the same size domain using the LCZ-Approach, 91,250 inputs would be required by the same model. The question of the effect of this approach on model performance is a key issue, which is addressed in Chapter 3 and Chapter 4 of this thesis.

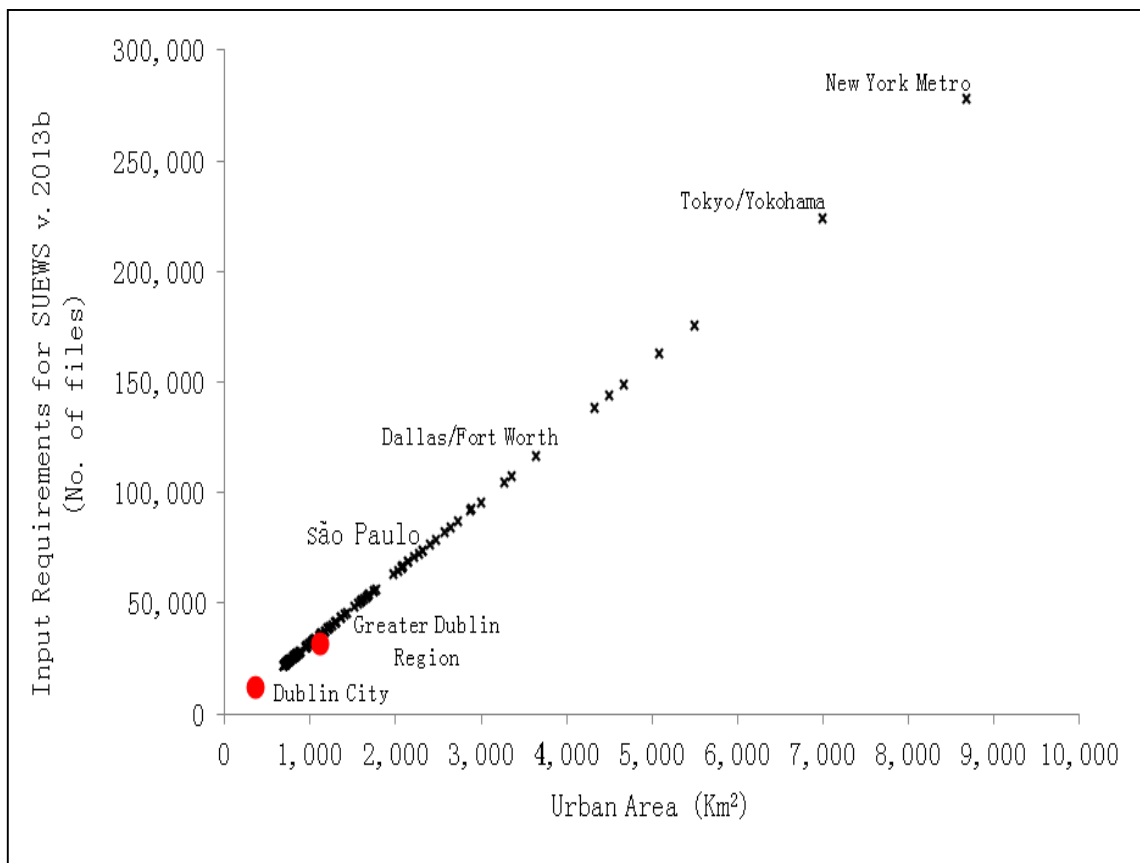


**Figure 2.3** Relationship between city size and number of input files required by SUEWS v.2013b if run at  $1 \times 1$   $\text{km}$  resolution for 1 year. Each  $1 \times 1$   $\text{km}$  grid contains 8 input files. Each data point represents the size of a real city based on data from GRUMPv1 (Balk, et al., 2006). The number of input files is used as a proxy for data requirements. The discussion in text provides a different estimate based on the rows of data contained within these 8 files, hence, this Figure is more conservative.

The notion of mapping LCZ across an entire city in order to examine potential source areas (urban forms and functions) for temperature measurements has already been established (Emmanuel & Krüger, 2012; Kovács & Németh, 2012). In mapping LCZ, the urban area is

broken down into smaller spatial units with relatively homogenous built and vegetative forms. Thus a LCZ map can also be used in designing sampling strategies to obtain more precise values for specific urban parameters required by many UCMs.

Further, it has been suggested that LCZ may provide insight into socio-economic patterns across urban areas (Romero, et al., 2010) which may form the basis for estimating the anthropogenic component of Eqn. 1.1. The use of the LCZ-Approach as a sampling strategy in urban settings where very little geographic (as well as demographic) data are available would appear to be particularly advantageous for efficiently deriving these data:

1. Firstly, identifying urban typologies across a city allows users to design targeted fieldwork campaigns / employ high-resolution remote sensing to derive land cover parameters for LCZ within their domain (Mills, et al., 2015). Rather than randomly sampling the urban area, researchers can focus their efforts on identifying representative areas, which can be reproduced across the entire urban area and extract the required urban parameters from these areas.
2. Secondly, using LCZ as a sampling framework enables users to examine the variability of parameter values which means the representativeness of LCZ parameters can be readily judged, or put slightly differently, how particular areas do or do not conform to the LCZ system.
3. Thirdly, since the LCZ system was developed using data from multiple cities globally and is based on identifying land cover features that serve to modify the thermal climate near the surface, they are well suited for urban climate research such as UCM application.

Related to these points, the first and second knowledge gap highlighted in AR5 (Section 1.2 – Chapter 1) on the uncertain relationship between urban form/function and GHG emissions, called for a standardised method of calculating GHG emissions across different cities – since

the LCZ system has been adopted as the appropriate standard in which to report on air temperatures within the field of urban climate, it is possible they can also be used for fine-scale GHG inventories within urban areas (Liu, et al., 2012).

### **2.3 Evaluation Approach**

Despite the obvious advantages of urban climate models for aiding decision making (Oke, 1984; Arnfield, 1990) there is little evidence to suggest they are being applied routinely to planning problems (Eliasson, 2000). In fact Oke (2006) highlights the need for more extensive validation and application of urban climate models for planning problems as a research priority for the urban climate community. The international urban energy balance model inter-comparison project (Grimmond, et al., 2010; Grimmond, et al., 2011) went a large way towards identifying the general ability of 33 different models. However, while recommendations surrounding parameter standardisation, initial conditions / forcing data and vegetation treatment emerged, there is still no agreed approach for model development and evaluation.

The nature of model evaluation is central to the present work. Within the body of literature reviewed, urban climate model (UCM) evaluation has tended to be carried out by model developers (individuals or groups) themselves with little coordination across the discipline - for instance (Grimmond & Oke, 1999; Oleson, et al., 2008; Hamdi & Masson, 2008; Chen, et al., 2011). However, commonalities in terms of evaluation approaches do emerge. Firstly, the models tend to be evaluated against datasets independent of those used for deriving parameterisation schemes, for example subsets of data are withheld during development and used in the subsequent evaluation. Secondly, common statistical metrics are used to judge performance which enables better communication across studies. Thirdly, there is usually some form of problem statement which defines the appropriate applications of the model.

However, in the absence of a community agreed framework, it is unlikely the utility of UCMs will be demonstrative effectively moving forward. The central aspects of the evaluation approach used in this thesis are discussed below. This approach informed each of the papers in this thesis. In the sections that follow, the main components of the evaluation approach are outlined.

### 2.3.1 *Model Assessment*

Within the wider earth sciences (but here with respect to atmospheric sciences) the terms model validation and model evaluation are used interchangeably. As argued by Oreskes *et al.* (1994) however, there is a key difference between the terms validation and evaluation. Such an argument can be trivialised on the basis that fundamentally, the use of language does not impact on a models' ability to capture and reproduce key processes or responses. However as stated by Oke (2006) and Oreskes (1998) the distinction is of critical importance in communicating judgements i.e. model performance to the wider public or policy makers, especially where long term implications of adopting these judgements may mean the difference between achieving (for instance) thermal comfort or discomfort within a city.

In order to ensure consistent and comparable communication with respect to model performance, the distinction must be addressed. There are two means of viewing models (i) as a scientific hypothesis or (ii) as a tool.

As a scientific hypothesis, a model may be validated in terms of its ability to reproduce physical processes. For example, if the air temperature of a parcel of air increases while the specific moisture content remains the same, the relative humidity would decrease. If a model is capable of reproducing this, then we may say it appears physically valid, but not by reproducing the heat capacity of air. Being able to reproduce reality (even for the wrong reasons) does not speak to model performance - the increase / decrease in relative humidity may be orders of magnitude off the observations. On the other hand, viewing a model as a tool

would implicitly require the user to assess how effective the tool is, or put slightly differently, to evaluate the quality of the model. This stance (and hence the term “evaluation”) appears more satisfactory, but it should be remembered that model evaluation does not consider the processes but rather it’s ability at reproducing some specific aspect of reality. Both evaluation and validation are not mutually exclusive approaches, though it would appear that in the cases referred to above, model evaluation is often what is being carried out.

### 2.3.2 *Evaluation Metrics*

Urban climate models have historically been developed by independent groups. As such, there is no agreed methodological approach to evaluate their quality. In other disciplines, standards do exist - see for instance Steyerberg & Vergouew (2014) and Moriasi *et al.* (2007). The approach employed here distinguished between “internal” and “external” evaluation. Internal model evaluation means employing of subsets of data used to derive parameterisation schemes to evaluate model performance. Examples of this can be identified within the existing urban climate model literature (Kusaka, et al., 2001; Hamdi, et al., 2012). While there is no specific reason to suggest internal evaluation is inappropriate, ideally models should be tested in a wide range of circumstances and demonstrate universality. External evaluation addresses this issue by evaluating model performance against data that are independent of the models development. However, given the sparsity of turbulent flux observation platforms or meteorological networks in urban areas globally (Muller, et al., 2013), this may require alternative means of evaluation, at least in the case of urban energy budget models, for example, the use of Remote Sensing (Hu *et al.*, 2014; Chapter 5) or crowd sourced data (Muller, et al., 2015).

In terms of practicing evaluation, a *de facto* convention is adhered to within the literature. Evaluation usually focuses on two broad aspects namely (1) the error (also referred to as the model accuracy) and (2) the direction of the error (also referred to as bias). These are

outlined below as these metrics are employed throughout each of the papers included within this collection.

### 2.3.2.1 Performance / Accuracy Metrics

Common metrics for error/accuracy are presented in this section while the next section presents common metrics for reporting the direction of the error or bias, all employ as their basis the error ( $e$ ) between observations ( $X_{obs}$ ) and model predictions ( $X_{model}$ ):

$$e = X_{obs,i} - X_{model,i} \quad \text{Eqn. 2.1}$$

The root mean squared error (RMSE) is given by:

$$RMSE = \sqrt{\frac{1}{n} \sum_{i=1}^n e_i^2} \quad \text{Eqn. 2.2}$$

The mean absolute error (MAE) is given by:

$$MAE = \sqrt{\frac{1}{n} \sum_{i=1}^n |e_i|} \quad \text{Eqn. 2.3}$$

For a given threshold (e.g. model errors within 1 standard deviation ( $\sigma$ ) of observational data) the accuracy ( $acc$ ) is the number of model predications within the defined threshold, divided by the total number of observations, given by:

$$acc = \frac{\sum_{i=1}^n X_{model} \leq \sigma}{\sum_{i=1}^n X_{obs}} \quad \text{Eqn. 2.4}$$

Additional metrics are the Pearson correlation coefficient ( $r$  – derivation not shown), the coefficient of determination ( $r^2$  – derivation not show) and Nash-Sutcliffe model efficiency coefficient ( $E$ ), which is given by:

$$E = 1 - \frac{\sum_{i=1}^n (e_i)^2}{\sum_{i=1}^n (X_{obs,i} - \bar{X}_{obs})^2} \quad \text{Eqn. 2.5}$$

In the case of Eqn. 2.2-2.4, the resulting statistic will be the same unit as the data used e.g. if  $X_{obs}$  and  $X_{model}$  are temperatures in °C, the resulting RMSE and MAE will be in °C. For the latter two metrics (Eqn, 2.5 and 2.6) the result will be a unit-less ratio between  $\infty$  - 1.0. Variations of these metrics are also employed, for instance, the centred RMSE (Taylor, 2001; Koh, et al., 2012) or mean absolute scaled error (Hyndman & Koehler, 2006). While wider arguments for and against particular performance metrics have been noted - see for instance Willmott & Matsuura (2005) and the response from Chai & Draxler (2014), it is generally favourable to employ multiple metrics, which represent different measures of the models' ability to accurately simulate the response, when reporting model performance.

### 2.3.2.2 Error Direction / Bias Metrics

While the previous section highlights metrics used to calculate and report on a models performance / accuracy, these metrics negate the effect of over-prediction and under-prediction, commonly referred to as "bias" (Moriassi, et al., 2007). Bias metrics on the other hand provide a measurement of the average tendency of modelled values to be larger or smaller than observed values. As with the previous section, common metrics are presented here.

The mean bias (MB) which returns a value in the same unit as the input measurements is given by:

$$MB = \frac{1}{n} \sum_{i=1}^n (X_{model,i} - X_{obs,i}) \quad \text{Eqn. 2.6}$$

As with Eqn. 2.1 MB can be affected by very large differences between model values and observations, moreover these metrics can be significantly affected by error cancelation. Therefore, it is often advisable to normalise the metric using observed values, this provides the normalised mean bias (NMB) given by:

$$NMB = \frac{\sum_{i=1}^n (X_{model,i} - X_{obs,i})}{\sum X_{obs}} \quad \text{Eqn. 2.7}$$

This returns a unit-less metric which takes on a value -1.0 to  $+\infty$  values where  $< 0$  indicates underestimation of model values relative to observations and  $> 0$  indicates overestimation relative to values. Additionally, the mean fractional bias (MFB) uses the mean difference between observational values and modelled values to normalise Eqn. 2.6 given by:

$$MFB = 2 \times \left( \frac{\overline{X_{model}} - \overline{X_{obs}}}{\overline{X_{model}} + \overline{X_{obs}}} \right) \quad \text{Eqn. 2.8}$$

This metric takes on a value between -2.0 and +2.0, as with Eqn. 2.7 values  $< 0$  indicate lower modelled values with respect to observational values and conversely values  $> 0$  indicate higher modelled values i.e. overestimation. Eqns. 2.6-2.8 refer to bias that is described as systemic i.e. model values are generally all higher (overestimation) or lower (underestimation) than observational values. To control for unsystematic errors, the variance (s) or standard deviation ( $\sigma$ ) of the modelled and observational values should be also be reported with the bias metric(s) used.

It should be noted that in all cases above the observational data used to calculate both error and bias are assumed to be the true state of the atmosphere. However, large variability is inherent to turbulent flux observations (Keogh, 2015), while observations undergo post-processing it is important to note that observational error will factor into reported model performance. Where possible, the same set of observational data are used to evaluate the LCZ-SUEWS approach, in this way, the *relative* change in error arising due to the use of generic land cover and/or off site meteorology is of primary interest, and ensures the error and bias statistics are comparable.

## 2.4 Case Study City

The approaches outlined in previous sections was applied to a test-case city (and others) to examine the LCZ-Approach for UCM application and determine the utility of UCMs for addressing planning problems. In this section, the rationale for choosing the Greater Dublin

Area (GDA), Ireland for the present work is given, followed by a detailed overview of the city and surrounds.

#### *2.4.1 Rationale for selecting the Greater Dublin Area*

There are a number of reasons why the GDA was selected to develop, apply and evaluate the proposed LCZ-Approach for deriving a first estimate of parameters for use in a UCM; this section highlights these reasons, however it should be noted that the modelling approach proposed is intended to be extendable beyond this case study area (as in Chapter 4).

Firstly, the majority of population increase in Ireland over the past number of decades has been concentrated in (and immediately proximate to) Dublin city. The city and the GDA currently houses almost 40% of the national population, thus significant land cover change has occurred (Figure 2.4) resulting in the largest urban area within Ireland. Hence, one of the main rationales for selecting Dublin city as a study location for urban climatological investigation is due to the fact it can be reasonably expected that the urban effect is detectable across large sections of the GDA and the scale of changes, while smaller than for other cities, is likely to be representative of urban changes more generally.

Secondly, recalling Table 1.1, Spate (1942) argues capital cities represent a nexus of socio-economic-political activities and as such have special status in terms of national development policies. Therefore, as a capital, a significant amount of autonomy may be expected of the Dublin / GDA planning authorities providing additional flexibility in determining their specific urban and social development plan(s). Therefore, outputs from the present work (specifically those from Chapter 6) have more direct relevance in Dublin; or put slightly differently, the outputs from the present research have a higher probability of being adoptable for Dublin and the GDA than in other urban areas in Ireland.

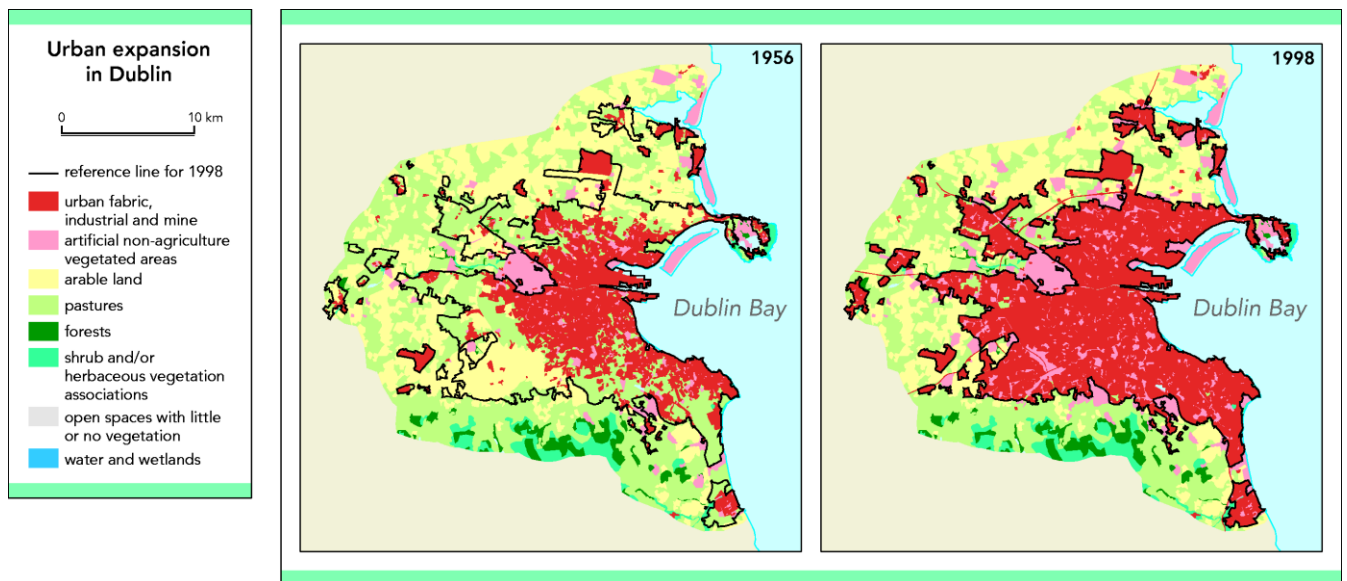


**Figure 2.4 Land use / Land cover change illustrating urban expansion across Dublin city between 1956-1998. The areas of the map in red illustrate the urban fabric. Source: EEA (1999)**

Thirdly, a significant amount of work has been carried out on the impact of Dublin city on the near-surface climate, particularly in terms of the UHI. Sweeney (1987) conducted mobile temperature measurements by traversing the city by car during winter nights, reporting that UHI magnitude ( $\Delta T_{U-R}$ ) could reach  $6.5^{\circ}\text{C}$  in settled anticyclonic conditions approximately 4 hours after local sunset. Graham (1993) adopted a similar approach, conducting mobile temperature traverses by car and bicycle during the summer months and reported a UHI intensity of approximately  $4.5^{\circ}\text{C}$  approximately 4 hours after local sunset.

Both Sweeney (1987) and Graham (1993) adopted mobile temperature measurements since no fixed urban network of meteorological stations existed. To overcome this limitation, Alexander and Mills (2014) established a small network of meteorological stations across different LCZ and additionally conducted mobile measurements during the summer - reporting a UHI intensity between the inner city (LCZ 2) and surrounding non-urban hinterland (LCZ D) of  $4.2^{\circ}\text{C}$ . Hence, the UHI has been extensively studied.

While the UHI has been the subject of study in Dublin since at least 1987, Keogh *et al.* (2012) were the first attempt to explore the energetic basis, that is fluxes of heat and moisture, of the urban effect in Dublin by means of Eddy Covariance (EC) observation. Two EC flux

sites were established in suburban (LCZ 6) and urban (LCZ 2) neighbourhoods and the UEB examined. Their analysis illustrates the differences in the partitioning of available energy (left side of Eqn. 1.1) into sensible and latent heating and heat storage (right side of Eqn. 1.1) whereby sensible heating ( $Q_H$ ) was ~10% higher at the urban site relative to the suburban site, and the magnitude of latent heat ( $Q_E$ ) at the suburban site was more than double that of the urban site. They conclude differences in flux partitioning is primarily due to different land cover and vegetative amounts surrounding the two EC sites.

Flux observations have been made continuously since this time. Additionally a third site was established in a second urban neighbourhood (LCZ 2) on a intensively instrumented site, reported in Sunderland *et al.* (2013) and continues to make observations up to the present work. This long time series of EC flux measurements made within different urban environments, coupled with the previous research on the modification of intra-urban air temperature (which may be considered as a proxy for differences in the UEB) and the network of meteorological stations means Dublin is an ideal location to evaluate model applications, explore the impact of the proposed LCZ-Approach and derive planning solutions that have a low impact on the UEB.

#### 2.4.2 *Geographical setting and climate*

In Chapters 3-6 of the present work, a mid-complex UCM is applied to an urban area referred to as the Greater Dublin Area (GDA) which encompasses Dublin city, Dublin county and surrounding conurbations contained within counties Meath, Kildare and Wicklow – see Figure 2.5. The GDA sits on the east coast of the country adjacent the Irish sea, though county Kildare is landlocked. The GDA distinguishes itself from other regions of Ireland in terms of its position as a nodal point for transport networks; including road, rail, seaports and airports. Moreover, the GDA is recognised formally as the financial, administrative and political capital of Ireland.

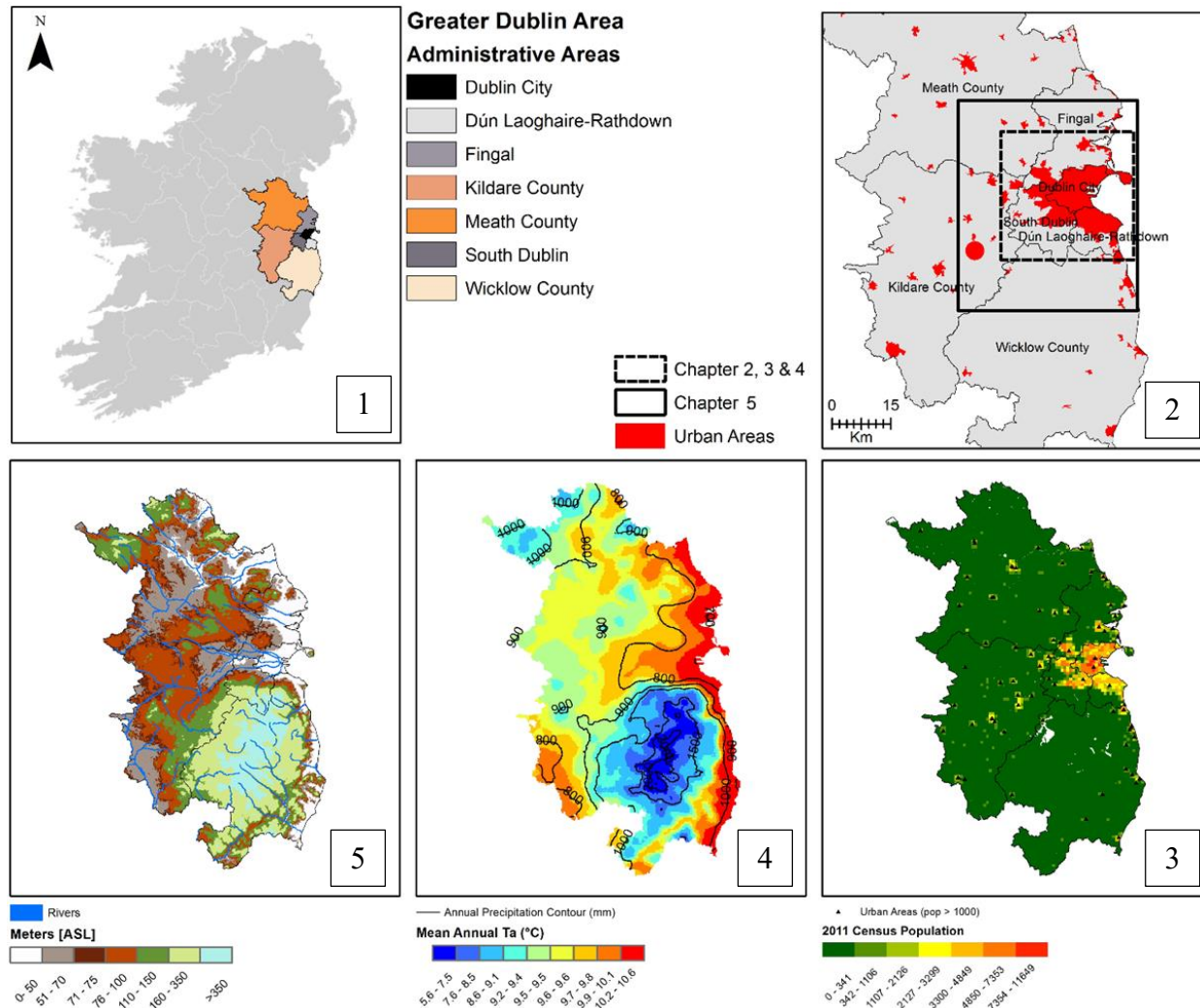


Figure 2.5 Overview of the case study city and surrounding area – referred to as the Greater Dublin Area (GDA). From Top left moving clockwise: (1) GDA in the context of the island of Ireland (2) Overview of the model domain employed in this work and the major urban areas encapsulated – areas in red are the administrative boundaries of major urban areas (defined as contiguous urban areas with a population of 1000 people or more – CSO 2012) (3) The population of the GDA based on the last census (2011) – CSO 2012 (4) Climatology of the GDA, shown is the mean annual 2m air temperature based on the climate normal (1989-2010) contours show mean annual isopleths (accumulated precipitation) – Met Éireann/Walsh (2012) (5) The physical features of the GDA, shown are major river ways and topography of the GDA - NASA, GDEM V2 and Water Body Data (SWBD)

The location of GDA impacts on the local climate which varies slightly throughout the region. In general, the climate of GDA is characterised as temperate oceanic climate (Koppen type Cfb) which implies a mild, wet climate. Dublin city and county receives an average of 600-800mm of precipitation annually; Kildare and Meath receives 800-1,000mm (Walsh, 2012). Wicklow receives comparably more precipitation than other counties in the GDA owing to the presence of the Dublin/Wicklow mountains which produces a high volume of relief rain, hence, the annual average precipitation in Wicklow ranges from 1,200mm in the lowlands to 2,400mm in the highlands - Figure 2.5 (4).

The location of the Dublin/Wicklow mountains also explains the lower amount of precipitation received by Dublin city / county. Since the climate of Ireland is dominated by the passage of mid-latitude cyclones (MLCs) moving west-east across the Atlantic, the high topography to the south of the city serves to predominantly block South-Westerly precipitation from reaching the city (Rohan, 1983). The majority of precipitation falls as rain, associated with frontal systems, though convective rain can occur during the late summer / early autumn.

Due to the proximity of the Irish sea, there is a general east-to-west trend moving inland in terms of air temperature – the mean annual temperature for Dublin city and county is  $\sim 10^{\circ}\text{C}$  whereas in Meath and Kildare, the mean temperature is a few degrees cooler ( $8-9^{\circ}\text{C}$ ). Dublin county holds the highest temperature record for 5 months of the year (that is, the record highest temperature recorded in any January, February, March, November and December) since records began, the GDA combined holds the record for 7 months (Walsh, 2012).

The presence of MLCs and associated active frontal systems means cloud cover is present throughout the year (generally clouds will cover 66% of the sky each hour). As a consequence, most parts of Ireland, including the GDA receive less than  $1/3^{\text{rd}}$  the amount of available sunshine hours at the surface. There is a wider synoptic trend from North-West to South-East of the country in terms of actual sunshine hours, however in terms of the GDA,

there is comparably less variation; the mean annual amount received is between 1,350-1,400 hours of sunshine (Walsh, 2012), though due to the latitude of Ireland, there is a great deal of variation between winter (150-175 hours) and summer (500-525 hours). Wind speed is largely controlled by the presence of cyclonic or anti-cyclonic systems over Ireland, the mean annual wind speed for the GDA is  $5.5 \text{ ms}^{-1}$  though there can be considerable diurnal variation.

### 2.4.3 Demographics

Currently the GDA houses 40% of the total population of the island of Ireland, this figure has doubled since the start of the 20<sup>th</sup> century and is expected to reach 45% in the next 15 years and 50% by the middle of this century (Central Statistics Office, 2013). In terms of population counts, two broad trends exist within the GDA since 1840; firstly, a slow but marked decrease in the population following the famine years (circa 1845) where the population decreased year on year from ~800,000 to less than 670,000. Secondly, from around 1911 and the establishment of Irish nationalism, the population within the GDA began to increase, in 1977, the population reached over 1 million and has not dipped below this level since that time – see Table 2.1 and Figure 2.5. Moreover, the pace of population growth has accelerated to a present growth rate of 78 people per day (28,324 persons per annum or 1.6%) from a baseline of about 19 people per day in 1977. The largest decade on decade increase occurred during 2000-2010 during a period of significant economic growth.

**Table 2.1 Population count at the last census (2011) and projected increase for the Greater Dublin Area (GDA) between 2011-2031 (Source: CSO, 2013)**

	<b>Population 2011</b>	<b>Natural increase</b>	<b>Internal migration</b>	<b>External migration</b>	<b>Total increase</b>	<b>Projected Population 2031</b>
<u>Population counts in Thousands</u>						
Greater Dublin Area (GDA)	1795	298	92	11	401	2197
Dublin city & county	1262	188	47	23	257	1519
Kildare, Meath & Wicklow	534	110	45	-11	144	678

Approximately 75% of the population within the GDA were between the ages of 15-64 around the start of the 20<sup>th</sup> century, this demographic as a proportion of the total population of the GDA has decreased at a rate of about 0.25% per decade. The proportion of the population aged 65 or over has increased by approximately 0.125% per decade, about half the rate of the 15-64 demographic decrease – see Figure 2.6. Combining Figure 2.5 and 2.6, the majority of the population resides within a fairly geographically discrete area around Dublin city, though fairly significant satellite towns do exist.

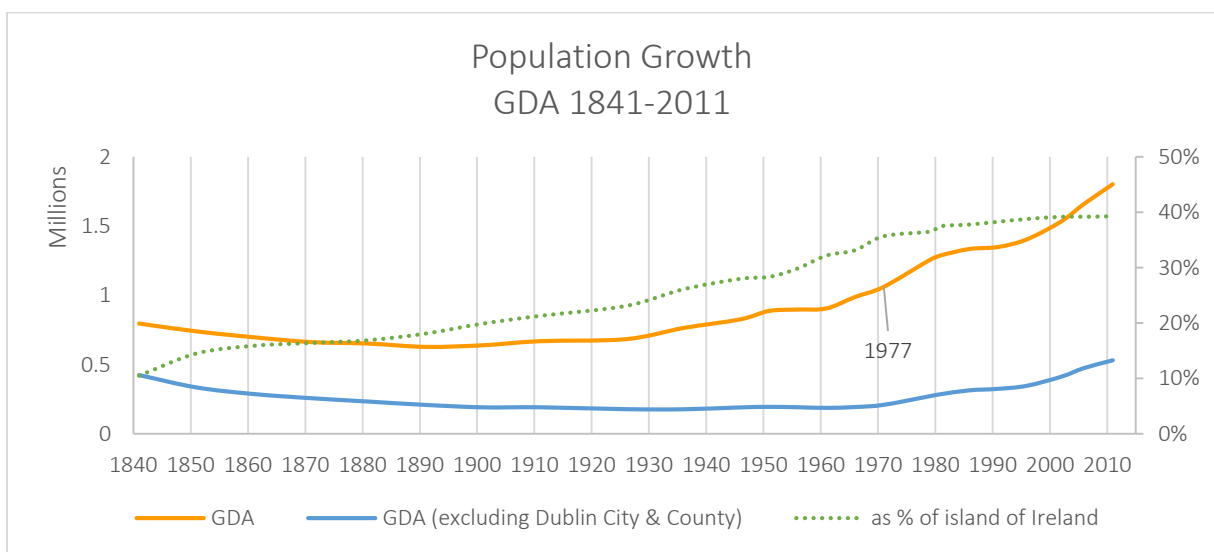


**Figure 2.6 Population growth in the GDA based on national census statistics, following the 1966 census year the slope of the line increases notably indicating an increased pace of urbanisation within the region. Also shown is the trend for the GDA excluding Dublin city and County, which illustrates the shift of surrounding populations towards the city. The 2<sup>nd</sup> series (right Y-axis) shows the proportion of the total population of Ireland living within the GDA. Statistics sourced from CSO (2012)**

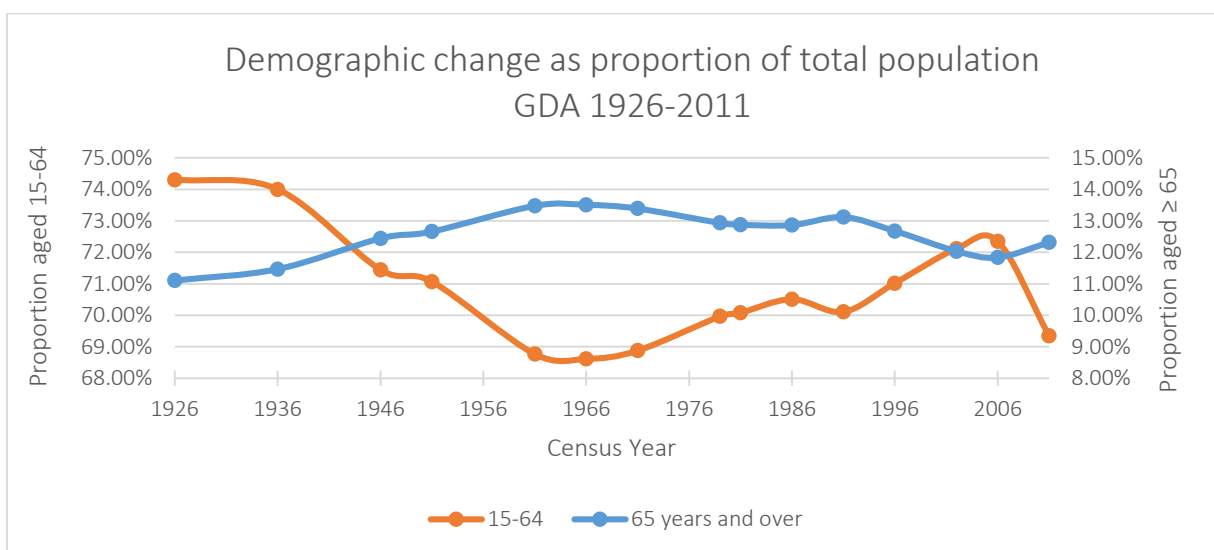


**Figure 2.7 Demographic change in terms of age profile of the Greater Dublin Area (GDA) based on census statistics. The older demographic (65 and over) are plotted against the 2<sup>nd</sup> (right) Y-axis. Statistics sourced from CSO (2012)**

## 2.5 Summary and Conclusion

This chapter has discussed the approach in which parameters for a mid-complex model were derived and the approach taken to evaluate model performance.

The proposed LZY-Approach for modelling seeks to reduce the data requirements of applying UCMs across an entire city by modelling ‘typical’ LCZ within an urban area and applying model outputs to areas which share the same LCZ class, rather than a more traditional tessellation approach. In terms of deriving detailed parameter estimates, the LCZ-Approach allows for the derivation of parameters required by many UCMs by enabling researchers to strategically sample based on the relative coverage of different LCZ within a city.

Given the sparsity of urban flux sites globally, it is understandable why subsets of observational data and limited spatial and temporal circumstances have been utilised for UEB model evaluation, however this is suboptimal. In the present work, evaluation is framed with a view to extend the circumstances in which the SUEWS model has been evaluated, both in terms of the background climate and urban environment and the impact of the LCZ-Approach on model performance. This is termed an external evaluation, and was designed to demonstrate the utility of the chosen model and modelling approach in multiple domains.

To gain a detailed insight into the impact on model performance the approach was applied to a case study city with a sufficient knowledge-base and necessary observation platforms in order to validate the approach and carry out an evaluation of the SUEWS model. Evaluating the SUEWS model and modelling approach was central to the chapters that follow, these approaches were taken in order to achieve the research aims outlined in the previous chapter.

The approach for model evaluation is based on the need for evaluation in a greater number of circumstances, this feeds directly into the proposed modelling approach i.e. that is should be evaluated in a number of circumstances. Data requirements were shown to be high

when considering an entire urban area, meaning that sub-domains are often required for modelling, thus limiting the opportunity for evaluation. By first segregating the urban domain into LCZs, accepting limitations of this approach, the number of input requirements to run a mid-complex model is reduced significantly, allowing models to be run a) across a larger portion of the urban area and b) in areas which suffer with data scarcity.

---

## Chapter 3 Using LCZ data to run an Urban Energy Balance Model

---

### 3.1 Preface

This chapter is published as:

Alexander, P.J., Mills, G., Fealy, R. (2015) Using LCZ data to run an urban energy balance model, *Urban Climate*, Volume 13, September 2015, Pages 14-37, ISSN 2212-0955, <http://dx.doi.org/10.1016/j.uclim.2015.05.001>.

This paper is positioned at the beginning of the present collection as it was designed to lay the ground work for subsequent papers. Here, the LCZ-Approach highlighted in Chapter 2 of this thesis was linked with a mid-complex urban energy budget model – SUEWS – hence is referred to in the paper (and others) as the LCZ-SUEWS approach. The broad questions that motivated this paper were (i) *what impact would low-quality data have on a model such as SUEWS?* (ii) *Does the LCZ-Approach satisfy the requirements of the SUEWS model?*

Within data-poor settings, it is anticipated that a researcher interested in the effect of their city on the climate may have at their disposal 1) meteorological data from a WMO standard weather station and 2) some form of land use cover data. Tangential to this paper, research on how to generate a local climate zone (LCZ) map for any city world-wide using free, open-source and standardised was carried out, in hopes to satisfy 2) above. With these two-components the LCZ-Approach may be utilised (recall Figure 2.2 in the previous Chapter). However, since this approach has not been applied elsewhere, the question remained as to how this might impact on model performance. Therefore, this chapter provides a proof-of-concept for the approach. The original submission evaluated model performance only during 1 month (June 2010). For the accepted version, this was extended so as to cover a longer period of time and ensure the proof-of-concept was truly robust, and that performance when using this approach to run SUEWS was more or less consistent throughout multiple seasons.

### 3.2 Abstract

In recent years a number of models have been developed that describe the urban surface and simulate its climatic effects. Their great advantage is that they can be applied in environments outside the cities in which they have been developed and evaluated. Thus, they may be applied to cities in the economically developing world, which are growing rapidly, and where the results of such models may have greatest impact with respect to informing planning decisions. However, data requirements, particularly for the more complex urban models, represent a major obstacle to their employment. Here, we examine the potential for running the Surface Urban Energy and Water Balance model (SUEWS) using readily obtained data. SUEWS was designed to simulate energy and water balance terms at a neighbourhood scale ( $\geq 1\text{km}^2$ ) and requires site-specific meteorological data and a detailed description of the surface. Here, its simulations are evaluated by comparison with measurements made over a seven month (approximately 3 seasons) period (April-October) at two flux tower sites (representing urban and suburban landscapes) in Dublin, Ireland. However, the main purpose of this work is to test the performance of the model under 'ideal' and 'imperfect' circumstances in relation to the input data required to run SUEWS. The ideal case uses detailed urban land cover data and meteorological data from the tower sites. The imperfect cases use parameters derived from the Local Climate Zone (LCZ) classification scheme and meteorological data from a standard weather station located beyond the urban area. For the period of record examined, the simulations show good agreement with the observations in both ideal and imperfect cases, suggesting that the model can be used with data that is more easily derived. The comparison also shows the importance of including vegetative cover and of the initial moisture state in simulating the urban energy budget.

### 3.3 Introduction

Within the next four decades the global population is projected to increase by 2.3 billion, within the same period it is expected that urban areas will gain 2.6 billion (UN 2012), absorbing projected growth and continuing to draw from existing rural populations. While this trend appears globally, there are regional differences. The urban population in more economically developed regions has already reached 78%, whereas in less developed regions it currently stands at 47%. Taking the projections for Asia and Africa together, their urban population will grow by 2.3 billion by the middle of the century. If these projections are realised, most of the urbanisation in the future will occur in the economically developing world (Satterthwaite, 2007). Responding to this challenge will result in large-scale housing and critical infrastructure projects (e.g. energy and water supply, waste removal facilities and transport) that, once in place, create an urban form that is difficult to change; hence, it is important that urban growth is well managed. At least two responses might be expected: horizontal expansion of the urban area and densification of the existing urban fabric (Moonen et al., 2012). If future urban development is to reduce environmental impacts (e.g. air quality, hydrology and thermal effects) that result from conventional urbanisation some guidance on development pathways is needed (Schwela, 2000; Schuster et al., 2005; Arnfield, 2003; Chen & Ng, 2012). One component of this guidance should be physically-based models that can simulate the effect of alternative urban plans and designs and inform decision-making. However, these models only have value if they have been tested, that is, applied to urban places, evaluated against observations and validated. Unfortunately, there are few examples of the application of urban climate models to these types of problems (Oke, 2006).

Although there are an increasing number of diverse urban climate models available, there is little evidence that they are routinely applied. A significant impediment to their routine use includes the paucity of relevant information on: the physical character of cities (that is the

buildings, materials, layout, etc.) needed to derive model parameters and; the meteorological data needed to ‘force’ the models and evaluate their simulations. In fact, the lack of urban specific data has been recently highlighted in the 5<sup>th</sup> assessment report (AR5) of the Intergovernmental Panel on Climate Change (IPCC, 2014). Specifically, AR5 highlights serious data limitations with respect to geophysical, biological and socio-economic data, as well as inadequate knowledge surrounding the vulnerability of the built environment and building materials to climate change. These issues are particularly acute for the rapidly growing cities of the economically developing world, many of which are outside the mid-latitude climates where the models have been developed and may lack the necessary urban and meteorological information required. Recently, a protocol for collecting urban parameters in an efficient and standardised manner has been proposed to address this problem (Ching, 2013; Bechtel et al. 2015).

This paper examines the issue of information quality and its impact on the performance of an urban energy balance model (UEB). The Surface Urban Energy and Water Balance model (SUEWS) is a moderately complex UEB that requires detailed information on the urban landscape and is usually run using on-site meteorological data. We use SUEWS to simulate the energy budget at two Dublin locations for which we have detailed energy flux stations and detailed spatial information (e.g. individual building footprints, heights) on the surrounding urban landscape. This allows us to run the model and evaluate its simulations of turbulent fluxes over a period of time. We then use readily available standard meteorological data and coarse land-cover data and perform the same evaluation. The performance of SUEWS is judged against two different urban landscapes - city centre and green suburbs - where eddy-flux towers are located that provide observations of the UEB terms. The results are compared with observations to assess the relative effect of input data quality. Specifically, we address two questions, which have implications for the use of UEB models in data-poor settings:

1. How does SUEWS perform in terms of discriminating between different urban environments when run using readily available but coarse land-cover data and standard meteorological data relative to using optimal data?
2. Specific to the Dublin case study, which is more important for running SUEWS; on-site detailed meteorological data or high quality, spatially detailed land-cover?

The answers are based on the application of the SUEWS in Dublin (Ireland), for which we have a range of data suitable for evaluating model performance under ideal and non-ideal circumstances.

### 3.4 Urban energy budget (UEB) models

A number of urban models have been developed at a variety of spatial and temporal scales with a range of applications, the most common of which are based on the surface energy budget,

$$Q^* + Q_F = Q_H + Q_E + \Delta Q_S, \quad W m^{-2} \quad \text{Eqn.3.1}$$

where  $Q^*$  is net radiation,  $Q_F$  is anthropogenic heat flux,  $Q_H$  and  $Q_E$  are the turbulent sensible and latent heat fluxes respectively and  $\Delta Q_S$  is storage heat flux. This equation refers to a representative urban volume that extends from of the surface in which there is no net horizontal transfer (that is, an extensive surface type) and no significant energy exchange across the lower boundary. Hence, assessing each of the terms at the upper surface of the volume, which is located above the canopy layer captures the exchanges between the urban surface and overlying boundary layer. The process of urbanisation results in the replacement of natural surfaces by hard impervious surfaces (e.g. roads, pavements, car parks) and buildings. This greatly alters the surface energy balance by, for example, increasing (decreasing) the sensible (latent) heat flux and increasing heat storage. One of the best known outcomes is the formation of an urban heat island (Oke, 1980).

There are three approaches for UEB modelling: deriving empirically based models; modification of existing models designed for non-urban areas and; development of new models with urban specific conceptualisation and physics (Hidalgo et al., 2008). The latter two approaches simulate the urban effect by describing the urban landscape using parameterisations that can range from the very simple e.g. concrete slab approach used by Taha (1999) and Kusaka & Kimura (2004) to more complex schemes that take into account building dimensions, materials, and internal energy use, see for example, Mills (1997), Masson (2000), Martilli et al., (2002) and Kanda et al., (2005). Most of these describe urban areas by partitioning the surface into cells each of which has distinct properties related to aspects of urban form (e.g. fraction that is impervious) and function (e.g. anthropogenic heat flux). Evaluating and comparing these models has proved difficult owing to their distinct histories, which reflects different designs that have evolved in response to user needs and data requirements and availability. In fact, there has been a call for the standardisation of how parameters are gathered regardless of which model is being employed (Ching, 2013; Bechtel et al., 2015). This would greatly aid communication among researchers, allow for better comparisons between models and allow the transfer of models (and results) between cities.

Grimmond et al., (2010 & 2011) categorised 33 UEB models into simple, medium and complex based on 12 characteristics and compared their simulations against observations of the UEB made across a range of urban settings (see Table 3.1). In these tests, each UEB model had distinct merits such that no single model performed best or worst in comparisons; however broad conclusions emerged. First, those models that included information on building facades (that is the walls and roof) and on vegetation had smaller errors when simulating outgoing shortwave radiation ( $K_{\uparrow}$ ), net radiation ( $Q^*$ ) and the turbulent fluxes ( $Q_H$  and  $Q_E$ ). Second, providing additional data on building materials (such as detailed thermal properties and albedo)

did not necessarily improve the models performance; for simple models, a net improvement was often observed but this was not the case for complex models.

Table 3.1 Aspects of UEB models which are used for classification of model complexity. For example, in the case of criteria 1, "simple" would be associated with modelling only one or two fluxes, "complex" would be associated with modelling all fluxes

Criteria	Characteristic	Typical Treatment (Categories)	Levels of Complexity
1	Fluxes Included	All fluxes / individual fluxes	4
2	Vegetation	Separated / integrated	3
3	$Q_F$	Internal building / modelled	4
4	Temporal $\Delta Q_s$	Fixed / Variable	3
5	Urban Morphology	Single layer(s) / multiple	7
6	Facet / Orientation	Bulk / canyons	4
7	Reflections	Single / multiple / infinite	3
8	Albedo / Emissivity	Bulk / multiple facets	3
9	$\Delta Q_s$	Residual / conduction	3
10	Resistance	Single layer / multi-layer	3
11	Surface Temperature / Moisture	Bulk / Single / Multiple	4
12	Air Temperature / Moisture	Forcing height / single / multi-layer	3

In other work, Loridan et al. (2010) evaluated the single-layer urban climate model (SLUCM), as a component of the mesoscale Weather Forecasting Model (WRF) model, and found that data on vegetative cover was especially important for improved simulations. Similarly, Loridan & Grimmond (2012) using the same model found that using data that described the character of urban neighbourhoods where flux observations are made, rather than using generic urban data, had a marked effect; SLUCM was better able to reproduce the turbulent fluxes at 15 sites across the US, Mexico, Canada, Australia, Finland and Poland.

These studies provide a cautionary tale; while information on the nature of the urban surface is critical for UEB simulations, there is no guarantee that acquiring more detailed information will improve model performance. This has significant implications for the acquisition of urban data suited for a model as it can take a considerable amount of time but might yield little benefit. For example, UEB model evaluations consistently show the value of information on vegetation for simulating the turbulent fluxes but this does not mean that

obtaining information on the details of trees (e.g. species, age, health, etc.) will make a difference to simulations. This is important as, from a planning and design perspective, city greening initiatives are a major component of climate-based policies and any UEB model chosen must be able to assess the impact of modifying vegetation cover/type (Breuste, 2004). However, it will be important to know what sort of data is needed, as this will guide the type of modelling exercise and help in interpreting the results. Practically then the challenge is to acquire urban data at a sufficient scale and detail to run a validated model suited for a purpose.

For many purposes, it may be possible that model ‘look-up’ Tables that link urban landscape types to typical climate-relevant parameters could address the lack of land-cover information. The Local Climate Zone (LCZ) classification scheme for example, partitions the landscape into 10 urban and 7 non-urban classes, permits mixed categories and allows seasonality to be taken into account (see Table 3.2; Stewart & Oke, 2012). The advantages of this approach include: LCZ types are purported to be universal in their depiction of landscapes and their climate impacts; it is relatively easy to categorise urban neighbourhoods into an LCZ type from fieldwork and readily available sources (e.g. GoogleEarth) and; each LCZ type is associated with a typical range of parameter values that describe surface cover, building heights and street aspect ratio, etc. (Table 3.2). The scheme has been applied most to the study of the Urban Heat Island (UHI), for which it was developed— see Fenner et al., (2014), Leconte et al., (2014), and Stewart et al., (2014). As an example, Figure 3.1 shows the LCZ map of Dublin, which was generated for an urban heat island study using available land-cover data, remote sensing and fieldwork (Alexander & Mills, 2014).

**Table 3.2 Outline of Local Climate Zone Classes and their properties (modified from Stewart and Oke, 2012). Those that are asterisked are present in the Dublin study area**

Local climate zone (LCZ)	Building surface fraction (%)	Impervious surface fraction	Pervious surface fraction	Height of roughness elements (m)
Compact high-rise	40–60	40–60	<10	>25
*Compact midrise	40–70	30–50	<20	10–25
*Compact low-rise	40–70	20–50	<30	3–10
Open high-rise	20–40	30–40	30–40	>25
*Open midrise	20–40	30–50	20–40	10–25
*Open low-rise	20–40	20–50	30–60	3–10
Lightweight low-rise	60–90	<20	<30	2–4
*Large low-rise	30–50	40–50	<20	3–10
Sparsely built	10–20	<20	60–80	3–10
*Heavy industry	20–30	20–40	40–50	5–15
*Dense trees	<10	<10	>90	3–30
Scattered trees	<10	<10	>90	3–15
Bush, scrub	<10	<10	>90	<2
*Low plants	<10	<10	>90	<1
*Bare rock or paved	<10	>90	<10	<0.25
Bare soil or sand	<10	<10	>90	<0.25
*Water	<10	<10	>90	–

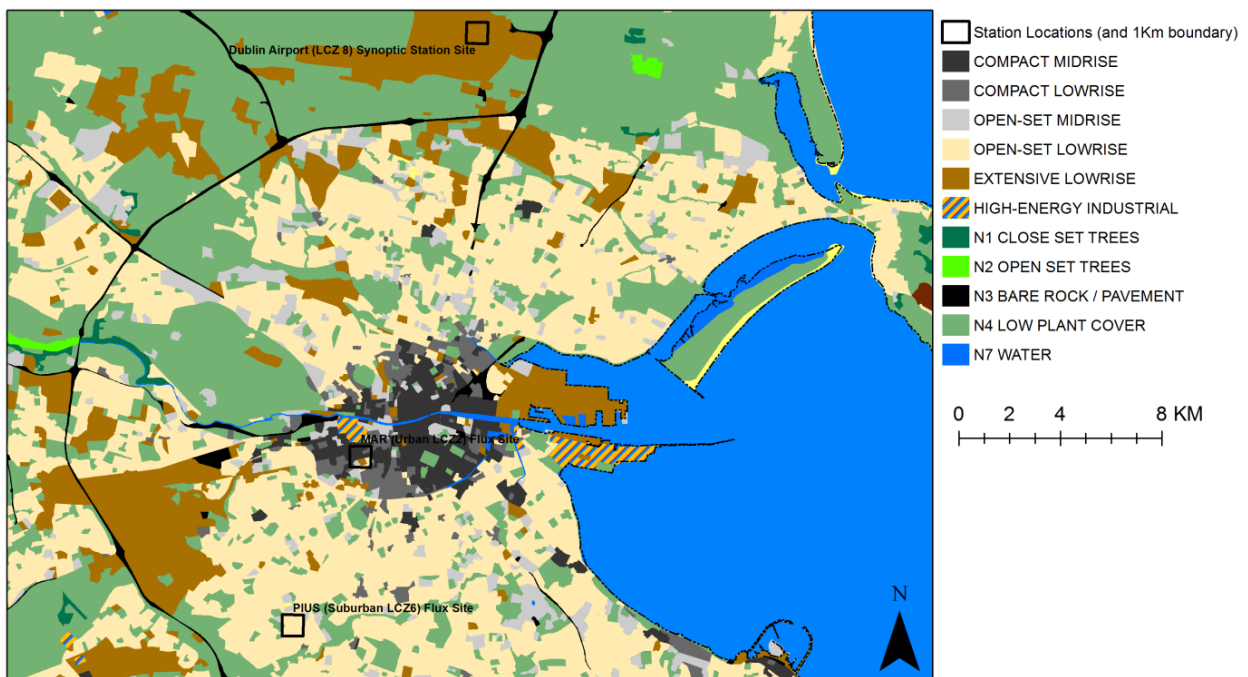


**Figure 3.1 LCZ Map of Dublin also shown are flux site locations and synoptic station location with 1 km grid which represents extent of area used to calculate surface fractions (Modified from Alexander & Mills, 2014)**

### 3.5 Methodology

In this work we examine the quality of the input data needed to run a moderately complex UEB model satisfactorily. Our examination is based on data gathered for Dublin,

Ireland (53° N, 6° W), which has a mild, mid-latitude climate (Cfb). It provides an ideal place for this study as it has two observation sites (located in urban and suburban neighbourhoods) where detailed energy flux and meteorological observations have been made since 2009; these data can be used to run the model and compare its simulations with observations. In addition: there is a LCZ description of the city that outlines major neighbourhood types and; a WMO standard weather station at Dublin Airport, which is 5-10 km distant from the flux sites, records hourly observations.

The Surface Urban Energy and Water Balance Scheme (SUEWS v.2013b) is used to simulate the UEB (Eqn. 3.1) of both neighbourhoods. SUEWS requires a relatively low number of input parameters that may include: meteorological data; socio-economic-demographic data and; surface cover and urban structure data. Some of these inputs are required to run the model, while other inputs are optional. At the very least the model requires standard meteorological data and details on the fractions of the landscape that is occupied by buildings, vegetation, impervious paving, etc. The challenges of operational employment of the earlier stages of model have been documented (Cleugh et al., 2005) and include the parameterisation schemes themselves along with acquiring the necessary forcing data.

Järvi et al. (2011) evaluated SUEWS using flux observations (spanning various time lengths from different years) from sites in Los Angeles (34°N, Köppen climate type, Csb) and Vancouver (49°N, Cfb). The results showed the model to be capable of simulating net radiation, sensible and latent and heat fluxes with RMSE ranges of 25-47 W m<sup>-2</sup>, 30-64 W m<sup>-2</sup> and 20-56 W m<sup>-2</sup>, respectively. Moreover, while the model reproduced the diurnal cycle of the turbulent fluxes, it tends to underestimate  $Q_E$  and overestimate  $Q_H$  in the day time. Here, we compare SUEWS model output with energy flux observations at two flux sites. The initial model runs use detailed site-specific meteorological and land-cover data. Subsequently, SUEWS is run using meteorological data from Dublin Airport and land-cover data representative of the LCZ

type in which each flux site is located. In the following Sections we describe the SUEWS model, the meteorological/flux data and the urban land-cover data used in this study. We then outline the structure of the experiment.

### 3.5.1 SUEWS

SUEWS was designed for urban simulations at a neighbourhood-scale, which corresponds to an area of approximately 1 km<sup>2</sup>. It simulates both the urban energy budget (Eqn. 3.1) and water budget,

$$P + I_e + F = E + R + \Delta S \quad mm \ h^{-1} \quad \text{Eqn.3.2}$$

Where P is precipitation, I<sub>e</sub> is externally piped water, F is anthropogenic water emission, E is evaporation (including transpiration) R is runoff and ΔS is change in storage. Eqns. 3.1 and 3.2 are connected directly through the evaporative terms (Q<sub>E</sub> and E) and indirectly via other terms; for example, a precipitation event may result in water storage in soil that will affect its thermal properties. The energy budget, eqn 3.1, which is the focus of this paper describes flux exchanges at a plane that separates the roughness sub-layer (between 2 to 4 times the mean height of the roughness elements) from the remainder of the boundary-layer. The modelled fluxes therefore correspond to the inertial sub-layer, where micro-scale variability driven by individual roughness elements becomes integrated into neighbourhood signals. Moreover, one should note the absence of advective terms in eqn 3.1, so that it assumes there is a negligible horizontal energy transfer. strictly speaking then, this limits the application of SUEWS to extensive neighbourhood types where the landscape may be described as relatively homogenous (Middel et al., 2012). The absence of detailed accounting for radiative transfer within the canyons below the simulated level should also be noted.

The data inputs employed by the model are listed in Table 3.3 and include hourly meteorological data, land cover parameters and anthropogenic fluxes. SUEWS describes the milieu of different surface types in a neighbourhood in terms of fractional coverage (λ) of

buildings, pavements, water, vegetated areas (both irrigated and non-irrigated) and trees (coniferous and deciduous) and unmanaged land cover such as bare soils or rock. Anthropogenic water and energy use can also be provided; hourly water use can be expressed as a proportion of the daily total and hourly anthropogenic heat fluxes can be estimated from typical daily patterns, divided into weekday and weekend values.

**Table 3.3 Summary of inputs required to run SUEWS model**

<b>Variable</b>	<b>Units</b>	<b>Comments</b>
<b><i>Meteorological</i></b>		
Air Temperature (T)	°C	
Relative Humidity (RH)	%	
Pressure (Pr)	kPa	
Precipitation (P)	mm h <sup>-1</sup>	
Wind speed (V)	m s <sup>-1</sup>	
Incoming short wave (K↓)	W m <sup>-2</sup>	
Incoming long wave (L↓)	W m <sup>-2</sup>	Optional (otherwise uses T and RH)
Observed Sensible Heat (Q <sub>H</sub> )	W m <sup>-2</sup>	Optional
Observed Latent Heat (Q <sub>E</sub> )	W m <sup>-2</sup>	Optional
Observed Storage Heat (ΔQ <sub>S</sub> )	W m <sup>-2</sup>	Optional
Cloud Fraction	Tenths	Optional
Soil moisture deficit	m <sup>3</sup> m <sup>-3</sup>	Optional
Leaf Area Index (LAI)		Optional
<b><i>Anthropogenic Inputs</i></b>		
Anthropogenic Heat (Q <sub>F</sub> )	W m <sup>-2</sup>	Optional, hourly values (otherwise modelled)
Anthropogenic Water Use	%	Optional, hourly ratio of total diurnal usage
<b><i>Surface Inputs</i></b>		
Fractional Coverage of Surface types (λ)	%	Urban, Pavement, Soil, Grass (irrigated and un-irrigated), Trees (coniferous and deciduous) Water
Surface Area	Ha	
Water Usage Area	Ha	Optional
Latitude / Longitude	°	
Storage Capacity of Pipes	mm	Optional
Frontal area fractions		Optional, buildings and trees separate
Roughness Length for momentum (z <sub>0</sub> )	m	Optional
Zero displacement height (z <sub>d</sub> )	m	Optional
Surface Element Heights	m	Optional, buildings and trees separate

### 3.5.2 Meteorological and energy flux data

The atmospheric observations used here are of two types. The first is standard meteorological information obtained from Dublin airport, which is located 5 km from the city centre in an area dominated by warehouses (Figure 3.1). Hourly observations are available for a number of elements: air temperature (T), precipitation (P), pressure (Pr), humidity (RH),

wind-speed ( $V$ ) and direction and solar radiation received ( $K_{\downarrow}$ ). Note that hourly values for  $K_{\downarrow}$  are a required model input.

The second is meteorological and energy flux data that is acquired at two stations (Figure 3.1) that are part of the International Urban Flux Network (Keogh et al., 2012). The measurement sites were selected to represent sites that typify Dublin’s urban land-cover. Each has an identical suite of instruments (see Table 3.4) and radiation and turbulent flux terms are recorded alongside the meteorological variables listed above. The suburban site is located in a residential area consisting of similar two-story houses about 6 m tall and much of the landcover is vegetated (open low-rise or LCZ6). The instruments are positioned on a mast that is located on the roof of a school at a height of 12 m (10 m for the net radiometer). The urban site is located in a mixed-use area closer to the city centre; much of the surrounding landscape is impermeable and the average building height is about 8 m (compact midrise or LCZ2). The support mast is on the roof of a 12 m tall building and the instruments are at a height of 17 m (15 m for net radiometer).

**Table 3.4 A list of the energy budget and meteorological variables and the instruments used at each site; the height of the instruments at urban and suburban sites respectively is shown in the parentheses. The final column lists the equivalent SUEWS parameters (Table 3.3).**

Variable	Instrument	SUEWS parameter
Radiation	Net radiation sensor (15/11) Hukseflux NR01	$K_{\downarrow}$ , $K_{\uparrow}$ , $L_{\downarrow}$ , $L_{\uparrow}$
3D wind velocity	Sonic anemometer (17/12) Campbell Scientific CSAT3	$V$ , $Q_H$ , $Q_E$
Water vapour density	InfraRed Gas Analyser (17/12) Licor Sciences LI-7500	$Q_E$
Air temperature and relative humidity	Temperature and relative humidity probe (17/12) Vaisala HMP45C	$T$ , $RH$

Upward and downward facing radiometers provide  $K_{\downarrow}$ ,  $K_{\uparrow}$ ,  $L_{\downarrow}$  and  $L_{\uparrow}$ . The turbulent fluxes  $Q_H$  and  $Q_E$  heat are obtained using an open-path eddy covariance system that is

interrogated at a rate of 10Hz; the recorded fluxes are based on 30 minute averages. These data are then corrected following Webb et al. (1980), which results in increasing  $Q_E$  and decreasing  $Q_H$  and somewhat reducing the residual. The heat storage term ( $\Delta Q_S$ ) is then estimated as a residual of the measured terms,

$$\Delta Q_S \approx Q^* - (Q_H + Q_E) \quad W m^{-2} \quad \text{Eqn.3.3}$$

Thus,  $\Delta Q_S$  includes any errors associated with the estimation of the other fluxes. Also, while the anthropogenic heat flux ( $Q_F$ ) is not distinguishable in the observations, it is present in all the measured terms.

Each tower is located well within its LCZ type and the flux instruments are positioned at a level that is approximately twice the height of the surrounding buildings and at about the height of the inertial sub-layer established by that surface type. In other words, we are assuming that advection is negligible and that  $\Delta Q_A$  can be ignored. Finally, it is also assumed that the *makeup* of source regions for the radiation ( $K\uparrow$  and  $L\uparrow$ ) and the turbulent ( $Q_H$  and  $Q_E$ ) fluxes are similar even though the source for the former is fixed and that for the latter changes with wind direction and stability (Oke 2006). In practice, this means that observations of  $K\uparrow$  and  $L\uparrow$  are strongly dependent on the surfaces directly below the sensors. In the case of the suburban site, which is located in the grounds of a small school, the underlying surface consists mostly of a dark roof surface and asphalt car park so that these terms are less likely to be representative of the open low-rise suburban setting than the turbulent terms.

For both data types, observations for the period April 08 – October 18 2010 were used. Both the winter period 2009 (i.e. November 2009 – January 2010) and 2010 (November 2010 – January 2011) saw atypical synoptic conditions, specifically widespread snow/ice was present across both Ireland and the UK for most of the period. This resulted in restricted access to on-site data loggers at the flux locations. As such, the period of observations utilised represents a contiguous period of observations without significant data gaps.

### 3.5.3 Urban land-cover parameters

The required urban land-cover fractions ( $\lambda$ , see Table 3.5) were derived using GoogleEarth. Values of  $\lambda$  were calculated for a 1 km<sup>2</sup> area around each flux site by digitizing polygons representing roads, buildings and vegetated surfaces and points to represent trees. The total tree canopy coverage was estimated based on the average canopy size for trees in Dublin (Ningal et al., 2011). All trees were classified as deciduous. The total area coverages of buildings, pavements, water, vegetated areas, trees and unmanaged land were computed and then converted to fraction values ( $\lambda$ ) for each site.

**Table 3.5 Local climate zones (LCZ) in Dublin city with estimated plan area fractions ( $\lambda$ ). These were computed by taking the average of n randomly sampled areas (1 km<sup>2</sup> in size) within each LCZ type. The equivalent fractions calculated for the area around the urban and suburban observation sites are listed in the final two rows.**

LCZ	Built	Impervious	Unmanaged	Trees	Grass	Water	(n)
2 Compact Mid	33	55	00	06	06	00	5
3 Compact Low	22	61	00	07	10	00	5
5 Open Mid	13	48	00	11	28	00	5
6 Open Low	14	52	00	11	23	00	10
8 Large Low	30	61	00	04	05	00	5
10 Industrial	16	69	00	08	07	00	5
101 Close Trees	01	02	04	48	45	00	5
104 Low Plant	03	08	03	18	67	00	10
105 Bare Rock	09	49	00	14	29	00	2
106 Bare Sand	06	20	55	19	00	00	1
107 Water	00	00	00	00	00	100	---
Urban site (LCZ2)	33	66	00	00	00	00	---
Suburban site(LCZ6)	18	48	00	05	29	00	---

The LCZ scheme also provides a range of  $\lambda$  values for each of the 17 types (Table 3.2) and for the Dublin study area, 11 of these types are present (Figure 3.1). Fractional areas were calculated for each of these by random sampling from within each type; the size of sample varied in proportion to the area that that LCZ type occupied in the city. Thus for example, we sampled at 10 locations within the large suburban swath around the city centre (Open low-rise type, LCZ 6) and at 5 places in the more densely built city centre (Compact mid-rise, LCZ 2).

None of the sampled places correspond with the observation site calculations. We treated the LCZ impervious fraction as pavement surface type in SUEWS. The final  $\lambda$  values calculated for each LCZ is the average of the sampled sites (Table 3.5); a comparison with the LCZ ranges presented in Table 3.2 is provided in the last two rows.

### 3.5.4 Model Experiment

SUEWS is run in four modes, which are used to represent optimal and suboptimal modes:

Mode	Land cover	Meteorological forcing	Description	Pairing
1	High-Resolution	Flux sites	Optimal situation that uses meteorological data and land-cover parameters for the observation sites	Modes 2 & 4
2	High-Resolution	Off-site standard weather station	Suboptimal as it uses meteorological data from a standard weather station to represent the city	Modes 1 & 3
3	LCZ	Off-site standard weather station	Suboptimal as it uses meteorological data from a standard weather station and land-cover parameters estimated for the larger LCZ neighbourhood type in which the sites are situated	Modes 4 & 2
4	LCZ	Flux sites	Suboptimal as it uses LCZ land cover parameters and $L_{\downarrow}$ is derived from T and RH (Loridan et. al, 2011)	Modes 3 & 1

Simulations were completed for the period April 08- October 18 2010 (that is, Julian dates 98 through 291), which corresponds with the period for which daily observations of  $Q^*$ ,  $Q_H$ ,  $Q_E$  and  $\Delta Q_S$  are available for both flux sites. Our comparison between different Modes is based on the hourly values and on the average diurnal (daily) profiles calculated for each month. The anthropogenic heat and water fluxes options in SUEWS are not implemented here; this is reasonable in the Irish climate which is mild and wet and the contributions of traffic is likely to be small (perhaps  $\leq 20 \text{ W m}^{-2}$  using Pigeon et al. (2007) as a guide).

At the start of the period (April) the soil moisture status in SUEWS is set at field capacity (150 mm). The recorded precipitation at stations around Dublin in March, 2010 was about 55 mm which represented 110% of the average for that month and resulted in wide spread localised flooding toward the end of the month. At agricultural meteorological stations proximate to Dublin, soil moisture deficit (SMD) was reported at -10mm (surplus) at stations. The spring period (February-April) of 2010 was especially cold so it might be expected that vegetation growth was inhibited, even in the city. To account for this, the Leaf Area Index (LAI) at the beginning of April was obtained from MODerate Resolution Imaging Spectroradiometer (MODIS) data (MOD-15), which are available at 1 km<sup>2</sup> resolution at 8-day intervals.

### 3.5.5 Model Evaluation and Sensitivity

The performance of SUEWS run in each of the Modes listed above is evaluated against the observations at the urban and suburban flux sites. A measure of the goodness of fit for each modelled term is provided by the RMSE,

$$\text{RMSE} = \left[ \sum_{i=1}^n \frac{(\hat{y}_i - y_i)^2}{n} \right]^{0.5} \quad \text{Eqn. 3.4}$$

Where  $(\hat{y}_i - y_i)$  represents the difference between the observed ( $y$ ) and simulated ( $\hat{y}$ ) flux term (e.g.  $Q^*$ ) at each hourly time interval ( $i$ );  $N$  represents the total number of hours. RMSE is commonly used to assess the total error, regardless of its direction. To measure any bias in the simulations the Mean Fractional Bias (MFB) is used,

$$\text{MFB} = \frac{1}{n} \sum_{i=1}^n \frac{(\hat{y}_i - y_i)}{(\hat{y}_i + y_i)/2} \quad \text{Eqn. 3.5}$$

Where all terms have the same meaning as in the RMSE; this statistic produces a value between -2 and +2 where the sign indicates over (+) or under (-) estimates. Additionally, to examine the relative performance across all months between each Mode we generated Taylor

diagrams for each of the simulated flux terms which employ three statistics: the centred RMSE ( $E'$ ), the correlation coefficient ( $R$ ), and the standard deviation ( $\sigma$ ) (Taylor, 2001).:

$$E' = \frac{1}{N} \sum_{i=1}^N [(\hat{y}_i - \bar{\hat{y}}) - (y_i - \bar{y})]^2 \quad \text{Eqn. 3.6}$$

$$R = \frac{\frac{1}{N} \sum_{i=1}^N (\hat{y}_i - \bar{\hat{y}})(y_i - \bar{y})}{\sigma_{\hat{y}} \sigma_y} \quad \text{Eqn. 3.7}$$

where  $\sigma_{\hat{y}}$  and  $\sigma_y$  are the standard deviations of the model and observed variable, respectively. The other terms are the same as eqn 3.4 and resulting values are in  $\text{W m}^{-2}$  with the exception of eqns 3.5 and 3.7. For the period of examination, there are a total 4656 hourly values (194 days) of observed ( $y$ ) and simulated ( $\hat{y}$ ) values for each model run for each site.

To test the sensitivity of SUEWS to differences in meteorological forcing data (for example differences which might arise between off-site and on-site stations) we employed a one-factor-a-time (OFAT) approach (Griensven et al., 2002). First, we generated highly typified data i.e. data derived from a loess curve for a 168-hour period for each required meteorological variable (see Table 3.3). We excluded precipitation from these data. To test SUEWS sensitivity to  $K_{\downarrow}$ , T/RH and V we perturbed these data  $\pm 10\%$  of the mean state in order to examine the impact on modelled turbulent fluxes ( $\Delta Q_S$ ,  $Q_H$  and  $Q_E$ ). For the purpose of our OFAT analysis we distributed land cover evenly across all land cover types (excluding water), meaning differences in our simulations of  $\Delta Q_S$ ,  $Q_H$  and  $Q_E$  between each perturbation would arise due to the modification of forcing data.

### 3.6 Results

In the following Section the *relative* performance of SUEWS in each Mode is examined by comparing simulated and observed fluxes at each site. Initially, the diurnal performance of SUEWS when run in different Modes is examined based on the hourly simulations for the

month of June. In this Section we also present the differences between our forcing data sites. Subsequently, the overall performance of the model based on daily outcomes is presented followed by an examination of the impact of modifying: the land cover and meteorological forcing data.

### *3.6.1 Hourly fluxes comparison - June 2010*

The meteorological forcing data available for the Dublin Airport (A) site and that available for the urban and suburban sites in June are shown in Table 3.6 and Table 3.7. Rainfall was recorded on 9 days in June and with two exceptions, all stations recorded rainfall on corresponding days. The total amount of rainfall recorded at the Airport was 53.6 mm (Table 3.6), which was higher and lower than that recorded at the urban and suburban sites, respectively; this is not surprising given the non-standard exposure of the gauges at the flux sites. Recorded wind-speed at the Airport averaged  $2.17 \text{ ms}^{-1}$ , which was lower than that measured over the ‘rougher’ urban surface at both sites, which may be surprising but mean wind-speed was lower than normal in June 2010 owing to the dominance of high pressure ( $\sim 1018 \text{ hPa}$  for the month). The difference between the sites is clearest when air temperature and solar radiation observations are compared (Table 3.7): T at the Airport is consistently lower than values in the city, especially at night and;  $K_{\downarrow}$  is higher on average especially in the morning hours. These differences are probably influenced by the local climate at the Airport, which is closer to the coast and may be affected by an afternoon sea-breeze in generally calm conditions. These types of differences might be expected of any station located ‘near’ the site of interest but subject to its own local influences; as such, using the observations from a WMO synoptic station (that might be expected to record the background climate) to force SUEWS is a good test of its robustness.

**Table 3.6 Daily rainfall receipt at Dublin Airport (RA) and the difference recorded at the urban ( $DR_{A-U}$ ) and suburban ( $DR_{A-S}$ ) flux sites**

Day	RA (mm)	$DR_{A-U}$	$DR_{A-S}$
Jun-01	14.2	-6.2	-8.2
Jun-07	7.8	-1.8	-6.2
Jun-08	15.2	7.4	0.6
Jun-09	1	-0.6	-0.6
Jun-10	0.2	0	0.2
Jun-14	11.8	5.6	1.4
Jun-27	2.7	1.7	1.1
Jun-28	0	-1.6	-0.2
Jun-29	0.7	0.7	0.5
Total	53.6	5.2	-11.4

The hourly observed and simulated fluxes for June 2010 for both sites are presented in Figure 3.2. The diurnal cycle at the urban site shows that most of the available energy ( $Q^*$ ) is partitioned into sensible heat, either as storage in the fabric ( $\Delta Q_S$ ) or as turbulent exchange with the atmosphere ( $Q_H$ ); relatively little is expended as evaporation ( $Q_E$ ), about 10% ( $25 \text{ W m}^{-2}$ ) of  $Q^*$  around noon. Before mid-day it is  $\Delta Q_S$  that dominates but  $Q_H$  is the largest non-radiative flux after noon. At the suburban site, the same basic pattern is present but  $Q_E$  is larger, reaching values of  $60 \text{ W m}^{-2}$  in early afternoon about one-third the magnitude of  $Q_H$ . The difference in patterns between the sites reflects their respective vegetated fractions.

Overall, SUEWS reproduces the diurnal cycle and shows good agreement with the observations at both locations, even when the model is run using standard meteorological data and urban parameters derived from the LCZ dataset, rather than the site specific data (Mode 3). Table 3.8 summarises the relative differences in hourly RMSE and MFB in terms of changing the land cover and meteorological forcing data. The run with optimal model inputs (Mode 1) uses measured values of  $K_{\downarrow}$  and  $L_{\downarrow}$  are provided by the observation platforms so not surprisingly  $Q^*$  is simulated closely at both sites ( $\text{RMSE} \approx 10 \text{ W m}^{-2}$  with little bias).

**Table 3.7 Mean hourly wind speed ( $V_A$ ), air temperature ( $T_A$ ), and shortwave radiation receipt ( $K_{\downarrow A}$ ) at Dublin Airport and the differences (D) recorded at the urban (u) and suburban (s) flux sites**

Hour	$V_A$	$DV_{A-U}$	$DV_{A-S}$	$T_A$	$DT_{A-U}$	$DT_{A-S}$	$K_{\downarrow A}$	$DK_{\downarrow A-U}$	$DK_{\downarrow A-S}$
0	1.7	-0.4	-0.5	11.37	-4.43	-5.03	0	0	0
1	1.83	-0.31	-0.39	11.2	-4.15	-4.63	0	0	0
2	1.81	-0.29	-0.4	10.7	-4.15	-4.7	0	0	0
3	1.84	-0.33	-0.42	10.46	-4.02	-4.81	0	0	0
4	1.74	-0.25	-0.54	10.61	-3.75	-4.79	2.1	1.7	1.7
5	1.63	-0.35	-0.5	11.32	-3.15	-4.36	38.7	11.6	7.8
6	1.82	-0.18	-0.48	12.36	-2.49	-3.94	108.8	20.7	12.7
7	2.05	-0.21	-0.62	13.59	-1.96	-3.15	194.9	30.1	9.1
8	2.25	-0.33	-0.62	14.58	-1.86	-2.7	311.6	43.1	9.8
9	2.35	-0.42	-0.83	15.35	-1.48	-2.45	385.6	22.4	-3.5
10	2.43	-0.54	-0.76	16.2	-1.3	-2.1	487.4	-2.6	20.78
11	2.49	-0.46	-0.78	16.71	-1.3	-1.83	569.1	60.5	37.8
12	2.57	-0.49	-0.82	17.03	-1.44	-1.84	546.9	32.2	57.9
13	2.58	-0.83	-1.06	17.47	-1.3	-1.53	559.4	27.6	43.8
14	2.55	-0.83	-1.3	17.63	-1.35	-1.59	524.4	-6.7	12.8
15	2.59	-0.79	-1.29	17.73	-1.56	-1.55	460.3	-29.1	28.9
16	2.69	-0.72	-1.17	17.8	-1.56	-1.6	388.2	-30.9	-21.3
17	2.58	-0.69	-1.28	17.64	-1.72	-1.74	332.4	-7.7	-1.7
18	2.45	-0.66	-1.07	17.2	-2.18	-2.12	229.1	-4	-17
19	2.38	-0.52	-0.94	16.62	-2.54	-2.49	116.8	-16.2	-12.1
20	2.13	-0.42	-0.75	15.61	-3.22	-3.16	40.1	-4.1	-4.8
21	1.92	-0.22	-0.58	14.21	-4.1	-3.94	1.9	-1.1	-1
22	1.86	-0.37	-0.53	13.07	-4.17	-4.46	0	0	0
23	1.73	-0.38	-0.51	12.34	-4.28	-4.56	0	0	0
Mean	2.17	-0.46	-0.76	14.53	-2.64	-3.13	220.7	6.1	7.6
St. Dev	0.98	0.79	0.87	3.6	1.64	1.97	255.5	94.6	76.9
Skewness	0.18	-0.15	0.64	-0.18	-0.66	-1.05	1	0.2	1.08
Median	2.22	-0.44	-0.79	14.6	-2.4	-2.77	107	0	0
Quartile 25	1.39	-0.93	-1.28	12	-3.5	-3.8	0	-9.1	-9.5
Quartile 75	2.78	0.01	-0.27	17.4	-1.5	-1.98	378.5	21.8	14.6

The error for  $K_{\uparrow}$  is 3.5 and 20.2  $W m^{-2}$  at the urban and suburban sites, respectively. Noticeably the bias and error in the simulation at the suburban site (MFB=0.55) indicates persistent overestimation by SUEWS; this is not unexpected given the nature of the urban surface directly below the net radiometer at the suburban site discussed earlier, which results

in a lower albedo than expected. The RMSE values for  $L\uparrow$  are 30 and 20  $W m^{-2}$  at the urban and suburban sites but the MFB values are close to zero. The errors in the non-radiative terms are 15 (19), 15 (17), 31 (27)  $W m^{-2}$  for  $Q_H$ ,  $Q_E$  and  $\Delta Q_S$ , respectively for the urban and suburban sites (the latter in parentheses). The  $Q_E$  term is overestimated at both sites (more so at the urban site where little evaporation was measured) but the overestimate in  $\Delta Q_S$  at the suburban site is a distinguishable feature.

**Table 3.8 Root mean square error (RMSE) and Mean fractional bias (MFB) and bias direction change for each energy budget term based on hourly fluxes for June 2010. The top is urban (LCZ 2 site) bottom is suburban (LCZ 6 site). RMSE values are in  $W m^{-2}$ . Negative values denote a reduction in RMSE (i.e. model improvement) whereas positive values denote an increase in RMSE. Negative values in MFB denote a decrease in absolute bias, positive denotes an increase in absolute bias. MFB directional changes denote if the model switches (>) from over (+) to under (-) prediction or if the direction of the bias remains the same (=)**

Degrading Meteorological forcing				Degrading land cover		
LCZ 2						
	RMSE	MFB	MFB direction	RMSE	MFB	MFB direction
$Q^*$	16.5	0.17	=	-0.9	-0.01	=
$K\downarrow$	---	---		0	0	=
$K\uparrow$	3	0.03	=	2.2	0.06	=
$L\downarrow$	---	---		0	0	=
$L\uparrow$	-11.7	-0.03	=	-0.1	0	=
$\Delta Q_S$	-3.5	0.26	->+	-6	-0.13	=
$Q_H$	6.1	0.09	=	-1.2	-0.01	=
$Q_E$	-0.3	-0.15	=	-5.6	0.72	=
LCZ 6						
$Q^*$	9.7	0.14	->+	-1.7	-0.01	=
$K\downarrow$	---	---		0	0	=
$K\uparrow$	4.7	0.02	=	-1.5	-0.02	=
$L\downarrow$	---	---		0	0	=
$L\uparrow$	3.5	-0.03	=	-0.2	0	=
$\Delta Q_S$	-4.1	0.28	->+	2.5	-0.02	=
$Q_H$	4.4	0.2	->+	-2.3	-0.01	=
$Q_E$	-4.5	-0.14	=	0.1	0	=

Running SUEWS in Mode 2 changes the source of meteorological input data, which are no longer collected *in situ* with the non-radiative flux terms. In addition,  $L\downarrow$  is now estimated from temperature and relative humidity (Loridan et al., 2011). The effect of these changes on the radiative terms is to introduce an error into  $K\downarrow$  of about 23 (25)  $W m^{-2}$  and into  $L\downarrow$  of about 7 (7)  $W m^{-2}$ , but no mean bias. The effect can be seen in the diurnal curve of  $Q^*$  (Figure 3.2b), which is lower in the daytime by about 20  $W m^{-2}$  near noon and higher at night-time (less

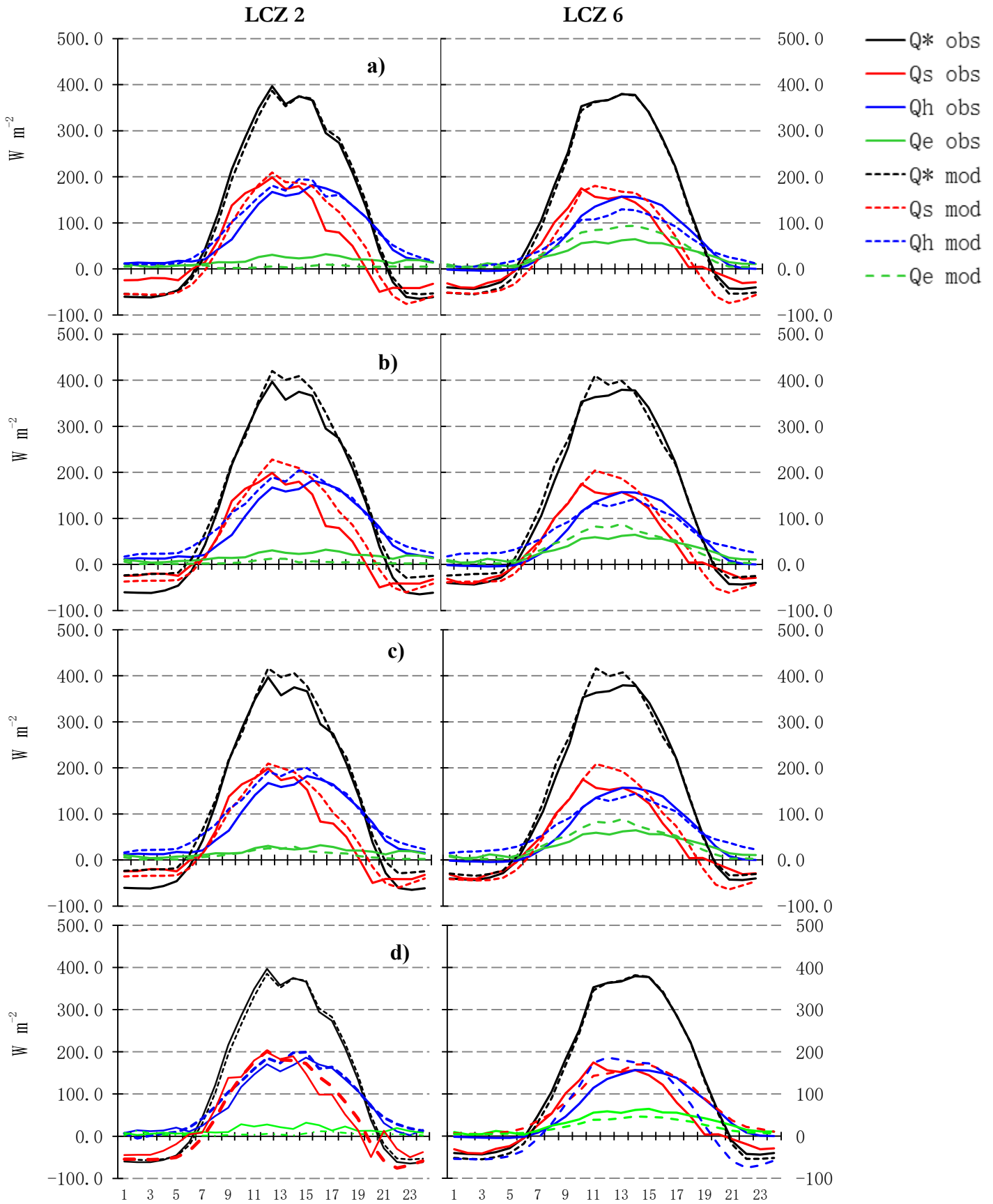


Figure 3.2 Average hourly energy fluxes (measured and simulated) in  $W m^{-2}$  for June 2010. The graphs on the left refer to the urban site and those on the right refer to the suburban site. The rows (a–d) show simulations when SUEWS is run in different modes (a: Flux Forcing (FF) with Site Specific (SS) land cover (Mode 1), b: Synoptic Forcing (SF) with SS land cover (Mode ..), c: SF with LCZ land cover d: FF with LCZ land cover). See text for details. X-axis is local time.

negative). However, change in RMSE is largest for  $Q^*$  at 15 (10)  $W m^{-2}$  but as  $Q^*$  is the largest component in the energy budget, this increase is not substantial. The patterns of the non-radiative terms are broadly consistent with the observations.

The changes in the hourly RMSE values for the non-radiative fluxes at both sites are not large ( $\pm 5 W m^{-2}$ );  $\Delta Q_S$  and  $Q_E$  are smaller but  $Q_H$  is larger. However, these changes do affect the bias; the MFB generally increases in magnitude and, in the case of  $Q_E$  at the urban site, the sign reverses. However, the magnitude of  $Q_E$  at this site is very small so it is especially sensitive. Running SUEWS in Mode 3 by using the typical LCZ values (given in Table 3.5) has a minor additional impact; RMSE values changed from between 2 and 6  $W m^{-2}$  at both sites. The additional error introduced to the non-radiative terms is relatively small, increasing RMSE values by about 6  $W m^{-2}$ .

Running the model in Mode 3 has little effect. Similarly, the difference between Mode 1 and 4 where the difference is in land cover representation utilising meteorology from the flux sites were negligible; at both sites the radiative RMSE difference was  $<1.0 W m^{-2}$  and difference in RMSE for the turbulent fluxes was  $<2.0 W m^{-2}$ .

Overall, the difference in the urban environments around each site is captured by the model; this is clearest in the  $Q_E$  differences between sites that correspond with their respective vegetated fractions. Most of the errors associated with using sub-optimum input data is associated with the use of off-site meteorological inputs that affected the incoming radiative terms ( $K_{\downarrow}$  and  $L_{\downarrow}$ ) most directly. However, the suburban site consistent overestimation of  $K_{\uparrow}$  suggests strongly that there is a discrepancy between the site-specific albedo and that of the neighbourhood generally. The diurnal and daily patterns of exchanges are simulated by SUEWS but there are obvious issues with simulating  $Q_E$  at both sites. The difference in running the model in Mode 2 and Mode 3 is small, which suggests that the use of off-site meteorological

input data is of greater significance than the use of the LCZ-based evaluation of urban land-cover.

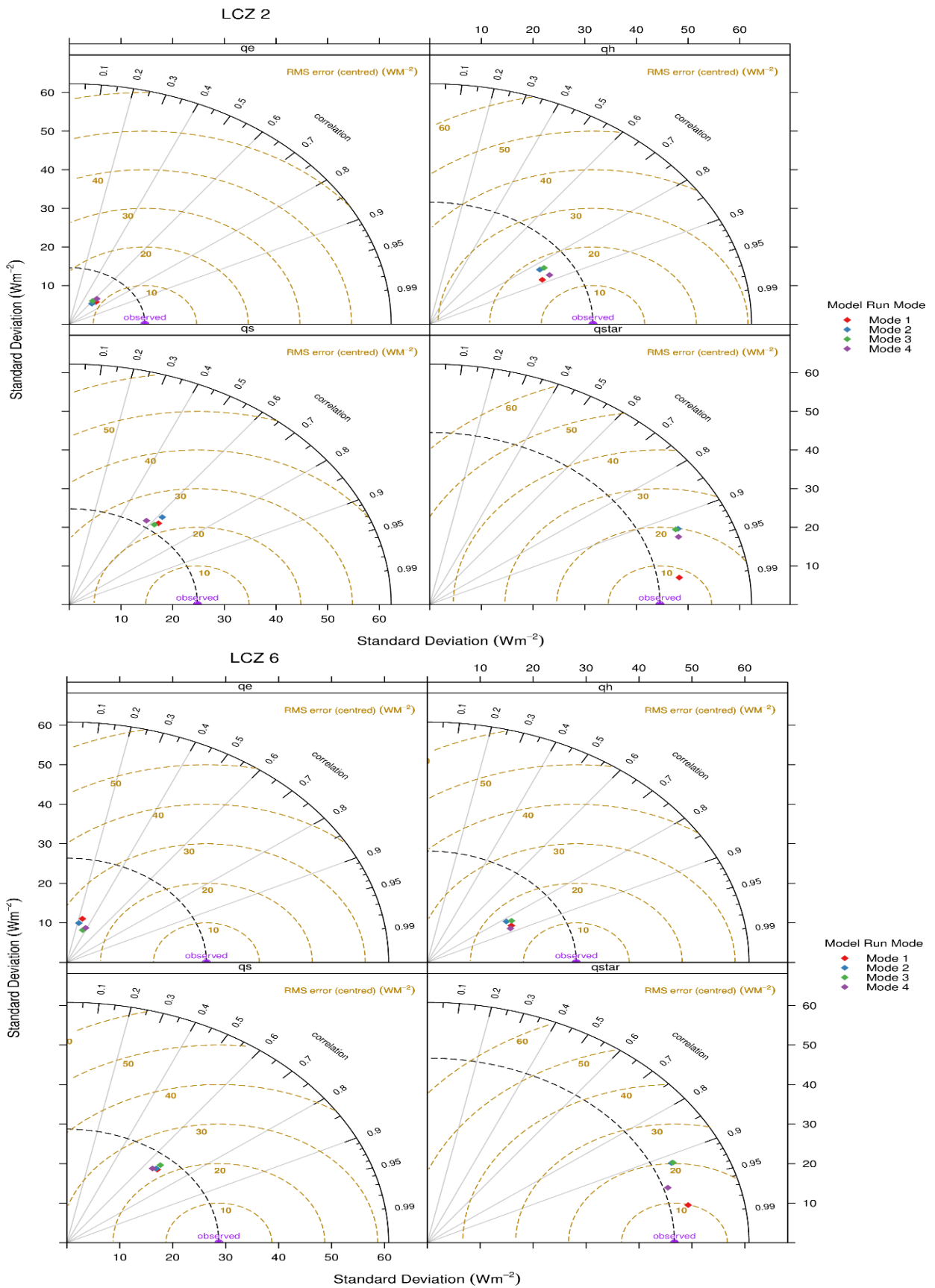
### 3.6.2 Daily fluxes comparison

Table 3.9 shows the average daily RMSE scores for each of the flux terms by month and by Mode for the urban and suburban observation sites. Thus, for example, for the entire period at the urban site, the average RMSE values for SUEWS run in Mode 1 are: 21.7 ( $\text{RMSE}_{Q^*}$ ); 25.3 ( $\text{RMSE}_{\Delta QS}$ ); 23.9 ( $\text{RMSE}_{QH}$ ) and; 16.7  $\text{W m}^{-2}$  ( $\text{RMSE}_{QE}$ ). The total ( $\Sigma_{\text{RMSE}}$ ) error (87.6  $\text{W m}^{-2}$ ) is the sum of the individual flux error terms and is a useful measure of overall model performance. For the optimal case (Mode 1) the  $\Sigma_{\text{RMSE}}$  for the urban site is 89.1  $\text{W m}^{-2}$  while that for the suburban site is 83.3  $\text{W m}^{-2}$ . The overall performance is also presented in Figure 3.3.

Changing the land-cover and meteorological data input data had little impact on the overall performance of the model. For the urban site,  $\Sigma_{\text{RMSE}}$  values are 90.3, 82.7 and 92.6  $\text{W m}^{-2}$  for Modes 2, 3 and 4, respectively. Similarly, for the suburban site, the differences compared to Mode 1 are all  $< 5.5 \text{ W m}^{-2}$ . The best performance (i.e. the lowest  $\Sigma_{\text{RMSE}}$ ) was found in Mode 1 for the LCZ 6 site and Mode 3 for the LCZ 2 site. The worst performance (highest  $\Sigma_{\text{RMSE}}$ ) was found in Mode 3 and Mode 4 for the LCZ 6 and LCZ 2 site respectively. The difference between the best and worst performances was 5.5  $\text{W m}^{-2}$  for the LCZ 6 site and approximately double this (9.9  $\text{W m}^{-2}$ ) for the LCZ 2 site. The range of RMSE across all fluxes was  $< 30 \text{ W m}^{-2}$  for the LCZ 2 site in all Modes and was  $< 40 \text{ W m}^{-2}$  for the LCZ 6 site in all modes.

**Table 3.9 Root mean square error (RMSE) values ( $W m^{-2}$ ) for each month based on daily values of all flux terms for each Mode (N = 744 per Mode) Mode 1 uses High-Resolution land cover (HRLC) and forcing data obtained at the flux sites, Mode 2 uses HRLC and forcing data obtained off-site by a standard weather station. Mode 3 uses LCZ derived land cover fractions and off-site forcing data Finally Mode 4 uses LCZ land cover and forcing data obtained at the flux sites.**

<b>Urban site (LCZ2)</b>																	
	Apr	May	Jun	Jul	Aug	Sep	Oct	MEAN		Apr	May	Jun	Jul	Aug	Sep	Oct	MEAN
Flux	Mode 1								Flux	Mode 2							
Q*	24.1	26.0	27.6	19.7	21.8	18.7	14.0	22.1	Q*	22.8	26.9	29.4	17.0	27.8	18.3	20.3	23.4
$\Delta Q_s$	18.7	34.1	28.2	35.1	25.6	16.4	19.1	26.0	$\Delta Q_s$	15.6	32.5	27.0	30.7	24.6	17.2	27.0	25.2
Q <sub>H</sub>	21.2	24.9	19.2	24.2	20.4	26.7	30.8	23.6	Q <sub>H</sub>	21.1	24.4	21.0	24.2	23.1	25.2	26.3	23.5
Q <sub>E</sub>	11.1	18.8	18.0	20.9	16.2	22.5	9.5	17.4	Q <sub>E</sub>	11.3	19.7	18.8	21.0	16.5	24.6	9.7	18.1
SUM	89.1								SUM	90.2							
	Mode 3									Mode 4							
Q*	21.8	25.9	28.0	16.5	26.9	17.7	20.1	22.6	Q*	36.7	33.4	31.0	28.8	26.2	25.0	21.1	29.1
$\Delta Q_s$	13.3	29.2	21.6	26.8	20.7	16.7	27.8	22.3	$\Delta Q_s$	20.0	32.5	24.7	34.2	22.8	17.2	28.5	25.8
Q <sub>H</sub>	21.3	24.5	20.6	23.1	22.5	23.8	25.7	23.0	Q <sub>H</sub>	26.8	27.7	19.2	24.9	21.3	26.1	26.6	24.5
Q <sub>E</sub>	8.5	16.6	14.6	16.3	12.7	22.3	8.6	14.8	Q <sub>E</sub>	7.8	15.9	13.5	16.6	12.2	19.7	8.0	13.9
SUM	82.7								SUM	92.6							
<b>Suburban site (LCZ6)</b>																	
	Apr	May	Jun	Jul	Aug	Sep	Oct	MEAN		Apr	May	Jun	Jul	Aug	Sep	Oct	MEAN
Flux	Mode 1								Flux	Mode 2							
Q*	18.5	21.5	17.8	14.7	14.3	13.4	5.9	15.6	Q*	15.5	21.9	26.7	23.8	19.1	15.2	13.6	19.9
$\Delta Q_s$	18.4	19.8	18.2	17.0	19.1	24.2	36.7	21.1	$\Delta Q_s$	23.8	23.3	22.2	20.3	17.7	25.3	35.1	23.2
Q <sub>H</sub>	15.1	25.2	16.5	23.0	16.6	30.3	30.9	22.2	Q <sub>H</sub>	11.9	21.1	17.3	19.9	16.0	28.2	30.5	20.4
Q <sub>E</sub>	13.9	15.0	17.8	30.8	21.4	42.7	28.1	24.3	Q <sub>E</sub>	11.3	14.1	17.1	28.2	22.9	45.3	28.7	24.1
SUM	83.3								SUM	87.6							
	Mode 3									Mode 4							
Q*	15.4	22.2	27.1	23.7	19.3	15.4	13.6	20.1	Q*	15.8	19.0	23.1	14.1	14.0	14.4	17.1	16.8
$\Delta Q_s$	22.6	22.7	22.1	20.4	17.8	25.2	34.8	23.0	$\Delta Q_s$	21.9	22.1	20.5	17.1	22.1	25.4	29.6	22.2
Q <sub>H</sub>	14.8	23.4	19.4	19.9	18.1	30.3	33.2	22.3	Q <sub>H</sub>	14.6	24.9	18.6	23.4	17.6	31.8	38.2	23.6
Q <sub>E</sub>	7.7	13.5	14.0	29.5	23.4	46.4	28.1	23.5	Q <sub>E</sub>	8.7	13.5	13.6	31.9	21.8	44.0	27.9	23.3
SUM	88.8								SUM	85.9							



**Figure 3.3 Taylor Diagrams for Mode 1-4 based on daily values of QE, QH,  $\Delta$ QS and Q\* for LCZ 2 (top) and LCZ 6 (bottom) Mode 1 uses High-Resolution land cover (HRLC) and forcing data obtained at the flux sites, Mode 2 uses HRLC and forcing data obtained off-site by a standard weather station. Mode 3 uses LCZ derived land cover fractions and off-site forcing data Finally Mode 4 uses LCZ land cover and forcing data obtained at the flux sites**

Examining the individual flux performance more closely looking firstly at  $Q^*$ ; the lowest mean RMSE value was  $22.1 \text{ W m}^{-2}$  for the LCZ 2 site in Mode 1 and  $15.6 \text{ W m}^{-2}$  for the LCZ 6 site, also in Mode 1. The highest mean RMSE value for  $Q^*$  was  $29.1 \text{ W m}^{-2}$  in Mode 4 for the LCZ 2 site and  $20.1 \text{ W m}^{-2}$  for the LCZ 6 site in Mode 3. Given the relatively large magnitude of this flux, this may be regarded as negligible. For the turbulent fluxes ( $Q_H$  and  $Q_E$ ), the lowest mean RMSE value for  $Q_H$  and  $Q_E$  (respectively) was  $23.0 \text{ W m}^{-2}$  (Mode 3) and  $13.9 \text{ W m}^{-2}$  (Mode 4) for the LCZ 2 site and  $20.4 \text{ W m}^{-2}$  (Mode 2) and  $23.6 \text{ W m}^{-2}$  (Mode 4) for the LCZ 6 site.  $\Delta Q_S$  mean RMSE ranged between a minimum of  $22.3 \text{ W m}^{-2}$  (in Mode 2) and maximum of  $26.0 \text{ W m}^{-2}$  (in Mode 1) for the LCZ 2 site and a minimum of  $21.1 \text{ W m}^{-2}$  (in Mode 1) and maximum of  $23.2 \text{ W m}^{-2}$  (in Mode 3) for the LCZ 6 site.

In general, the model was consistently biased (MFB) across all months and all Modes. The model exhibited a minor positive bias ( $< 0.5$ ) for both  $Q^*$  and  $Q_H$  for both sites in all Modes. For both sites,  $\Delta Q_S$  exhibited a strong negative bias ( $< -1.0$ ) in all Modes, whereas  $Q_E$  varied between a strong negative bias for the LCZ 2 site and a minor negative bias for the LCZ 6 site (see Table 3.10).

### *3.6.3 Impact of Meteorological Forcing Data on Performance*

Comparing model performance between Mode 1 to Mode 2 and Mode 4 to Mode 3 reveals an insight into the impact of meteorological forcing data when utilising the same quality of land cover information. This is summarised by Table 3.11. For the high-resolution land cover cases, utilising off-site meteorological data to force SUEWS decreased the performance (i.e. increase RMSE) of  $Q^*$  by  $1.5 \text{ W m}^{-2}$  for the LCZ 2 site and by  $4.2 \text{ W m}^{-2}$  for the LCZ 6 site.

**Table 3.10 Mean Fractional Bias (MFB) results for urban (LCZ2) site and suburban (LCZ6) site April-October. Mode 1 uses High-Resolution land cover (HRLC) and forcing data obtained at the flux sites, Mode 2 uses HRLC and forcing data obtained off-site by a standard weather station. Mode 3 uses LCZ derived land cover fractions and off-site forcing data Finally Mode 4 uses LCZ land cover and forcing data obtained at the flux sites**

Q*	LCZ2								LCZ6							
	apr	may	jun	jul	aug	sep	oct	Mean	apr	may	jun	jul	aug	sep	oct	Mean
Mode1	0.22	0.20	0.20	0.16	0.20	0.26	0.27	0.21	0.12	0.16	0.11	0.11	0.10	0.15	0.02	0.11
Mode2	0.18	0.13	0.17	0.05	0.16	0.15	0.02	0.12	-0.03	0.04	0.08	-0.07	0.05	0.00	-0.02	0.01
Mode3	0.16	0.12	0.16	0.04	0.15	0.14	0.00	0.11	-0.02	0.04	0.08	-0.06	0.05	0.01	-0.02	0.01
Mode4	0.31	0.24	0.19	0.21	0.20	0.28	0.05	0.21	0.02	0.11	0.11	0.05	0.09	0.12	0.25	0.11
$\Delta Q_s$																
Mode1	0.37	0.49	0.47	0.72	0.59	0.24	-1.12	0.25	-0.27	-0.06	-0.09	0.22	0.11	0.18	-3.60	-0.50
Mode2	0.30	0.39	0.43	0.57	0.55	-0.04	-1.63	0.08	-0.55	-0.26	-0.14	-0.08	0.02	-0.35	-3.95	-0.76
Mode3	0.14	0.26	0.31	0.43	0.41	-0.30	-1.41	-0.02	-0.49	-0.20	-0.08	-0.02	0.08	-0.23	-3.82	-0.68
Mode4	0.39	0.44	0.35	0.68	0.49	0.10	-1.97	0.07	-0.40	-0.08	-0.04	0.18	0.14	0.19	-2.16	-0.31
$Q_E$																
Mode1	-1.17	-1.29	-1.32	-1.19	-0.97	-0.88	-1.06	-1.13	0.44	0.04	0.19	-0.26	-0.09	-0.54	-0.18	-0.06
Mode2	-1.21	-1.39	-1.42	-1.21	-1.03	-1.02	-1.22	-1.22	0.35	0.04	0.15	-0.27	-0.13	-0.62	-0.33	-0.12
Mode3	-0.56	-0.85	-0.68	-0.75	-0.55	-0.69	-0.89	-0.71	0.15	-0.15	-0.01	-0.43	-0.29	-0.74	-0.48	-0.28
Mode4	-0.41	-0.76	-0.56	-0.74	-0.47	-0.55	-0.68	-0.59	0.23	-0.14	0.03	-0.47	-0.28	-0.67	-0.52	-0.26
$Q_H$																
Mode1	0.27	0.21	0.19	0.15	0.21	0.47	0.74	0.32	0.22	0.32	0.15	0.23	0.20	0.84	1.17	0.45
Mode2	0.25	0.17	0.18	0.08	0.20	0.44	0.66	0.28	0.14	0.21	0.15	0.07	0.16	0.79	1.18	0.38
Mode3	0.25	0.18	0.17	0.06	0.18	0.41	0.65	0.27	0.20	0.26	0.20	0.13	0.23	0.84	1.23	0.44
Mode4	0.33	0.25	0.18	0.19	0.20	0.46	0.65	0.32	0.20	0.32	0.21	0.25	0.26	0.88	1.29	0.49

**Table 3.11** The impact of degrading meteorological forcing data (top Mode 1 versus Mode 2) and land cover (bottom, Mode 1 versus Mode 4) on daily RMSE values for the LCZ2 and LCZ6 site. Values are in  $W\ m^{-2}$ ; negative values denote a reduction in RMSE (i.e. model improvement) whereas positive values denote an increase in RMSE.

	April	May	June	July	August	September	October
<i>Impact of degrading forcing data on daily RMSE values</i>							
LCZ2							
$Q^*$	-1.3	0.9	1.8	-2.7	6.0	-0.4	6.3
$\Delta QS$	-3.1	-1.6	-1.2	-4.4	-1.0	0.8	7.9
$QH$	-0.1	-0.5	1.8	0	2.7	-1.5	-4.5
$QE$	0.2	0.9	0.8	0.1	0.3	2.1	0.2
LCZ6							
$Q^*$	-3.0	0.4	8.9	9.1	4.8	1.8	7.7
$\Delta QS$	5.4	3.5	4.0	3.3	-1.4	1.1	-1.6
$QH$	-3.2	-4.1	0.8	-3.1	-0.6	-2.1	-0.4
$QE$	-2.6	-0.9	-0.7	-2.6	1.5	2.6	0.6
<i>Impact of degrading land cover quality on daily RMSE values</i>							
LCZ2							
$Q^*$	-1.0	-1.0	-1.4	-0.5	-0.9	-0.6	-0.2
$\Delta QS$	-2.3	-3.3	-5.4	-3.9	-3.9	-0.5	0.8
$QH$	0.2	0.1	-0.4	-1.1	-0.6	-1.4	-0.6
$QE$	-2.8	-3.1	-4.2	-4.7	-3.8	-2.3	-1.1
LCZ6							
$Q^*$	0.1	-0.3	-0.4	0.1	-0.2	-0.2	0.0
$\Delta QS$	1.2	0.6	0.1	-0.1	-0.1	0.1	0.3
$QH$	-2.9	-2.3	-2.1	0	-2.1	-2.1	-2.7
$QE$	3.6	0.6	3.1	-1.3	-0.5	-1.1	0.6

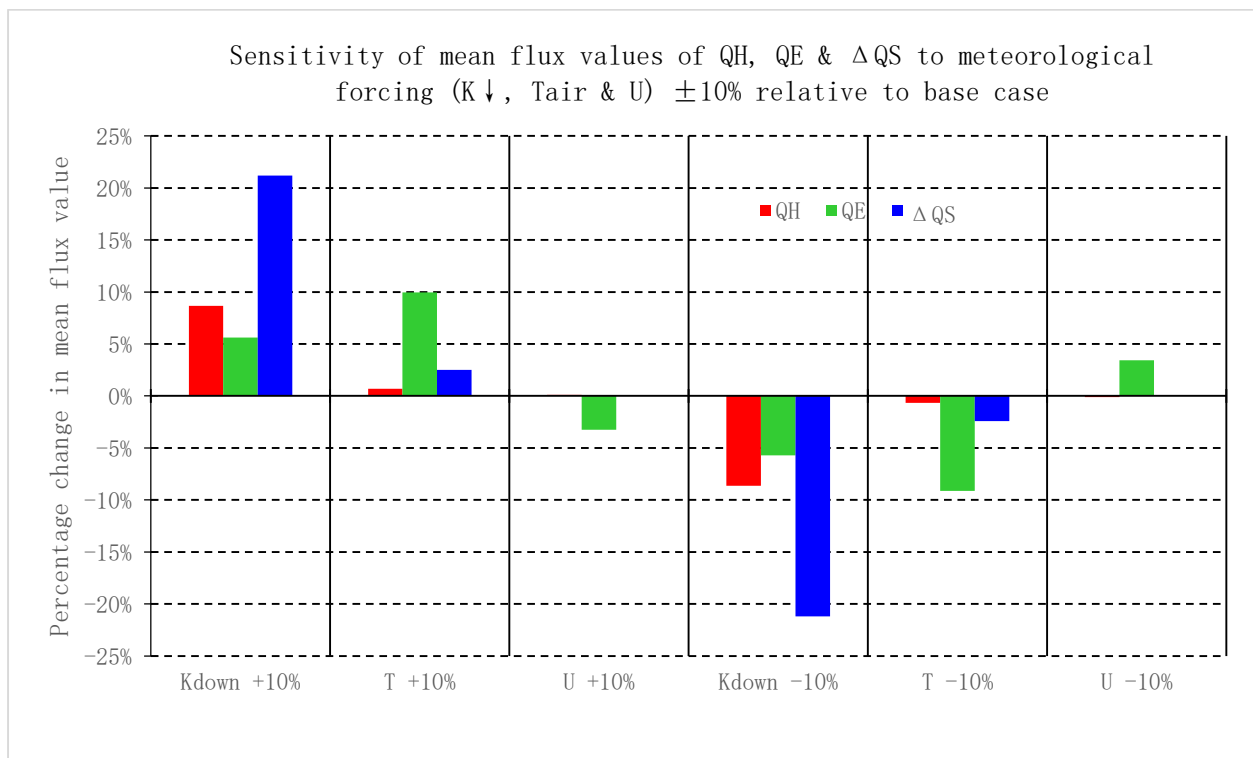


**Figure 3.4** One-Factor-A-Time (OFAT) analysis of forcing data impact on SUEWS simulation of turbulent fluxes. A based case (168 hours) was established using data derived from loess curve of required meteorological forcing (see Table 3.3). We then perturbed  $K\downarrow$ ,  $T$  and  $u$   $\pm 10\%$  of the base case. Presented above is the % difference in the mean value (over the 168hours) of  $QH$ ,  $QE$  and  $\Delta QS$ . It should be noted that  $RH$  was not modified when perturbing  $T$ , hence the apparent increase/decrease in  $QE$

This decrease in performance did not cascade through all turbulent fluxes, model performance increased (i.e. decreased RMSE) marginally for  $Q_H$  and  $\Delta Q_S$  (by 0.4 and 0.3  $W m^{-2}$  respectively) for the LCZ2 site whereas RMSE was increased by 0.7  $W m^{-2}$  for  $Q_E$ . For the LCZ6 site, RMSE for  $Q_H$  decreased by 1.8  $W m^{-2}$  and by 0.3  $W m^{-2}$  for  $Q_E$  when utilising off-site meteorology,  $\Delta Q_S$  RMSE increased by 2.0  $W m^{-2}$ . Accounting for performance increases and decreases, the mean RMSE difference taken across all the turbulent fluxes for both sites is 0  $W m^{-2}$ . By including off-site meteorological data for the Modes which utilised LCZ land cover information, RMSE decreased by 6.5, 3.4 and 1.6  $W m^{-2}$  for  $Q^*$ ,  $\Delta Q_S$  and  $Q_H$  respectively for the LCZ2 site. RMSE for  $Q_E$  increased by 0.8  $W m^{-2}$ . For the LCZ6 site, RMSE increased by 2.7, 1.0 and 0.2  $W m^{-2}$  for  $Q^*$ ,  $\Delta Q_S$  and  $Q_E$  respectively. RMSE for  $Q_H$  decreased by 1.4  $W m^{-2}$ . MFB direction did not change between Modes.

The impact of meteorological forcing data had a larger impact on  $\Delta Q_S$  and  $Q_H$  than for  $Q_E$ . This was also borne out during our OFAT analysis over a grid with equal distribution of urban, paved, and vegetated and tree cover. Differences in  $K_{\downarrow}$  had the largest impact on simulated turbulent fluxes, followed by temperature. The model was insensitive to variation in wind speed ( $V$ ) – see Figure 3.4. The mean difference in daily RMSE across both sites for all fluxes and all months when using off-site meteorological data in place of on-site was  $\sim 0.7 W m^{-2}$ .

#### *3.6.4 Impact of Land Cover on Performance*

Table 3.11 also presents the impact on relative performance when land cover data are changed. Using on site meteorological forcing data (Mode 1) and subsequently utilising LCZ for land cover (Mode 4) had a larger impact on the performance of  $Q^*$  for both sites. For the LCZ 2 site, RMSE increased by 7.2  $W m^{-2}$  (to 28.9  $W m^{-2}$ ) for  $Q^*$  when employing the LCZ data. Again, given the large magnitude of this flux this is rather small. As for the turbulent fluxes,  $Q_H$  RMSE increased by  $< 1 W m^{-2}$  (0.7  $W m^{-2}$ ),  $Q_E$  decreased (i.e. improved model

performance) by  $3.3 \text{ W m}^{-2}$  and  $\Delta Q_S$  increased by  $0.4 \text{ W m}^{-2}$ . For the LCZ6 site, again comparing Modes which utilised on-site meteorological forcing, RMSE for  $Q^*$  increased by  $1.6 \text{ W m}^{-2}$  when utilising the LCZ, by  $1.5 \text{ W m}^{-2}$  for  $Q_H$ ,  $0.8 \text{ W m}^{-2}$  for  $\Delta Q_S$  and decreased by  $1.2 \text{ W m}^{-2}$  for  $Q_E$ . There was no impact on model bias between Modes 1 and 4 and Modes 2 and 3 with the exception of  $\Delta Q_S$  for the LCZ2 site, where the model exhibited a minor positive MFB (over-prediction) of heat storage in Mode 1 (0.25), and a close to zero (-0.07) negative MFB in Mode 4.

Examining the impact of land cover input when off-site meteorological forcing data was utilised (i.e. comparing Mode 2 and Mode 3), often a net improvement in model performance was observed when utilising the LCZ data. However as with the performance changes arising between the on-site meteorological Modes, the changes here can be summarised as marginal improvements. Utilising the LCZ for the LCZ 2 site improved model performance by  $0.8 \text{ W m}^{-2}$  for  $Q^*$ ,  $2.6 \text{ W m}^{-2}$  for  $\Delta Q_S$ ,  $0.5 \text{ W m}^{-2}$  for  $Q_H$  and  $3.3 \text{ W m}^{-2}$  for  $Q_E$ . For the LCZ6 site, RMSE increased by  $0.1 \text{ W m}^{-2}$  for  $Q^*$  and by  $2.0 \text{ W m}^{-2}$  for  $Q_H$ . RMSE decreased by  $0.3 \text{ W m}^{-2}$  for  $\Delta Q_S$  and  $0.7 \text{ W m}^{-2}$  for  $Q_E$ . As with the on-site Modes, MFB did not change direction when utilising the LCZ for land cover. The mean difference in daily RMSE across both sites for all fluxes and all months when using LCZ land cover in place of high-resolution land cover was  $\sim -1 \text{ W m}^{-2}$ .

### **3.7 Discussion**

#### *3.7.1 SUEWS accuracy and measurement errors*

It would be incorrect to attribute the difference between ‘best case’ (Mode 1) simulations by SUEWS and site observations (i.e. performance) to model errors only. The fractional coverage values used by the model represent the surrounding neighbourhood but the observation site may still be exposed to atypical surface characteristics. This appears to be the case for the suburban site here where  $K\uparrow$  is consistently overestimated owing to the exposure

of the radiometer to low albedo surfaces directly below the instrument. As a result, the magnitude of  $\Delta Q_S$  computed from observations (Eqn. 3.3) for this site is probably an overestimation for the neighbourhood; this partly explains the differences between observations and simulations. In this regard it is interesting to note the simulated values for  $K\uparrow$  at the LCZ 6 site is likely more realistic representation for the surrounding area than observed  $K\uparrow$ .

The Objective Hysteresis Model (OHM) which is the sub model within SUEWS which directly relates to  $\Delta Q_S$  in all modes overestimates storage relative to the observational data. It is also important to consider the energy balance closure problem (see for example: Kanda et al., 2004; Kawai and Kanda, 2010; Foken, 2008) which relates to the underestimation of the turbulent fluxes in observational data. The observational data here are corrected following Webb et al. (1980), which results in increasing  $Q_E$  and decreasing  $Q_H$  and somewhat reducing the residual. Nevertheless, as per Eqn. 3.3 the likelihood is that  $\Delta Q_S$  is exaggerated by the observational data. This especially important to highlight if examining the nocturnal withdrawal of heat from the substrate leading to (for instance) the UHI effect.

Overall the daily and hourly flux patterns simulated by SUEWS at both urban and suburban sites show good agreement with the observed fluxes. When provided with observed  $K\downarrow$  and  $L\downarrow$ , SUEWS distinguishes between the two sites on the basis of the non-radiative terms: the model results under(over)-estimated  $Q_E$  and over(under)-estimated  $Q_H$  and  $\Delta Q_S$  at the urban (suburban) site. The role of  $Q_E$  appears to be critical as its magnitude is managed by the availability of water and plant growth. The former here is expressed in terms of the soil moisture content, which is set to field capacity. The latter is a function of the vegetative fraction and leaf area fraction. Looking at the daily and hourly simulations of SUEWS (Figure 3.2, Figure 3.4) it seems that the description of plant growth (canopy cover, tree species, etc.) may be critical, which is consistent with Grimmond et al., (2011). In addition, the model has

difficulty in responding quickly to precipitation events when rapid increases in the magnitude of  $Q_E$  are observed.

### 3.7.2 *Impact of non-local meteorological and LCZ data*

Using off-site meteorological observations of  $K_{\downarrow}$  and of temperature and relative humidity to estimate  $L_{\downarrow}$  increases the difference between the observations at the site and SUEWS simulations but nevertheless the model still shows itself capable of discriminating between neighbourhood types. The use of LCZs to capture information about the type of neighbourhood in which the observation site is located has a marginal effect. The differences in meteorology between the off-site and on-site stations are highlighted in Table 3.6 and Table 3.7. Such differences may be expected of most cities where off-site meteorological stations conforming to WMO standards will likely record higher wind speeds (due to less friction), colder air temperatures (more evapotranspiration, less heat storage) and higher levels of precipitation. This was not the case for Dublin, where off-site recordings were cooler, but wind speeds were also lower. In order to verify this finding, additional situations comparing off-site and on-site data with respect to model performance are needed; we plan to undertake this in a subsequent paper.

Nevertheless, the differences between Modes were relatively minor, moreover the model showed itself to be relatively insensitive to such differences. This suggests that SUEWS may be used to discriminate between different urban neighbourhoods by sampling from within LCZs and obtaining land-cover fractions and forcing the model with off-site meteorology.

To test this proposition, we ran SUEWS in Mode 3 for four additional LCZ types present in the Dublin area to represent other urban and non-urban covers. These include: compact low-rise (LCZ3) for inner-city residential area; large low-rise (LCZ8) for warehouse areas found at the edge of the city; low plant cover (LCZ104) for grass-covered landscape and; closed trees (LCZ101) for forested areas. Each LCZ area was sampled (Table 3.5) as before

and fractional areas were calculated. Figure 3.5 shows the mean value for each non-radiative flux for June 2010 for each LCZ, including the urban and suburban LCZs used in the body of this study. The values are presented as a difference from the overall mean calculated for the six LCZs; thus,  $Q_H$  for an LCZ is shown as the difference from the mean  $Q_H$  value for all LCZ. This highlights the partitioning of the UEB across different LCZs. The results make intuitive sense. Note that the LCZs with the highest combined fractions of buildings and impervious surface cover (LCZs 2,3 and 8) exhibit above average values of  $Q_H$  and  $\Delta Q_s$ ; these areas store more sensible heat (higher surface temperatures) and heat the overlying atmosphere rather than evaporate water. Oppositely, the well vegetated suburbs and the natural land-covers partition available energy into  $Q_E$  rather than  $Q_H + \Delta Q_s$ .

Stewart and Oke (2012) speculate that energy partitioning zones are unlikely to coincide exactly with LCZs because similar flux densities can occur above canopy layers with distinctly different microscale structure, land cover, and thermal climate. The profiles for June presented in Figure 2.5 illustrates this problem, note for instance  $Q_H$  profiles for LCZ 2 and LCZ 3 vary by  $<10 \text{ W m}^{-2}$ . However, these data have been averaged in order to examine the signal for the entire month of June. Diurnal variations exhibited a higher degree of variation than the mean value for June; moreover, energy partitioning for specific boundary layer conditions (for instance high pressure, little wind, no precipitation) maybe of greater importance to one user than other, reinforcing the earlier point on the need for models to undergo extensive validation in differing circumstances and conditions.

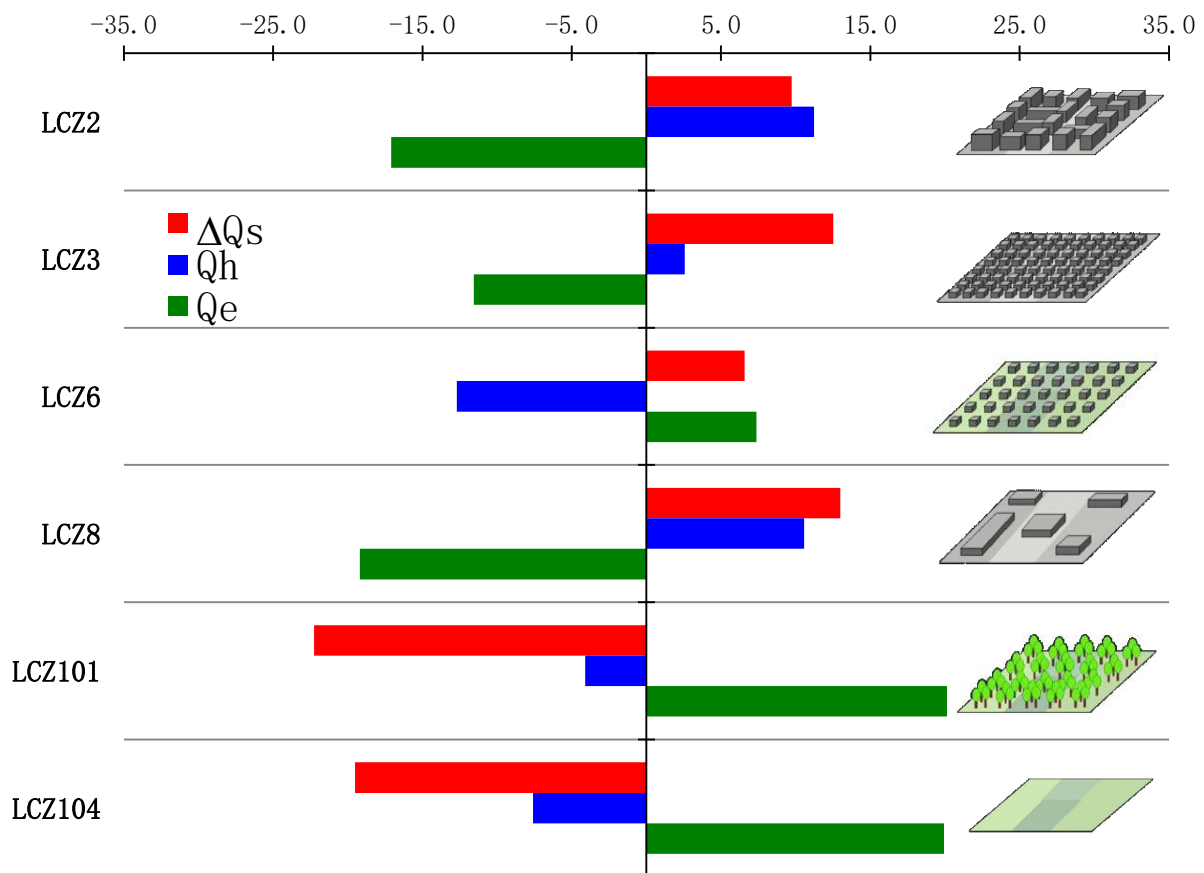


Figure 3.5 Relative partitioning of Turbulent fluxes at each LCZ site for June (2010) the mean value of QH QE and  $\Delta Q_S$  for each LCZ are subtracted from the group mean. X-Axis is W m<sup>-2</sup>. LCZ images reproduced from Stewart and Oke (2012)

Nevertheless, the LCZ classification provides a useful sampling framework for the derivation of the land-cover fractions needed to run SUEWS. This proved an efficient and effective means of gathering LCZ data here and provided a means of extending the model to other parts of the city. However, using the LCZ for this, does introduce a degree of subjectivity into data acquisition as there is no objective means of delineating a spatially contiguous LCZ type for individual cities. Ultimately users should avoid simply employing the mid-range of values which are provided for each LCZ type to derive land cover and/or anthropogenic parameters. For example, within Dublin, the fractional coverage of buildings for LCZ 2 was at the lowest end of the provided LCZ range, while impervious fraction was at the highest end of the range. Meaning the generic LCZ 2 mid-range would not accurately describe this LCZ in Dublin.

While the scheme allows for sub-categories within each LCZ category, for example: dense compact midrise / open compact midrise etc. the development of mean values for the objective discrimination between LCZ types (rather than within a single LCZ class) would allow for a more consistent usage and allow comparisons between LCZs across cities and climate types.

### **3.8 Summary and Conclusion**

The input needs of urban atmospheric models present a barrier to their application in many places where information on the physical characteristics and urban energy budgets are sparse. Here we examined a means to overcome this obstacle by presenting a modelling framework that draws upon basic descriptions of the characteristics of city (Local Climate Zones) and tested this with a moderately complex urban energy budget model (SUEWS) which was forced with meteorological data obtained from outside the urban area. The use of forcing data obtained from a WMO synoptic station in lieu of data obtained from flux observation platforms in SUEWS resulted in a slight reduction in *relative* model performance against two urban types. The use of parameters that represent LCZ types however had no significant impact in this case study.

Our primary aim was to demonstrate/validate a modelling approach that could apply a moderately complex UEB model utilising readily available data beyond one or two instrumented sites. Based on the results from Dublin, SUEWS appears capable of being run with easily obtainable meteorological and land cover data with no significant impact on model performance across multiple seasons.

---

## Chapter 4 Linking urban climate classification with an urban energy and water budget model: multi-site and multi-seasonal evaluation

---

### 4.1 Preface

This chapter is submitted as:

Alexander, P.J., Bechtel, B., Chow, W., Fealy, R., Mills, G. (2016) Linking urban climate classification with an urban energy and water budget model: multi-site and multi-seasonal evaluation 1-23pp - *Urban Climate*

Here, the modelling approach is tested in cities beyond where the LCZ-Approach was developed and in different background climates. The objective here was to test the robustness of the approach against independent datasets. As with the previous paper, SUEWS was used with the approach (hence, LCZ-SUEWS). This also provided an opportunity to evaluate the latest version of the SUEWS model in background climates well beyond those used for evaluation previously. The primary question motivating this paper was *Does the LCZ-Approach work in different cities beyond Dublin? Is the impact on model performance consistent across different cities?*

The primary objective of the paper was to derive the necessary input parameters for SUEWS in a consistent manner, apply and evaluate the model in a standardised way so as to ensure comparability across the different sites. The experimental design used in paper 1 / Chapter 3 were refined to align more with the PILPS-URBAN approach (i.e. adding more detailed data in “stages” rather than a cross-validation approach).

The paper was submitted to the Journal of Urban Climate in February 2016.

### 4.2 Abstract

There are a number of models available for examining the interaction between cities and the atmosphere over a range of scales, from small scales - such as individual facades, buildings, neighbourhoods - to the effect of the entire conurbation itself. Many of these models

require detailed morphological characteristics and material properties along with relevant meteorological data to be initialised. However, these data are difficult to obtain given the heterogeneity of built forms, particularly in newly emerging cities. Yet, the need for models which can be applied to urban areas (for instance to address planning problems) is increasingly urgent as the global population becomes more urban. In this paper, a modeling approach which derives the required land cover parameters for a mid-complex urban energy budget and water budget model (SUEWS) in a consistent manner is evaluated in four cities (Dublin, Hamburg, Melbourne and Phoenix). The required parameters for the SUEWS model are derived using local climate zones (LCZs) for land cover, and meteorological observations from off-site synoptic stations. More detailed land cover and meteorological data are then added to the model in stages to examine the impact on model performance with respect to observations of turbulent fluxes of sensible ( $Q_H$ ) and latent ( $Q_E$ ) heat. Replacing LCZ land cover with detailed fractional coverages was shown to marginally improve model performance, however the performance of model coupled with ‘coarse’ LCZ data was within the same range of error (20-40  $Wm^{-2}$  for  $Q_E$  and 40-60  $Wm^{-2}$  for  $Q_H$ ) as high resolution data.

### **4.3 Introduction**

There has been considerable progress in the representation of urban-scale processes within atmospheric models. A variety of urban-scale models now exist which are capable of simulating the urban heat island either empirically or using physical models (Taha et al., 1988; Myrup, 1969; Atkinson, 2003; Bottyán & Unger, 2003; Kusaka & Kimura, 2004; Hoffmann et al., 2012), urban air quality (Shir & Shieh, 1974; Huang et al., 2000; Karppinen et al., 2000), human thermal comfort in the outdoor urban environment (de Dear & Brager, 1998; Ali-Toudert & Mayer, 2006), energy demand and anthropogenic emissions of heat (Block et al., 2004; Fan & Sailor, 2005; Allen et al., 2011). There are a wide number of surface schemes for modeling fluxes of mass, momentum and energy in urban areas (i.e. the urban energy balance

- UEB), which vary in complexity in terms of their parameterisation and hence, their input requirements. More complex UEB schemes have been shown to be very useful in examining, for instance, the detailed hygrothermal impact of different urban forms and functions on the micro-scale climate (Barlow et al., 2004; Harman et al., 2004; Dupont et al., 2004). Such models are invaluable for understanding the processes in operation within urban environments. Moreover, there are some examples of where UEB models have been coupled with meso-scale models (Harman & Belcher, 2006; Bueno et al., 2013; Stewart et al., 2014; Onomura et al., 2015; De Ridder et al., 2015) which would effectively allow for micro-scale meteorological forecasts.

These complex UEB models however are incapable of being run in many data poor settings, or at least routinely, for cities in the economically developing world where the application of such models to planning problems and adaptation to extreme weather conditions would have the largest potential benefit. There is now a clear need to overcome this knowledge gap so as to allow greater integration of urban climate knowledge with the planning and policy communities (Mills et al., 2010; Ching, 2013; Hebbert & Mackillop, 2013; Heaphy, 2015). For instance, a comparison of 33 models by Grimmond *et al.* (2010) highlighted the large number (145) of input parameters required by the group of models considered. Providing such parameters for a single neighbourhood is challenging, and this is before we consider the parameters required for an entire urban area. In order to carry out simulations across an entire urban domain, generalisations will be needed in the interim.

Obtaining the necessary input parameters in data poor settings is only part of the problem, greater rigour in evaluating models in differing background climates and in different cities is also urgently needed. As stated by Oke (2006), without extensive model evaluation exercises the utility of UEB models for planning problems remains dubious. The international urban climate model comparison (Grimmond et al., 2010; Grimmond et al., 2011) went a large

way towards discovering the general ability of UEB models in simulating the urban effect on turbulent fluxes and prioritising the most important input parameters. Research on specific model performance in different settings is also beginning to emerge (Loridan & Grimmond, 2012). Despite this there is still a noted lack of integration of urban climate knowledge in the planning process. Very few examples exist of UEB models being applied to real planning problems in collaboration with city planners (Eliasson, 2000). In order to bridge this knowledge gap, more specific evaluation of individual UEB models needs to be undertaken, with clearer links to planning applications, as proposed by Masson *et al.* (2014). It is unlikely that there will emerge a one-model-fits-all scheme that will apply to all situations, however a starting point may be to seek a balance between realistically representing urban processes, ensuring good model accuracy and requiring readily obtained input parameters that are derived in a consistent manner so as to allow inter-city comparisons.

While concerted effort has been placed on model development (Hidalgo *et al.*, 2008) to better represent urban climate processes and move towards operational use in forecasting models, there is a clear need for more general models which are also capable of studying the impacts of urbanisation on the environment with fewer input requirements. One example is the local scale urban meteorological parameterisation scheme (LUMPS – Grimmond & Oke, 2002) which has been shown to accurately simulate the UEB in multiple cities requiring only simple input parameters. The simple treatment of vegetation and water availability i.e. urban water balance (UWB) within LUMPS limits its application to real planning challenges. Hence a mid-complex scheme, the surface urban energy and water balance scheme (SUEWS – Järvi *et al.*, 2011) was subsequently developed which has a high potential to fill this intermediate space between complex parameterisation, accuracy and ease of implementation.

SUEWS requires more input parameters than LUMPS, however it is still relatively straightforward to carry out simulations and due to its inclusion of the UWB can be applied for

planning problems. The model has already been evaluated in Helsinki, Los Angeles (Järvi, et al., 2011; Järvi, et al., 2014) and Dublin (Alexander et al., 2015) where the necessary inputs to force the model and evaluate its performance were available.

Here we evaluate SUEWS further in three additional background climates and urban configurations. However, our primary aim is to consider the impact of data quality and evaluate model accuracy in a systematic way across multiple sites. In order to derive a means to apply SUEWS in data poor situations we employ a modeling approach which links the local climate zone (LCZ) classification (Stewart & Oke, 2012) with SUEWS. LCZ are linked with SUEWS to derive the necessary land cover parameters easily and in a consistent manner across an entire urban domain. Here, we extend the proof of concept established in a previous paper (Alexander et al., 2015) to include additional background climates and multiple urban environments in order to validate the LCZ-SUEWS approach and answer the following questions:

- 1) Can off-site meteorological data be used to force SUEWS and what is the impact on performance?
- 2) Is the impact of “low quality” (i.e. LCZ) land cover data on SUEWS performance comparable across different cities?

The answer to these questions will have a direct impact on applying the model in data-poor settings such as rapidly expanding urban areas. Prior to outlining the methods employed in this paper, the use of LCZ with the SUEWS model is discussed.

#### **4.4 LCZ-SUEWS approach**

The traditional approach for modeling urban areas involves a number of procedures. Firstly, the urban area is parameterised in terms of fraction coverage ( $\lambda$ ) of buildings, roads and pathways, vegetation, soils and water. Building form (morphology) and vegetation are then derived based either from LiDAR, aerial imagery or field work. From these other parameters are derived for example the sky view factor ( $\psi$ ) and height/width (H/W) ratio. The function (as

well building materials) are derived using local expert knowledge. Finally, the derivation of meteorological forcing data, either from observations made on site or through an atmospheric model such as a regional climate model. A number of different methods and data can be employed in each of these stages, a standard does not exist for any scale, and thus inter-site comparisons remain largely elusive. Moreover, in some data starved regions the availability of high-quality data (i.e. multispatial, multitemporal) required by some methods is sparse or simply non-existent.

The basic premise of the linked LCZ-SUEWS approach is address this disparity. Rather than view the urban area as a collection of individual surfaces (walls, rooftops, roads, materials) the approach employs as its starting point the notion that the urban area is a collection of discrete homogenous neighbourhoods of similar characteristics, seeks to identify these neighbourhoods and standardise the approach for deriving parameters for these neighbourhoods required by models.

The thermal differentiation of urban areas using LCZ as a basis has already been demonstrated both empirically and through modeling (Fenner et al., 2014; Stewart et al., 2014; Leconte et al., 2015; Colunga et al., 2015). Moreover, the ability to identify LCZ across entire urban areas i.e. to map LCZ has also been demonstrated (Bechtel et al., 2015). Therefore, LCZ are ideally placed for standardising the collection of model parameters and for applying the outputs of UEB models across a much larger domain, thus reducing computational expense. There are a number of advantages of the approach:

1. The LCZ scheme itself is defined based on fractional coverages of different land cover types and urban parameters (building height / roughness,  $\psi$  and H/W) thus enables a first estimate of these parameters for models

2. The classification of a city into LCZ enables subsequent strategic sampling of the urban area to derive details parameters and characteristics such as building materials, population density and land use
3. LCZ were designed to better describe the site characteristics of urban temperature sensors, hence can aid in the placement of instruments, the interpretation and evaluation of model simulations based on these observations
4. The scheme was designed to be universally understood and since they employ standard building forms are likely to coincide (either in part or entirely) with other land use land cover classifications that have already been established (Alexander & Mills, 2014; Leconte et al., 2015)

Figure 4.1 illustrates the approach in terms of linking LCZ to a UCM across multiple urban scales, highlighting points 1-4 from above. Methods are currently being tested to create LCZ maps for most cities using readily obtained open source data (Bechtel et al., 2015). Therefore, we are assuming for the approach either (i) a LCZ map of the urban area is available or (ii) another LULC map which can be translated into LCZ is available.

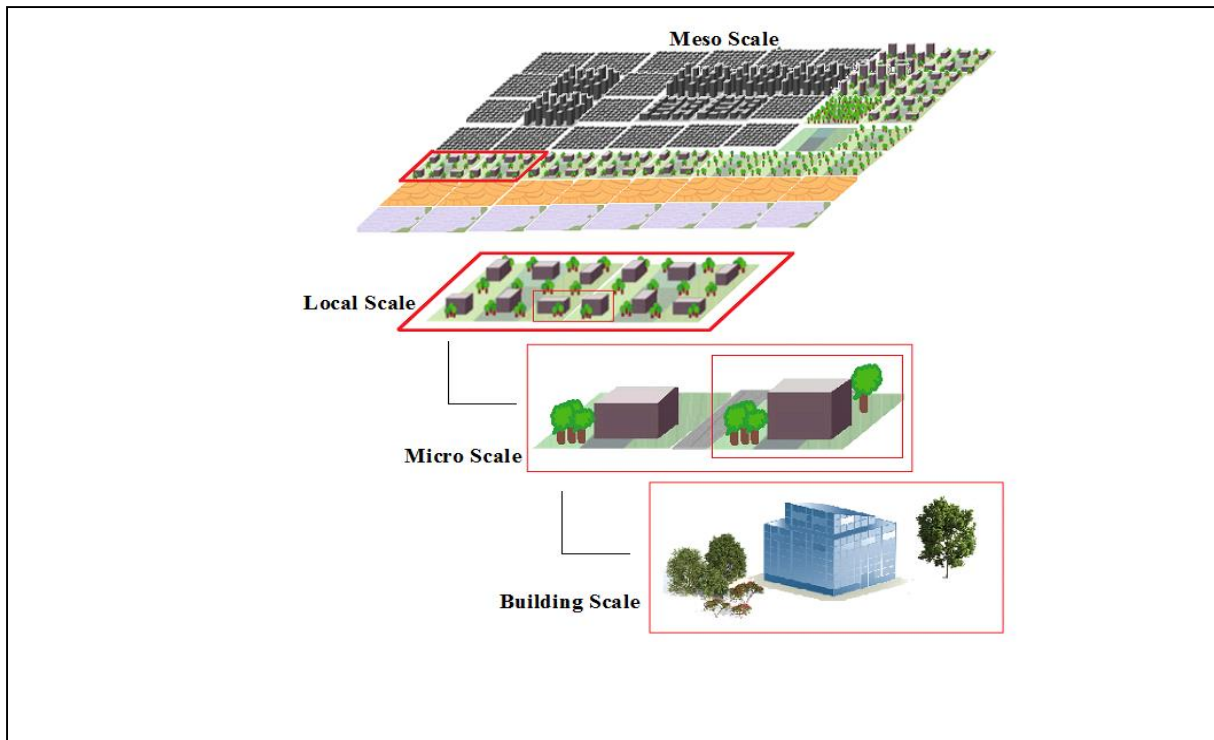


**Figure 4.1 LCZ-SUEWS approach:** At the mesoscale (10s-100s of Km<sup>2</sup>), model parameters are derived by integrating all LCZ across the entire domain. At the local scale (1-10s of Km<sup>2</sup>) specific model parameters for individual LCZ types are derived. At the microscale and building scale (10s-100s of m<sup>2</sup>) the approach is as yet untested, but would involve the addition of building dimensions and spacing, individual vegetative species as well as detailed material data.

It should be noted there are only a few examples of where LCZ have been linked to microscale ( $\leq 100$  m) models (see Middel *et al.* (2014) for example) essentially where subsets of a neighbourhood are examined using the LCZ framework. There are currently no examples in literature of linking LCZ to building scale ( $\leq 10$  m) models. This may be possible in some instances where particular forms and functions can be inferred from individual LCZ classes (for instance, it would be unlikely LCZ 10 would ever describe a residential area and more likely to be required to conform to particular design/material regulations). While examining building scale through the LCZ may seem impractical, it potentially allows for later upscaling to micro, local and meso scale therefore may be useful. However, for this work the approach employs the local scale (500-1000m) to derive model parameters and apply model outputs.

## 4.5 Experimental outline

We test the effect of using LCZ data which is derived in a consistent way on SUEWS performance by carrying out simulations of the UEB at four locations and compare the results against observations of turbulent fluxes of sensible ( $Q_H$ ) and latent heat ( $Q_E$ ). The SUEWS model (v.2014b) is outlined in detail in (Järvi, et al., 2011) and (Järvi et al., 2014). In brief, the model calculates hourly radiative fluxes ( $Q^* = K^* + L^*$ ) using the net all-wave radiation parameterisation (NARP - Offerle et al., 2003) latent heat,  $Q_E$ , using a modified Penman-Monteith equation (Grimmond & Oke, 1991) heat storage,  $\Delta Q_S$ , using the Objective Hysteresis Model (OHM - Grimmond & Oke, 1999) and anthropogenic heat,  $Q_F$ , using the Sailor and Vasireddy approach (Sailor & Vasireddy, 2006). Finally,  $Q_H$  is calculated as the residual from the calculated fluxes i.e.  $Q_H = Q^* - [Q_E + \Delta Q_S + Q_F]$ .

### 4.5.1 Experimental setup

In order to evaluate the LCZ-SUEWS approach, we designed a systematic experiment to test the impact of improving data quality on model performance. Our evaluation is carried out in four cities. The locations and data descriptions are outlined in section 4.5.2 below, here we provide an outline of the experimental procedure – see table 4.1 for overview.

We adopted a similar approach to the inter-model comparison project (Grimmond et al., 2011) whereby SUEWS was initially run using baseline land cover parameters and off-site meteorology (“low” quality data sampled using LCZ maps). Subsequently more detailed land cover fractions and meteorological data were added in stages. Each step was intended to reveal the importance of information quality on the model output. Due to the uncertainty/assumptions required in relation to  $Q_F$  for several of the sites we opted to exclude this flux from the model runs – though estimates are provided for some of the sites which indicate the magnitude is low ( $\leq 30 \text{ W m}^{-2}$ ).

**Table 4.1 Outline of systematic experiment used to test the LCZ-SUEWS approach across multiple sites / climates / urban configurations. Each stage subsequent to stage 1 adds additional detail, hence, when interpreting results, the additional effort in providing these data should be considered.**

Stage	Experiment Alias	Land cover data use for model run	Meteorological data used for model run
1	Base-line	Local Climate Zone fractions derived from sampling sites across the urban area	Proximate WMO standard synoptic station (airport sites): T, RH, K↓, Pr, P, U, V
2	Detailed land cover	Fractional values derived from 1 km <sup>2</sup> immediately surrounding flux site	Proximate WMO standard synoptic station (airport sites): T, RH, K↓, Pr, P, U, V
3	Detailed meteorology	Fractional values derived from 1 km <sup>2</sup> immediately surrounding flux site	Meteorological data collected adjacent flux observation platforms: T, RH, K↓, L↓, Pr, P, U, V

Data from urban flux observations sites and proximate WMO standard synoptic stations were obtained by contacting data holders at each of the four sites. Once these data were released and collated for a period of approximately one year for each site, we generated a LCZ classification following the method outlined in Bechtel *et al.* (2015) for each city where data were available. Land cover parameters were then derived by sampling LCZs (excluding the area surrounding the flux sites) and manually computing fractional coverages, this was done in Google Earth Pro similar to the method proposed by See *et al.* (2015). For high-resolution land cover we used the reported meta-data values for the flux sites. Where this was unavailable, we derived detailed fractional coverages, building heights and vegetation type(s) surrounding each of the sites out to radius of 500m from the flux platforms.

The model was span up prior to each of the experiments using the following approach: for each of the sites, we saturated the surrounding landscape i.e. soil moisture content (SMC) was set to maximum, and the model was span up until SMC reached an equilibrium and appropriate estimates of leaf area index were thus obtained for the initiation period (January 1<sup>st</sup>).

#### 4.5.2 Test locations

Tables 4.2 and Figure 4.2 below provides an overview of the four sites included in this work. SUEWS has mostly been applied in temperate climates though the simpler model LUMPS has been applied in arid environments before (Middel et al., 2012). Here we applied SUEWS to a newly (<2 years) instrumented site in Dublin, Ireland; a long term (5-10 years) site in Hamburg; Germany; a long term site in Melbourne, Australia; and an established site (2-4 years) in Phoenix, USA. The latter two sites represent environments with low precipitation and high annual temperatures, whereas the former two represent (i) a cool temperate climate with little annual temperature variation and high precipitation and (ii) a warm humid continental climate respectively. In Table 4.3, we highlight the required fractional values of land cover types required by SUEWS as computed using high resolution data and the LCZ approach.

**Table 4.2 Meta-data of the sites included in this study. Shown is the year in which observations were obtained, the background climate type, the location of both the flux sites and alternative synoptic stations. Shown also in meters are the instrument height of the flux towers ( $Z_m$ ) the displacement height ( $Z_0$ ) and the mean building height surrounding the site ( $Z_b$ ).**

Location	Year	Köppen	Site	LAT	LONG	WMO ID	$Z_m$	$Z_0$	$Z_b$
Dublin, Ireland Site code: DUB	2013	Cfb	Flux	53.34	-6.27	---	37	0.6	16.3
			Synoptic	53.43	-6.25	39690			
Hamburg, Germany Site code: HAM	2014	Dfb	Flux	53.52	10.10	---	50	0.6	8.8
			Synoptic	53.63	10.00	101470			
Melbourne, Australia Site code: MEL	2004	Cfb	Flux	-37.73	145.01	---	40	0.4	6.4
			Synoptic	-37.67	144.83	948660			
Phoenix, USA Site code: PHX	2012	BWh	Flux	33.48	-112.14	---	22.1	0.5	4.5
			Synoptic	33.42	-112.02	722780			

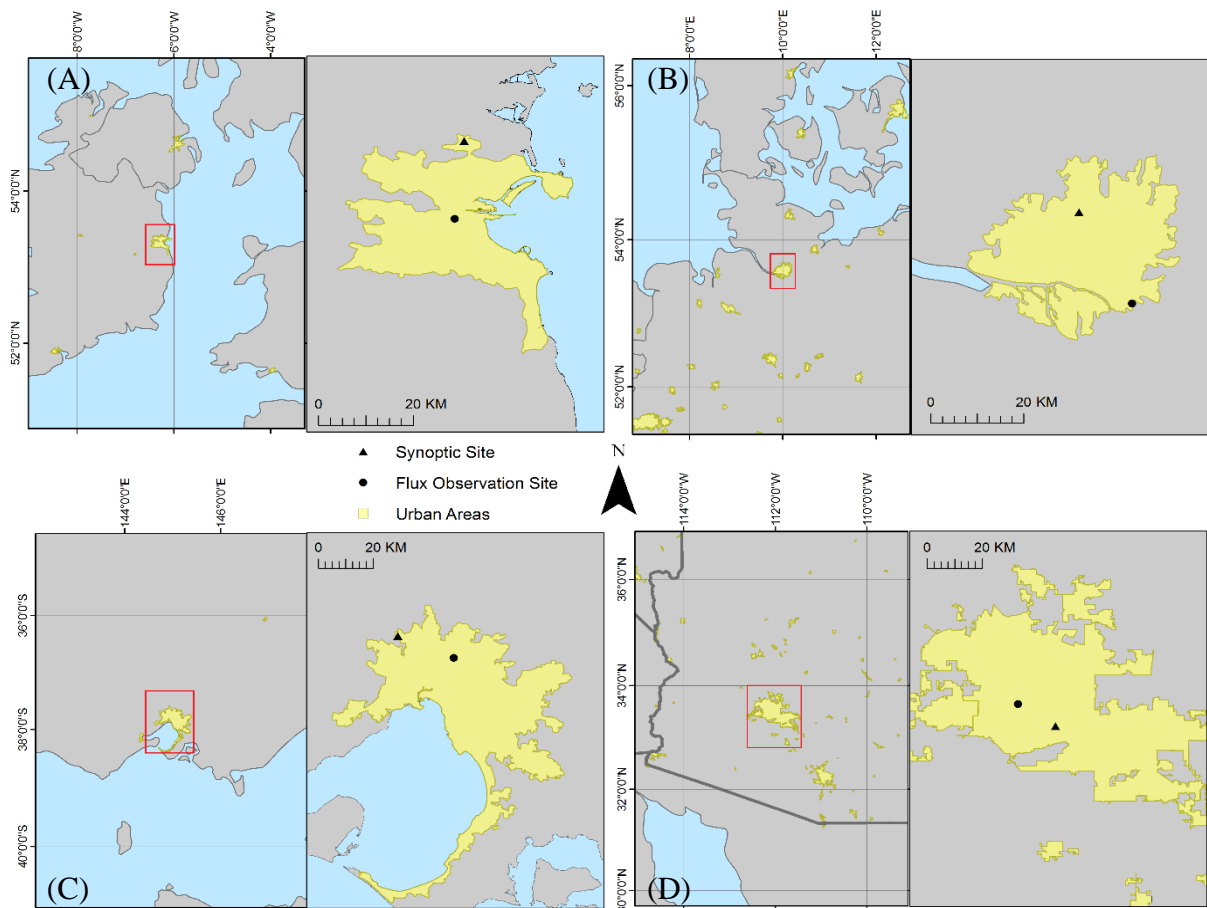


**Figure 4.2** Location of the four sites used in this experiment (A) is Dublin, Ireland (B) is Hamburg, Germany (C) is Melbourne, Australia (D) is Phoenix, USA.. Shown are the locations of the synoptic and flux sites. Urban land cover obtained from Global Rural-Urban Mapping Project, Version 1 (GRUMPv1)

**Table 4.3** Land cover fractions ( $\lambda$ ) used to force the model calculated using the LCZ approach (stage 1) and traditional approach using high resolution (HR) data immediately surrounding the sites (stage 2 and 3)

Location	Land cover	Building	Pavements	Unmanaged	Trees	Grass	Water
Dublin, Ireland [DUB]	LCZ 2 - Compact Midrise	33	55	00	06	06	0
	HR <sup>1</sup>	39	49	00	10	02	0
Hamburg, Germany [HAM]	LCZ 8 - Large low-rise	40	20	10	17	11	2
	LCZ D <sup>2</sup> - Low plants	05	02	07	35	49	2
	HR <sup>1</sup>	27	15	07	22	18	11
Melbourne, Australia [MEL]	LCZ 6 - Openset low-rise	37	16	0	21	26	0
	HR <sup>3</sup>	44	16	0	29	11	0
Phoenix, USA [PHX]	LCZ 6 - Openset low-rise	49	18	27	02	04	0
	HR <sup>4</sup>	26	22	37	05	10	0

<sup>1</sup> Based on 1 km immediately surrounding flux site,  $\lambda$  calculated using 2.5m imagery in GoogleEarth Pro

<sup>2</sup> Data not used in this study <sup>3</sup> Based on values reported in Coutts *et al.*, (2007) <sup>4</sup> Based on values reported in Chow *et al.*, (2014)]

The first site, Dublin Ireland – DUB – the flux observations are made on a mast located in a recently instrumented flat rooftop located on the grounds of a technical institute, just south of the centre of the urban area amidst a mix of dense commercial units and residential apartments (Sunderland et al., 2013; Keogh, 2015). The buildings surrounding the flux site are between 15-20m tall, compact spacing with little vegetation. The site was not present during the initial test case of the LCZ-SUEWS approach in Dublin (Alexander et al., 2015). The synoptic station for DUB is located approximate 15km north of the urban centre adjacent Dublin International Airport conforming to WMO standards; large homogenous fetch of short grass, no tall trees, and no nearby buildings.

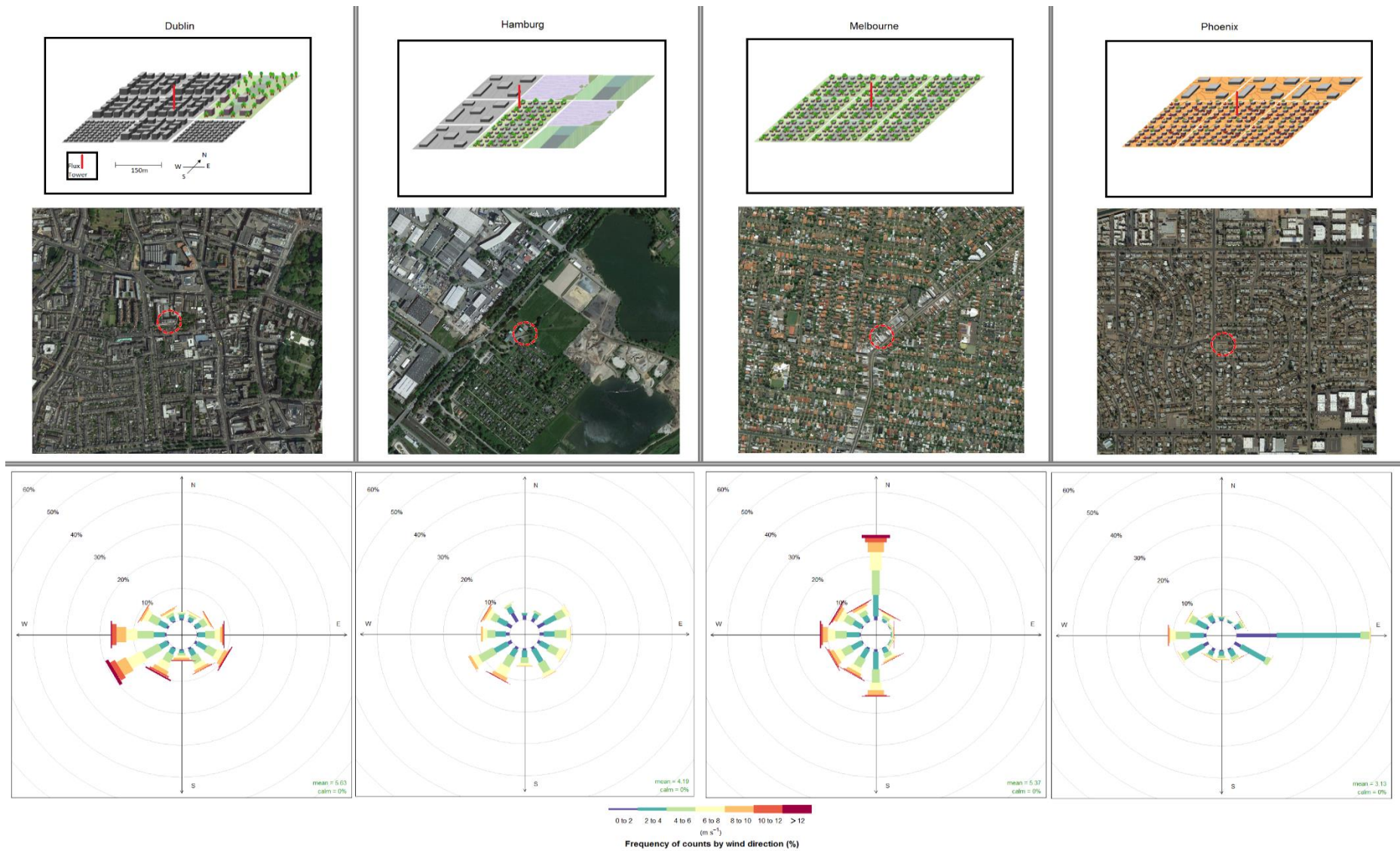
The second site, Hamburg Germany – HAM – the flux observations are made at various height levels of a large telecommunications mast located 8km east of the urban centre (Brümmer et al., 2012). This site essentially straddles two differing LCZs, to the west of the flux site, is characterised by large warehousing units <15m tall with little vegetation. To the East of the mast there is largely green vegetation, trees and little building coverage. The synoptic station for HAM is located at Hamburg International Airport approximately 11km north of the urban centre, again conforming to WMO standards.

The third site, Melbourne Australia – MEL – here the flux observations are made in Preston, a suburban area located approximately 10km north of the centre of Melbourne (Coutts, et al., 2007). The instruments are located on a mast surrounded by medium density residential houses 5-8m tall, open spacing and an ample amount of vegetation both grass and trees. The accompanying synoptic data were obtained from Melbourne Airport, located 23km north-west of the urban centre.

The final site, Phoenix USA – PHX – for this location, observations are made within a residential area located 7.5km North-West of downtown Phoenix in the suburban area of Maryvale (Chow et al., 2014). The surrounding area is comprised almost entirely of low rise

residential housing 5-8m tall with dry xeric landscaping i.e. little green vegetation. The synoptic data for this site were obtained from Phoenix Skyharbor airport which is proximate to the centre of the urban area (approximately 3.5km southeast of downtown Phoenix). Solar radiation data were unavailable at Skyharbor airport, therefore solar radiation data for a nearby Arizona Meteorological network (AZMET) station located 1km northwest of the airport at Encanto were used.

Figure 4.3 illustrates the LCZ descriptions applicable immediately below and surrounding each of the sites along with satellite imagery and annual wind roses from each location. These LCZ descriptions along with wind direction were used to filter the observational data to ensure the source area for each site was consistent with the LCZ type used for the model runs. For example, for DUB site, this meant including westerly vectors while excluding easterly winds. For HAM, observational data were split into 2 sub datasets corresponding with LCZ 8 (westerly flows) and LCZ D (easterly flows). For the purposes of this study we only considered the LCZ 8 data. For both MEL and PHX the relative homogeneity of the surrounding urban area (along with the low wind speeds) meant no additional filtering was carried out on the provided observational data.



∞

Figure 4.3 – Top: LCZ description of the land cover immediately surrounding each site. Middle: Satellite imagery surrounding each of the sites. Bottom: Annual wind roses collected at the flux sites, each coloured bar represents a different wind speed (m s<sup>-1</sup>), wind direction was partitioned into 16 compass vectors.

### 4.5.3 Evaluation of experiments

The performance of SUEWS run in each stage of the experiment is evaluated against the observations at each of the sites. Table 4.4 highlights the observational data available against which the model is judged, Table 4.5 highlights the raw data post-processing steps undertaken at each site along with the instruments used at each site. We employed root mean squared error (RMSE) and mean fractional bias (MFB) and Taylor diagrams which further employ the centred RMSE ( $E'$ ), the correlation coefficient ( $R$ ), and the standard deviation ( $\sigma$ ) (Taylor, 2001) to assess the model performance in each of the stages highlighted previously. Additionally, regression analysis was carried out between model simulations and observations, for this the coefficient of determination ( $R^2$ ) is reported. For comparing seasonal model performance across stages, the RMSE is normalised (nRMSE) using a normalisation factor, which is computed using the difference between the maximum and minimum observed values (Shcherbakov et al. 2013).

**Table 4.4 Descriptive statistics illustrating the availability of flux data (top rows) as a percentage of the entire year considered. Note: DOY 1 = January 1<sup>st</sup>. Also given are the means ( $\mu$ ) and standard deviations ( $\sigma$ ) of wind speed ( $u$ ) relative humidity (rh) air temperature ( $T_{air}$ ) air pressure (pres) and insolation (kdown) recorded at the synoptic sites.**

		Site	DUB	HAM <sub>LCZ 8</sub>	MEL	PHX
		Year	2013	2014	2004	2012
		DOY span	1-109, 149-305	1-365	1-70, 87-183, 210-242, 275-333	1-77, 108-110, 121-157, 164-223, 242-366
		N (valid)	3567 (45%)	4536 (57%)	3705 (47%)	6784 (86%)
U ms <sup>-1</sup>	$\mu$	5.6	4.2	5.3	1.1	
	$\sigma$	2.9	2.1	2.8	0.9	
RH %	$\mu$	81.7	80.7	67.5	28.2	
	$\sigma$	12.3	15.4	18.8	16.8	
T <sub>air</sub> °C	$\mu$	9.5	10.8	13.7	25.1	
	$\sigma$	5.5	7	5.3	9.3	
pres kPa	$\mu$	101.4	101.4	101.6	101.1	
	$\sigma$	1.2	0.8	1.7	1.2	
rain mm	Max	12.9	14.9	8.5	14.7	
	Sum	763.9	679.4	448.6	114.19	
kdown W m <sup>-2</sup>	$\mu$	115.1	121	164.38	231.49	
	$\sigma$	188.2	197.7	253.29	308.92	

**Table 4.5 Meta-data illustrating instrumentation at the four flux site along with corrections carried out on flux measurements**

Site	DUB	HAM	MEL	PHX
Instruments [ Model ]	<p><u>Tower (48 m AGL)</u></p> <ul style="list-style-type: none"> <li>3D sonic anemometer [WindMaster Pro, Gill]</li> <li>Gas analyser [LI-7200]</li> <li>Temperature-relative humidity sensor [HMP45C]</li> <li>Net radiometer [NR-01] 47 m</li> </ul> <p><u>Roof level (37 m)</u></p> <ul style="list-style-type: none"> <li>Tipping bucket rain gauge [ARG100]</li> </ul>	<p><u>Tower (50 m AGL)</u></p> <ul style="list-style-type: none"> <li>3D sonic anemometer [USA-1]</li> <li>Gas analyser [LI-7500]</li> <li>Thermometer [Pt-100]</li> <li>Humidity sensor [HMP 45] 12 m</li> <li>Pyranometer [Kipp+Zonen]</li> <li>Pyrgeometer [Eppley]</li> </ul> <p><u>Ground level</u></p> <ul style="list-style-type: none"> <li>Pressure sensor [PTB 200 A]</li> <li>Tipping bucket rain gauge</li> </ul>	<p><u>Tower (40m AGL)</u></p> <ul style="list-style-type: none"> <li>3D sonic anemometer [CSAT3]</li> <li>Infrared gas analyser [LI-7500]</li> <li>Krypton hygrometer [KH20]</li> <li>Temperature-relative humidity [HMP45C]</li> <li>Net radiometer [Q7.1]</li> <li>Albedometer [CM 7B]</li> <li>Pyrgeometer [CG2]</li> </ul>	<p><u>Tower (22m AGL)</u></p> <ul style="list-style-type: none"> <li>3D sonic anemometer [CSAT3]</li> <li>Infrared gas analyser [LI-7500]</li> <li>Temperature-relative humidity sensor [HMP45AC]</li> <li>Net radiometer [NR-01]</li> </ul> <p><u>Ground level</u></p> <ul style="list-style-type: none"> <li>Rain gauge [TB4]</li> </ul>
10/20 Hz data corrections	<ol style="list-style-type: none"> <li>Planar fit rotation (Wilczak et al.,2001)</li> <li>Block averaged (30 min)</li> <li>Offset for sensor lag (co-variance maximization)</li> <li>Signal de-spiking (Vickers and Mahrt, 1997), accepted spikes: 1 %</li> <li>Missing sample allowance 10 %</li> <li>Density effects (Webb <i>et al.</i>, 1980)</li> <li>Flagging according Foken 2003, QC &gt;= 7 discarded</li> </ol> <p>Foot print model: Kormann and Meixner 2001</p>	<ol style="list-style-type: none"> <li>Double rotation</li> <li>Block averaged (60 min)</li> <li>Offset for sensor lag (co-variance maximization)</li> <li>Signal de-spiking (Mauder <i>et al.</i> 2013), accepted spikes: 2 %</li> <li>Missing sample allowance 10 %</li> <li>Density effects (Webb <i>et al.</i>, 1980)</li> <li>Flagging according Foken 2003, QC &gt;= 7 discarded</li> </ol> <p>Foot print model: Kormann and Meixner 2001</p>	<ol style="list-style-type: none"> <li>Signal de-spiking</li> <li>Oxygen absorption (Tanner <i>et al.</i>, 1993)</li> <li>Offset for sensor lag</li> <li>Block averaged (30 min)</li> <li>Density effects (Webb <i>et al.</i>, 1980)</li> </ol> <p>Foot print model: None reported</p>	<ol style="list-style-type: none"> <li>Signal de-spiking</li> <li>Aligned into natural wind coordinates (w = 0) (Kimal &amp; Finnigan, 1994)</li> <li>Offset for sensor lag</li> <li>Block averaged (30 min)</li> <li>Frequency response correction</li> <li>Density effects (Webb <i>et al.</i>, 1980)</li> </ol> <p>Foot print model: Schmid <i>et al.</i>, 1991</p>

## 4.6 Results

In the following sections the results of the systematic experiment for the four flux sites across each of the stages are presented. The differences in model performance between stages and how these differences related across the four sites is the primary focus. The performance of SUEWS in simulating the radiative fluxes where they have direct bearing on the subsequent estimation of the turbulent fluxes is also highlighted. Our analysis focused on two key temporal scales; (i) hourly / mean diurnal simulations and (ii) daily flux densities. We also examined seasonal performance focusing on two key periods where solar insolation is at a minimum / maximum and where phenological conditions result in different surface processes occurring, namely (i) winter-time, conventionally defined as the months of December January and February (DJF) in the northern hemisphere and (ii) summer-time, defined as June July and August (JJA). When reporting seasonal results, the months of DJF are used for MEL for summer and JJA for winter.

### 4.6.1 Stage 1: Daily and Hourly Performance Results

The first stage of the experiment established a base-line performance against which the subsequent addition of more detailed meteorological and land cover data is judged. In this stage of the experiment, landcover data are not obtained directly from the area surrounding each of the flux sites, but rather by sampling the LCZ. The performance for each of the sites are highlighted in Table 4.6.

The ranking from lowest to highest RMSE (values reported in parenthesis) based on the daily estimates of  $Q_E$  - PHX performed best in stage 1 ( $9.66 \text{ W m}^{-2}$ ), followed by DUB ( $9.98 \text{ W m}^{-2}$ ), MEL ( $30.99 \text{ W m}^{-2}$ ) and HAM ( $37.72 \text{ W m}^{-2}$ ). In terms of model bias, PHX and MEL underestimate  $Q_E$  ( $-1.02$ ,  $-0.18$  respectively). DUB and HAM both showed negligible negative and positive biases ( $-0.02$  and  $0.02$ ) respectively. For  $Q_H$  the ranking from lowest to highest daily RMSE values was DUB ( $24.65 \text{ W m}^{-2}$ ) HAM ( $32.07 \text{ W m}^{-2}$ ) MEL ( $32.31 \text{ W m}^{-2}$ )

and PHX ( $47.27 \text{ W m}^{-2}$ ) in stage 1.  $Q_H$  was underestimated for the DUB site (-0.16) and overestimated for HAM (0.67), MEL (0.62) and PHX (0.31).

For  $Q_E$  the highest  $R^2$  value achieved in stage 1 was for HAM the lowest value was for PHX followed by MEL and DUB.  $Q_H$  in stage 1 is characterised by relatively high  $R^2$  values compared to  $Q_E$  (ranging from 0.26-0.69).

The calculation of RMSE based on hourly values often includes large isolated errors which can occur between specific hourly flux densities, these errors can arise either due to observational errors which were not filtered correctly or poor model performance. Unsurprisingly for most sites / variables, hourly RMSE was higher than daily RMSE, for instance, for DUB  $Q_E$  RMSE was  $37.11 \text{ W m}^{-2}$  which was approximately 3.5 times higher (i.e. worse) than the daily performance, though this was an extreme example. Generally hourly performance was 1.5 times poorer than daily for  $Q_E$  and  $Q_H$  in stage 1.

**Table 4.6 Root Mean Square Error (RMSE) statistics ( $W m^{-2}$ ) calculated for daily mean flux density and individual hourly flux densities. Also shown are mean fractional bias (MFB) calculated using the daily flux densities (-2 to +2). Also shown are the coefficient of determination ( $R^2$ ). A colour key summary for highest and lowest daily RMSE scores illustrating the best performance (lowest RMSE) to worse performance (highest RMSE): Lowest RMSE (best performance) = Green, Highest RMSE (worst performance) = Red, intermediate RMSE = Yellow**

[DUB]					[HAM]				[MEL]				[PHX]			
$Q_E$																
Stage	$R^2$	RMSE	RMSE (hourly)	MFB	$R^2$	RMSE	RMSE (hourly)	MFB	$R^2$	RMSE	RMSE (hourly)	MFB	$R^2$	RMSE	RMSE (hourly)	MFB
1	0.11	9.98	37.11	-0.02	0.45	37.72	23.96	0.02	0.06	30.99	26.11	-0.18	0.01	9.66	20.91	-1.02
2	0.10	10.51	21.54	0.01	0.48	47.02	27.78	0.20	0.07	32.70	25.75	-0.35	0.06	13.16	21.40	-0.80
3	0.06	19.47	25.79	0.67	0.47	51.53	48.81	0.17	0.05	32.67	23.55	-0.46	0.00	7.99	21.43	-1.26
$Q_H$																
Stage	$R^2$	RMSE	RMSE (hourly)	MFB	$R^2$	RMSE	RMSE (hourly)	MFB	$R^2$	RMSE	RMSE (hourly)	MFB	$R^2$	RMSE	RMSE (hourly)	MFB
1	0.67	24.65	28.61	-0.16	0.56	32.07	43.51	0.67	0.26	32.31	49.36	0.62	0.69	47.27	65.38	0.31
2	0.67	25.48	25.41	-0.17	0.54	38.96	37.87	0.58	0.25	31.77	52.39	0.69	0.67	43.59	60.40	0.27
3	0.59	39.89	32.68	-0.74	0.57	40.74	59.48	0.61	0.31	33.66	41.89	0.48	0.79	45.37	61.32	0.46
n		128	3567			353	4536			235	3705			291	6784	

#### 4.6.2 Stage 2 and Stage 3: Performance Results

In the second stage of the experiment, the land cover types used for the model runs were modified using fractional values calculated out to 1 km<sup>2</sup> surrounding each site. While these fractional values relate to the area directly surrounding the flux site, they require additional effort to compute. The largest difference between stage 1 and 2 in terms of land cover fractions was HAM and PHX which both had significantly lower building fractions than those calculated using the LCZ approach – recall Table 3. This was borne out in the model performance – Table 4.6. The impact of high resolution land cover was to increase daily RMSE marginally for Q<sub>E</sub> at all sites. The largest RMSE increase was 9.3 W m<sup>-2</sup> compared to stage 1 for HAM, followed by PHX, RMSE increased by 3.5 W m<sup>-2</sup>. The increase was 0.53 W m<sup>-2</sup> and 1.71 W m<sup>-2</sup> for DUB and MEL respectively. The impact on daily Q<sub>H</sub> was less consistent across the sites compared to Q<sub>E</sub>. For MEL and PHX a slight improvement was seen (RMSE decreased by 0.54 and 4.77 W m<sup>-2</sup> respectively) whereas performance decreased slightly for DUB (0.83 W m<sup>-2</sup>) and HAM (6.89 W m<sup>-2</sup>).

Model bias did not change direction in stage 2, for HAM the positive bias (i.e. model overestimation) for Q<sub>E</sub> increased by 0.18. For MEL and PHX, which both exhibited negative bias (i.e. model underestimation) in stage 1 also had negative biases in stage 2. The bias increased by 0.17 for MEL but a significant improvement was seen in PHX, bias was reduced by 0.22, though the model still underestimated Q<sub>E</sub>. For DUB, there was no change in bias for Q<sub>E</sub> and Q<sub>H</sub> between stage 1 and 2. Interestingly, the impact on RMSE calculated from the hourly flux densities in stage 2 was an average reduction in RMSE of 2.5 W m<sup>-2</sup>. The largest improvement in hourly flux calculation was Q<sub>E</sub> for DUB which reduced RMSE by 15.57 W m<sup>-2</sup>.

For the final stage of the experiment, off-site meteorological forcing data was replaced with measurements made on site. The most significant difference for this stage is the use of

observations of the incident radiation ( $K_{\downarrow}$ ,  $L_{\downarrow}$ ) made at the four sites. There was little impact on daily RMSE in stage 3 for HAM, MEL and PHX when compared to values for stage 2. For DUB, daily RMSE increased by 8.96 and 14.41  $\text{Wm}^{-2}$  for  $Q_E$  and  $Q_H$  respectively. For HAM, RMSE increased by 4.51 and 1.78  $\text{Wm}^{-2}$  for  $Q_E$  and  $Q_H$ , whereas for PHX, RMSE was decreased by 5.17  $\text{Wm}^{-2}$  for  $Q_E$  and increased by 1.78  $\text{Wm}^{-2}$  for  $Q_H$ . RMSE for MEL was practically unchanged in terms of  $Q_E$  between stage 2 and 3 (improved model performance by 0.03  $\text{Wm}^{-2}$ ) similarly to HAM and PHX the difference in  $Q_H$  was  $< 2 \text{ Wm}^{-2}$  (1.89  $\text{Wm}^{-2}$ ).

A larger impact was seen in the hourly flux density RMSE, particularly for HAM - moving from stage 2 to 3, RMSE increased by a similar amount for both  $Q_E$  (21.03  $\text{Wm}^{-2}$ ) and  $Q_H$  (21.61  $\text{Wm}^{-2}$ ) though the bias remained positive indicating overestimation by the model compared to the observations. For DUB, model RMSE also increased between stage 2 and 3 by 4.25 and 7.27  $\text{Wm}^{-2}$  for  $Q_E$  and  $Q_H$ . For MEL, hourly performance improved (RMSE decreased) slightly for  $Q_E$  (2.2  $\text{Wm}^{-2}$ ) and  $Q_H$  (10.5  $\text{Wm}^{-2}$ ) between stage 2 and 3. There was no impact on hourly RMSE for PHX between stage 2 and 3 (0.03 and 0.92  $\text{Wm}^{-2}$ ) – though it should be noted hourly  $Q_H$  RMSE was the highest amongst the four sites with a persistent positive bias (model over estimation of  $Q_H$  compared to observations).

#### 4.6.3 Seasonal and Annual Performance Results

The seasonal RMSE values are given in Table 4.7. Model performance tended to be better in winter than summer for all sites during all stages based on the RMSE. RMSE for  $Q_E$  was lower than  $Q_H$  for all sites in both seasons. Looking initially at difference between the seasonal RMSE for individual stages, the largest difference in model performance was for  $Q_H$  for PHX, performance in summer was 31.11, 18.83 and 33.57  $\text{Wm}^{-2}$  worse than winter in stage 1, 2 and 3 respectively. The smallest difference in seasonal performance was for  $Q_E$  for DUB.

Examining the seasonal difference across all stages reinforces the trend between summer and winter performance. The performance in summer is worse for both  $Q_H$  and  $Q_E$ , the

exception was  $Q_E$  for MEL which exhibits higher RMSE in winter and  $Q_H$  for DUB which was slightly higher, though this was due to large wintertime RMSE in stage 3: for stage 1 and 2 RMSE was higher in summer. While there was a clear difference in the seasonal performance for all sites, the difference between stages were small with only some exceptions.

To account for the seasonal differences in the magnitude of available energy between winter and summer and enable comparison across seasons, the nRMSE was also calculated, which normalises the RMSE using the range of observed turbulent flux magnitude. This relates the magnitude of the error to the magnitude of the observed flux. Where the mean of the observed flux approaches  $0 \text{ Wm}^{-2}$  (values highlighted in Table 4.7) the nRMSE should be interpreted with some caution. Nevertheless, nRMSE for  $Q_E$  and  $Q_H$  tended to be lower in winter than summer for stages 1-2.

The overall annual performance for each of the sites are presented as Taylor diagrams in Figure 4.4, which compares the individual stages. Taking the entire annual performance across all sites, the difference between stages 1 and 2 are generally lower than between stages 1 and 3. The centred RMSE for  $Q_H$  tended to be higher for all sites, there was also stronger correlation with observations for  $Q_H$  than for  $Q_E$ . The simulated annual variation ( $\sigma$ ) across the entire period was close with the variation in observations, the clear exceptions were  $Q_E$  for DUB which exhibited significant higher variation in observations compared to the model in all stages. The other exception was  $Q_H$  for MEL which illustrated higher variation in the model compared with the observations. Stage 1 (LCZ derived inputs) and Stage 2 (high-resolution land cover) exhibited similar performances on an annual basis.

**Table 4.7 Seasonal RMSE values calculated for each site. Summer refers to June July and August for DUB, HAM and PHX and December January February for MEL. Winter refers to December January February for DUB, HAM and PHX and June July and August for MEL. Values are in  $\text{Wm}^{-2}$ . RMSE values are derived using daily flux densities thus are slightly more conservative than hourly RMSE values. Given also is the nRMSE which normalises the RMSE using the range of observational data, hence the effect of larger flux magnitudes in summer are removed. Highlighted are values where the mean observed flux density was close to  $0 \text{ Wm}^{-2}$  meaning the normalised values should be interpreted with caution.**

$Q_E$						$Q_H$					
Stage	Metric	DUB	HAM	MEL	PHX	Stage	Metric	DUB	HAM	MEL	PHX
Summer						Summer					
1	RMSE	12.13	27.69	16.08	29.27	1	RMSE	25.86	46.86	39.29	48.70
2	RMSE	12.75	26.76	17.05	22.46	2	RMSE	27.39	35.22	40.89	39.65
3	RMSE	18.09	25.98	16.84	31.40	3	RMSE	28.85	31.74	34.37	57.04
1	nRMSE	51.7%	22.9%	24.1%	23.0%	1	nRMSE	16.7%	36.7%	20.9%	32.3%
2	nRMSE	54.4%	22.1%	25.6%	17.6%	2	nRMSE	17.7%	27.6%	21.8%	26.3%
3	nRMSE	77.1%	21.5%	25.2%	24.6%	3	nRMSE	18.6%	24.8%	18.3%	37.8%
Winter						Winter					
1	RMSE	8.28	10.78	20.39	13.32	1	RMSE	23.05	21.93	39.92	17.59
2	RMSE	8.73	12.08	20.38	18.71	2	RMSE	25.40	22.87	44.31	20.82
3	RMSE	21.42	41.36	19.90	13.65	3	RMSE	41.85	48.32	24.44	23.47
1	nRMSE	21.4%	19.6%	16.7%	84.8%	1	nRMSE	15.2%	19.9%	38.4%	24.3%
2	nRMSE	22.6%	21.9%	18.3%	119.1%	2	nRMSE	16.7%	20.8%	42.2%	28.8%
3	nRMSE	55.4%	75.1%	17.7%	86.9%	3	nRMSE	27.6%	43.9%	24.1%	32.5%

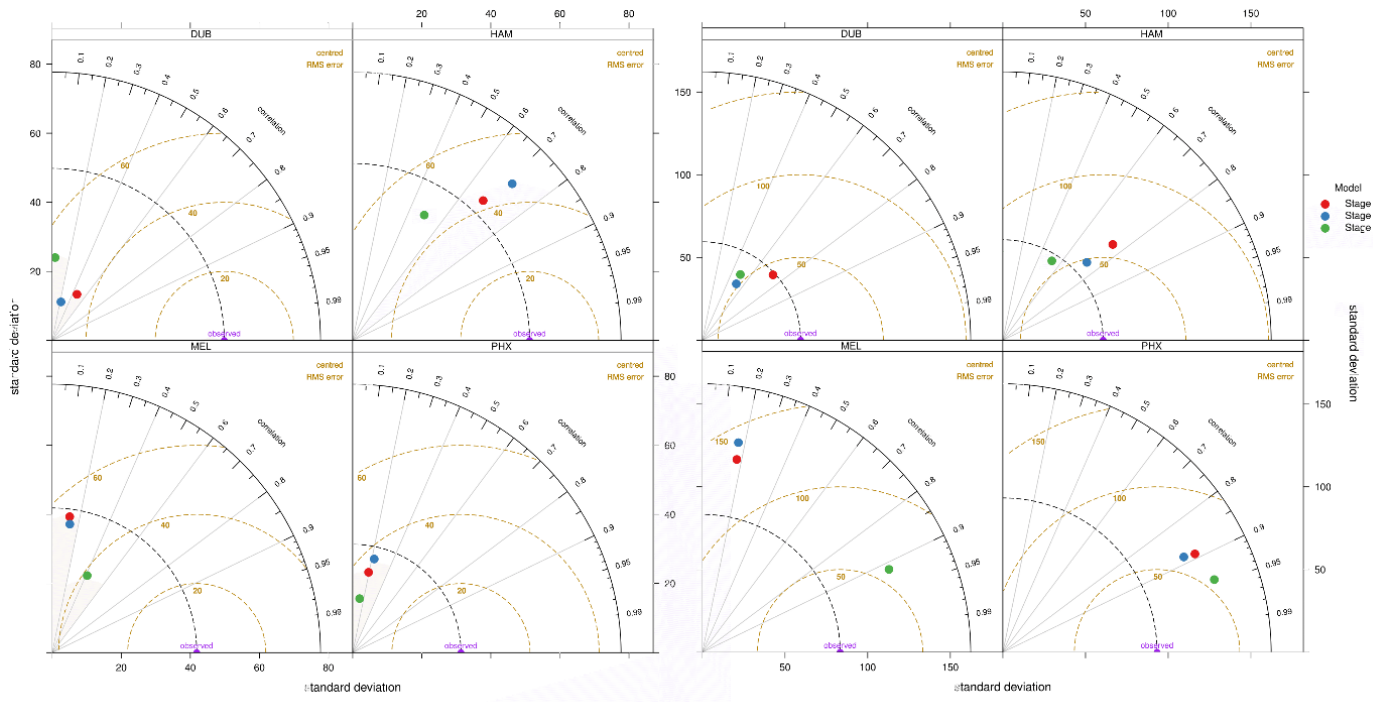


Figure 4.4 Taylor diagrams based on all (i.e. hourly) observations for  $Q_E$  (left) and  $Q_H$  (right)

## 4.7 Discussion

Despite differences in background climate, urban land cover type, building materials, and vegetative species, the performance of SUEWS in simulating the turbulent fluxes  $Q_E$  and  $Q_H$  is broadly consistent between sites. RMSE for  $Q_E$  falls into a range of between 20-30  $Wm^{-2}$  while a RMSE range of 40-60  $Wm^{-2}$  for  $Q_H$  captures all sites, ranges similar to those reported in Järvi *et al.* (2011) for Los Angeles and Vancouver. The improved ability of the model in simulating  $Q_E$  is evident, errors were consistently lower than  $Q_H$  for most of the sites.

The addition of high resolution land cover fractions did not significantly impact on model performance across any of the sites considered, despite large differences between those calculated by the LCZ approach. Given the increased amount of effort required to derive the high resolution fractions, it appears LCZ fractional values can satisfactorily be used in combination with the SUEWS model.

In all stages, the model captures well the relative differences between the four sites when considering both latitude and urban density. For the urban LCZ considered here,  $Q_H >$

$Q_E$  while  $Q_E$  is higher in summer owing to phenological development and higher amount of energy. Both of these factors may explain the seasonal variation in performance whereby performance was better in winter than summer. Vegetation, even small amounts, have been identified as a critical component for most UEB models (Loridan et al., 2010; Grimmond et al., 2011), here single species (i.e. deciduous or coniferous) were used for all sites, it is possible that increased detail on annual phenological development, observed LAI progression for example, along with multiple species will reduce the seasonal differences in model performance.

As different levels of data are added to the model for the experiment, the impact on performance relative to the observation sites was largely consistent across all domains. In terms of hourly simulations of  $Q_H$ , using additional details on surrounding land cover fractions improved the model performance, though the reduction in RMSE was relatively minor (often  $< 15 \text{ Wm}^{-2}$ ) compared to stage 1 - there was no impact on bias direction. Similar magnitudes were found in previous work.

The impact of adding meteorological data collected adjacent the flux sites is the most difficult finding to explain. Generally, performance was diminished using on-site meteorological data coupled with high resolution land cover in all cases except PHX, though the differences were extremely small. This may be due to observational error whereby the meteorological data collected alongside the towers are unduly influenced by local effects whereas the flux platforms have a more representative fetch. This would certainly be the case for DUB and HAM which had relatively heterogeneous fetches surrounding the flux sites.

As with previous studies, errors should not be attributed solely to model performance; observations of  $Q_E$  are notoriously difficult and subject to large errors / uncertainty particularly immediately during and after precipitation events. Observations at each of the flux sites included underwent post processing of some kind however some observational errors may have

been included despite this and despite the additional filtering carried out using the LCZ approach and wind vectors. For instance, the magnitude of observed  $Q_E$  for DUB [LCZ 2] was larger than would be expected given the sparse amount of vegetation surrounding this site. A similarly instrumented site also classed as LCZ 2 (reported in Alexander *et al.* 2015) exhibited a much lower magnitude and range of  $Q_E$  during summer months, where the maximum observed value was about  $60 \text{ Wm}^{-2}$  and a median value of  $25 \text{ Wm}^{-2}$ . Here, the observed median value for DUB during summer was  $67.57 \text{ Wm}^{-2}$  with a maximum of  $215 \text{ Wm}^{-2}$  around midday. There is nothing that readily accounts for the large magnitude of  $Q_E$  observed at this site, again given the lack of vegetation. The instruments for DUB are located about 5 m lower than the alternative LCZ 2 site, so it is unlikely to be due to measurements being made within the roughness sublayer. However, this only occurred for the diurnal profiles, taking hourly and daily values goes some way towards filtering out such erroneous observations. In terms of the HAM site, the addition of more detailed land cover data resulted in a decrease in model performance – this is likely attributed to the source area of the observations following the filtering process. Note the fractional values immediately surrounding the site have a higher fraction of vegetation and water coverage however the observational dataset sought to exclude the influence of these land cover types. It is unsurprising the model overestimated the magnitude of  $Q_E$  in this instance.

Another important component for UEB model performance is net radiation. Here, there was a consistent overestimation of  $Q_H$  for PHX, this was due to the model underestimation of albedo ( $\alpha$ ) leading to lower value of  $K\uparrow$  (not shown). The model estimated  $\alpha$  to be 0.15 – however in reality, the building material in PHX are much lighter than the group average, as such,  $\alpha$  based on observations was  $\sim 0.25$ . Therefore, the model retained more energy, leading to overestimation of both  $Q_E$  and  $Q_H$ . This means a subset of LCZ material properties may need to be compiled for applying the model in environments with similar building materials, but it

should be noted the partitioning of energy normalised by available energy, that is  $Q_H/Q^*$  and  $Q_E/Q^*$ , was similar between observations and the modelled fluxes.

Nevertheless, SUEWS simulations for both daily and hourly turbulent fluxes agree well with observations using the LCZ approach, with errors well within previously reported ranges. This enables us for the first time to carry out inter-site comparisons in the UEB across similar LCZ types. Figure 4.5 shows the diurnal flux profiles for three LCZ 6 sites (derived using the setup in stage 1) to illustrate this point. As shown, the partitioning of energy amongst these sites are remarkably similar. Day length (i.e. positive  $Q^*$ ) is shown to be slightly longer in the DUB data with a lower amount of energy at midday as would be expected of this climate. As a consequence,  $Q^*$  at midday was  $457.25 \text{ Wm}^{-2}$ ,  $65 \text{ Wm}^{-2}$  lower than MEL and  $132 \text{ Wm}^{-2}$  lower than PHX. PHX exhibits slightly higher proportion of energy expended towards  $Q_H$  throughout the course of the day compared to both DUB and MEL, as would be expected given the lack of vegetation/water in this environment. The differences in land cover can also be examined e.g. building material and artificial surface extent across all sites can be examined in detail to explore the effect on  $\Delta Q_s$  – a principle component of nocturnal UHI formation.

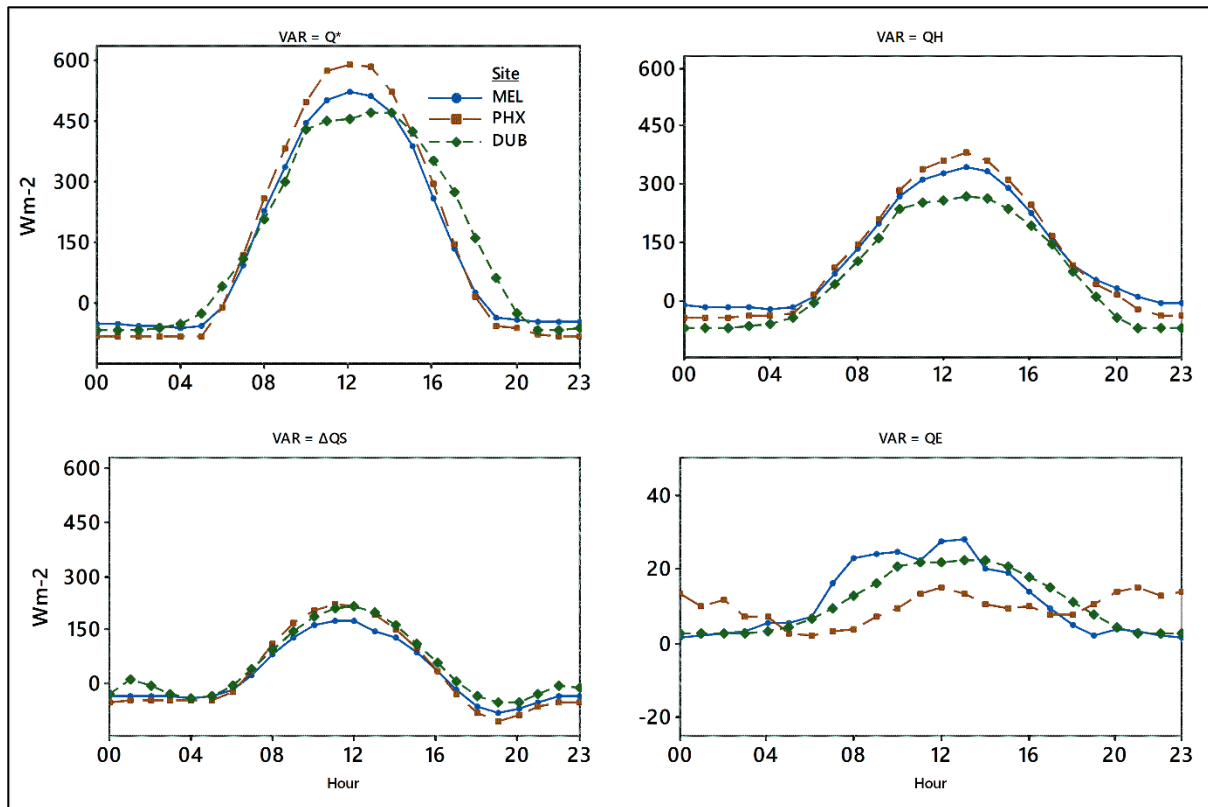


Figure 4.5 - LCZ 6 summer time Diurnal profile for MEL, PHX and also shown is LCZ 6 site from Alexander et al. (2015) Top left panel is  $Q^*$ , followed by  $Q_H$  (top right),  $\Delta Q_S$  (bottom left) and  $Q_E$  (bottom right)

The use of a standardised method for collecting land cover (LCZ) and meteorological data in order to perform initial assessments of an area's urban energy and water balance should not discourage the continued establishment of high-quality and long-term flux towers in cities. Here, we considered only three LCZ classes, namely LCZ 2, 6 and 8 as these represented the sites with available data. As additional instrumented sites become available, the approach outlined here should undergo further evaluation.

While the approach has obvious applications in overcoming fiscal/computational limitations in cities with limited resources, the application of the approach needs to be further validated in sparse urban environments, as well as non-urban environments. Different background climates should also be considered. While we requested urban flux data for a range of background climates the four sites included in this study were the only cities for which data were made available. Therefore, eddy-covariance platforms are still an essential investment in any city. Despite the limited sites included here, the extension of the LCZ-SUEWS approach

into additional arid / continental type climates undertaken here builds upon the original case study, which further supports the notion that the approach employed with the SUEWS model is capable of realistically simulating the UEB in a variety of circumstances and urban environments.

#### **4.8 Conclusions**

In this study we systematically tested a modeling approach which seeks to overcome data scarcity in terms of urban morphology and meteorological observations made within the urban environment. To that end, we coupled the local climate zone (LCZ) scheme of Stewart and Oke (2014) with the surface energy and water balance scheme (SUEWS) v.2014b (Järvi et al., 2014). The approach was tested in four background climates and different urban configurations. Detailed land cover data and meteorological observations were added to the SUEWS model in stages to examine the impact on model performance relative to the coarse LCZ data and meteorological observations made at airports conforming to WMO standards.

The results show that the addition of detailed data on model performance varied across the sites considered, however root mean squared error (RMSE) consistently fell within a range of between 20-40  $\text{Wm}^{-2}$  for  $Q_E$  and between 40- 60  $\text{Wm}^{-2}$  for  $Q_H$ . The difference between the use of LCZ and detailed land cover was generally small indicating that utilising LCZ data with SUEWS for the initial assessment of the urban energy and water balance is an appropriate approach to take. Furthermore, meteorological observations which are designed to exclude the urban effect are appropriate as forcing data for SUEWS, without impacting significantly on model performance. The results indicate that this modelling approach can be used in data poor settings to rapidly derive in a consistent manner the parameters required by most urban climate models, provided an LCZ map of the city is available.

---

## Chapter 5 Spatial validation of an urban energy balance model using multi-temporal remotely sensed surface temperature

---

### 5.1 Preface

This chapter is published as:

Alexander, P.J., Fealy, R., Mills, G. (2015) Spatial validation of an urban energy balance model using multi-temporal remotely sensed surface temperature, in *IEEE Urban Remote Sensing Event (JURSE), 2015 Joint*, vol., no., pp.1-4, March 30 2015-April 1 2015 doi: 10.1109/JURSE.2015.7120500

An abridged version of this chapter containing its core findings was published in *IEEE*, as part of the Joint Urban Remote Sensing Event conference (JURSE) proceedings, Lausanne, Switzerland. An extended version of this paper is presented here based on reviewer feedback of the abridged version along with comments received at JURSE. Two aspects are examined in this chapter 1) the spatial validity of the LCZ-SUEWS approach for Dublin based on land surface temperature (LST) and 2) an evaluation of LCZ-SUEWS LST based on observations from the MODIS sensor. This latter aspect was excluded from the abridged version, however both 1) and 2) were presented at JURSE.

As highlighted in Chapter 2 of this thesis, validation and evaluation are separated on the basis of how the model is viewed. Here, validation refers to the ability of the LCZ-SUEWS approach to reproduce observed spatial patterns of LST, irrespective of accuracy, the hypothesis being that there would be *some* demarcation in LST between the urban centre of Dublin and the surrounding non-urban hinterland by SUEWS based on differences in thermal characteristic (principally albedo) and vegetative coverage. Evaluation on the other hand refers specifically to the accuracy of simulated LST with respect to observations, a smaller subset of the domain used for validation was used for the evaluation and the temporal scale was also shifted to examine the mean surface urban heat island (SUHI) based on monthly values over the course of an entire year both during daytime and nighttime.

## 5.2 Abstract

Despite a growing number of urban energy balance (UEB) model applications being undertaken within urban climate literature, the number of independent validation exercises remains very limited. This in turn has raised questions as to the value of model applications without due consideration to the models performance in space and time. The PILPS-URBAN project (Grimmond, et al., 2010; Grimmond, et al., 2011) went some ways towards understanding the general performance of 33 UEB models and highlighted the need for careful treatment of urban and non-urban land surfaces within model parameterisation and also the derivation of input parameters. Nevertheless, the need for independent external validation of specific models is now evident. While there are some examples of model evaluation at point locations where eddy-covariance (EC) platforms measure turbulent fluxes, very few studies have evaluated UEB models across a wider space. EC platforms must remain fixed at a location for a significant period of time in order to determine source areas and must also be elevated above the urban canopy layer, roughly twice the height of the surrounding roughness elements e.g. buildings and vegetation. Therefore, in order to evaluate model performance across space, novel approaches are needed. Here we undertake an external evaluation of the SUEWS model in Dublin (Ireland). We present a method for spatially validating and evaluating the model across the Dublin area by employing remotely sensed surface temperatures obtained through the MODIS sensor. Our analysis focussed on two principle aspects: firstly, the validity of simulated LST from SUEWS, that is, the ability of the model to demarcate the urban area from its surrounding non-urban hinterland and secondly an evaluation of modelled LST in terms of reproducing the magnitude of the surface urban heat island.

### 5.3 Introduction

Urban areas are the most significant biome for human habitation with over half of the world's population residing within cities across the globe (Satterthwaite, 2007). The introduction of hard, impervious surfaces results in a significantly modified land cover which in turn modifies the energetics at the interface between the surface and the atmosphere (Oke, 1988; Kimura & Takahashi, 1991). Understanding this modification both historically and into the future is now critical as continued urbanisation and demographic changes means more urban residents will become at risk to heat-related stresses especially as cities come to realise global climate change (National Research Council, 2012). In order to assess whether responses seeking to mitigate risk to urban dwellers are appropriate and cost effective requires detailed meteorological forecasting prior to their implementation. Atmospheric models are useful in this regard.

Broadly speaking, this requires two primary considerations in order to effectively aid decision making; 1) how urban areas are described in terms of their morphology and 2) the accuracy/ability of models to capture the key processes that impact on the urban population (Arnfield, 2003). In terms of the former, much work has gone into extracting detailed urban parameters for use in urban canopy models (UCMs) both from field work (Grimmond & Oke, 1991; Cleugh, et al., 2005) and remotely sensed data (Grimmond & Souch, 1994; Middel, et al., 2012). Whereas the latter has received much less attention, generally UCMs are only validated by model developers themselves. Moreover, it is typical that urban models are validated against in-situ measurements made within distinctive urban landscapes. This approach assumes that the area in which observations are made can be reproduced across the entire urban area, however in light of the difficulty in placing observational platforms (both in terms of urban heterogeneity and identifying a location that is safe and secure) often it is the case that this assumption cannot be upheld except in very specific circumstances.

Employing a modelling and observational approach which deliberately generalises an urban area into its key components which yield the most significant impact on land-atmosphere exchanges can go some ways towards alleviating this problem (Chapter 2, Chapter 3). However, if more UCMs are to include dynamic effects such as advection (the horizontal transfer of energy and/or mass) there will be a growing need to assess how models performance spatially.

Reformulating observational approaches can achieve this, but will inevitably encounter the same issues highlighted above when brought to bear on a real urban situation. Recently it has been proposed to utilise remotely sensed (RS) observations for model validation which have an obvious spatial advantage over in-situ platforms (Tomlinson, et al., 2011; Hu, et al., 2014).

Here we build upon the work carried out by others by undertaking to spatially validate and evaluate the Surface Energy and Water Balance Scheme (SUEWS) model in Dublin, Ireland. We employ standard metrics to evaluate model performance at two flux observation platforms, providing an estimate of its performance at 2 points. Subsequently we employ RS land surface temperature (LST) data from the MODIS sensor to assess how the model performs across Dublin city during conditions that are conducive to strong urban modification of the atmosphere. Following on from establishing whether or not the model is spatially valid, we evaluate its simulations of LST by examining the surface urban heat island (SUHI) across a one-year period.

#### **5.4 Urban Energy Balance Models**

A number of urban models have been developed at a variety of spatial and temporal scales with a range of applications, the most common of which are based on the urban energy budget (UEB):

$$Q^* + Q_F = Q_H + Q_E + \Delta Q_S \quad \text{W m}^{-2} \quad \text{Eqn. 5.1}$$

$Q^*$  is net radiation,  $Q_F$  is anthropogenic heat flux,  $Q_H$  and  $Q_E$  are the turbulent sensible and latent heat fluxes, respectively and  $\Delta Q_S$  is storage heat flux. This equation refers to a representative urban volume that extends from the surface in which there is no net horizontal transfer (that is, an extensive surface type) and no significant energy exchange across the lower boundary. Hence, assessing each of the terms at the upper surface of the volume, which is located above the canopy layer captures the exchanges between the urban surface and overlying boundary layer. The process of urbanisation results in the replacement of natural surfaces by hard impervious surfaces (e.g. roads, pavements, car parks) and buildings. This greatly alters the surface energy balance by, for example, increasing (decreasing) the sensible (latent) heat flux and increasing heat storage. One of the best known outcomes is the formation of an urban heat island.

The UEB model used here is the Surface Urban Energy and Water Balance Scheme (SUEWS v.2013b). SUEWS is able to simulate both the UEB (Eqn. 5.1) and urban surface water balance of an urban neighbourhood and requires a relatively low number of input requirements that may include: meteorological data; population-economy related data and; surface cover and urban structure data. Some of these inputs are required to run the model, while other inputs are optional. At the very least the model requires standard meteorological data and details on the fractions of the landscape that is occupied by buildings, vegetation, impervious paving, etc. Järvi, et al. (2011) evaluated SUEWS using flux observations (spanning various time lengths from different years) from individual neighbourhoods in Los Angeles (34°N, Köppen climate type dry-summer subtropical, Csb) and Vancouver (49°N, Maritime temperate climate, Cfb). The results showed the model to be capable of simulating net radiation, sensible and latent and heat fluxes with root mean squared error (RMSE) ranges of 25-47  $Wm^{-2}$ , 30-64  $Wm^{-2}$  and 20-56  $Wm^{-2}$ , respectively.

We examine the performance of the SUEWS model at both individual points (flux sites) and across a wider space. Our examination is based on data gathered for Dublin, Ireland (53° N, 6° W), which has a mild, mid-latitude climate (Cfb). It provides an ideal place for this study as it has two observation sites (located in urban and suburban landscapes) where detailed energy flux and meteorological observations have been made since 2009; these data can be used to run the model and compare its simulations with observations. In addition, there is a local climate zone (LCZ) description of the city that outlines major neighbourhood types and standard weather station observations available at Dublin Airport, which is between 5 and 10 km distant from the urban and suburban flux sites, respectively.

## 5.5 Methods

### 5.5.1 SUEWS model

The SUEWS model (V.2014b used here) was designed for urban simulations at a neighbourhood-scale, which corresponds to an area of 1 km<sup>2</sup>. It simulates both the urban energy budget (Eqn. 5.1) and urban water budget:

$$P + I_e + F = E + R + \Delta S \text{ mm h}^{-1} \quad \text{Eqn. 5.2}$$

Where P is precipitation,  $I_e$  is externally piped water, F is anthropogenic water emission, E is evaporation (including transpiration), R is runoff and  $\Delta S$  is change in storage. Eqns. 5.1 and 5.2 are connected directly through the evaporative terms ( $Q_E$  and E) and indirectly via other terms; for example, a precipitation event may result in water storage in soil that will affect its thermal properties. The energy budget (Eqn.5.1), describes flux exchanges at a plane that separates the roughness sub-layer (between 2 to 4 times the mean height of the roughness elements) from the boundary-layer above. The modelled fluxes therefore correspond to the inertial sub-layer, where micro-scale variability driven by individual roughness elements becomes integrated into neighbourhood signals. This corresponds with the spatial resolution of the MODIS satellite platform (1km). One should note the absence of explicit advective terms

in Eqn. 5.1, so that it assumes there is a negligible horizontal energy transfer. Strictly speaking then, this limits the application of SUEWS to extensive neighbourhood types where the landscape may be described as relatively homogenous. The inclusion of a working UWB is an important component as this will directly impact on the partitioning of energy at the surface (Figure 5.1). Hence, the SUEWS model was chosen since it includes both the UEB and UWB. SUEWS employs the Net All-wave Radiation Parameterisation (NARP) which approximates LST (for the purpose of calculating  $L\uparrow$ ) based on  $T_a$  and corrects using observations of  $K\downarrow$  and surface albedo during the daytime (Offerle, et al., 2003).

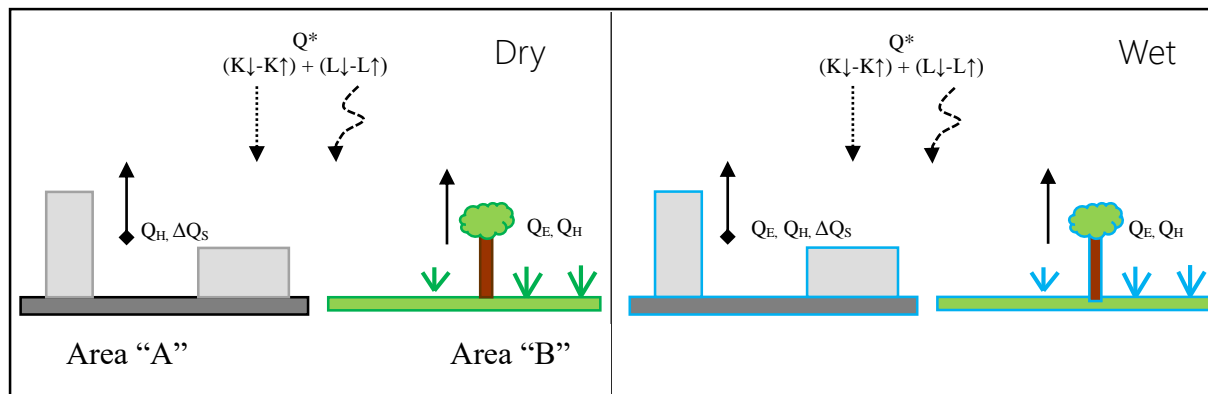


**Figure 5.1 Overview of the conceptual relationship between the UWB and LST. In the dry case for Area “A” - available energy ( $Q^*$ ) will be used to heat the surface / air ( $Q_H$ ) and be stored within the urban volume ( $\Delta Q_s$ ). In the wet case, assuming all surfaces are covered in water (water bucket approach) the available energy is channelled into evaporation until the surface is dry, hence less energy is gained relative to the dry case which results in lowering of LST to compensate. SUEWS includes a ‘running’ UWB, different surfaces can transfer water to others e.g. water can runoff from roof-tops to pavements therefore SUEWS is far more physically realistic compared to a simple water bucket approach**

### 5.5.2 Forcing data and observation platforms

The atmospheric observations used here come from standard meteorological information obtained for Dublin airport, which is located 5 km from the city centre in an area dominated by warehouses, LCZ 9 and low plant cover, LCZ D - Figure 5.2. Hourly observations are available for a number of elements: air temperature ( $T$ ), precipitation ( $P$ ), pressure ( $Pr$ ), humidity ( $RH$ ), wind-speed ( $V$ ) and direction and solar radiation receipt ( $K\downarrow$ ). Note that hourly values for  $K\downarrow$  are a required model input. These data are used to force the model.

SUEWS also requires fractional coverage of land cover types. The model was furnished with land cover fractions (i.e. % building, pavements, grass, trees, water and soil) for Dublin based on typologies generated from the LCZ classes present in Dublin (Chapter 3, Chapter 4). We employ LCZ as the basis for examining the correlation between MODIS LST and modelled LST. The model simulations of  $Q_H$  and  $Q_E$  are evaluated against flux data that is acquired at two stations (see Figure 5.2) that are part of the International Urban Flux Network.

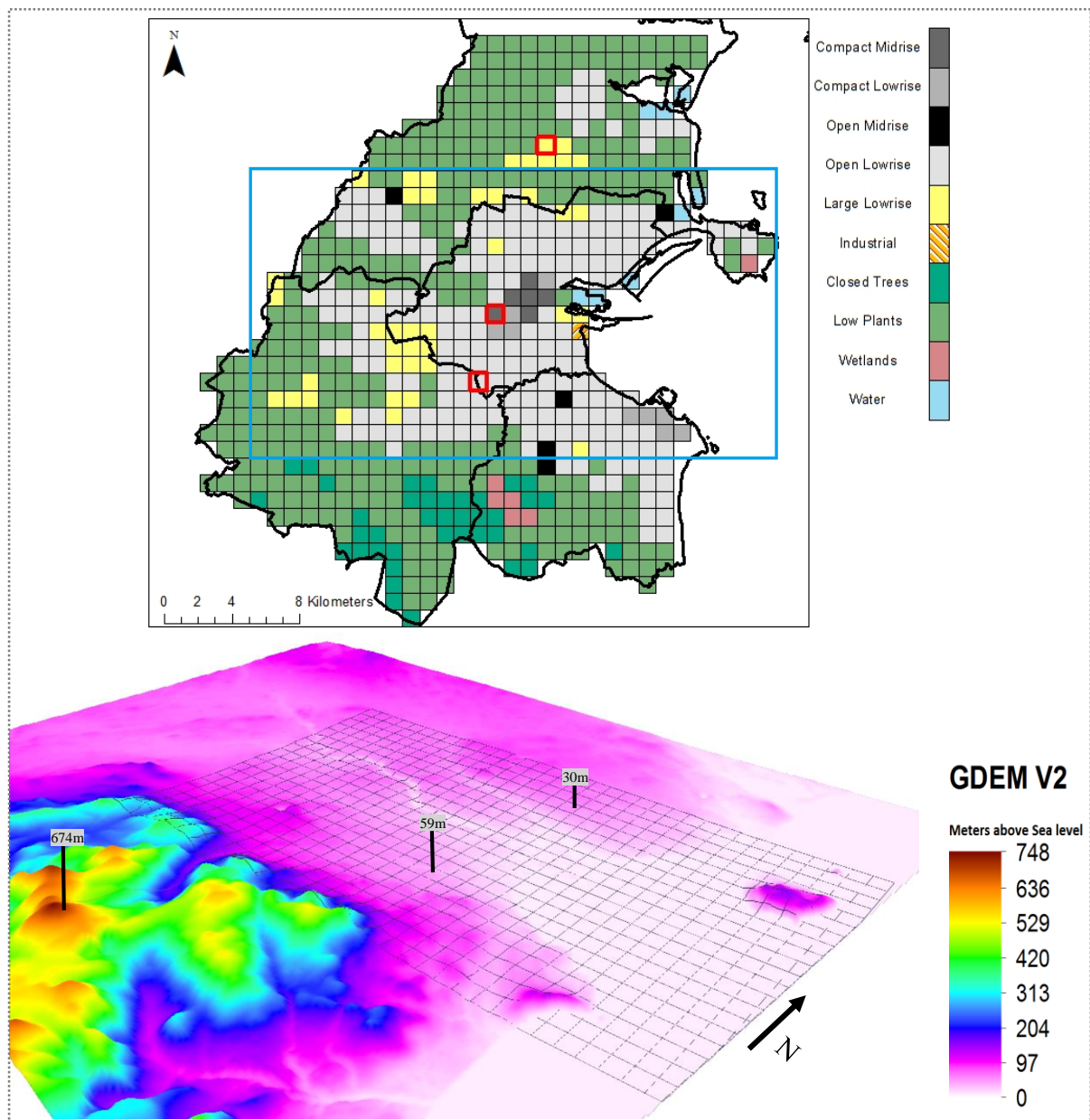


Figure 5.2 Above – overview of the model domain for validation and the subset used for evaluation The red boxes show the location of the flux towers and the location of the WMO site adjacent Dublin airport. The southernmost grid is the suburban flux tower (LCZ 6) the centre grid contains the urban flux site (LCZ 2) and the northernmost grid is the airport synoptic station. Below – visualisation of the relief of the evaluation subset (DEM data from NASA, GDEM V2), the callouts show the general pattern of elevation from south to north. Note the area considered is relatively consistent in terms of topography, which was done to minimise the effect of relief on LST

The measurement sites were selected to represent sites that typify Dublin's urban land-cover (Keogh, et al., 2012). The suburban site is located in a residential area consisting of similar two-story houses about 6 m tall; much of the landcover is vegetated (open lowrise or LCZ6). Each has an identical suite of instruments and radiation and turbulent flux terms are recorded alongside the meteorological variables listed above. The instruments are positioned on a mast that is situated on the roof of a school at a height of 12 m (10 m for the net radiometer). The urban site is located in a mixed-use area closer to the city centre; much of the surrounding landscape is impermeable and the average building height is about 8 m (compact midrise or LCZ2). The support mast is on the roof of a 12 m tall building and the instruments are at a height of 17 m (15 m for net radiometer).

Upward and downward facing radiometers provide  $K_{\downarrow}$ ,  $K_{\uparrow}$ ,  $L_{\downarrow}$  and  $L_{\uparrow}$ . The turbulent fluxes  $Q_H$  and  $Q_E$  heat are obtained using an open-path eddy covariance system that is interrogated at a rate of 10Hz; the recorded fluxes are based on 30 minute averages. The heat storage term ( $\Delta Q_S$ ) is estimated as a residual of the measured terms:

$$\Delta Q_S \approx Q^* - (Q_H + Q_E) \text{ W m}^{-2} \quad \text{Eqn. 5.3}$$

Each tower is located well within its LCZ type and the flux instruments are positioned at a level that is approximately twice the height of the surrounding buildings and at about the height of the inertial sub-layer established by that surface type. In other words, we are assuming that advection is negligible and that  $\Delta Q_A$  can be ignored. A measure of the goodness of fit is provided by the Root Mean Squared Error (RMSE):

$$\text{RMSE} = \left[ \sum_{i=1}^n \frac{(\hat{y}_i - y_i)^2}{n} \right]^{0.5} \quad \text{Eqn. 5.4}$$

Where  $(\hat{y}_i - y_i)$  represents the difference between the observed ( $y_i$ ) and simulated ( $\hat{y}_i$ ) flux term (e.g.  $Q^*$ ) at each hourly time interval ( $i$ );  $N$  represents the total number of hours. RMSE is commonly used to assess the total error, regardless of its direction.

### 5.5.3 Spatial Validation

Our spatial validation is based on data obtained by the MODIS sensor on board the Terra Platform. This provides users with LST obtained four times per day at a 1km resolution. To spatially validate the model, that is, examine the extent to which SUEWS is capable of demarcating the urban area from the non-urban, we took the following approach:

- We obtained 1km LST for Dublin for a one-year period (2010) from MODIS sensor on board the Terra platform (Aqua was excluded due to computational limitations)
- These data were clipped to the domain of interest (Figure 5.2) and a model grid generated to align with the LST pixels (1x1 km)
- The clipped data were filtered for cloud cover by only selecting scenes where no-data pixels did not exceed 20% of the model domain
- These data were further filtered so as to only include periods with several runs of consecutive days
- Daytime LST was extracted due to the correction used within the NARP model (as discussed in Section 5.5.1 above)

The resulting period for validation ran from 07 April 2010 – 21 April 2010 (see Table 5.1). This limited temporal scope reflects the number of scenes that were cloud free over Dublin city, and somewhat restricts the interpretation of the results obtained. However, in our judgement while this covers a limited period to validate SUEWS spatially, it corresponds with conditions where the model may be expected to perform well i.e. clear-skies, little wind, no precipitation, therefore provides a best-case estimate of its performance across space. To validate simulated LST against observations from MODIS we generated our model grid to align with the LST pixels for each scene. Thus, each grid contained LST from MODIS for each of the days considered, as well as hourly modelled output from SUEWS.

As the objective was to examine the spatial validity of the model, our analysis focussed on relative partitioning of LST across different LCZ classes. We plotted MODIS LST against SUEWS at the corresponding overpass time by first calculating the mean LST for each LCZ class and subtracting this from the overall group mean for both the modelled (mod) and observed (obs) LST:

$$LST'_{mod,obs(i)} = \overline{LST}_{mod,obs(i)} - \sum_{i=1}^{i=7} \overline{LST}_{mod,obs(i)} \quad 5.5$$

This provides a deviation from mean state for each LCZ class, whereby a LCZ class can be above the mean state (i.e. positive thermal anomaly) or below the mean state (i.e. negative thermal anomaly).

**Table 5.1 Summary meteorological conditions for the period selected for validation of SUEWS. Data is from Dublin airport station (see Figure 5.1).  $T_a$  denotes mean 2m air temperature, U denotes mean wind speed, Sun denotes the number of sunshine hours,  $Sun_{pot}$  is the fraction of the day with sunshine relative to the number of available hours,  $G_{Rad}$  denotes the mean global radiation,  $E_v$  denotes daily evaporation. Note the 11-17<sup>th</sup> are particularly clear periods. Data sourced from National Meteorological Service of Ireland (Met Eireann)**

Date	$T_a$ °C	Pres hPa	U ms <sup>-1</sup>	Sun hours	$Sun_{pot}$ -	$G_{Rad}$ j/cm <sup>2</sup>	$E_v$ Mm
07/04/2010	7.3	1010.5	5.0	7.6	0.6	1528	2.8
08/04/2010	9.5	1019.5	4.8	3.9	0.3	1109	2.6
09/04/2010	8.3	1021.9	2.3	4	0.3	1352	2.3
10/04/2010	6.9	1022.3	3.1	7.5	0.6	1541	2.6
11/04/2010	8.9	1021.1	2.9	12	0.9	2034	1.4
12/04/2010	8.1	1019.9	2.7	10.7	0.8	1898	3.1
13/04/2010	6.4	1018.2	4.1	12.6	0.9	2131	3.2
14/04/2010	4.7	1015.8	4.2	7	0.5	1526	2.3
15/04/2010	4.6	1017.3	4.4	3	0.2	1127	1.9
16/04/2010	6.1	1018.1	3.4	13.3	0.9	2201	3.3
17/04/2010	8.4	1011.2	3.6	12.5	0.9	2155	3.8
18/04/2010	6.6	1007.1	2.6	3.2	0.2	1167	2.2
19/04/2010	5.2	1009	3.2	7.2	0.5	1299	2.2
20/04/2010	6.1	1011.6	4.5	9.4	0.6	1569	3
21/04/2010	3.4	1013	2.5	9.1	0.6	1919	2.9

#### 5.5.4 Spatial Evaluation

Following our point evaluation of simulated turbulent fluxes (5.5.2 above) and spatial validation (5.5.3 above) of LST deviations, we evaluated the ability of SUEWS to reproduce the annual cycle of the surface urban heat island (SUHI). For this, MODIS LST was averaged on a pixel by pixel basis for each month. These mean monthly LST values were then separated into daytime (DT) and night time (NT) LST values. The LCZs were then used to generate an average monthly LST for each LCZ class, thus, removing any spatial variation between the same LCZ class – see Figure 5.3. We defined the DT and NT SUHI as the difference between LST for the inner city (in the case of Dublin, LCZ 2) and the surrounding non-urban hinterland (LCZ D) hence, the SUHI is expressed as  $\Delta T_{LCZ 2 - LCZ 6}$ .

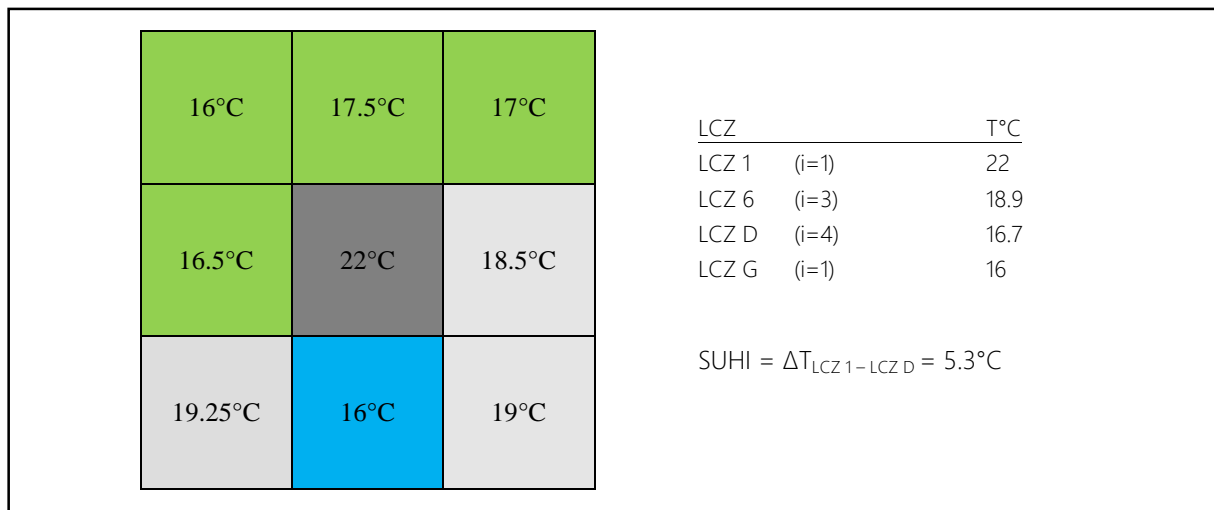


**Figure 5.3 Conceptual summary of the evaluation of LST. Each grid above represents an LST pixel from MODIS with an observed LST value (given in °C for convenience). The colours represent different LCZ classes, where Green is low plants (LCZ D) Blue is water (LCZ G) dark grey is compact highrise (LCZ 2) and light grey is openset lowrise (LCZ 6). LST is averaged across grids with the same LCZ class ('i'), hence the SUHI is expressed as a difference between mean LST for LCZ classes**

To evaluate SUEWS simulation of the SUHI we employed the RMSE (eqn. 5.4 above) and additionally generated Taylor Diagrams (Taylor, 2001) which employ three model performance metrics, namely the correlation coefficient (R) the centred RMSE ( $\sigma_D$ ) and Standard Deviation ( $\sigma$ ). Our overall aim in both validating and evaluating SUEWS was to demonstrate the general ability of the model for end users, as well as establish the value of employing remotely sensed land surface temperatures for carrying out model evaluation.

## 5.6 Results

We ran the SUEWS model during a period of relatively fine weather in April (April 11-17) 2010. We evaluated the models performance in simulating turbulent fluxes of energy against two point locations in our model domain. Subsequently, we employed RS LST from the MODIS sensor in order to examine the ability of SUEWS to demarcate urban LST from non-urban LST and in reproducing the SUHI. Initially, we present the model evaluation at our flux locations, followed by the results of the spatial validation and finally the evaluation of SUEWS simulations of the SUHI.

### 5.6.1 Point Performance for turbulent fluxes

The model performance at the flux sites for the one-week period is summarised in Table 5.2. Generally, SUEWS reproduced the turbulent fluxes ( $Q_H$ ,  $Q_E$  and  $\Delta Q_S$ ) well. The performance at the suburban flux site, LCZ 6, was slightly better than the urban flux site (LCZ 2) based on the sum of the RMSE (that is the combined RMSE for  $Q_H$ ,  $Q_E$  and  $\Delta Q_S$ ). RMSE for the LCZ 6 site (RMSE for LCZ 2 shown in parenthesis) were as follows:  $Q_H$  36.83 (58.43)  $Q_E$  15.77 (17.29) and  $\Delta Q_S$  34.96 (61.14)  $W m^{-2}$ .

**Table 5.2 Model performance at two locations in Dublin. Shown is the hourly RMSE (Eqn. 5.4) for sensible ( $Q_H$ ) latent ( $Q_E$ ) and storage ( $\Delta Q_S$ ) heat flux for the period April 11-17, 2010. The sum of the RMSE is given in the final row, which provides a quick overview of where the model performance was best**

April 11-17 2010	RMSE ( $Wm^{-2}$ )		
	<i>Turbulent Flux</i>	<i>LCZ 2 site (Urban)</i>	<i>LCZ 6 site (Suburban)</i>
	$Q_H$	58.43	36.83
	$Q_E$	17.29	15.77
	$\Delta Q_S$	61.14	34.96
	$\Sigma_{RMSE}$	136.86	87.56

Though  $Q_E$  is a relatively minor term at the LCZ 2 site, SUEWS reproduces the diurnal trend poorly relative to the observed diurnal trend (see Figure 5.4), however there is a noted improvement at the LCZ 6 site. The poorest simulated flux in terms of high RMSE at the LCZ

6 site was  $Q_H$  which was routinely overestimated by the model particularly at night; conversely  $\Delta Q_S$  was underestimated around this site during daylight hours (peaks in Figure 5.4). The simulation of  $Q_H$  and  $\Delta Q_S$  at the LCZ 2 site was remarkably similar to the observation tower though  $Q_E$  was underestimated routinely by a large amount hence the relatively large RMSE for this term. It is worth remembering that the model was forced with off-site data obtained at Dublin airport, which perhaps is closer in morphological characteristics to the LCZ 6 site. Nevertheless, the model performs well over the week simulated with respect to following a logical diurnal pattern, furthermore, given the morphology of both sites in terms of vegetative cover, the model reproduces well the differences in energy partitioned into evapotranspiration ( $Q_E$ ) between the urban and suburban site.

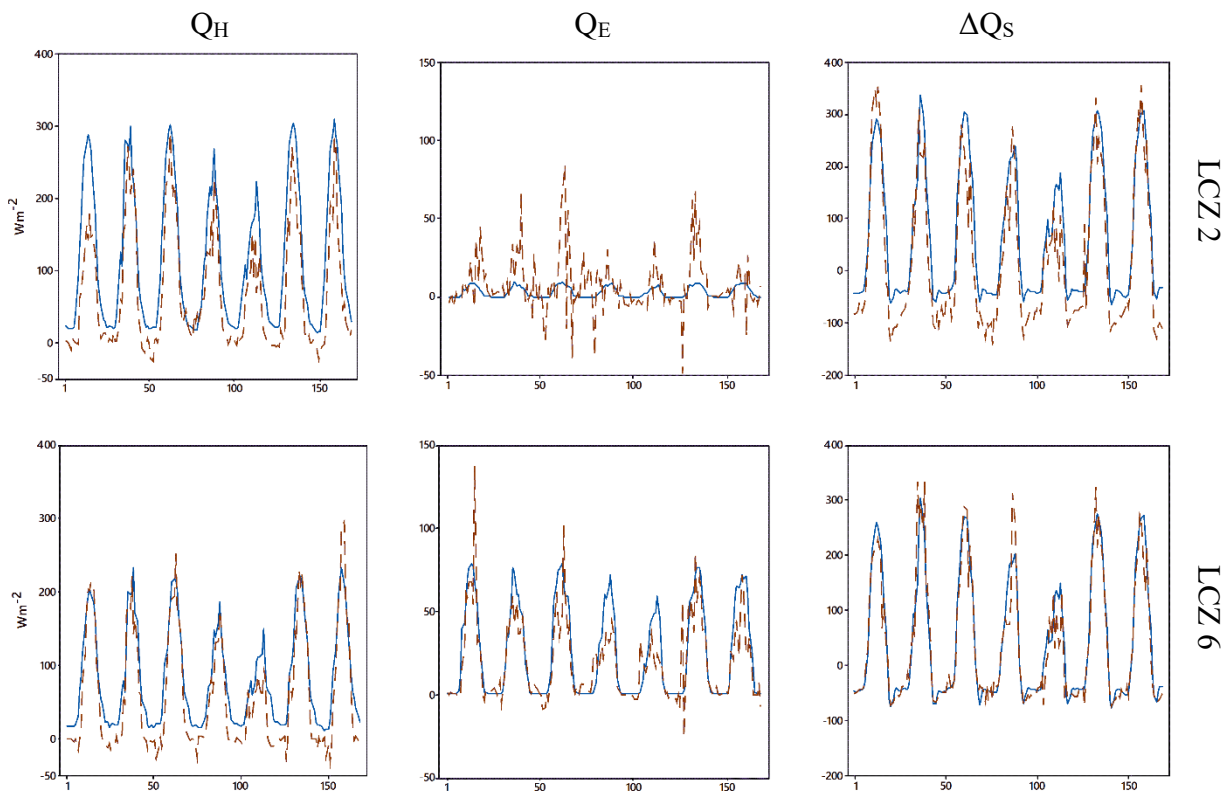


**Figure 5.4** Diurnal evolution of observed (dashed lines) and simulated (solid lines)  $Q_H$  (first column)  $Q_E$  (second column) and  $\Delta Q_S$  (third column) for LCZ 2 (top row) and LCZ 6 (bottom row) sites April 11-17, 2010. The corresponding RMSE values are given in Table 5.2 above

### 5.6.2 Spatial Correspondence of land surface temperature

The main goal of the present study was to evaluate how SUEWS performs spatially, without the need for a dense observational network. To accomplish this, we compared SUEWS LST, which is an integration of various surface LST across each grid, with MODIS LST (see Figure 5.5). SUEWS provides LST for each hour of simulation, thus, we obtained LST values which correspond with the overpass / acquisition time of Terra platform (approximately 11am local time). Due to the method of calculating LST within SUEWS, only daytime acquisitions were selected for comparing the spatial extent of LST. Rather than giving a raw comparison pixel by pixel, we derived typologies of LST based on LCZ land cover (eqn. 5.5). This is deemed to be a more appropriate measure of the spatial performance of SUEWS in terms of the LST relationships it simulates e.g. more built-up areas are expected to exhibit higher LST than extensively vegetated areas etc. though SUEWS was not expected to capture intra-LCZ variation as would occur in reality.

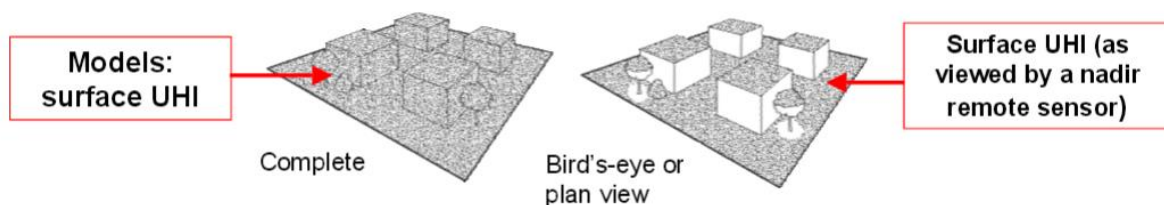


**Figure 5.5** Idealised overview of the difference between LST / SUHI as modelled by SUEWS (left) which is an integrated LST from roof tops, walls, vegetation and pavements and observed by the MODIS sensor (right) which is based on surfaces visible to the satellite. Image is adapted from Voogt & Oke (1997)

Generally, simulated LST from SUEWS was routinely lower than the observations obtained by MODIS (Figure 5.6). However, the relationship between LST both from observations and the model are more or less consistent with one another. Taking a typical day for closer examination (April 11 2010) LST in LCZ 2 was  $\sim 1^{\circ}\text{C}$  warmer than the group mean based on the MODIS data, whereas SUEWS LST was almost half this value ( $\sim 0.6^{\circ}\text{C}$ ). The next clearest signal was Low Plants LCZ which exhibited lower than average LST, again as would be expected *a priori*. This LCZ was  $1.2^{\circ}\text{C}$  lower than the group mean based on MODIS

observations, whereas this value was 0.9°C based on SUEWS. The most promising result appears in the spatial patterns of LST revealed by both MODIS and SUEWS during exceptionally fine weather, during which time a clear urban / non-urban divide can be seen (Figure 5.7). For instance, the warmest LST correspond with the compact inner city of Dublin based on both LST values, whereas the surrounding non-urban area can be clearly demarcated based on lower LST.

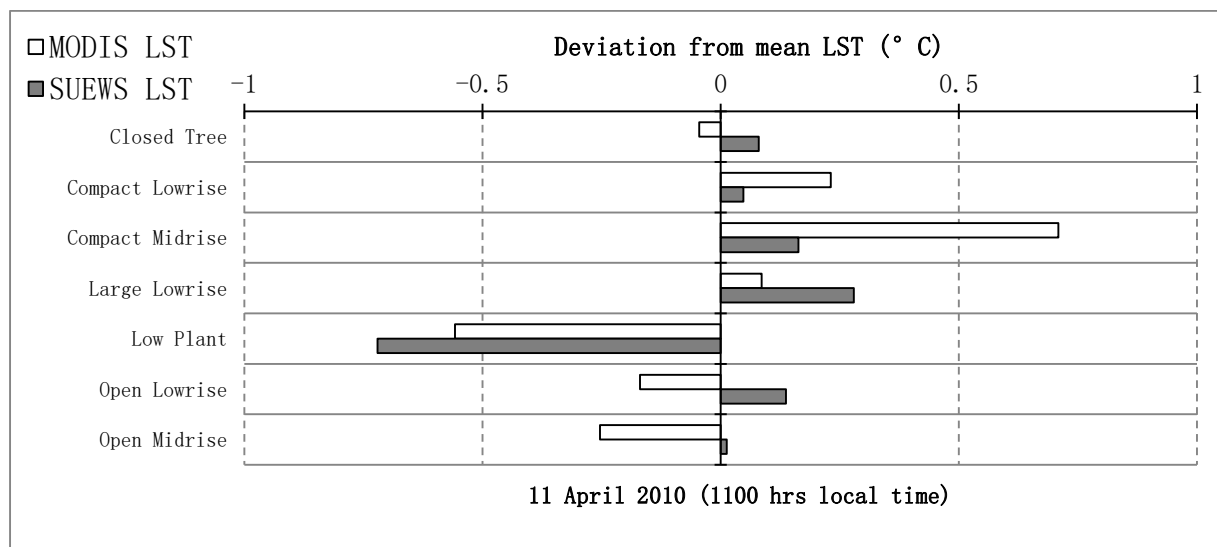


**Figure 5.6** Deviation of individual LCZ from mean observed and simulated daytime LST averaged across the entire domain (recall eqn 5.5). Show are the results for April 11 which is typical of the period examined. Of interest here is whether the demarcation of LST are similar between MODIS and SUEWS for urban and non-urban LCZ

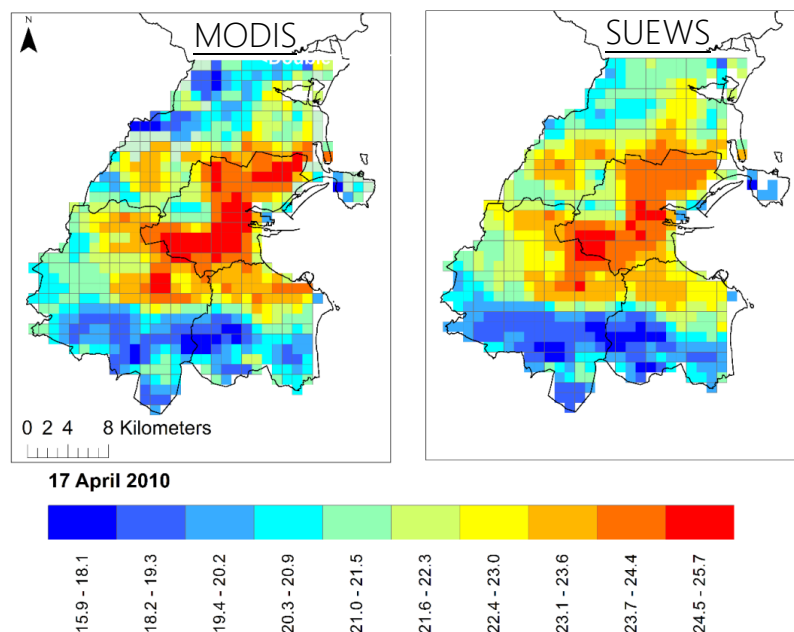


**Figure 5.7** Spatial pattern of daytime LST for the 17 April 2010 as observed by MODIS (left) and simulated by SUEWS (right). The April 17 was chosen as it was exceptionally clear period, hence, observed LST was available for the entire domain

### 5.6.3 *Surface Urban Heat Island evaluation*

Our evaluation of SUEWS in this section centres on simulations of mean monthly LST differences between Dublin inner city and surrounding hinterland i.e. LCZ 2 and LCZ D respectively, throughout the course of an entire year (2010). The simulations of LST are evaluated against observations from the MODIS sensor - both daytime and night time acquisitions are considered. We define the difference in LST between these LCZ as SUHI intensity. By amalgamating LST into LCZ typologies, we no longer consider detailed spatial patterns, hence, both daytime and nighttime values can be considered. The observed LST from MODIS are summarised in Table 5.3 below, the corresponding SUHI intensity from both MODIS and SUEWS are given in Figure 5.8.

Based on observations from the MODIS sensor, the annual course of SUHI intensity almost followed a Platykurtic Gaussian distribution for both daytime and night time. Daytime SUHI intensity peaked around June, reaching a magnitude of 4.5°C. The apparent dip in intensity between June and July is likely due to the high level of precipitation and associated cloud cover experienced during July. Reported sunshine totals for the city were 80-100% of the climate normal for the month while precipitation was 125-225% compared to the normal. Air temperatures around the inner city were -0.5 to 0°C lower than normal, while outside the city the immediate surrounding air temperatures were 0 to 0.5°C higher than normal (Walsh, 2010). Observed night time SUHI intensity varied little throughout the year the magnitude was approximately 2.6°C, with the exception of the first two months of the year.

Simulated SUHI intensity during the daytime throughout the course of the year appears more bimodal, with a peak around March and a second peak around September. Despite the differences in annual development, the magnitude of SUHI intensity during the day shows remarkable similarities with that observed by MODIS during certain months. For example, SUHI intensity in May was 3.8°C based on MODIS observations, simulated SUHI intensity

for the corresponding time was 3.4°C. For July, which as highlighted above was mostly atypical in terms of the weather experienced, SUHI from both MODIS and SUEWS was 3.1°C. Similar to MODIS, SUHI intensity at night from SUEWS was broadly consistent throughout the year, at around 2.4°C. However, despite the similarities highlighted, there are also a number of anomalies with respect to observations. During the late summer / autumn period (August-October) SUHI intensity during the daytime from SUEWS was 1-3°C higher than MODIS.

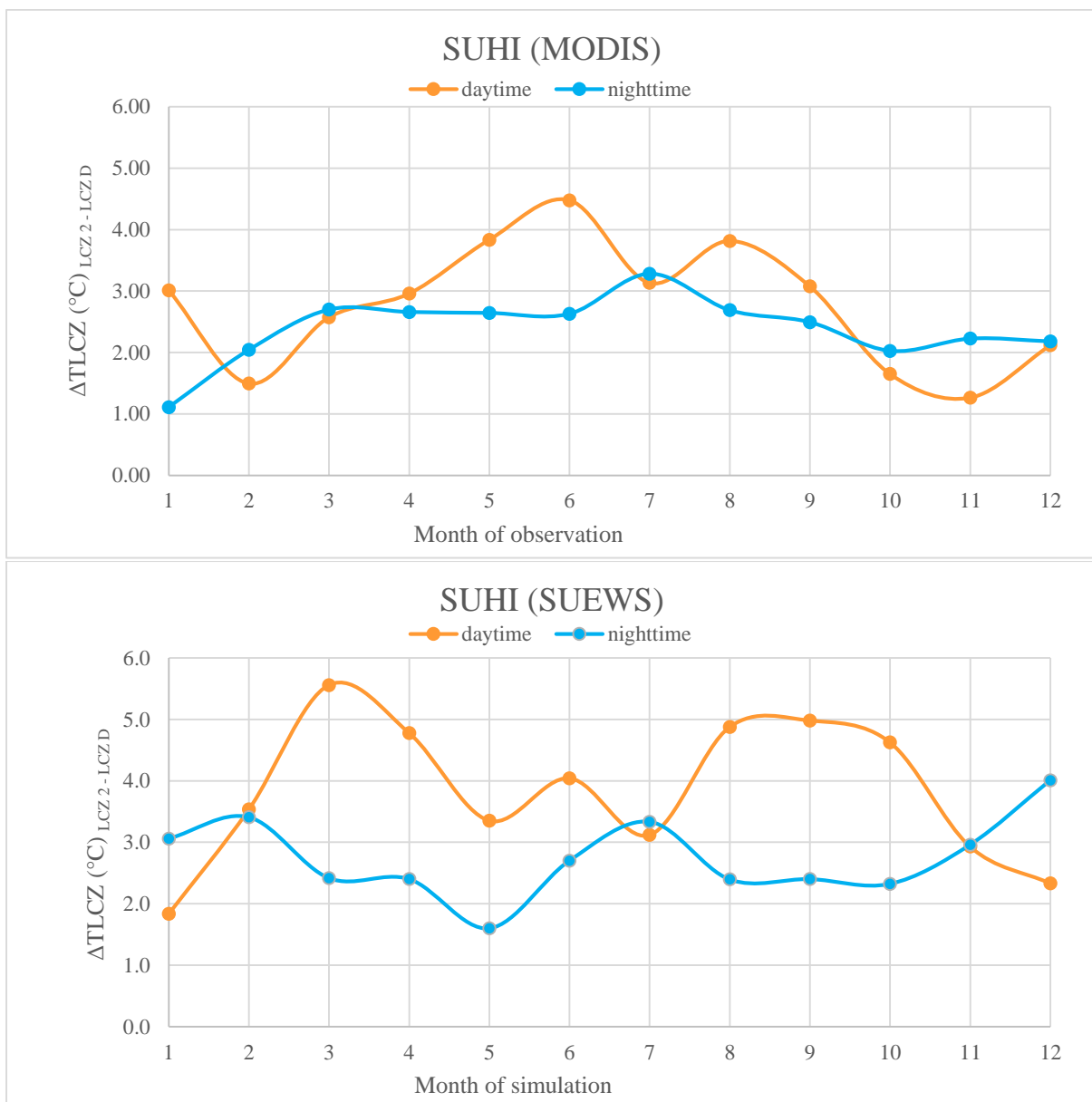


**Figure 5.8 Top: Mean monthly SUHI intensity ( $T_{LCZ2} - T_{LCZD}$ ) based on observations from MODIS sensor (MOD11A2) for daytime and nighttime acquisitions. Bottom: As for panel, but LST is derived from SUEWS model. Hourly values corresponding to MODIS overpass times were used for averaging**

**Table 5.3 Mean monthly MODIS LST for the sub-domain used for evaluation against SUEWS. Shown are LST for each LCZ type across 2010. Values are given in °C – recall Figure 5.3 for calculation method**

LCZ		January	February	March	April	May	June	July	August	September	October	November	December
<b>Day</b> (~1100hrs local time)													
Compact mid-rise	<i>i = 5</i>	2.98	1.99	12.31	19.4	23.16	27.65	22.89	22.88	20.86	15.32	4.8	-2.92
Compact low-rise	<i>i = 9</i>	2.15	1.03	9.85	14.83	18.32	23.59	19.65	19.11	17.3	13.02	4.15	-1.74
Open mid-rise	<i>i = 4</i>	1.04	1.06	11.01	17.47	21.23	24.77	21.39	20.42	18.07	14.07	4.01	-3.91
Open low-rise	<i>i = 185</i>	1.32	1.17	10.7	17.4	21.06	25.72	21.81	20.76	18.86	14.28	4.09	-3.56
Large low-rise	<i>i = 36</i>	0.74	0.72	10.62	18.24	21.5	26.3	22.08	20.66	19.51	14.65	4.19	-4.15
Low plants	<i>i = 124</i>	-0.03	0.5	9.74	16.44	19.33	23.17	19.76	19.07	17.79	13.67	3.53	-5.04
<b>Night</b> (~2200hrs local time)													
Compact mid-rise	<i>i = 5</i>	-2.89	0.08	1.29	6.62	9.75	13.74	13.78	12.81	10.84	8.82	3.63	-3.49
Compact low-rise	<i>i = 9</i>	-0.92	-1.12	1.37	5.45	8.56	12.18	11.54	11.67	9.35	8.33	2.95	-2.23
Open mid-rise	<i>i = 4</i>	-2.6	-1.33	0.04	4.49	7.77	12.12	12.7	11.34	9.49	7.76	2.46	-4.85
Open low-rise	<i>i = 185</i>	-2.73	-1.25	0.08	5.07	8.12	12.37	11.46	11.55	9.56	7.88	2.9	-4.61
Large low-rise	<i>i = 36</i>	-3.17	-1.73	-0.52	4.69	7.49	12.07	9.97	11.06	9.06	7.31	2.75	-5.06
Low plants	<i>i = 124</i>	-4	-1.96	-1.41	3.96	7.11	11.12	10.5	10.12	8.35	6.79	1.41	-5.67

To better understand why SUHI intensity was overestimated by SUEWS during these months, we examined the calculated LST for LCZ 2 and LCZ D – and additionally LCZ 6 as this was the most extensive urban LCZ class across the domain – by generating Taylor diagrams which compare observed LST against those simulated by SUEWS - Figure 5.9. RMSE was routinely higher for daytime LST, though both daytime and nighttime LST had high  $R^2$  values. Based on LST development across the year considered, the model exhibited less variation in LST compared to observations.

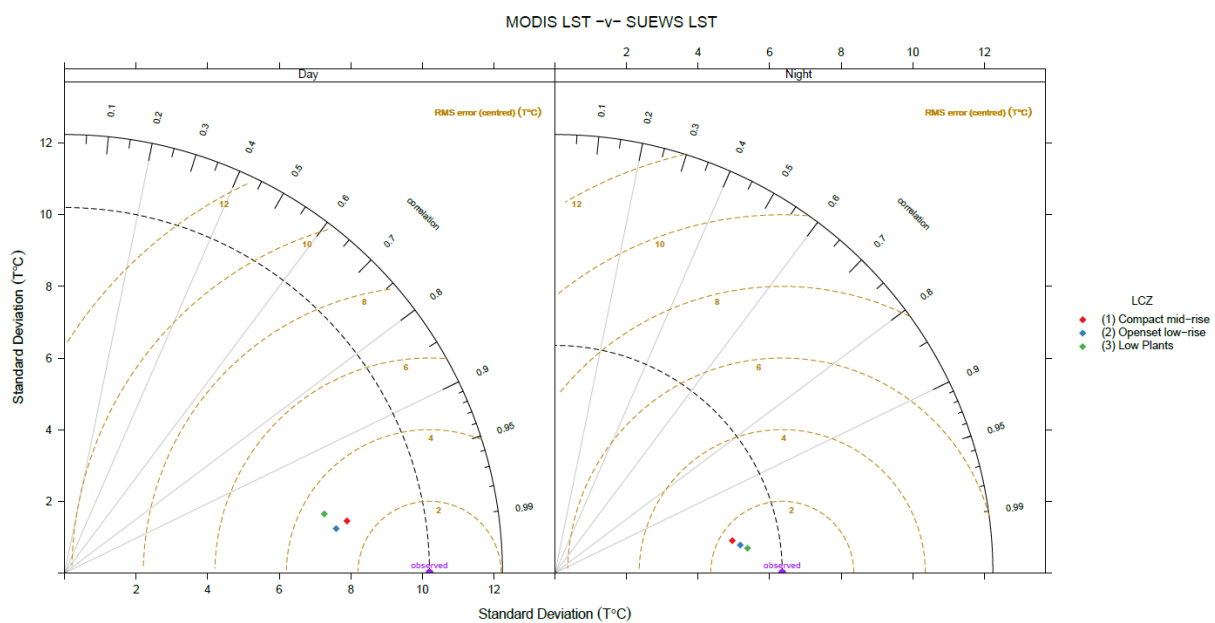


**Figure 5.9 Taylor diagrams based on monthly LST for 2010 from MODIS and SUEWS. The left pane is daytime LST and the right is night time LST, the points represent 3 different LCZ classes, LCZ 2 (red) LCZ 6 (blue) and LCZ D (green), the purple point represents observations from MODIS, hence night time LST performance was higher than daytime,  $R^2$  and RMSE are given in Table 5.4**

The overestimation of SUHI was primarily due to the model underestimating daytime LST for LCZ D, whereas the error for LCZ 2 was comparatively lower and closer resembled the observations - Table 5.4 / Figure 5.10.

**Table 5.4 Model performance metrics for LST, given are the RMSE and  $R^2$  of SUEWS LST compared to MODIS LST**

<b>RMSE (°C)</b>	<b>LCZ 2</b>	<b>LCZ 6</b>	<b>LCZ D</b>
<b>Daytime</b>	2.23	2.6	3.11
<b>Nighttime</b>	1.13	1.34	0.76
<b><math>R^2</math></b>	<b>LCZ 2</b>	<b>LCZ 6</b>	<b>LCZ D</b>
<b>All Hours</b>	0.9675	0.9741	0.9623

As a result of these daytime anomalies, model performance was lower for daytime LST, with a higher RMSE compared to nighttime LST.

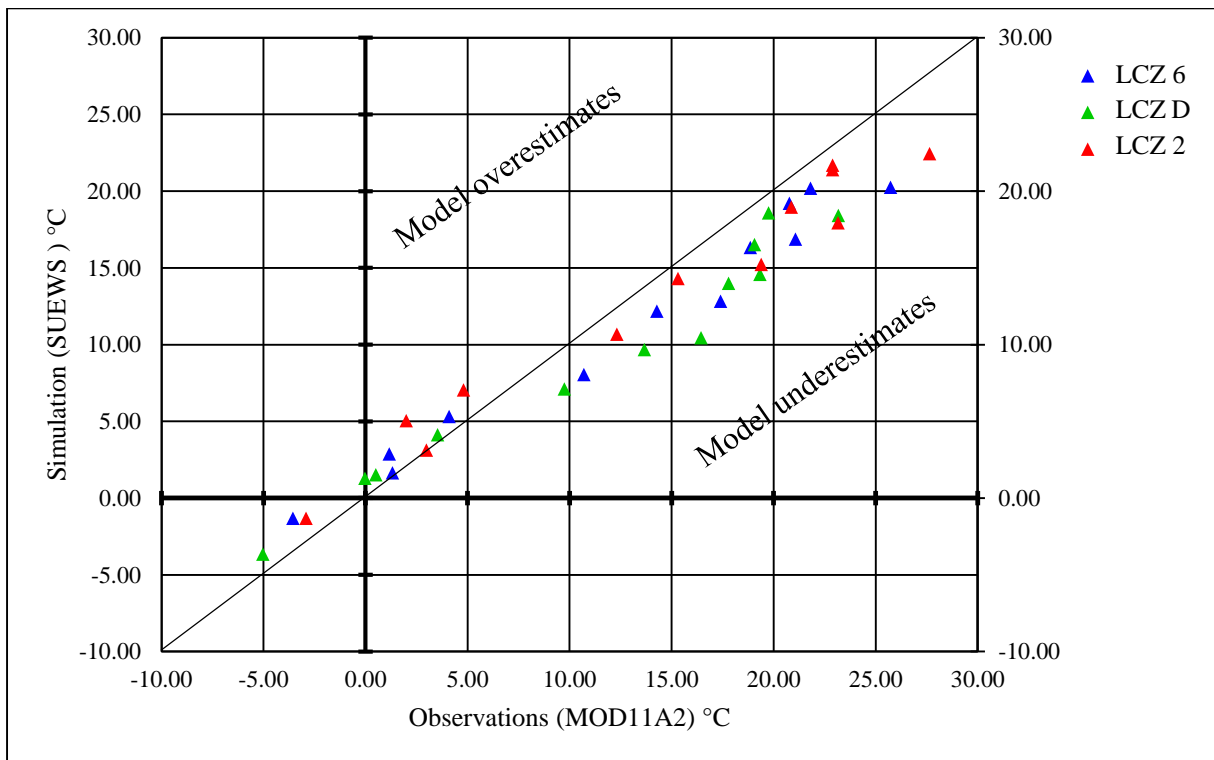


**Figure 5.10 Scatter between observed daytime LST and simulated LST, the 1:1 line is included in order to illustrate points where the model over or underestimates LST**

The apparent overestimation of nocturnal SUHI by SUEWS at the end of 2010 was primarily due to abnormal synoptic conditions across much of Europe during the winter period, with high amounts of snow cover and cold temperatures. Snow cover / depth was omitted from the meteorological forcing data. As a result of snow cover across much of the domain observed differences in LST between LCZ 2 and LCZ D was  $\sim 2^{\circ}\text{C}$ , around half the value as simulated by SUEWS. The inclusion of snow cover data in meteorological forcing may improve the estimation of SUHI intensity in this instance. Nevertheless, the correspondence between observed and simulated nocturnal LST is encouraging.

## 5.7 Conclusion

In this study we sought to spatially validate the surface urban energy and water balance scheme (SUEWS) model by employing remotely sensed (RS) land surface temperatures (LST) in Dublin, Ireland. Furthermore, SUEWS was evaluated at 2 point locations, one urban and one suburban, to ensure good agreement with observations of the urban energy balance (UEB) flux densities during a calm, clear one-week period in April, 2010. During this same period, we examined the spatial pattern of LST as observed by MODIS (MOD11A2) and LST calculated by SUEWS to determine if simulated LST was capable of demarcating the urban area from the surrounding non-urban area. We subsequently generated LST typologies based on (i) the local climate zone (LCZ) classification scheme (ii) data obtained through the MODIS sensor and (iii) LST simulated by SUEWS. By comparing LST obtained for the inner city (LCZ 2) and non-urban hinterland (LCZ D), we were able to derive the mean monthly surface urban heat island (SUHI) intensity across an entire year. We then compared SUHI intensity between MODIS and as simulated by SUEWS.

During the one-week period considered, the model performed well at the point locations in terms of simulations of turbulent fluxes, consistent with previous studies; RMSE values ranged between 35-60  $\text{Wm}^{-2}$  for  $Q_H$  and  $\Delta Q_S$  and between 15-20  $\text{Wm}^{-2}$  for  $Q_E$ . While LST was generally underestimated by SUEWS when compared to observations, the demarcation of the urban / non-urban area was very promising.

The simulation of mean monthly SUHI intensity was split into daytime and night time intensities. Daytime SUHI intensity tended to be overestimated by the model, whereas modelled mean nocturnal intensity was slightly underestimated. Nocturnal SUHI intensity from MODIS was 2.6°C whereas for SUEWS it was 2.4°C. We conclude that RS data can be used for model evaluation / validation, though additional studies demonstrating the use of RS in this manner are required to ensure consistency in its employment.

---

## Chapter 6 Simulating the impact of different urban development pathways on the local climate of a mid-latitude city

---

### 6.1 Preface

This chapter is in press as

Alexander, P.J., Fealy, R., Mills, G. (2016) Simulating the impact of different urban development pathways on the local climate: A scenario-based analysis in the greater Dublin region, Ireland. *Landscape and Urban Planning*. DOI: 10.1016/j.landurbplan.2016.02.006

The final paper in this collection applies the knowledge generated through papers 1-3. Having demonstrated that the LCZ-SUEWS approach produces realistic simulations of the turbulent exchanges of energy between different local-scale urban forms and the near surface atmosphere, the approach is applied to a current planning problem in Dublin, Ireland. As documented in national and international news, there is now a significant housing crisis in Dublin as economic recovery begins to take hold and concentrate in the city. This has led to high demand for both housing and office space with virtually no new supply in the past 7 years. In turn, there is increased pressure for the Dublin local authorities to begin development of new residential and commercial units to ease the rising demand. In response to this unprecedented situation the government of Ireland recently announced an emergency €1.5 billion investment in direct provision for some 35,000 additional social housing and commercial units with development to begin as early as 2016.

In some respects, this is analogous (though notably less extreme) to the situation in urban areas in developing economies where the pace of inward migration outstrips the pace of planned development. Hence, evidence based development policies are urgently needed. Here the impact of individual development pathways on the urban surface energy and water balance of Dublin city are simulated using the LCZ-SUEWS method.

## **6.2 Abstract**

In this study, the impact of different urban development pathways on neighbourhood climate are examined. The investigation considers the relative impact differing policy / planning choices will have on the local-scale climate across a city during a typical climatological year (TCY). The aim is to demonstrate a modelling approach which couples a climate-based land classification and simple urban climate model and how this can be used to examine the impact differing urban forms and design strategies have on neighbourhood scale partitioning of energy and resulting consequences. Utilising the Surface Urban Energy and Water Balance (SUEWS) model (Järvi et al., 2011) hourly fluxes of sensible, latent and stored heat are simulated for an entire year under four different urban development pathway scenarios. The land cover scenarios are based on those obtained by the MOLAND model for 2026 (Brennan et al., 2009) in our case study city Dublin (Ireland). MOLAND LULC are translated into local climate zones (Stewart & Oke, 2011) for examination. Subsequently, the types of building forms, vegetation type and coverage are modified based on realistic examples currently found across Dublin city. Our results focused on 2 principle aspects: the seasonality of energy partitioning with respect to vegetation and average diurnal partitioning of energy. Our analysis illustrates that compact scenarios are suitable form of future urban development in terms of reducing the spatial impact on the existing surface energy budget. Design interventions which maintain the level of vegetation at a ratio  $> 9:16$  to artificial surfaces reduces the impact.

## **6.3 Introduction**

Globally, city planners face significant pressures to accommodate a rapidly growing urban population. In the past 60 years, the urban population has increased by 3.154 billion and more than 50% of the global population are now urban; by 2050, it is projected that this proportion will exceed 66% (UN, 2014). Urban areas are a focus of human activity and are

major drivers of global climate change; moreover, their locations at low altitude, along rivers and close to coasts exposes them to hazards (such as coastal flooding) that are likely to be exacerbated in climate change scenarios (IPCC, 2014). Urban areas also modify the local climate profoundly, producing well known climatic phenomena such as the urban heat island (UHI) (Karl, et al., 1988; Patz, et al., 2005), CO<sub>2</sub> dome (Balling, et al., 2001; Idsoa, et al., 1998) and photochemical smog (Gray & Finster, 2000; Moussiopoulos, et al., 1995). These local to global climate effects are caused by two different, but related, aspects of cities. Urban form describes the surface cover (e.g. impervious fraction), the construction materials (e.g. asphalt) and the built geometry (e.g. the building dimensions and their juxtaposition). Urban function describes the activities in cities that require water, energy, materials etc.; the waste heat, vapour and materials are deposited into the atmosphere, hydrosphere and lithosphere. Urban form and function are strongly related so that, for example, more compact and densely occupied cities have lower per capita fuel use for transportation (Bramley & Power, 2009; Breheny, 1991; Elkin, et al., 1991; Mills, 2007).

As the world continues to urbanise, the global sustainable development challenges (and opportunities) will be increasingly concentrated in cities. Urban policies that address these must manage aspects of urban form and functions to mitigate (and adapt to) climate changes at different scales. This is especially true for economically developing countries where the rates of urbanisation are greatest and population growth outstrips the pace of planned development (Jorgenson & Rice, 2010; Martine, et al., 2008). The emerging layout of these fast-growing cities (e.g. urban extent, population and building density) will have long-term implications as once constructed, cities have proved difficult to alter. Incorporating climate knowledge into urban decision-making will be an important component in planning and creating more sustainable cities. In this respect, urban climate models (UCMs) are a potentially valuable tool for evaluating some of the impacts of different urban designs, land use, population densities

and activities on the surface energy and water balances and the consequent effects on the local atmosphere and hydrology, respectively. Addressing local climate conditions (such as the UHI) can help reduce the contribution of individual cities to global climate change. In fact a variety of UCMs have been applied for precisely this purpose (see Table 6.1), yet there is little evidence that they have been used to inform decision making (Eliasson, 2000; Hebbert & Mackillop, 2013; Mills, 2008; Oke, 1984). By comparison, climatic considerations are routinely employed to assist building design (Brager & de Dear, 1998; Givoni, 1992; Shaviv, 1984).

This ‘knowledge circulation failure’ (Hebbert and MacKillop, 2013) has been attributed to many causes, including a mismatch between urban climate knowledge and planning/design concerns. For example, while climate research has examined the nocturnal UHI in considerable detail, architects and planners are most interested in daytime conditions when people occupy outdoor spaces and building energy demands are highest (Svensson & Eliasson, 2002). To overcome this failure, existing research should be codified for planning use (Alcoforado, et al., 2009; Mills, et al., 2010) but also new research needs to be undertaken that meets urban planning needs (Gál & Unger, 2009; Marland, et al., 2003; Ward, 2003). UCMs can help address these issues as they encapsulate much of our knowledge of the urban climate effect and have become increasingly sophisticated in their descriptions of the urban landscape; in addition, the results of the models have been evaluated in many circumstances (Grimmond, et al., 2010; Grimmond, et al., 2011).

Previous research has demonstrated how available meteorological data can be used to run mid-to-complex urban energy balance models, which would allow the urban climate effect to be included in the planning process (Alexander, et al., 2015; Grimmond & Oke, 2002). However, there has been little guidance on how to run UCMs, interpret their findings and integrate their projections to inform policy.

**Table 6.1 Overview of a selection of Urban Climate Models (UCMs) for planning and research applications. The list below is non-exhaustive and based on non-proprietary models. The list also excludes building-scale energy models. Scale refers to the resolution of the model output, where  $\mu$  = micro (1-100m)  $\alpha$  = local (1-2km)  $\beta$  = meso (> 2 km) scale**

Model Name	Model reference	Scale	Reviewed exemplar applications
ENVI-met	(Bruse, 1999)	$\mu$ - $\alpha$	Building form impacts on microclimate (Middel, et al., 2014) Green-roof strategies and HTC (Peng & Jim, 2013)
MITRAS	(Schlünzen, et al., 2003)	$\mu$	Wind flow patterns, dispersion (Schlünzen, et al., 2011)
SOLWEIG	(Lindberg, et al., 2008)	$\mu$ - $\alpha$	Vegetation and building form impacts on shadow patterns, mean radiant temperatures (Lindberg & Grimmond, 2011) Impact of urban planning on HTC (Goldberg, et al., 2013)
SLUCM (WRF)	(Kusaka, et al., 2001)	$\alpha$ - $\beta$	Simulating urban expansion impacts on temperature, wind speed and surface ozone concentrations (Wang, et al., 2007) Land-Sea breeze and UHI development (Lin, et al., 2008)
SUEWS	(Järvi, et al., 2011)	$\alpha$ - $\beta$	BRIDGE project, ensembles modelling for urban hydrology (Chrysoulakis, et al., 2013)
TUF-3D	(Krayenhoff & Voogt, 2007)	$\mu$	Use of artificial turf to reduce surface and air temperature (Yaghoobian, et al., 2010)
TEB	(Masson, 2000)	$\mu$ - $\beta$	Impact of climate change on temperature and cooling demands in Paris (Lemonsu, et al., 2013)

In this study, we demonstrate the utility of the surface urban energy and water balance scheme (SUEWS v.2014b) for evaluating the climatic impact of different urban development pathways. SUEWS is parameterised using values obtained from the Local Climate Zone (LCZ) scheme that describes neighbourhood types and is run using available meteorological data. This approach is applied to a case study city (Dublin, Ireland, 53.3° N, 6.3° W) where the pathways for future growth are based on scenarios generated by the MOLAND model to 2026. These scenarios generate distinct land use and land cover (LULC) outcomes, which are translated into LCZ types to provide parameter values. The output of the model illustrates the impacts of the different development pathways. Before discussing the methodology in detail, the potential value of the SUEWS model - linked with the LCZ scheme - for planning purposes is presented.

#### **6.4 Integrating LCZ and SUEWS to support planning decisions**

The LCZ scheme categorises landscapes into types based on their impact on the near-surface air temperature (Stewart & Oke, 2012); it consists of 17 standard types, 10 of which are urban, 7 are non-urban (Figure 6.1) but it can also accommodate mixed types. The scheme is properly applied to a neighbourhood-scale (areas greater than about 1 km<sup>2</sup>) where each type is differentiated from another based on a range of variables such as the fractional impervious cover, mean building height, sky view factor and anthropogenic heat generation. The net effect of these properties is to modulate the thermal response of the overlying atmosphere and create the urban heat island (UHI) phenomenon; this link has been validated in published work (Levlovics, et al., 2013; Stewart, et al., 2014). The value of the LCZ scheme extends beyond the UHI however, and could provide a platform for incorporating much urban climate knowledge into planning practice for a number of reasons:

- First, the UHI may be regarded as an indicator of urban climate effects generally, so mitigating it addresses other effects such as the lack of greenspaces and of available water. So a map of LCZ types in a city identifies where the urban effect is greatest.
- Second, LCZ types are designed to be culturally neutral (applicable internationally) and intuitive (user-friendly). As such they can clarify communication between climate scientists and planners e.g. Picone & Campo (2015) see Figure 6.2. Moreover, they can facilitate knowledge transfer between cities.
- Third, LCZs are useful for both observational and modelling studies of the local scale climate. A LCZ map of a city can be used to sample the urban landscape to measure climate variables and to gather more detailed information on surface characteristics to run UCMs. Even the current variables in the LCZ scheme correspond with the many UCM parameters.

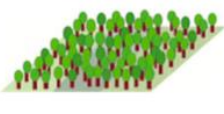
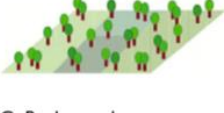
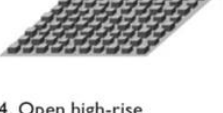
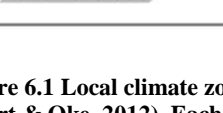
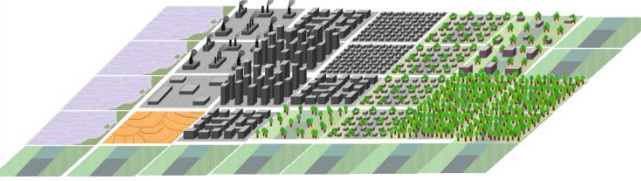
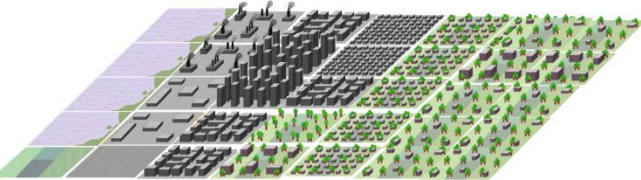
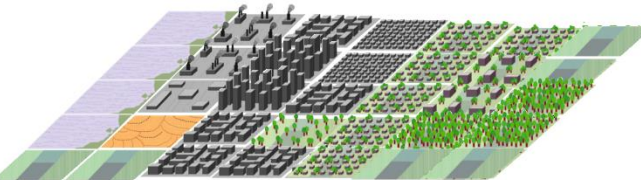
Built types	Definition	Land cover types	Definition
 <p>1. Compact high-rise</p>	Dense mix of tall buildings to tens of stories. Few or no trees. Land cover mostly paved. Concrete, steel, stone, and glass construction materials.	 <p>A. Dense trees</p>	Heavily wooded landscape of deciduous and/or evergreen trees. Land cover mostly pervious (low plants). Zone function is natural forest, tree cultivation, or urban park.
 <p>2. Compact midrise</p>	Dense mix of midrise buildings (3–9 stories). Few or no trees. Land cover mostly paved. Stone, brick, tile, and concrete construction materials.	 <p>B. Scattered trees</p>	Lightly wooded landscape of deciduous and/or evergreen trees. Land cover mostly pervious (low plants). Zone function is natural forest, tree cultivation, or urban park.
 <p>3. Compact low-rise</p>	Dense mix of low-rise buildings (1–3 stories). Few or no trees. Land cover mostly paved. Stone, brick, tile, and concrete construction materials.	 <p>C. Bush, scrub</p>	Open arrangement of bushes, shrubs, and short, woody trees. Land cover mostly pervious (bare soil or sand). Zone function is natural scrubland or agriculture.
 <p>4. Open high-rise</p>	Open arrangement of tall buildings to tens of stories. Abundance of pervious land cover (low plants, scattered trees). Concrete, steel, stone, and glass construction materials.	 <p>D. Low plants</p>	Featureless landscape of grass or herbaceous plants/crops. Few or no trees. Zone function is natural grassland, agriculture, or urban park.
 <p>5. Open midrise</p>	Open arrangement of midrise buildings (3–9 stories). Abundance of pervious land cover (low plants, scattered trees). Concrete, steel, stone, and glass construction materials.	 <p>E. Bare rock or paved</p>	Featureless landscape of rock or paved cover. Few or no trees or plants. Zone function is natural desert (rock) or urban transportation.
 <p>6. Open low-rise</p>	Open arrangement of low-rise buildings (1–3 stories). Abundance of pervious land cover (low plants, scattered trees). Wood, brick, stone, tile, and concrete construction materials.	 <p>F. Bare soil or sand</p>	Featureless landscape of soil or sand cover. Few or no trees or plants. Zone function is natural desert or agriculture.
 <p>7. Lightweight low-rise</p>	Dense mix of single-story buildings. Few or no trees. Land cover mostly hard-packed. Lightweight construction materials (e.g., wood, thatch, corrugated metal).	 <p>G. Water</p>	Large, open water bodies such as seas and lakes, or small bodies such as rivers, reservoirs, and lagoons.
 <p>8. Large low-rise</p>	Open arrangement of large low-rise buildings (1–3 stories). Few or no trees. Land cover mostly paved. Steel, concrete, metal, and stone construction materials.	<b>VARIABLE LAND COVER PROPERTIES</b>	
 <p>9. Sparsely built</p>	Sparse arrangement of small or medium-sized buildings in a natural setting. Abundance of pervious land cover (low plants, scattered trees).	<p>b. bare trees</p>	Leafless deciduous trees (e.g., winter). Increased sky view factor. Reduced albedo.
 <p>10. Heavy industry</p>	Low-rise and midrise industrial structures (towers, tanks, stacks). Few or no trees. Land cover mostly paved or hard-packed. Metal, steel, and concrete construction materials.	<p>s. snow cover</p>	Snow cover >10 cm in depth. Low admittance. High albedo.
		<p>d. dry ground</p>	Parched soil. Low admittance. Large Bowen ratio. Increased albedo.
		<p>w. wet ground</p>	Waterlogged soil. High admittance. Small Bowen ratio. Reduced albedo.

Figure 6.1 Local climate zone scheme for universally describing neighbourhood morphology and thermal climate (Stewart & Oke, 2012). Each zone is defined on the basis of parameters which impact on the hydrothermal properties such as the % imperviousness, sky-view factor, building materials, waste heat, building and vegetation height and so forth

	Present day
	Future land cover scenario "A" (Sprawl)
	Future land cover scenario "B" (Compact)

**Figure 6.2** A hypothetical city comprised of different neighbourhood types (LCZ – Figure 6.1), with future land cover scenarios classified into LCZ, thus allowing for initial assessment and modelling of climatic impacts of policy / planning decisions at the neighbourhood scale (see for instance fig. 12/13 in Ching, 2013)

Here, we link the LCZ scheme with SUEWS climate model v.2013b (Järvi, et al., 2011) to explore the impacts of urban development scenarios on neighbourhood scale climate. By integrating LCZ with SUEWS, urban form is accounted as either sparse, open or compact neighbourhood areas as well as lowrise, midrise or highrise building elements. While SUEWS cannot explicitly account for building configurations (unlike for example, the ENVI-MET model) it employs several parameters that are determined by the extent of open spaces, buildings and vegetation height and coverage. These form choices will impact on the local scale partitioning of energy – eqn (6.1) below.

SUEWS simulates the effect of urbanisation on the processes responsible for local-scale climate changes. These processes are encapsulated in the urban energy budget (UEB), which states

$$Q^* + Q_F = Q_H + Q_E + \Delta Q_S + \Delta Q_A, \quad W m^{-2} \quad \text{Eqn.6.1}$$

$Q^*$  is net radiation,  $Q_F$  is anthropogenic heat,  $Q_H$  and  $Q_E$  are the turbulent sensible and latent heat respectively and  $\Delta Q_S$  is storage heat and  $\Delta Q_A$  is advection (i.e. the horizontal transfer of energy). Each term is expressed as a flux density ( $Wm^{-2}$ ) across the sides of an imaginary volume that encloses a Section of urban landscape. The volume encloses the urban surface features (buildings, trees, etc.) and extends to a depth within the substrate where energy exchanges are close to zero; in other words,  $Q^*$ ,  $Q_F$ ,  $Q_H$ ,  $Q_E$  and  $\Delta Q_S$  can each be assessed at the top of the volume. SUEWS does not account for advection which is significant at the boundary between surface types, and so is limited to ‘homogenous’ landscapes (both urban and non-urban) where  $\Delta Q_A \approx 0$ . Moreover, the lack of explicit accounting for advection (strictly speaking) further limits the model to synoptic conditions conducive to a strong urban effect i.e. low winds, clear sky, high pressure. Thus, the UEB simulates the total amount of energy available at the urban surface ( $Q^*+Q_F$ ) and its use for heating the air ( $Q_H$ ), evaporating water ( $Q_E$ ) and heating the substrate ( $\Delta Q_S$ ). The partitioning of available energy will govern the urban impact on the substrate, surface and air temperatures and atmospheric humidity; it will also affect the UHI, building energy management and the partitioning of precipitation into runoff and storage (Table 6.2).

SUEWS is well suited to this study as it requires a relatively low number of input parameters including: meteorological data; socio-economic-demographic data and; surface

We simulated neighbourhood/local scale ( $\sim 1 \text{ km}^2$ ) turbulent fluxes in order to examine the impact of different development pathways on neighbourhood scale climate across a typical climatological year (TCY). We simulated hourly fluxes using the Surface Urban Energy and Water balance (SUEWS v.2013b) model (Järvi, et al., 2011). We forced the model with meteorological data obtained from a WMO standard station located approximately 5 km outside of the metropolitan area. These data are based on 10-year hourly averages, thus represent a TCY, but for clarity, the 10-year period runs from 2005-2014 which contained 3 of

the warmest years on record for the region (Walsh, 2014). Hence while the TCY simulations are intended to be *a-temporal*, they are based on the present climate regime. The model has already been evaluated under a number of different circumstances i.e. background climates and different cities (Alexander, et al., 2015; Järvi, et al., 2011; Järvi, et al., 2014) and its potential utility for urban planning has been discussed (Chrysoulakis, et al., 2014).

cover and urban structure data, which is provided by the LCZ scheme.

**Table 6.2 Link between urban development/features, impact on energy balance terms and resulting impact on local scale climate / urban heat island relevant for planners particularly in warm climates**

Urban Feature	Energy Balance Term (Relative to non-urban areas)	Urban Effect
Canyon Geometry	Increased $K^*$	Increased surface area and trapping of radiation
Air Pollution	Increased $L_{\downarrow}$	Greater absorption and re-emission
Canyon Geometry	Decreased $L^*$	Reduced Sky View Factor (less nocturnal loss to atmosphere)
Buildings and Traffic	Addition of $Q_F$	Direct addition of heat
Construction Materials	Increased $\Delta Q_S$	Increased thermal admittance at night
Absence of water bodies / vegetation	Increased $Q_H$	Increased surface / air heating
Construction Materials	Decreased $Q_E$	Increased water-proofing / increase runoff
Canyon Geometry	Decreased $Q_A$	Reduces wind speed

## 6.5 Methods

### 6.5.1 Case study area

Our case study area to apply LCZ-SUEWS model and demonstrate its utility is the Greater Dublin Region (GDR) which covers Dublin city (Ireland) and parts of the surrounding counties containing several large satellite towns. Dublin is the capital city of Ireland and located on the east coast, flanked by the Irish Sea to the East, and the Dublin/Wicklow mountains to the South. With the exception of the mountainous southern part, most of the city occupies a flat and low-lying basin (<100 meters above sea level.) and is bisected by the Liffey River – Figure 6.3. Given its latitude, it has a mild climate with little temperature variation through the

year (Köppen type *Cfb*) although day-length is significant longer in summer (16 h in June) than in winter (8 h in December). The extent of the urban area under investigation extends to  $\sim 700$  km<sup>2</sup> as the city has expanded outside its administrative boundaries over the last three decades. The population of the defined model extent is  $\sim 1.4$  million. It provides an ideal place for this case study as it houses two flux observation sites (located in urban and suburban neighbourhoods) where detailed energy flux and meteorological observations have been made since 2009 (Keogh, et al., 2012), this allowed for model evaluation and calibration. In addition there is a LCZ description of the city that outlines major neighbourhood types (Alexander & Mills, 2014) and a WMO standard weather station located outside the urban area. These data allow SUEWS to be parameterised and run.

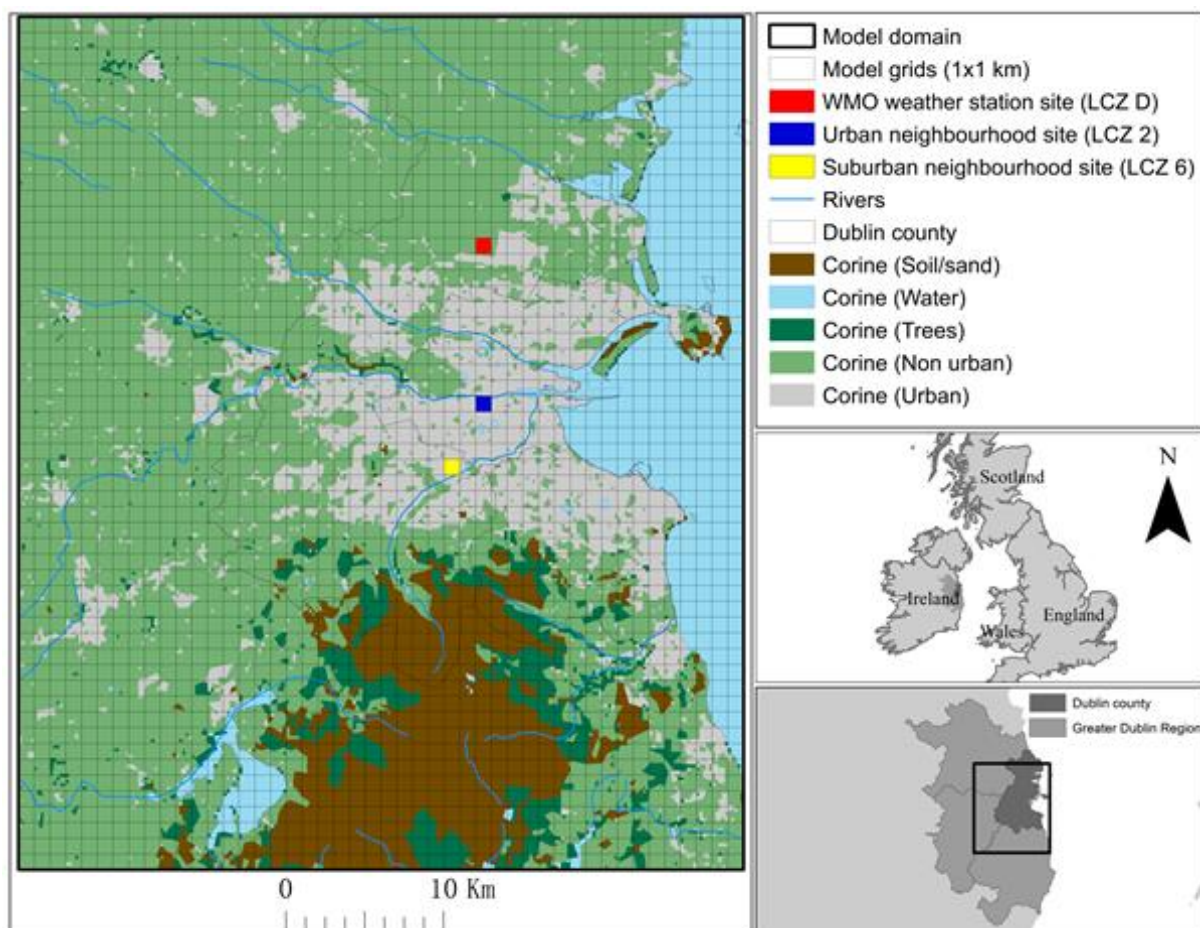


**Figure 6.3 Study area overview. Main image shows the model domain and grids. LULC classes from CORINE were combined to show urban –v- non urban extent. The grids highlighted in blue and yellow represent the two neighbourhoods (inner city and southern suburb respectively) used to evaluate the models’ accuracy, and the red grid shows the location of the synoptic station used to force all model simulations**

## 6.6 Data

SUEWS requires hourly meteorological data, land cover parameters and estimates of anthropogenic fluxes – see Table 6.3. In terms of land cover, the model describes different surface types in a neighbourhood in terms of fractional coverage of buildings, pavements, water, vegetated areas (both irrigated and non-irrigated) and trees (coniferous and deciduous) and unmanaged land cover such as bare soils or rock. Anthropogenic water and energy use can also be provided; hourly water use can be expressed as a proportion of the daily total and hourly anthropogenic heat fluxes can be estimated from typical daily patterns, divided into weekday and weekend values. In the following Sections, the various input data utilised are described.

**Table 6.3 INPUT requirements of SUEWS model (\*) indicates inputs which were used in this study**

Variable	Units	Used in this study marked with *	Comments
<i>Meteorological</i>			
Air Temperature (T)	°C	*	
Relative Humidity (RH)	%	*	
Pressure (Pr)	kPa	*	
Precipitation (P)	mm h <sup>-1</sup>	*	
Wind speed (V)	m s <sup>-1</sup>	*	
Incoming short wave (K <sub>↓</sub> )	W m <sup>-2</sup>	*	
Incoming long wave (L <sub>↓</sub> )	W m <sup>-2</sup>		Optional (otherwise uses T and RH)
Observed Sensible Heat (Q <sub>H</sub> )	W m <sup>-2</sup>		Optional
Observed Latent Heat (Q <sub>E</sub> )	W m <sup>-2</sup>		Optional
Observed Storage Heat (ΔQ <sub>S</sub> )	W m <sup>-2</sup>		Optional
Cloud Fraction	Tenths	*	Optional
Soil moisture deficit (SMD)	m <sup>3</sup> m <sup>-3</sup>	*	Optional
Leaf Area Index (LAI)		*	Optional
<i>Anthropogenic Inputs</i>			
Anthropogenic Heat (Q <sub>F</sub> )	W m <sup>-2</sup>	*	Optional, hourly values (otherwise modelled)
Anthropogenic Water Use	%		Optional, hourly ratio of total diurnal usage
<i>Surface Inputs</i>			
Fractional Coverage of Surface types (λ)	%	*	Urban, Pavement, Soil, Grass (irrigated and un-irrigated), Trees (coniferous and deciduous) Water
Surface Area	Ha	*	
Water Usage Area	Ha		Optional
Latitude / Longitude	°	*	
Storage Capacity of Pipes	mm		Optional
Frontal area fractions			Optional, buildings and trees separate
Roughness Length for momentum (z <sub>0</sub> )	m		Optional
Zero displacement height (z <sub>d</sub> )	m		Optional
Surface Element Heights	m	*	Optional, buildings and trees separate

### 6.6.1 Forcing Data

We obtained hourly values for temperature, relative humidity, precipitation, pressure, wind speed and incoming solar radiation for the past 10 years from a meteorological station located close to Dublin airport, approximately 5 km north of the inner city. We averaged the hourly values for each day of the year in order to derive a typical climatological year (TCY). The resulting hourly dataset was used to force the model in each of the four MOLAND scenario runs and an additional run for the base line case (BLC) to examine the impact on the urban energy budget (UEB). This allowed for an evaluation of the modelled output for turbulent fluxes ( $Q_H$ ,  $Q_E$  and  $\Delta Q_S$ ) against observations made at two flux sites; one urban and one suburban. Each of the flux sites carries the same suite of instruments and measures  $Q^*$ ,  $Q_H$  and  $Q_E$  using an open path eddy-covariance method (see Keogh et al., 2012 for details).  $\Delta Q_S$  is estimated as the residual of the observations (i.e.  $\Delta Q_S \approx Q^* - Q_H + Q_E$ ) The instruments are located approximately twice the height of their surrounding roughness elements with relatively homogenous land cover fetches (extending outwards to approximately  $\geq 1 \text{ km}^2$  radius from the flux towers) thus are assumed to be making observations within the inertial sublayer and are representative of the neighbourhood type in which they are located. The flux data are provided as half-hourly averages of each of the flux terms, and have been shown to correspond well with SUEWS simulations forced with off-site meteorological data previously run in Dublin (Alexander, et al., 2015).

### 6.6.2 Land cover scenarios

The land cover data used here are based MOLAND scenarios for Dublin up to 2026 (see Brennan *et al.*, (2009) and Williams *et al.*, (2012) for further details). Rather than provide an overview of the MOLAND cellular automata model, which is discussed in detail by Barredo *et al.* (2003), a summary of the scenarios utilised in this study and how these were converted into land cover parameters required by SUEWS are given below.

The development scenarios used in this study are illustrated in Figure 6.4. In total four scenarios were examined which are differentiated by different policy priorities and hence, development pathways pursued in order to adhere to the policy chosen. The policies informing the scenarios can be divided into two broad categories; 1) those based on current regional planning guidelines which emphasise strategic green belts between the Dublin metropolitan area and surrounding satellite towns, we refer to this development pathway as urban-densification 2) consolidation of the metropolitan footprint (MF) with surrounding urban areas by expansion along transport corridors, we refer to this development pathway as urban-expansion (sprawl). Table 6.4 provides additional details on each of the four development pathway (DP) scenarios, to summarise;

- (i) DP-1; Business as usual development based on recent trends
- (ii) DP-2; Urban-Expansion along transport corridors
- (iii) DP-3; Urban-Consolidation with strategic satellite towns
- (iv) DP-4; Urban-Densification of existing MF and satellite towns

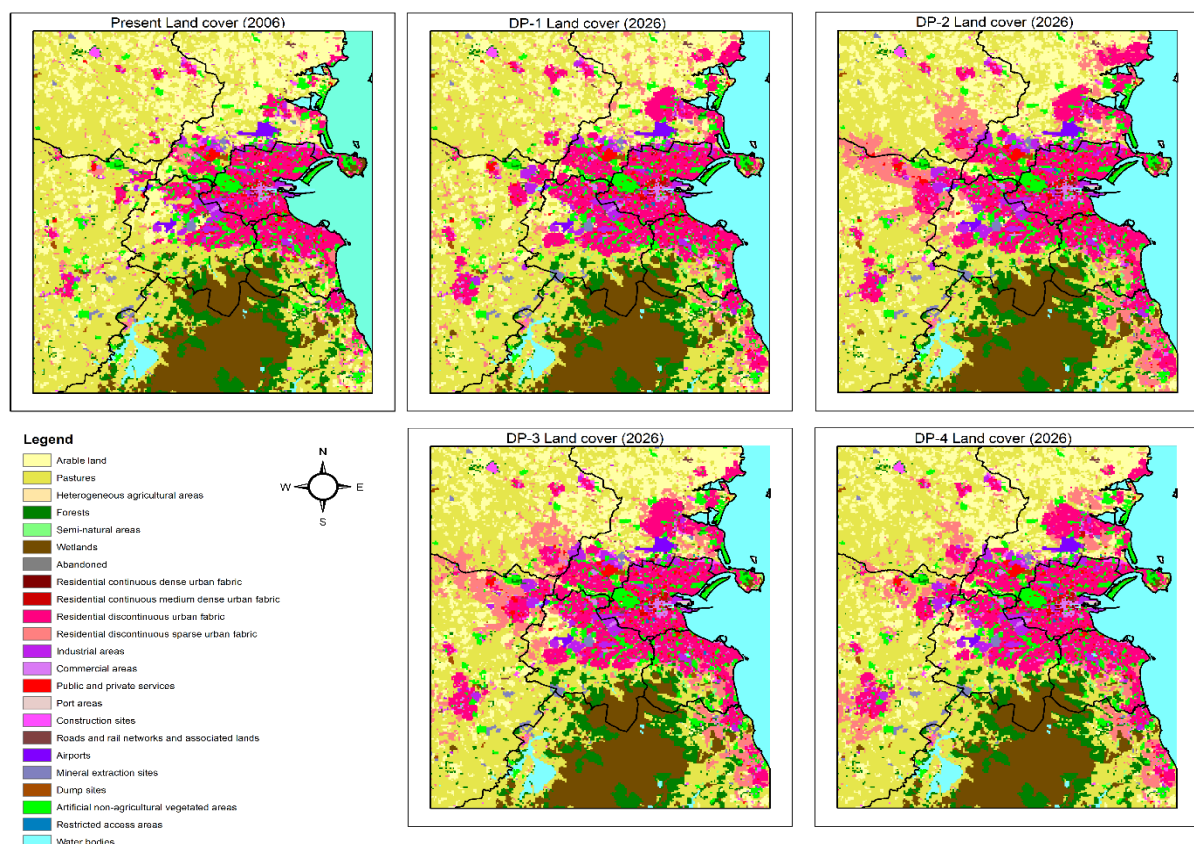


**Figure 6.4** Overview of present day CORINE land cover classes for study area (top left panel) with development pathway scenarios 1-4 - see text / Table 6.4 for more details

**Table 6.4 Outline of the development pathway (DP) scenarios utilised in this study. Further details are provided in Brennan et al. (2009). Urban extent is defined as % of modelled grids that are classed as urban Local Climate Zones (LCZ) the % in parenthesis is the increase in urban LCZ from the 2006 base line case– see Table 6.5 and Figure 6.3**

Scenario short name	Alias	Description	Urban Extent
DP-1	Business as usual	As the alias suggests, this scenario explores a continuation of the current, dispersed settlement patterns. Therefore, simulates a “business as usual” future, whereby implementation of pre-existing development policies have been weak. Reflecting the current economic climate, several transportation projects are delayed in this scenario until 2020. With the divergence of policy and practice concerning Green Belts in mind, this scenario does not contain a greenbelt layer as outlined in Brennan et al. (2009).	19.8% (+6.1%)
DP-2	Undirected sprawl	In this scenario development is strongly directed toward an expanded metropolitan footprint (MF), which is extended along key transport corridors. Strictly enforced Strategic Green Belts are used to discourage excessive development in rural areas and link protected areas together. Two types of Green Belts were created; large Outer Green Belts designed to designate areas where development should be kept to a minimum; and smaller Connector Green Belts, designed to preserve links between urban green space and rural areas.	25.8% (+12.1%)
DP-3	Directed Sprawl	This scenario explores a strong consolidation policy, whereby growth was focused within the existing envelope of the MF and towards a limited number of key towns in the Hinterland. Increased densities were delivered by infilling areas within the MF and in the main towns of the Hinterland. Green Belts were more extensive and strategically placed than DP-2.	25.4% (+11.7%)
DP-4	Densification	In this scenario, consolidation is promoted; development is focused within the existing MF and development centres. Growth in the Mid-East at public transport nodes within the MF and in designated towns on high quality public transport routes. Although densification within the existing MF was a focus of this scenario, there was a drive to keep towns distinct from one another.	23.2% (+9.5%)

The majority of all planned development in each DP are residential areas, which reflects the increasing demand for housing within the case study area. In order to translate the different land cover classes utilised in the scenarios to a format usable by SUEWS (fractional coverages of buildings / pavements / vegetation / trees / water / unmanaged soils) we took the following approach:

1. The MOLAND land-use land-cover (LULC) classes were spatially correlated with a pre-existing LCZ dataset for Dublin. After we established a link between MOLAND and LCZ LULC we converted each MOLAND LULC both 2006 and 2026 into a corresponding LCZ code.
2. Model grids (1 km<sup>2</sup>) were then coded into LCZ based on a majority rule (see Figure 6.5) and assigned fractional coverage based on the values given in Table 6.5
3. These values, obtained from Alexander *et al.* (2015), were generated by randomly sampling LCZ across Dublin and deriving a more precise fractional value for each cover type per LCZ.
4. To incorporate densification as a development policy into the model's land cover based on DP-4, the land cover fractions and building heights for several urban LCZ were modified for the DP-4 model run.

**Table 6.5 MOLAND LULC classes converted into corresponding Local climate zones (LCZ) in the study area, the parenthesis in the LCZ column contains the number of grids (n) that are coded to that LCZ class for the BLC. Plan area fractions (given in % below) were obtained from Alexander et al. (2015). Population are given as persons per km<sup>2</sup>, the values in parenthesis in this column represent population in 2026. The final row illustrates % changes for LCZ 2 DP-4 only**

MOLAND LULC	LCZ Name "Code"	Built	Impervious	Unmanaged	Trees	Grass	Water	Population
Residential continuous medium dense urban fabric; Commercial areas; Public and private services	2 Compact Midrise "LCZ 2" (12)	33	55	00	06	06	00	10130.2 (11981.0)
Residential continuous dense urban fabric	3 Compact Lowrise "LCZ 3" (1)	22	61	00	07	10	00	3867.6 (4574.2)
Port areas; Roads and rail networks and associated lands	5 Open Midrise "LCZ 5" (1)	13	48	00	11	28	00	2335.2 (2761.8)
Residential discontinuous urban fabric; Residential discontinuous sparse urban fabric	6 Open Lowrise "LCZ 6" (270)	14	52	00	11	23	00	3887.9 (4598.2)
Industrial areas; Construction sites; Airports; Mineral extraction sites	8 Large Lowrise "LCZ 8" (58)	30	61	00	04	05	00	1380.7 (1633.0)
<b>Non Urban LCZ (n=2142)</b>								
Forests; Semi-natural areas	A Dense Trees "LCZ 101" (104)	01	02	04	48	45	00	48.3 (57.1)
Arable land; Pastures; Heterogeneous agricultural areas; Dump sites; Artificial non-agricultural vegetated areas; Restricted access areas	D Low Plant "LCZ 104" (1492)	03	08	03	18	67	00	185.5 (219.4)
Wetlands	F Bare Soil/Sand "LCZ 105" (245)	06	20	55	19	00	00	0.0
Water bodies	G Water "LCZ 107" (301)	00	00	00	00	00	100	0.0
2 Compact Midrise (DP4)		+11	-5	---	-3	-3	---	---

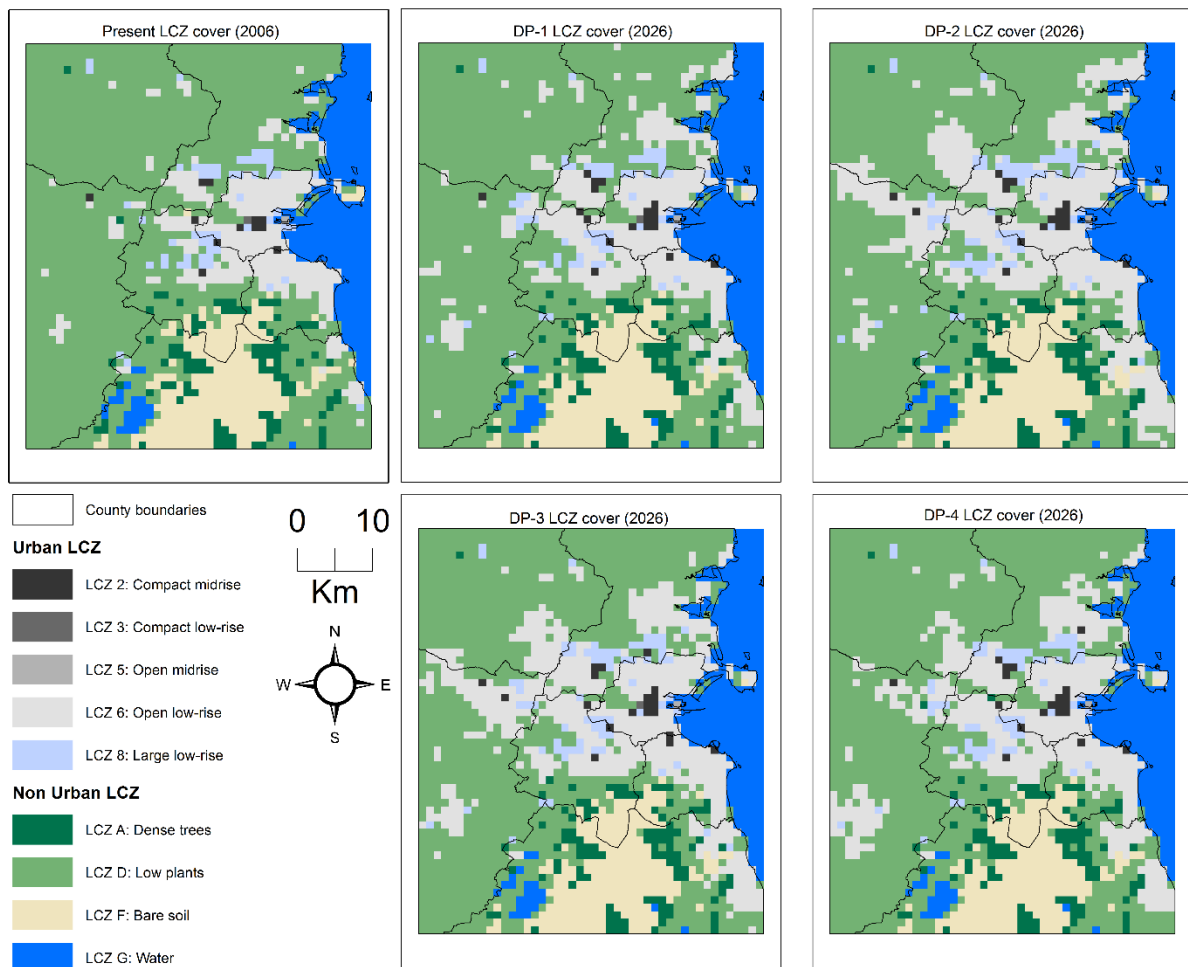


**Figure 6.5 Overview of model treatment of development pathway scenarios. Development pathways (DP-1 to DP-4) are detailed in Table 4 and in text. LCZ fractional coverages are given in Table 6.5. Each grid is coded into LCZ based on majority rule**

### 6.6.3 Anthropogenic Data

SUEWS is capable of simulating the addition of local scale anthropogenic heat ( $Q_F$ ) utilising specified population density per grid and a daily mean  $Q_F$  value, which is adjusted based on a diurnal energy use profile. The population density per grid was obtained from the national census of Ireland (Central Statistics Office, 2012). Population density extrapolated for 2026 was based on the population growth trends from previous census statistics – see Table 6.5. For the model simulations, weekday and weekends are differentiated with two separate hourly  $Q_F$  profiles. The weekday profile assumes an increase in  $Q_F$  from 05:00hrs (local time) through to 09:00hrs associated with commuting patterns and business activity hours. A second peak occurs between 17:00hrs – 18:00hrs associated with traffic flows leaving the city, with a

gradual-steady decline thereafter. The weekend profile is similar, but has no peak around the so-called rush hours, rather a steady increase and consistent  $Q_F$  throughout the day,  $Q_F$  declines at 22:00hrs rather than 17:00hrs which is the case for the weekday profile. An estimate of annual  $Q_F$  was obtained from a lookup Table (Flanner, 2009) and was then weighted for each month.  $Q_F$  was set to be slightly lower in summer months (May-September) than the winter months to reflect reduced space heating demand in summer / increased heating in winter and increased car usage etc. as would be expected for a middle-latitude city (Offerle, et al., 2005).

## 6.7 Results

In the following Sections, an analysis of SUEWS simulations of local scale turbulent fluxes across each neighbourhood is given, focusing on how form (openset verses compact) and function impacts the local climate. Firstly, the impact of the four MOLAND development pathways (DPs) relative to the base line case (BLC) is analysed with respect to the annual and seasonal partitioning of available energy into sensible, latent and stored heat and the spatial distribution across the study area in each DP. To highlight the impact of each DP, we derived the sensible heat index ( $\chi$ :  $Q_H/Q^*$ ) the evaporation index ( $\gamma$ :  $Q_E/Q^*$ ) the storage index ( $\Lambda$ :  $\Delta Q_s/Q^*$ ) and the Bowen ratio ( $\beta$ :  $Q_H/Q_E$ ) since these have direct impact on the local climate (recall Table 5.2). The diurnal profiles of each local climate zone (LCZ) class are then discussed in relation to areas which undergo urban development in each of the four DPs. An assessment of urban design interventions designed to reduce the amount of energy challenged into sensible and stored heat are then presented.

### 6.7.1 Annual and seasonal flux variation

The annual magnitude of sensible heating for LCZ 2 was 60.52% compared to 55.82%.0 and 53.98% for LCZ 6 and LCZ D respectively in the BLC. The impact of DP1-3 was to increase sensible heating by 2.7% and by 7.0% in DP4 for LCZ 2 areas. The increase in LCZ 6 and LCZ D was the same for all DPs, 1.2% and 0.1% respectively. Mean heat storage

for non-urban LCZ in the BLC was 16.04-19.03% excluding water bodies which as expected were a significant store of energy (for water bodies, LCZ F, 26.54% of incoming energy was stored on average). LCZ 2 had an annual value of 53.02% which was higher than the most abundant non-urban LCZ class (LCZ D) value which only stored 19.03% of available energy. For LCZ 6, which is spatially related to residential areas, heat storage was 31.95%. This ranking (highest to lowest energy store) was maintained across all DPs, though there was a slight difference. In DP1-3 LCZ heat storage increased by ~3% for LCZ 2 (inner city areas) and by 1% for LCZ 6 (residential suburban areas) whereas for DP4, storage was decreased by ~2% from the BLC, the increase for LCZ 6 was the same as DP1-3. This LCZ relationship relates to the urban heat island, leading to warmer air temperatures in compact areas of the city compared to vegetated areas and has been demonstrated previously (Alexander & Mills, 2014; Graham, 1993; Sweeney, 1987). The differences in the annual mean values in terms of the amount of energy for surface / air heating and evapotranspiration in each LCZ type are illustrated in Figure 6.6a. In all DP scenarios, the presence of water and vegetated LCZ reduced the annual magnitude of sensible heating and heat storage and increased the annual magnitude of evapotranspiration thus decreasing temperatures day and night and reducing surface runoff as more energy was used for evaporation.

The seasonal differences between LCZ in each DP was similar to annual partitioning of energy, although there was a greater distinction during the summer and winter period in terms of differences in mean  $Q_H$  and  $Q_E$  respectively – Figure 6.6b. During the summer period, mean  $Q_H$  was 82.7, 70.2 and 66.9  $W m^{-2}$  for LCZ 2, 6 and D respectively. In winter, mean  $Q_H$  was 34.4, 22.3 and 11.2  $W m^{-2}$  for the same three classes. Hence, there was a larger difference in sensible heat in winter between LCZ 2 and D than in summer. The opposite relationship existed between these LCZ for evapotranspiration, where the difference in summer was greater compared to winter as expected.

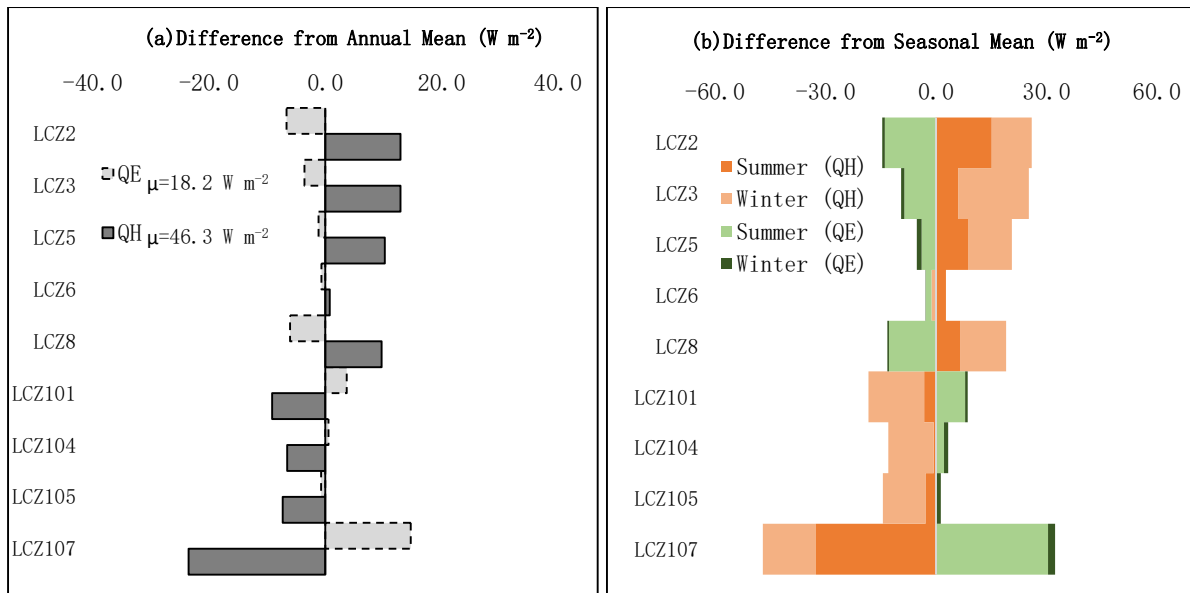


**Figure 6.6 (a) Difference from annual mean  $Q_H$  and  $Q_E$ , this is the mean value taken across all LCZ types, positive values indicate above average annual flux magnitude, in the case of sensible heat, this indicates higher surface / air heating. Negative values indicate below average annual flux magnitude. (b) Differences as with (a) however the values are further divided into seasonal  $Q_H$  (orange shades) and  $Q_E$  (green shades). Note the width of the individual color bars indicates the value above (+) or below (-) average for example,  $Q_H$  for LCZ 101 in summer is  $-3.2 W m^{-2}$  and  $-15.2 W m^{-2}$  in winter.**

The annual and seasonal differences in energy partitioning between LCZ are summarised in Table 6.6. Generally the ratio of turbulent fluxes to available energy follows previous work (Grimmond & Oke, 1995; Keogh, et al., 2012; Ward, et al., 2014). For urban LCZ, the available energy was predominantly channelled into surface/air heating and heat storage (annual sensible heat = 56-68%, evapotranspiration = 10-19% and heat storage = 24-50%) whereas for the non-urban LCZ a higher fraction of the available energy was partitioned into evapotranspiration (annual sensible heat = 24-50%, evapotranspiration = 20-34% and heat storage = 16-26%). There was also a seasonal pattern to the Bowen ratio (the relationship between  $Q_H$  and  $Q_E$ ) found in all LCZ. All areas showed lower  $\beta$  values in summer relative to winter, meaning a slightly higher proportion of turbulent exchange was channelled into evapotranspiration during summer months.

**Table 6.6 Proportioning of  $Q^*$  ( $\chi$ ,  $\gamma$ ,  $\Lambda$ ) and the Bowen ratio ( $\beta$ ) when  $Q^* \geq 0 \text{ W m}^{-2}$ . Presented are unit-less flux ratios for annual and seasonal partitioning.**

LCZ Code	$\chi$ ( $Q_H/Q^*$ )			$\gamma$ ( $Q_E/Q^*$ )			$\Lambda$ ( $\Delta Q_S/Q^*$ )			$\beta$ ( $Q_H/Q_E$ )		
	Ann	Sum	Win	Ann	Sum	Win	Ann	Sum	Win	Ann	Sum	Win
LCZ2	0.675	0.572	1.024	0.115	0.103	0.178	0.507	0.465	0.634	5.884	5.541	5.764
LCZ3	0.568	0.449	0.953	0.139	0.133	0.195	0.323	0.397	0.042	4.098	3.368	4.882
LCZ5	0.591	0.499	0.896	0.168	0.166	0.215	0.265	0.346	-0.038	3.522	3.001	4.160
LCZ6	0.573	0.507	0.771	0.192	0.196	0.227	0.330	0.357	0.226	2.976	2.586	3.401
LCZ8	0.563	0.468	0.873	0.115	0.107	0.171	0.236	0.332	-0.115	4.901	4.387	5.102
LCZ101	0.515	0.504	0.512	0.268	0.282	0.255	0.158	0.211	-0.033	1.921	1.787	2.005
LCZ104	0.544	0.519	0.593	0.228	0.239	0.236	0.187	0.237	0.014	2.383	2.176	2.515
LCZ105	0.516	0.489	0.573	0.205	0.216	0.213	0.223	0.277	0.036	2.513	2.262	2.688
LCZ107	0.241	0.214	0.308	0.339	0.396	0.249	0.264	0.338	0.002	0.713	0.541	1.239

### 6.7.2 Spatial differences between different development pathways

To examine the spatial variation between DPs impact on the BLC, the annual average of each of the indices were calculated in each grid cell (Figure 6.7) based on hourly values across the entire TCY. To assess the impact relative to the BLC, differences on a grid-by-grid basis were calculated by subtracting the annual mean of the BLC from each of the DPs. To examine significant spatial clustering of differences from the BLC, Getis-Ord  $G_i^*$  (Getis & Ord., 1992; Ord & Getis, 1995) was employed which compares local averages to the global averages. In this case,  $G_i^*$  illustrates where there are spatial clustering of increases and decreases in the turbulent fluxes relative to the BLC – see Figure 6.8. This reveals the geographical impact of each DP and identifies specific areas ideal for planning interventions. The partitioning of the annual fluxes for the LCZ classes follows what would be expected in each of the DP scenarios, grids which contain highly urbanised land cover (for instance the compact LCZ 2 and 3) exhibited the highest annual value of sensible heating and heat storage and the lowest annual magnitude of evapotranspiration concentrated around the inner city, whereas grids containing a higher vegetative fraction exhibited comparatively lower values of sensible heating and heat storage and higher evapotranspiration.

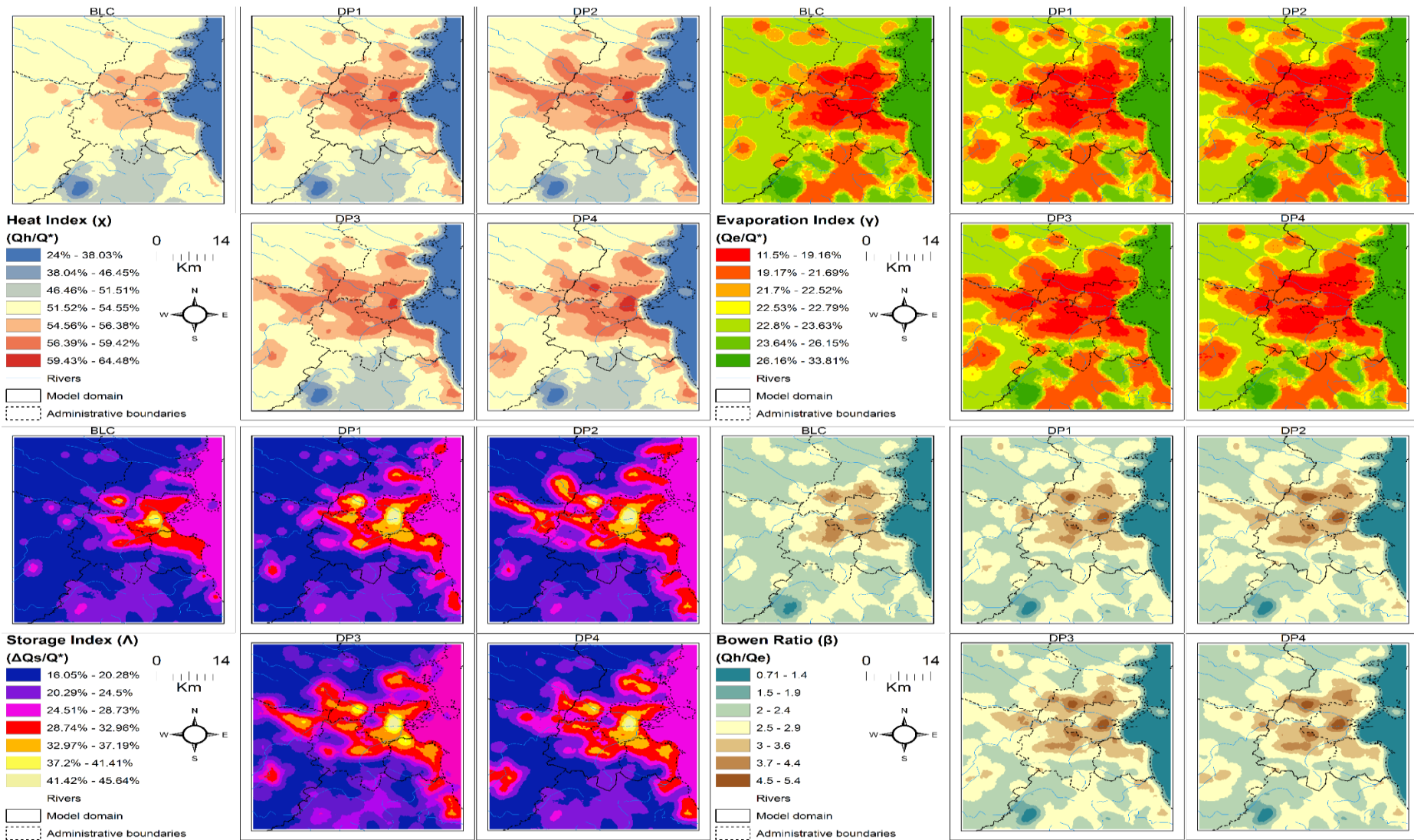


**Figure 6.7** Impact indices for BLC and DPs 1-4. Top left is the heat index ( $\chi$ ) which is the proportion of available energy used for surface / air heating. Top right is the evaporation index ( $\gamma$ ) which is the proportion of energy used for evapotranspiration. Bottom left is the storage index ( $\Lambda$ ) which shows the proportion of available energy stored in the substrate (buildings/pavements/soils), this effectively shows the potential UHI extent. Bottom right is the Bowen ratio ( $\beta$ ) which is the relationship between the heat and evaporative index, a higher number indicates more energy is used for surface / air heating meaning less water is evaporated hence is available for runoff.

As expected, the sprawling scenarios (DP2 and DP3) exhibited the largest spatial increase (that is, the number of areas with higher annual values compared to the BLC) in sensible heating and heat storage coupled with the largest decrease in evapotranspiration (see Table 6.7). Taking the number of areas with increased sensible heating relative to the BLC; DP3 exhibited the largest spatial increase (increasing in 14.1% of the modelled area) followed by DP2 (13.3% increase in area) DP1 (9.9% increase in area) and finally DP4 (6.4% increase in area). When the number of grids with decreases relative to the BLC were also taken into account, the ranking remained the same. The ranking for the number of areas with decreases in evapotranspiration were similar, however the number of areas in DP2 relative to the BLC was marginally higher than DP3 (6.9% and 6.3% respectively). Decreases in evapotranspiration were greater in DP1 than DP4. For storage, which illustrates the potential of the UHI, the ranking was DP2 (15.6%) followed closely by DP3 (15.5%) then DP1 (9%) and DP4 (6.4%). Out of the four scenarios DP4 had the least impact in respect to the number of areas with surface/air increases, evapotranspiration decreases and heat storage increases.

To further investigate the spatial differences between DP scenarios, 3 subsets of the model domain were examined based on these impact hotspots (see Figure 6.9) located around the inner city and 2 non-urban areas which became urbanised in each DP scenario. These were also used for examination of the diurnal energy profiles (Section 6.5.3). Within these subset areas, the type of development in each DP controlled the impact relative to the BLC. The replacement of LCZ D with LCZ 6 in the case of DP1-3 had the largest impact relative to BLC sensible heating. There were marginal increases in sensible heating and heat storage in the inner city where LCZ 3 was replaced with LCZ 2 in DP1-4. The impact on evapotranspiration was lower in LCZ 6 areas owing to their higher level of vegetation compared to LCZ 2 / 3. In the suburban subsets, DP4 was again identified as having the least impact compared to DP1, 2 and 3.

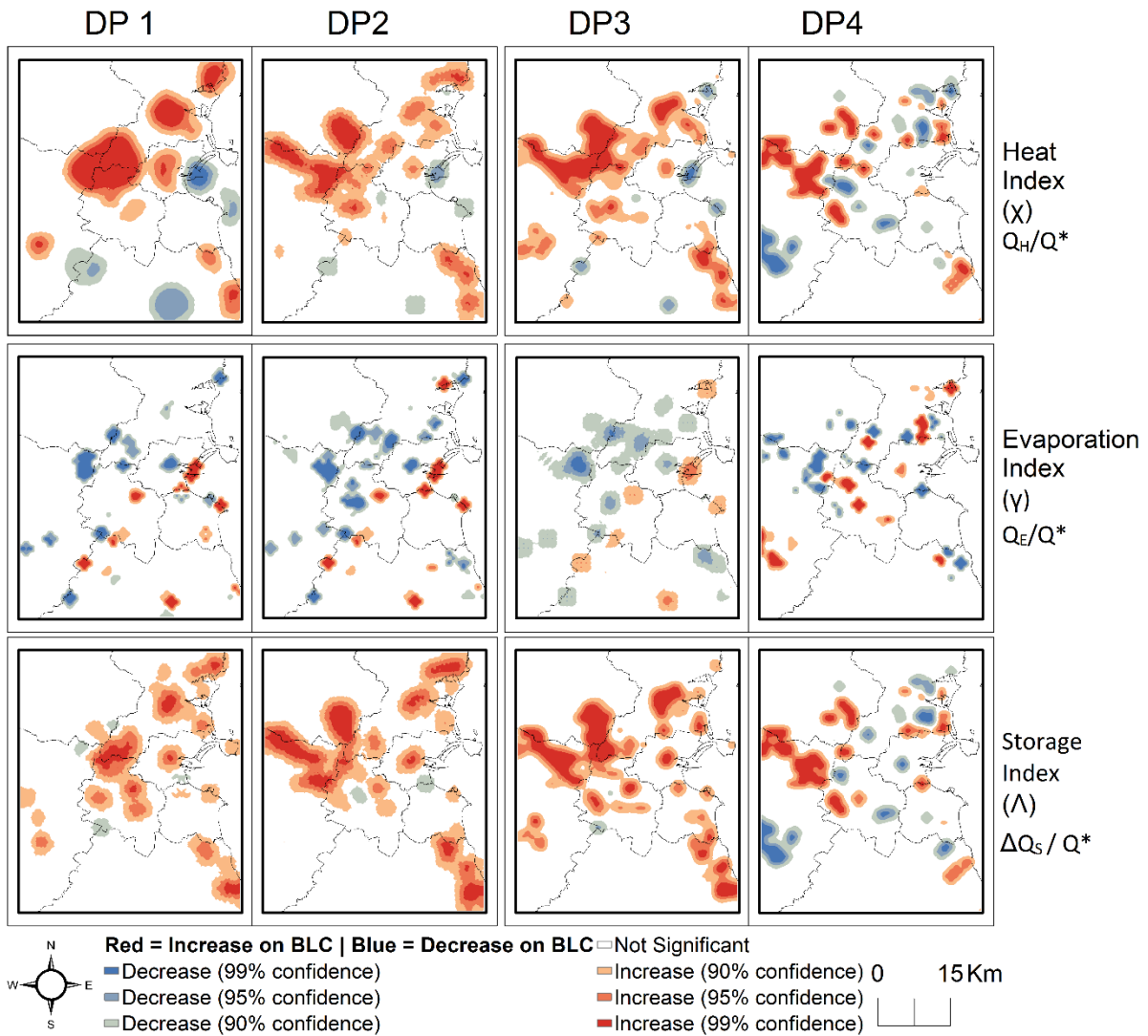


**Figure 6.8** Spatial distribution of increases/decreases in impact indices compared to BLC for each DP (columns). The differences are based on annual mean values

In a study by Demuzere et al., (2013) which simulated the impact of different urban environments on the surface energy balance, a similar energetic-hierarchy to what was established here was found between compact and open-set residential thermal climate zones, which are an earlier iteration of the LCZ 2 and LCZ 6 classes respectively. The reduction in vegetation fraction leads to a minor decrease in evapotranspiration though the larger impact is found in terms of heat storage as the heat capacity of these areas significantly increases due to the additional buildings and pavements. Work by Stewart et al., (2014) which examines the impact of this hierarchy on air temperature differences across LCZ highlights the impact of this on the UHI and diurnal temperature range across different LCZ.

**Table 6.7** The number of areas (as % of total model domain) with higher/lower annual values of  $\chi$ ,  $\gamma$  and  $\Lambda$  relative to BLC broken down into each DP. Note DP4 has the lowest net spatial impact meaning increases in one part of the city are offset by decreases in other parts.

Development Pathway	Net spatial increase/decrease compared to BLC		Significance level					
	( $\Sigma$ Increase - Decrease)		+99%	+95%	+90%	-90%	-95%	-99%
<b>DP1</b>								
Heat index $\chi$ ( $Q_H/Q^*$ )	8.9%		4.8%	4.9%	0.2%	0.0%	0.0%	1.0%
Evaporation index $\gamma$ ( $Q_E/Q^*$ )	-2.2%		1.3%	0.3%	0.7%	0.9%	1.7%	1.9%
Storage index $\Lambda$ ( $\Delta Q_s/Q^*$ )	7.7%		7.9%	0.4%	0.7%	0.8%	0.1%	0.4%
<b>DP2</b>								
Heat index $\chi$ ( $Q_H/Q^*$ )	12.1%		7.8%	3.4%	2.1%	0.0%	0.1%	1.1%
Evaporation index $\gamma$ ( $Q_E/Q^*$ )	-4.4%		1.5%	0.3%	0.7%	2.0%	2.4%	2.5%
Storage index $\Lambda$ ( $\Delta Q_s/Q^*$ )	14.9%		9.2%	2.1%	4.3%	0.1%	0.5%	0.1%
<b>DP3</b>								
Heat index $\chi$ ( $Q_H/Q^*$ )	12.9%		8.5%	2.7%	2.9%	0.0%	0.0%	1.2%
Evaporation index $\gamma$ ( $Q_E/Q^*$ )	-4.0%		1.4%	0.3%	0.6%	0.8%	2.5%	3.0%
Storage index $\Lambda$ ( $\Delta Q_s/Q^*$ )	14.9%		9.0%	2.8%	3.7%	0.5%	0.1%	0.0%
<b>DP4</b>								
Heat index $\chi$ ( $Q_H/Q^*$ )	0.1%		6.1%	0.1%	0.2%	3.1%	0.5%	2.7%
Evaporation index $\gamma$ ( $Q_E/Q^*$ )	0.0%		1.9%	0.3%	1.2%	0.2%	1.1%	2.1%
Storage index $\Lambda$ ( $\Delta Q_s/Q^*$ )	0.7%		5.6%	0.4%	0.4%	2.9%	0.2%	2.6%

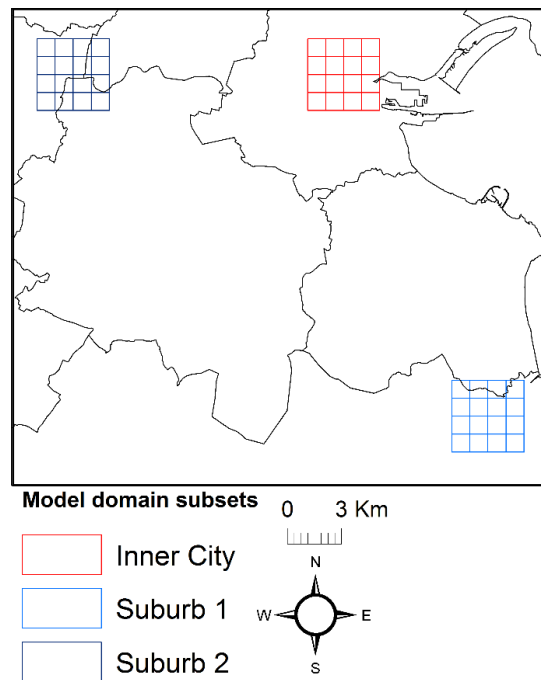


**Figure 6.9** Illustration of the domain subsets for detailed analysis of change in each DP and diurnal analysis (i.e. Section 6.7.3)

### 6.7.3 *Impact of development on seasonal diurnal fluxes*

Figure 6.10 illustrates the findings related to seasonal differences in energy budgets within the subset areas due to land cover change. For the inner-city subset, compact lowrise areas (LCZ 3 – Figure 6.10c) in the BLC were replaced with compact midrise areas (LCZ 2 – Figure 6.10a) in each of the four DP scenarios. The most distinguishable effect of this was to increase heat storage during both winter and summer and introduce significant hysteresis into the energy budget around these areas. Note for instance, LCZ 3 (BLC) the close temporal correspondence between available energy and heat storage in terms of the diurnal profile, whereas for LCZ 2 (DPs) a lag of 6 hours between the time available energy and heat storage both reach a minima value. We hypothesise due to decreased Sky View Factor ( $\Psi$ ), increased height to width ratio (H/W) and decreased effective albedo, which area parameterised in the LCZ concept, heat withdrawal became less efficient across the inner-city urban subset in each DP scenario relative to the BLC. This applied for both winter and summer.

For the suburban subsets, vegetated areas with low plant cover (LCZ D – Figure 6.10d) were replaced with residential areas (LCZ 6 – Figure 6.10b) in each of the DP scenarios, though the number of areas in the subset varied between DP1-4. In cases where LCZ D was replaced with LCZ 6, the impact during winter was an increase in surface / air heating during all hours, though the increase was slightly higher during daylight hours. Heat storage was increased by during daylight hours. There was little distinction in evapotranspiration though it was marginally higher for LCZ 6.

During the summer, daytime surface / air heating in the urban subset increased significantly at midday. Evaporation during the day was reduced. In the suburban subsets, the largest impacts were on heat storage, which increased significantly at midday, and a reduction in evapotranspiration for all hours similar to winter, though there was a tenfold increase in the difference during summer.

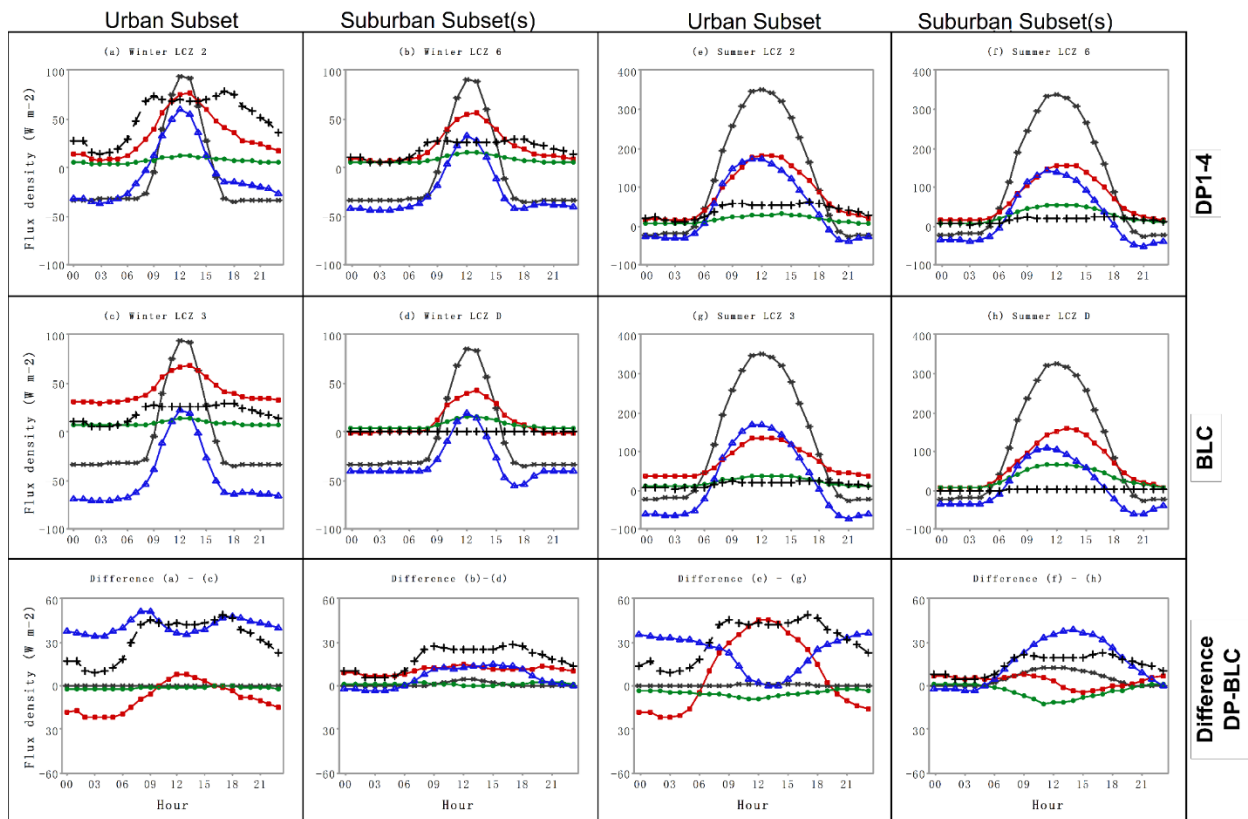


**Figure 6.10** Seasonal diurnal profiles for dominant LCZ in BLC (2<sup>nd</sup> row) and DP scenarios (1<sup>st</sup> row). The first 2 columns show winter diurnal profiles; the last 2 columns show summer profiles. The 3<sup>rd</sup> row illustrates the difference in the first 2 rows in each column. Stars (\*) show  $Q^*$ , squares ( $\square$ ) show  $Q_H$ , circles ( $\circ$ ) show  $Q_E$ , triangles ( $\Delta$ ) show  $\Delta Q_s$  and crosses (+) show  $Q_F$ . The impact (final row) from left to right can be interpreted as follows: 1) increased heat storage in the inner city and higher anthropogenic heat source in winter 2) in the suburbs, increased heat storage (UHI) and surface/air heating day and night in winter 3) Increased surface/air heating during the daytime hours in the inner city during summer 4) increased heat storage and surface /air heating in summer in suburbs during summer

#### 6.7.4 Design interventions for low impact development

Based on the previous Sections, DP4 had the least impact on the annual, seasonal and spatial fluxes across the model domain across all growth scenarios, hence this is the optimum growth pathway in terms of reducing the spatial impact on the local climate. To examine how sustainable design might be coupled with this type of growth to further reduce the impact on the UEB, several design interventions were tested using DP4 as the growth scenario – see Table 6.8. The first design intervention was simply to rebalance the ratio of vegetated to paved areas and modify the type of tree species. The second design intervention was to reduce the overall building footprint by instead promoting upward development. Therefore, building heights were modified and expansive green spaces encouraged, as with the first intervention, tree species were modified however an equal mix of deciduous and coniferous trees were used. The third

intervention was an extension of this, however additionally roof tops for all buildings were greened. The aim was to reduce the seasonality in evapotranspiration i.e. increase energy partitioning into evapotranspiration during winter and decrease annual fluxes of surface / air heating and heat storage relative to LCZ D areas in the BLC.

The first design intervention is the most modest, in that it simply controls the type and level of vegetation in future developments, specifically, the replacement of LCZ D with LCZ 6. The result was to reduce the impact of urban development on summertime evapotranspiration by 34.0%. Both the second and third design interventions which further modified the coverage and type of buildings reduced the impact further. The second design reduced the impact on summertime evapotranspiration by 47.7%, the third design reduced the impact by 52.2%.

The impact of urban development on the annual magnitude of surface / air heating was reduced by 30.1%, 37.5% and 38.6% in design 1, 2 and 3 respectively, the impact on heat storage was reduced by 7.9%, 15.8% and 21.7%, meaning the green roof design reduced the impact of urban development the most.

**Table 6.8 Design interventions tested here. LCZ 6 areas in DP4 were modified as per description and the model re-run. Exemplar images in the first three rows are all existing locations for Dublin city**

GIS model of example area	Exemplar image of existing area	Description
		<b><u>BLC area (LCZ 6)</u></b> Area comprises Lowrise buildings ( $\mu = 2.45\text{m}$ ) 15% building cover 10% tree cover (all deciduous) and remainder split between pavements and unirrigated grasses
		<b><u>Design intervention 1</u></b> Buildings as with BLC area (above). Tree cover and unirrigated grasses are increased (5% each) replacing paved areas. Tree species are modified to be predominantly coniferous (80:20 split between coniferous and deciduous)
		<b><u>Design intervention 2</u></b> Building coverage is reduced by 5% height increased by 2.45m. Tree cover and unirrigated grasses are increased (2.5% each) replacing building areas. Trees are modified to be a mix of species (50:50 split between coniferous and deciduous)
		<b><u>Design intervention 3</u></b> As with design intervention 2, however additionally green roof design are introduced to all buildings. Unirrigated vegetation type used to modify OHM coefficients for storage. Albedo and emissivity values ( $\alpha$ , $\epsilon$ ) for building roof tops also modified

## 6.8 Discussion

The impact of neighbourhood form and development on the urban energy budget (UEB) was examined under 4 distinct development scenarios in order to examine the optimum development pathway for Dublin city. The UEB was examined in terms of spatial changes due to urbanisation (primarily on the existing urban fringes), the seasonal differences in sensible, latent and stored heat and the impact on the diurnal profiles in different areas. Employing the local climate zone (LCZ) scheme allowed for this examination and provides useful guidance (Stewart & Oke, 2012). However as with most urban areas, individual areas though similar in form and function will differ (i.e. intra-LCZ differences) somewhat in terms of specific fractional coverages of vegetation, buildings and pavements. The use of very high resolution data, for example individual building footprints, heights, trees derived from a LIDAR system, would have allowed for examination of the UEB in greater detail and address the limitation of treating all LCZ areas equally. However, in data starved settings for example, cities in the economically developing countries, such an approach is not feasible, therefore this approach was not employed here. Moreover, there has been a recent call for standardisation in how urban areas are described in order to allow for more robust inter-city comparisons with respect to climate, impacts on human comfort, pollution and urban development (Ching, 2013; Bechtel, et al., 2015).

While the replacement of natural, vegetated landscapes with artificial materials associated with urban areas will inevitably impact upon the surface energy budget the results here illustrate the type of urban development plays a significant role on this impact at the local scale, moreover seasonal considerations should be taken into account. The densification (i.e. upward development) of existing urban plots was shown to increase winter time storage of heat, thus reducing the level of temperature changes within these areas (sensible heat). However, this will lead to increased levels of heat released back into the atmosphere at night, which serves to

enhance the urban heat island effect under the right synoptic conditions. During the summer months, daytime surface/air heat increased in these areas due to multiple reflectance (i.e. increased net radiation) which has major implications for daytime cooling requirements and human thermal comfort. Urban sprawl was shown to increase surface/air heating and heat storage significantly in both winter and summer, and decrease evapotranspiration in summer months. Again this has implications for energy use and human comfort thus strengthens the case for including such information in planning decisions. Moreover, since most of the projected development will occur along river basins, the decrease in evapotranspiration and increase in impermeability will increase runoff levels in these areas, creating a potential flood hazard. This strengthens the case for DP4 as being the DP with the lowest potential impact in terms of local climate.

The design interventions tested here focused on local scale mitigation of the impact on the UEB, undoubtedly such interventions will have a larger impact on the micro-to-building scale climate. The inclusion of coniferous vegetation in mid-latitude city such as Dublin (design intervention 1) served to reduce the seasonality of evapotranspiration which is lower in winter for deciduous vegetation (Lindberg & Grimmond, 2011; Peng & Jim, 2013) this in turn reduces the amplitude of surface/air heating during both winter and summer months. The inclusion of green roof tops (design intervention 3) served to further reduce local scale partitioning of energy into both surface/air heating and heat storage which was the intended outcome. However, the decrease was similar in magnitude to the first design intervention. As such the justification for including this design feature into future planning may appear weak, however the multiple benefits of natural roofing material at different scales should also be considered and will be part of future work.

Overall the SUEWS model proved to be capable of reproducing the expected differences between urban and non-urban UEB when linked with LCZ and forced with off-site

meteorological data, thus enabling background climate data to be translated into urban specific data for identifying specific areas for planning / policy interventions.

## **6.9 Conclusion**

The aim of this study was to investigate the optimum development pathway for a mid-latitude city with respect to reducing the spatial and temporal impact on the surface energy budget. Different policy priorities informing distinct development scenarios were examined. The MOLAND cellular-automata model was linked with the SUEWS urban energy and water budget model, the local climate zone classification and meteorological data from outside the urban area.

Drawing from the results of this study, we conclude that the optimum development scenario is one which preserves a higher overall proportion of vegetated land cover. Such development inevitably leads to an increased proportion of energy channelled into sensible heating of the near surface atmosphere and additionally heat storage within the urban fabric across the domain.

Therefore, design interventions which aimed to reduce this impact locally were investigated. An effective solution is the inclusion of vegetation that is photosynthetically active throughout the summer months and remains active during the winter months which serves to promote energy uptake by vegetation and thus increase latent heating. We conclude that incorporating urban climate data into development and design processes where meteorological observations are otherwise absent is possible and allows for a range of development pathways and local scale impacts to be examined. Such applications serve to increase the incorporation of urban climate knowledge into the planning and design process which can ameliorate environmental conditions for the urban population and reduce the negative impacts of development.

---

## Chapter 7 Discussion and Conclusions

---

The main objective of this thesis was to devise a method by which a mid-complex urban climate model (UCM) could be parameterised, using an existing classification technique suitable for use in data sparse locations, and applied in order to improve the integration of urban climate knowledge with the urban planning community. UCMs can be utilised to examine the potential impacts of land cover change on surface-atmosphere exchanges of heat and moisture. These exchanges have implications for issues such as human comfort, heat stress and energy use, all of which have a direct bearing on city design, and consequently anthropogenic emissions of greenhouse gases. In order to achieve this objective, several aspects were examined by this thesis, including:

- I. **Deriving forcing data and model applications:** The issue of data availability and the application of UCMs to planning problems in a standardised way are critical to the main objective of this research. Therefore, a modelling approach was developed and applied which seeks to directly overcome issues of data scarcity, while at the same time providing an approach which is user friendly for the planning community. The main aspect of the approach was to derive the necessary morphological parameters for large sections of the urban area, rather than the more traditional tessellation approach. To that end, the Local Climate Zone (LCZ) scheme of Stewart and Oke (2012) was employed to derive model parameters required by a mid-complex model. Ultimately, the work responds to Ching's (2013) assertion that the LCZ could provide first estimates of the parameters required to run a UCM.
- II. **The state of urban climate knowledge *vis a vis* models:** Once the necessary input parameters were derived, the ability of the Surface Urban Energy and Water Balance Scheme (SUEWS) of Järvi *et al.* (2011) to reproduce exchanges of radiant, sensible and

latent heat between the surface and near surface atmosphere in urban areas was examined. This was taken as a proxy for the state of urban climate knowledge, hence, a thorough and robust examination into the ability of SUEWS was conducted in order to demonstrate the general ability of the model to simulate urban-scale processes and to understand where knowledge gaps still exist.

III. **Methods of model evaluation:** The methods employed in examining model performance have heretofore been applied in an *ad hoc* and unsystematic manner, often in limited spatial and climatic circumstances. Yet, evaluating models in a wide variety of circumstances is a major research priority for the field of urban climate. Therefore, model evaluation was undertaken here using a mix of traditional and novel methods. However, there is still a need to a) formalise the examination of model performance and consolidate previous (and future) model evaluation exercises, b) incorporate additional novel methods to the evaluators' arsenal and c) provide an objective or aspiration to the wider urban climate community to better coordinate model evaluation in as many circumstances as possible.

## 7.1 Discussion

While these aspects were examined separately by individual papers, it is argued here that together they form a cohesive piece of work. In the sections that follow, the findings of each of the papers are discussed in relation to aspects I-III, the linkages between these papers are also commented upon.

### 7.1.1 Urban land cover data for modelling

The main aspect examined by this thesis relates to the manner in which the data necessary to force a UCM can be obtained universally, in a standardised and efficient manner. Arising from this is an additional aspect relating to the applicability of such an approach for planning problems, or put differently, whether there is a trade-off between satisfying data

requirements and the range of model applications. All papers included in this thesis deal with this aspect directly through the employment of the LCZ-Approach (Chapter 2, Section 2.3). In the case of Chapters 3 and 4, the use of the LCZ-Approach was examined in relation to the performance of SUEWS at the different sites. It was illustrated that the LCZ-Approach obtains data in standardised way and is applicable in data poor settings (Bechtel *et al.*, 2014; Ching, 2013). Moreover, the use of this approach did not significantly impact negatively on model performance. In Chapter 5, the use of the LCZ-Approach to derive LST typologies meant relative differences could be examined between urban and non-urban LCZ, which allowed for both validation and evaluation of SUEWS based on statistically averaged LST, which represents a new departure for the SUEWS model.

Chapters 3-5 demonstrate that the use of typologies of land cover fractions obtained through the LCZ approach combined with off-site meteorological data are sufficient for applying the SUEWS model and obtaining reasonable results between different neighbourhood types. In Chapter 6, the question shifted to whether or not the use of this approach limited the application of SUEWS to a real planning problem, namely the impact of future planning choices on local scale climate. Without the employment of the LCZ-Approach, obtaining the necessary inputs to run SUEWS for the future land cover scenarios would have been far more challenging; given the fact that a large number of permutations of urban form exist across the Greater Dublin Region – Figure 2.5 / Figure 6.4. The employment of the LCZ-Approach to derive the necessary input parameters and apply SUEWS to each of the scenarios overcame this issue, hence, can be seen as advantageous in data poor settings – Figure 2.3.

In these cases, using a LCZ map of an urban area to sample different neighbourhoods was an effective means to derive the necessary land cover inputs for SUEWS in a standardised way across multiple sites and for an entire region quickly and efficiently compared to a more detailed (grid-based) approach. Naturally, differences occurred between both approaches. In

the best case, fractional coverages of different land cover types using the LCZ-Approach fell within 5% of fractional coverages derived using high resolution satellite imagery and/or field work i.e. values that would be obtained through tessellation. In the worst case, fractional coverages deviated by 23% for specific LCZ classes between both methods.

Despite this, SUEWS proved to be relatively insensitive to such differences, and was still capable of accurately simulating turbulent fluxes for multiple sites. The larger impact on SUEWS performance was found to be the use of off-site meteorological data conforming to WMO standards. The use of these data increased the model error by twice that of using LCZ-derived land cover fractions, though the increase in error in both cases were modest. The greatest issue with the LCZ-Approach was found in its application to areas which straddle two different LCZ types e.g. Chapter 4, the case of Hamburg, Germany. Even with strict filtering by means of employing a footprint model for observational data to only include data representative of the modelled LCZ class, RMSE was relatively high ( $>50 \text{ Wm}^{-2}$ ) in some instances. This limits its application to areas with homogeneous neighbourhood types, be it urban or non-urban. Hence, simulations produced using the LCZ-SUEWS approach should be interpreted with caution at the boundaries between contrasting land cover types.

Nevertheless, the use of the LCZ-Approach moved the methodology to derive the necessary inputs (and interpret the simulations of SUEWS) into a GIS environment, which is arguably more familiar to practicing planners (Lindberg, et al., 2015). All papers demonstrate that the LCZ-Approach is advantageous for deriving the necessary inputs to satisfy the input requirements of a state-of-art UCM, with Chapter 6 further demonstrating how this can then be employed by planners, which has been lacking in the field of urban climate for some time (Hebbert & Mackillop, 2013; Oke, 2006).

### 7.1.2 *Urban climate model performance*

Be it in the development of dynamical (numerical) models, or capturing these processes appropriately through the use of empirical (statistical) parameterisation, UCMs demonstrate state-of-the-art understanding of the physical, biological and chemical processes which operate within the urban climate. Naturally, the ability of UCMs can then be seen as a reflection on the quality of this understanding.

While model development has been relatively successful, in that there is now a healthy ecosystem of UCMs available, model performance as a topic is less well developed (Oke, 2006; Masson, 2006). The international urban energy budget comparison experiments (PILPS-Urban) have been vital in progressing this (Grimmond *et al.*, 2010; 2011). While general conclusions may be drawn from PILPS-Urban, attention on individual model performance is still deserved, particularly as the focus begins to shift towards specific applications of models for solving urban problems. To that end, model evaluation formed a major component of the present work, having established that LCZ could provide parameters for use in the selected UCM. The selected model, the Surface Urban Energy and Water Balance Scheme – SUEWS (Järvi *et al.*, 2011, 2014), was chosen on for the following reasons:

1. SUEWS includes both physically realistic water balance and vegetative components, which were identified as being critical in UEB model performance during PILPS-Urban study
2. SUEWS requires a relatively low number of input parameters, which suggests it may be applied in data poor settings
3. SUEWS was developed at the neighbourhood or local scale, which is argued to be the scale at which planning decisions and interventions are most likely (Eliasson, 2000).

All of these criteria i.e. that the chosen model be physically realistic, applicable in data poor settings and applied to the local-scale were identified as essential in light of the main objective of this thesis.

The first paper in this collection, Chapter 3, examined the ability of SUEWS to reproduce the differences in the urban energy balance (UEB) between a highly urban and a suburban site in Dublin (Ireland). A modified form of the PILPS-Urban approach was employed whereby more sophisticated forcing data, both meteorological and morphological, were added in stages and the impact on model performance examined. The performance of the model, expressed through the RMSE, in simulating turbulent fluxes under a number of stages was remarkably good – Table 3.9.

Two critical aspects of SUEWS performance were identified in this paper: firstly, model performance was relatively insensitive to land cover parameters, whether they are derived in a detailed manner or based on statistical averaging of morphological features e.g. building fractions, paved fractions, roughness height and so forth. Secondly, the use of meteorological data collected off-site and, strictly speaking, in violation of the assumptions of the model (see Figure 7.1 for illustration) reproduced well the differences between an urban and suburban area, despite having a large impact on model performance – Table 3.11.

While every effort was made to ensure the results could be generalised to similar pairings of sites (LCZ 2 and LCZ 6), ultimately this is based on an assessment carried out over two sites in Dublin (Ireland) which were instrumented during a carefully designed observational campaign (Keogh *et al.*, 2012; Keogh, 2015).

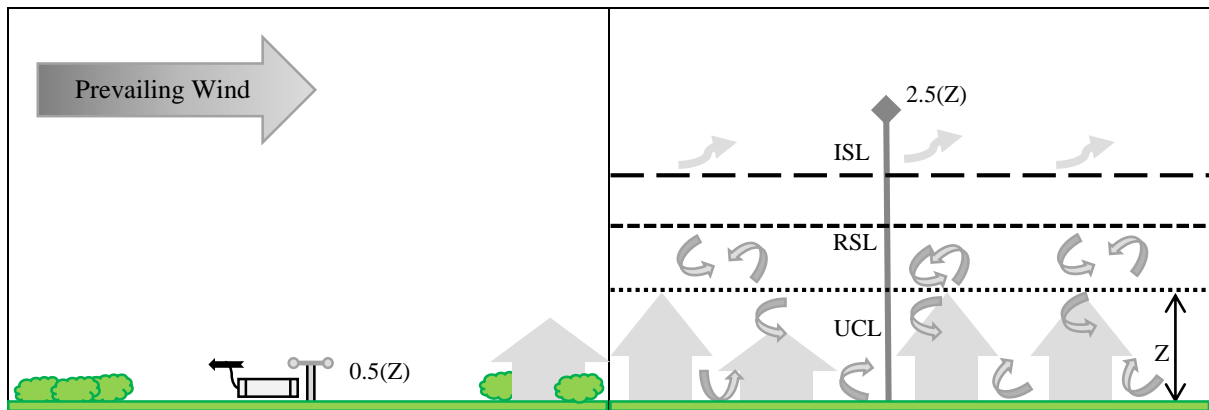


**Figure 7.1** Illustration of the findings of Paper 1: The right-hand pane illustrates the correct circumstances in which forcing data should be provided for SUEWS i.e. based on observations made within the inertial sublayer, approximately twice the height of the surrounding roughness elements ( $Z$ ) which should be relatively homogenous (adapted from Grimmond & Oke 2002). The left-hand pane illustrates the forcing data used for specific stages of the experiment in Paper 1, based on WMO standard observations at roughly 0.5 times  $Z$ . In both cases, SUEWS performance was capable of reproducing differences in turbulent processes between an urban and suburban area

### 7.1.3 Interpretation of model performance: observational considerations

In Section 2.3 it was highlighted that in calculating model performance metrics, the observations are assumed to be a truthful representation of the state of the atmosphere, it was also highlighted that this assumption should be treated with some caution. The temporal and spatial representativeness of observations contain significant uncertainties, particularly in urban areas - as highlighted by Oke (2006). Averaging observations and model outputs over the course of a year reduces the spatial variability, therefore model performance over the course of an entire year maybe regarded as robust, at the same time it should be generally accepted that hourly and daily observations used to quantify error and bias exhibit far more variability. This was a concern for Chapter 5 on the use of daily LST data from the MODIS sensor, hence why LST were averaged over the course of each month in order to derive a more reliable signal for model evaluation of the surface urban heat island.

Within urban areas, deriving the source area for point observations can be particularly problematic (Lowry 1977) which will also impact on the model performance metrics. The use of the LCZ concept goes some ways towards reducing the uncertainty of thermal source areas for urban observations (Stewart & Oke 2012) however, eddy covariance (EC) observations in urban areas are complex and often contain large errors.

In all cases, post processing techniques were used to remove these errors from EC observations, however observational errors will remain, particularly due to the energy balance closure problem (Foken 2008; Keogh 2015). Moreover, estimating  $\Delta Q_s$  as the residual of the observations will contain errors from all other terms. The impact of this on the calculation of model performance is reduced by careful documentation of the siting of the instruments e.g. Chapter 3 and the representativeness of  $K\uparrow$  from the observation platform located in the suburban site. Nevertheless, in all cases, the same set of observational data were used to compare the LCZ-SUEWS approach with more high resolution data, meaning direct comparison between model performance at individual sites was possible, cross-site comparisons should be interpreted with more caution.

Where possible, a long series of observational data were used to derive model performance metrics - this was done to ensure the sample size for these statistical measures were as large as possible. The exception here was on the use of a short period for validating SUEWS spatially (Chapter 5) rather than evaluating its performance. Here, the goal was to identify the ability of the model to spatially disaggregate the urban area of Dublin from surrounding non-urban hinterland, as the spatial validity of the model has not been addressed previously.

Since the urban effect is known to be strongest under calm settled synoptic conditions, the use of a limited amount of data was justified for spatial validation in the first instance, as during synoptic conditions known to militate the urban effect (rain, cloudy, windy conditions) no clear demarcation could have been expected. However, further examination using a larger dataset would be required to draw definitive conclusions on the spatial validity of the model. Therefore, it is important to remember the specific objectives of model assessment i.e. evaluation or validation, as discussed in Section 2.3, the availability of observational data and accuracy of these data when interpreting the results presented here.

#### 7.1.4 Utilising remotely sensed data for assessing model performance

Following on from recent work by Hu *et al.* (2014), remotely sensed land surface temperature (LST) was employed for validating the model spatially and evaluating its ability to reproduce the surface urban heat island (SUHI).

This represents a novel approach in model evaluation within the urban setting. Most UEB models are evaluated against observations of turbulent fluxes obtained by means of the eddy-covariance (EC) technique, for example, in Łódź, Poland, and Baltimore, Maryland (Loridan, 2011), Phoenix, Arizona, and Portland, Oregon, (Middel *et al.*, 2012). Due to their expense and sophistication, EC observations are often made during defined observational campaigns, which are limited both spatially and temporally. Therefore, remote sensing offers an additional means in which to evaluate UCMs. The advantage of remote sensing is clearly the large spatial coverage and the number of years in which observations are made, for instance, The MoDerate-resolution Imaging Spectroradiometer (MODIS) instrument on board the Terra platform has been making observations of LST since 1999. In addition, these data are delivered to evaluators free of cost. The disadvantage is that the observations are made at an instantaneous point in time, referred to as the sensor overpass time. This means rather than being able to evaluate models on a diurnal basis, evaluation must be carried out at specific local time(s). Moreover, if there is persistent cloud cover over the region of interest during the overpass times, there can be little if no basis for evaluation.

To overcome this issue, LST for Dublin were integrated on a monthly basis for an entire year. This served to filter out cloud cover (and partial cloud cover) days during the sensors' overpass times. However, this limits the resultant analysis, since LST is spatially averaged across 30 days. However, this still allowed for model evaluation in both space and time across an entire year. The parameterisation for LST employed by SUEWS appeared spatially valid; a clear demarcation between urban and non-urban LST was seen – Figure 5.6/5.7.

On the validity of the LST parameterisation within SUEWS (again, forced using the LCZ-Approach), the model was capable of distinguishing LST between high-density urban, mid-density and low-density urban LCZ (intra-urban) and non-urban LCZ (inter-urban) differences. The model overestimated LST for low-density (e.g. LCZ 6) urban areas and underestimated LST for non-urban (e.g. LCZ D) areas. In relation to the SUHI, the parameterisation of daytime LST (which employs a correction based on  $K_{\downarrow}$ ) appears to increase RMSE by between 1.1-2.4°C by underestimating daytime LST compared to simulated nighttime LST. The simulated SUHI from SUEWS for Dublin peaked around mid-summer (July) reaching a magnitude of 3.3°C at night with corresponded with observations from the MODIS sensor (3.2°C for nighttime acquisitions in July). Therefore, SUEWS appears to be capable of simulating the SUHI under ideal conditions i.e. meteorological conditions favourable to UHI development. This is the first instance where SUEWS has been spatially validated across an entire urban domain, though more work in other urban areas are necessary to confirm this finding.

While traditional methods of evaluation remain essential, it is critically important to ensure evaluations can be carried out a) using more widely available data and b) ensuring a variety of spatial circumstances are included. Chapter 5 of this thesis argues that remotely sensed data offers both of these aspects. Other methods of evaluation may include dense observational networks of standard instruments and/or crowd-sourced data (Muller *et al.*, 2013; 2015).

#### 7.1.5 SUEWS performance in context

When using detailed land cover data and forcing data obtain on-site i.e. in ideal circumstance, SUEWS simulations of  $Q_H$ ,  $Q_E$  and  $\Delta Q_S$  for three instrumented sites in Dublin, Ireland, exhibited realistic diurnal curves across multiple seasons, with RMSE values ranging between 20.4-30.8  $Wm^{-2}$  for  $Q_H$ , 9.5-20.9  $Wm^{-2}$  for  $Q_E$  and 18.7-35.1  $Wm^{-2}$  for  $\Delta Q_S$  at the

urban (LCZ 2) site. The RMSE ranges for the suburban (LCZ 6) site for the same three flux terms were 15.1-30.9  $\text{Wm}^{-2}$ , 13.9-30.8  $\text{Wm}^{-2}$  and 18.4-36.7  $\text{Wm}^{-2}$ . When forced using imperfect data (both land cover and meteorology), SUEWS still performed well: the RMSE for the fluxes at the LCZ 2 site were 20.6-25.7  $\text{Wm}^{-2}$ , 8.5-16.3  $\text{Wm}^{-2}$  and 13.3-29.2  $\text{Wm}^{-2}$  for  $Q_H$ ,  $Q_E$  and  $\Delta Q_S$  respectively. RMSE ranges for the LCZ 6 site in these circumstances were 14.8-33.2  $\text{Wm}^{-2}$ , 7.7-46.4  $\text{Wm}^{-2}$  and 17.8-34.8  $\text{Wm}^{-2}$ . Again, using imperfect data as forcing for SUEWS, the mean RMSE for a seven-month period in 2010 for  $Q_H$  and  $Q_E$  was 23.0  $\text{Wm}^{-2}$  and 14.8  $\text{Wm}^{-2}$  for the LCZ 2 site, 22.3  $\text{Wm}^{-2}$  and 23.5  $\text{Wm}^{-2}$  for the LCZ 6. The mean RMSE for twelve-month period in 2013 (non-consecutive) for a second LCZ 2 site in Dublin for  $Q_H$  and  $Q_E$  was 24.6  $\text{Wm}^{-2}$  and 9.9  $\text{Wm}^{-2}$ .

A comparison of 33 UEB models conducted by Grimmond *et al.* (2010; 2011) exhibited a similar range of error for turbulent fluxes (30-60  $\text{Wm}^{-2}$  for  $Q_H$ , 20-40  $\text{Wm}^{-2}$  for  $Q_E$ ). The performance of SUEWS here indicates that SUEWS is performing as well as any state-of-the-art model. The range of error using the LCZ-SUEWS approach was similar to values achieved using high resolution land cover data, this implies the model is relatively insensitive to land cover data, yet is capable of distinguishing between urban and non-urban areas (Chapter 3, Chapter 5) as well as accounting for intra-urban differences (Chapter 3).

The performance of the model was affected by the homogeneity of the area in which it is applied; notably the Hamburg site proved problematic in terms of model performance despite additional filtering of the observational data against which performance was judged. Model performance was best in areas with relatively consistent coverage, roughness characteristics, buildings materials and so forth.

This provides a cautionary tale for complex topographic, highly mixed and/or informal urban types, for instance in subtropical regions and rapidly developing cities. This also limits the application of SUEWS to the centre of neighbourhoods, with a great deal of uncertainty

surrounding the edges of different neighbourhood types. The second paper also demonstrated that regional characteristics must be retained, or put differently, generalisations can only take us so far, as seen in the case of the Phoenix site. The performance for Phoenix was characterised by systematic error due to the use of thermal properties (albedo and emissivity) that were not designed for buildings and land cover found in this area. Using thermal properties derived for buildings in similar background climates would undoubtedly improve SUEWS performance. Nevertheless, model performance at all sites fell within similar ranges for the turbulent fluxes.

## **7.2 Future research priorities**

The work here has contributed to the generation of input parameters in a consistent and efficient manner for urban areas, and has contributed to the evaluation of a state-of-the-art UCM. While the work here extends to several background climates and different urban types, it should not be viewed as exhaustive; for instance, the LCZ-SUEWS approach has not been evaluated in cities which experience a tropical climate, nor has it been evaluated in high-rise or any non-urban LCZ classes. The LCZ-Approach provides a means for applying SUEWS in data poor settings, such as rapidly developing cities, where the application of the approach may have the greatest impact. Application and evaluation of the approach in areas not considered here is an immediate priority for future research, which would significantly contribute to global urban databases (e.g. WUDAPT – Bechtel *et al.* 2015) providing a more complete picture of the range of urban land cover. Future work on the spatial validity of the SUEWS model is another research priority as it further demonstrates the ability of the model to be applied for spatial problems. This may be achieved by employing remotely sensed data. This was done in limited circumstances here for Dublin city, future work should seek to expand this to other cities and increase the temporal-span to consider multiple years. Such work would ensure that application of the model can be undertaken with confidence as well as highlight the limitations

of the model (e.g. at the boundary between LCZ types) which would aid future model development.

Finally, Chapter 6 highlighted the potential of the LCZ-SUEWS approach to reduce the impact of future planning decisions on the local scale climate – while the time horizon considered was relatively short (up to the year 2026) allowing the climate to be held constant, urban forms (e.g. buildings, roads) are likely to exist for 80 years or more (Mills 2007) which will experience a much changed climate in the future if the impacts of anthropogenic climate change are to be realised.

Recently, Masson *et al.* (2016) called for a systematic approach for modelling urban areas, which should include locally downscaled projections for climate change in and around the urban area in question along with land cover change scenarios. The former was not considered in Chapter 6, meaning the assertion that the compact development of the city into the future is the optimal route presently may present problems under a changed climate. Therefore, incorporating projections of future climate of Dublin is urgently needed to ensure that climate-resilience is built into future urban designs. Work on this is already underway.

### 7.3 Final conclusions

The issue of devising a comparative, climatically based description of urban areas has historically been a major challenge within the field of urban climatology. The challenges of deriving such a view of urban and non-urban sites include the cultural, regional and linguistic sensitivity of landscape interpretation, along with the heterogeneity of urban form, function and materials. A number of classification schemes have been proposed for describing urban sites, for example, urban land use types of Auer (1978); urban terrain zones of Ellefsen (1990/91) and urban climate zones of Oke (2004). These classification attempts are regarded as being limited since they lack non-urban zones, and classes are derived based on broad neighbourhood descriptions.

Building on these earlier attempts, the local climate zone scheme (LCZ) of Stewart and Oke (2012) was developed on the basis of physical characteristics which are then subsequently grouped into distinctive classes, additionally, the scheme is regarded as the first fully comprehensive scheme with the inclusion of non-urban sites. The identification of physical characteristics that yield the greatest impact on the near surface thermal climate builds on decades of research within the field of urban climatology. The transferability of LCZ across different regions means they have wider appeal than previous classification schemes.

Within the urban climate modelling community, it has been recognised that greater accuracy in urban representation (vegetation fractions, species, urban morphology and so forth) within models are required for accurate modelling of the urban climate. To that end, urban classification based on morphological characteristics have also been suggested, for instance Lee *et al.* (2011) suggest three urban classes, namely: commercial/industrial areas, high-density residential areas and low-density residential areas. Loridan and Grimmond (2011; 2012) proposed a classification of urban zones to characterise energy partitioning based on a built index, vegetated index and the proportioning of turbulent energy expenditure, identifying High, Medium and Low Density sites. Unlike the development of the LCZ scheme, the classifications utilised for the purposes of UCM applications arise out of a lack of sufficient detail of urban form and function globally required to force these models. This has limited the extent of model applications and inhibited the transfer of UCMs into the urban planning community.

Both the empirical and modelling communities have developed classifications to satisfy specific user needs, for instance, the number of UHI studies combined with the issue of miscommunication across these studies motivated the LCZ scheme (Stewart, 2011) the lack of a comprehensive classification prior to the LCZ scheme is regarded as one of the key reasons for the poor quality in reporting UHI studies. In the case of classifications for modelling purposes, the lack of relevant morphological data for urban areas necessitates generalisations,

however these classifications are more far more recent, hence are less well developed. As stated by Oke (2006), given the diversity of researchers within the field of urban climate, there is a clear need to avoid cliques and over specialisation by individual groups, in short dissimilarities in approaches and methods. Standardisation and multidisciplinary interactions are required to promote a healthy and robust scientific field. The application of the LCZ scheme by urban climatologists, urban planners, geographers and GIS experts illustrates its wide appeal across multiple aspects of the discipline, it stands to reason that it may have utility in the urban climate modelling community, as suggested by Ching (2013).

Hence this thesis is placed at a nexus between the LCZ scheme, which has been proven to be useful for characterising urban and non-urban areas, and a mid-complex UCM, which requires a range of input parameters to run. The principle motivation for this thesis was in generating the required inputs for UCMs in a standardised and efficient manner with minimal data requirements. This enables application in data sparse areas, where data scarcity prohibits their use and hence the integration of urban climate knowledge for planning problems.

Based on the findings from Papers 1-4 of this thesis, the following conclusions are drawn:

- 1. The LCZ-Approach works well with the SUEWS model, and overcomes modelling situations that would otherwise require large amounts of input data / high-resolution urban forcing data**

This has direct implications for urban areas for which we have little information in terms of urban meteorological, demographic and land cover data. The use of the LCZ modelling approach as an alternative to the traditional tessellation approach removes the requirements of a high-number of parameter values required to run mid-complex UCMs, which has inhibited the application of UCMs in such areas. While this approach necessitates the need to employ certain assumptions about urban form - for example, a residential neighbourhood in one area of the city is assumed to behave the same as other areas with similar morphological

characteristics - it is still capable of distinguishing between high-density and low-density urban areas, even when forced with off-site meteorological data. This will potentially allow for a greater number of model applications to be undertaken in the future.

**2. The SUEWS model performed well in a variety of circumstances examined here.**

The issue of model performance remains challenging for the urban climate community in light of the fact model development has outpaced model evaluation. Specifically, there is a universal recognition within the field of urban climate that more needs to be done by ways of evaluating models in a variety of circumstances and examining the transferability of models between different cities. This thesis directly addresses this knowledge gap by evaluating the SUEWS model. By evaluating the model in a standardised way in multiple urban areas and cities, model performance could be judged across different neighbourhoods and background climates. The model performed well across different cities when using high-resolution and low-resolution data, which provides an additional evidence base for its subsequent employment in other urban domains.

**3. Repositioning Remote Sensing from a means to derive input parameters to being used for model evaluation is a worthwhile endeavour**

Given the fact the LCZ approach for deriving parameters enables the possibility of modelling the UEB in cities where data scarcity has previously prohibited the application of UCMs, additional evaluations in these new areas will also be required. However, the deployment of eddy-covariance flux observation platforms remains challenging within the urban context. Therefore, employing remotely sensed data provides an opportunity for validation and evaluation to be undertaken where flux observations are absent. While this is a recent proposal and more work is required to demonstrate this further, the case study

undertaken here on the SUHI of Dublin using MODIS data to evaluate SUEWS contributes to the evidentiary basis of using these data in this manner.

**4. Given its parameterisations, and on the basis of the evaluation undertaken here and elsewhere, LCZ-SUEWS is an ideal approach for examining planning problems**

The SUEWS model is robust and capable of being used with the LCZ-Approach presented here. This overcomes data scarcity and/or the need for specialist understanding of urban parameters employed by the model while at the same time minimising the impact on model performance. Using SUEWS in this way enables the examination of planning problems such as the impact of land cover change, driven by planning choices, on local-scale climate. While this was applied to a specific case here, LCZ were designed to be culturally neutral and user friendly which suggests LCZ-SUEWS has applicability in many other circumstances. Using this approach in Dublin, Ireland, it was illustrated that urban form choices have distinct spatial impacts on local-scale turbulent fluxes. For instance, while increasing urban density across the existing urban extent had a larger impact on the magnitude of sensible and stored heat compared to allowing low-density sprawl, simple design strategies such as increasing urban greenery reduced this impact significantly. Therefore, the use of the LCZ-SUEWS approach has direct provision for aiding planning decisions which will encourage communication with the planning community, benefit the future design of cities, and reduce the impact of urbanisation on the urban population.

---

## Bibliography

---

- Acero, J., Arrizabalaga, J. K. S. & Katzschner, L., 2013. Deriving an Urban Climate Map in coastal areas with complex terrain in the Basque Country (Spain). *Urban Climate*, 4(1), pp. 35-60.
- Alcoforado, M., Andrade, H., Lopes, A. & Vasconcelos, J., 2009. Application of climatic guidelines to urban planning: The example of Lisbon (Portugal). *Landscape and Urban Planning*, 90(1-2), pp. 56-65.
- Alexander, P. & Mills, G., 2014. Local Climate Classification and Dublin's Urban Heat Island. *Atmosphere*, 5(4), pp. 755-774.
- Alexander, P., Mills, G. & Fealy, R., 2015. Using LCZ data to run an Urban Energy Balance Model. *Urban Climate*, 13(3), pp. 14-37.
- Ali-Toudert, F. & Mayer, H., 2006. Numerical study on the effects of aspect ratio and orientation of an urban street canyon on outdoor thermal comfort in hot and dry climate. *Building and Environment*, 41(2), pp. 94-108.
- Ali-Toudert, F. & Mayer, H., 2006. Numerical study on the effects of aspect ratio and orientation of an urban street canyon on outdoor thermal comfort in hot and dry climate. *Building and Environment*, 41(2), pp. 94-108.
- Allen, L., Lindberg, F. & Grimmond, C., 2011. Global to city scale urban anthropogenic heat flux: model and variability. *International Journal of Climatology*, 31(4), pp. 1990-2005.
- Allen, L., Lindberg, F. & Grimmond, C., 2011. Global to city scale urban anthropogenic heat flux: model and variability. *International Journal of Climatology*, 31(13), pp. 1990-2005.
- Arnfield, A., 1990. Street design and urban canyon solar access. *Energy and Buildings*, 14(1), pp. 117-131.

- Arnfield, A., 2003. Two decades of urban climate research: A review of turbulence, exchanges of energy and water, and the urban heat island. *International Journal of Climatology*, Volume 23, pp. 1-26.
- Ashie, Y., Ca, V. & Asaeda, T., 1999. Building canopy model for the analysis of urban climate. *Journal of Wind Engineering and Industrial Aerodynamics*, 81(1-3), pp. 237-248.
- Aston, Q., 2012. *Issues in Global Environment: Biology and Geoscience*. 2011 Edition, ISBN: 9781464965760 ed. s.l.:Scholarly Editions.
- Atkinson, B., 2003. Numerical Modelling of Urban Heat-Island Intensity. *Boundary-Layer Meteorology*, 109(3), pp. 285-310.
- Auer, A., 1978. Correlation of Land Use and Cover with Meteorological Anomalies. *Journal of Applied Meteorology*, 17(5), pp. 636-643.
- Balk, D. et al., 2006. Determining Global Population Distribution: Methods, Applications and Data. *Advances in Parasitology*, Volume 62, pp. 119-156.
- Balling, R., Cervený, R. & Idso, C., 2001. Does the urban CO<sub>2</sub> dome of Phoenix, Arizona contribute to its heat island?. *Geophysical Research Letters*, 28(24), pp. 4599-4601.
- Barlow, J., Harman, I. & Belcher, S., 2004. Scalar fluxes from urban street canyons. Part I: laboratory simulation. *Boundary-Layer Meteorology*, 113(3), pp. 369-385.
- Barredo, J., Kasanko, M. M. N. & Lavalle, C., 2003. Modelling dynamic spatial processes: simulation of future scenarios through cellular automata. *Landscape and Urban Planning*, 6(3), pp. 145-160.
- Bechtel, B. et al., 2015. Mapping Local Climate Zones for a Worldwide Database of the Form and Function of Cities. *ISPRS Int. J. Geo-Inf*, 4(1), pp. 199-219.
- Bechtel, B. & Daneke, C., 2012. Classification of Local Climate Zones Based on Multiple Earth Observation Data. *IEEE Journal of Selected Topics in Applied Earth Observations and Remote Sensing*, 5(4), pp. 1191-1202.

- Betsill, M. & Bulkeley, H., 2006. Cities and the Multilevel Governance of Global Climate Change. *Global Governance*, 12(2), pp. 141-159.
- Block, A., Keuler, K. & Schaller, E., 2004. Impacts of anthropogenic heat on regional climate patterns. *Geophysical Research Letters*, 31(12).
- Bottyán, Z. & Unger, J., 2003. A multiple linear statistical model for estimating the mean maximum urban heat island. *Theoretical and Applied Climatology*, 75(3), pp. 233-243.
- Brager, G. & de Dear, R., 1998. Thermal adaptation in the built environment: a literature review. *Energy and Buildings*, 27(1), pp. 83-96.
- Bramley, G. & Power, S., 2009. Urban form and social sustainability: the role of density and housing type. *Environment and Planning B: Planning and Design*, Volume 36, pp. 30-48.
- Breheny, M., 1991. *Sustainable development and urban form*. London, Pion, p. 292.
- Brennan, M. et al., 2009. Regional planning guideline review : using MOLAND as part. *Urban Institute Ireland Working Papers Series; 09/07*, pp. 1-23.
- Brümmer, B., Lange, I. & Konow, H., 2012. Atmospheric boundary layer measurements at the 280 m high Hamburg weather mast 1995-2011: mean annual and diurnal cycles. *Meteorologische Zeitschrift*, 21(4), pp. 319-335.
- Bruse, M., 1999. *The influences of local environmental design on microclimate- development of a prognostic numerical Model ENVI-met for the simulation of Wind, temperature and humidity distribution in urban structures*, Germany: University of Bochum: Ph.D. Thesis.
- Bruse, M., 1999. *The influences of local environmental design on microclimate-development of a prognostic numerical Model ENVI-met for the simulation of Wind, temperature and humidity distribution in urban structures.*, PhD Thesis: Temperature and Humidity

- Distribution in Urban Structures (in German), Germany, Institute of Geography, University of Bochum.
- Bueno, B., Norford, L., Hidalgo, J. & Pigeon, G., 2013. The urban weather generator. *Journal of Building Performance Simulation*, 6(4), pp. 269-281.
- Bulkeley, H., 2010. Cities and the Governing of Climate Change. *Annual Review of Environment and Resources*, Volume 35, pp. 229-253.
- Central Statistics Office, 2012. *Census of Ireland 2011*, Dublin: CSO.
- Central Statistics Office, 2013. *Regional Population Projections 2016-2031*, Dublin, Ireland: Government of Ireland.
- Chai, T. & Draxler, R., 2014. Root mean square error (RMSE) or mean absolute error (MAE)? - Arguments against avoiding RMSE in the literature. *Geoscientific Model Development*, Volume 7, pp. 1247-1250.
- Chandler, T., Fox, G. & Winsborough, H., 1974. *3000 Years of Urban Growth*. New York: Academic Press.
- Chen, F. et al., 2011. The integrated WRF/urban modelling system: development, evaluation, and applications to urban environmental problems. *International Journal of Climatology*, 31(2), pp. 273-288.
- Ching, J., 2013. A perspective on urban canopy layer modeling for weather, climate and air quality applications. *Urban Climate*, Volume 3, pp. 13-39.
- Ching, J., 2013. A perspective on urban canopy layer modeling for weather, climate and air quality applications. *Urban Climate*, 3(1), pp. 13-39.
- Chow, W. et al., 2014. Seasonal dynamics of a suburban energy balance in Phoenix, Arizona. *International Journal of Climatology*, 34(15), pp. 3863-3880.

- Chrysoulakis, N., Anselmo de Castro, E. & Moors, E., 2014. *Understanding Urban Metabolism: a tool for urban planning*. London, United Kingdom: Routledge (Taylor and Francis).
- Chrysoulakis, N. et al., 2013. Sustainable urban metabolism as a link between bio-physical sciences and urban planning: The BRIDGE project. *Landscape and Urban Planning*, 112(0), pp. 100-117.
- Cleugh, H. et al., 2005. *Evapotranspiration in Urban Water Balance Models: A Methodological Framework*. Canberra, Australia, International Congress on Modelling and Simulation (MODSIM05).
- Cohen, A. et al., 2004. Urban Air Pollution. In: *Comparative Quantification of Health Risks: Global and Regional Burden of Disease due to Selected Major Risk Factors*. Geneva: World Health Organisation, pp. 1353-1434.
- Colunga, M. et al., 2015. The role of urban vegetation in temperature and heat island effects in Querétaro city, Mexico. *Atmósfera*, 28(3), pp. 205-218.
- Convery, F., 2008. *Green City Guidelines: Advice for the protection and enhancement of biodiversity in medium to high-density urban developments*, Dublin: Urban Institute Ireland.
- Coutts, A., Beringer, J. & Tapper, N., 2007. Impact of Increasing Urban Density on Local Climate: Spatial and Temporal Variations in the Surface Energy Balance in Melbourne, Australia. *Journal of Applied Meteorology and Climatology*, 46(4), pp. 477-493.
- Coutts, A., Beringer, J. & Tapper, N., 2007. Impact of Increasing Urban Density on Local Climate: Spatial and Temporal Variations in the Surface Energy Balance in Melbourne, Australia. *Journal of Applied Meteorology and Climatology*, 46(4), pp. 477-493.

- Coutts, A., Beringer, J. & Tapper, N., 2008. Investigating the climatic impact of urban planning strategies through the use of regional climate modelling: a case study for Melbourne, Australia. *International Journal of Climatology*, 28(2), pp. 1943-1957.
- de Dear, R. & Brager, G., 1998. Developing an adaptive model of thermal comfort and preference. *ASHRAE Transactions. Center for the Built Environment*, 104(1), pp. 1-18.
- De Ridder, K., Lauwaet, D. & Maiheu, B., 2015. UrbClim – A fast urban boundary layer climate model. *Urban Climate*, 12(June 2015), pp. 21-48.
- De Vries, J., 2007. *European Urbanization, 1500-1800*. Abingdon, Oxon: Routledge.
- Demuzere, M. et al., 2013. Simulating the surface energy balance over two contrasting urban environments using the Community Land Model Urban. *International Journal of Climatology*, 33(15), pp. 3182-3205.
- Dupont, S., Otte, T. & Ching, J., 2004. Simulation of Meteorological Fields Within and Above Urban and Rural Canopies with a Mesoscale Model. *Boundary-Layer Meteorology*, 113(1), pp. 111-158.
- Eliasson, I., 2000. The use of climate knowledge in urban planning. *Landscape and Urban Planning*, 48(1-2), pp. 31-44.
- Elkin, T., McLaren, D. & Hillman, M., 1991. *Reviving the City: Towards Sustainable Urban Environment*.. London: Friends of the Earth.
- Ellefsen, R., 1990/91. Mapping and measuring buildings in the urban canopy boundary layer in ten US cities. *Energy and Buildings*, Volume 15-16, pp. 1025-1049.
- Emmanuel, R. & Krüger, E., 2012. Urban heat island and its impact on climate change resilience in a shrinking city: The case of Glasgow, UK. *Buildings and Environment*, Volume 53, pp. 137-149.
- European Environment Agency, 1999. *Environment in the European Union at the turn of the century*, Copenhagen (Denmark): EEA (European Environment Agency) .

- Fan, H. & Sailor, D., 2005. Modeling the impacts of anthropogenic heating on the urban climate of Philadelphia: a comparison of implementations in two PBL schemes. *Atmospheric Environment*, 39(1), pp. 73-84.
- Fenner, D., Meier, F., Scherer, D. & Polze, A., 2014. Spatial and temporal air temperature variability in Berlin, Germany, during the years 2001–2010. *Urban Climate*, 10(2), pp. 308-331.
- Flanner, M., 2009. Integrating anthropogenic heat flux with global climate models. *Geophysical Research Letters*, 36(2).
- Frumkin, H., 2002. Urban Sprawl and Public Health. *Public Health Reports*, 117(3), pp. 201-217.
- Gál, T. & Unger, J., 2009. Detection of ventilation paths using high-resolution roughness parameter mapping in a large urban area. *Building and Environment*, 44(1), pp. 198-206.
- Getis, A. & Ord., J., 1992. The Analysis of Spatial Association by Use of Distance Statistics. *Geographical Analysis*, 24(3), pp. 189-206.
- Giridharan, R., Lau, S., Ganesan, S. & Givoni, B., 2008. Lowering the outdoor temperature in high-rise high-density residential developments of coastal Hong Kong: The vegetation influence. *Building and Environment*, 43(10), pp. 1583-1595.
- Givoni, B., 1992. Comfort, climate analysis and building design guidelines. *Energy and Buildings*, 18(1), pp. 11-23.
- Goldberg, V., Kurbjuhn, C. & Bernhofer, C., 2013. How relevant is urban planning for the thermal comfort of pedestrians? Numerical case studies in two districts of the City of Dresden (Saxony/Germany). *Meteorologische Zeitschrift*, 22(6), pp. 739-751.
- Graham, E., 1993. The Urban Heat Island of Dublin City During the Summer Months.. *Irish Geography*, 26(1), pp. 45-57.

- Gray, K. & Finster, M., 2000. *The Urban Heat Island, Photochemical Smog, and Chicago: Local Features and the Problem and Solution*, Evanston, IL: Northeastern University.
- Grimmond, C., 1992. The suburban energy-balance - methodological considerations and results for a mid-latitude west coast city under winter and spring conditions. *International Journal of Climatology*, 12(3), pp. 481-497.
- Grimmond, C. et al., 2010. The International Urban Energy Balance Models Comparison Project: First Results from Phase 1. *Journal of Applied Meteorology and Climatology*, Volume 49, pp. 1268-1292.
- Grimmond, C. et al., 2010. The International Urban Energy Balance Models Comparison Project: First Results from Phase 1. *Journal of Applied Meteorology and Climatology*, 49(6), p. 1268–1292.
- Grimmond, C. et al., 2011. Initial results from Phase 2 of the international urban energy balance model comparison. *International Journal of Climatology*, 31(2), pp. 244-272.
- Grimmond, C. et al., 2011. Initial results from Phase 2 of the international urban energy balance model comparison. *International Journal of Climatology*, 31(2), pp. 244-272.
- Grimmond, C. & Oke, T., 1991. An evaporation-interception model for urban areas. *Water Resource Research*, 27(7), pp. 1739-1755.
- Grimmond, C. & Oke, T., 1995. Comparison of Heat Fluxes from Summertime Observations in the Suburbs of Four North American Cities. *Journal of Applied Meteorology*, 34(4), pp. 873-889.
- Grimmond, C. & Oke, T., 1999. Heat Storage in Urban Areas: Local-Scale Observations and Evaluation of a Simple Model. *Journal of Applied Meteorology*, 38(2), pp. 922-940.
- Grimmond, C. & Oke, T., 2002. Turbulent Heat Fluxes in Urban Areas: Observations and a Local-Scale Urban Meteorological Parameterization Scheme (LUMPS). *Journal of Applied Meteorology*, 41(7), pp. 792-810.

- Grimmond, C. & Souch, C., 1994. Surface description for urban climate studies: a GIS based methodology. *Geocarto International*, Volume 1, pp. 47-59.
- Hamdi, R., Degrauwe, D. & Termonia, P., 2012. Coupling the Town Energy Balance (TEB) Scheme to an Operational Limited-Area NWP Model: Evaluation for a Highly Urbanized Area in Belgium. *Weather and Forecasting*, 27(2), pp. 323-344.
- Hamdi, R. & Masson, V., 2008. Inclusion of a Drag Approach in the Town Energy Balance (TEB) Scheme: Offline 1D Evaluation in a Street Canyon. *Journal of Applied Meteorology and Climatology*, 47(10), pp. 2627-2644.
- Harman, I., Barlow, J. & Belcher, S., 2004. Scalar fluxes from urban street canyons part II: Model. *Boundary-Layer Meteorology*, 113(3), pp. 387-410.
- Harman, I. & Belcher, S., 2006. The surface energy balance and boundary layer over urban street canyons. *Quarterly Journal of the Royal Meteorological Society*, 132(621), pp. 2749-2768.
- Heaphy, L., 2015. The role of climate models in adaptation decision-making: the case of the UK climate projections 2009. *European Journal for Philosophy of Science*, 5(2), pp. 233-257.
- Hebbert, M. & Mackillop, F., 2013. Urban climatology applied to urban planning: a postwar knowledge circulation failure. *International Journal of Urban and Regional Research*, 37(5), pp. 1542-1558.
- Hidalgo, J. et al., 2008. Advances in urban climate modeling. *Annals of the New York Academy of Sciences*, Volume 1146, pp. 354-374.
- Hoffmann, P., Krueger, O. & Schlünzen, K., 2012. A statistical model for the urban heat island and its application to a climate change scenario. *International Journal of Climatology*, 32(8), pp. 1238-1248.

- Houet, T. & Pigeon, G., 2011. Mapping urban climate zones and quantifying climate behaviors - An application on Toulouse urban area (France). *Environmental Pollution*, 159(8-9), pp. 2180-2192.
- Huang, H., Akutsu, Y., Arai, M. & Tamura, M., 2000. A two-dimensional air quality model in an urban street canyon: evaluation and sensitivity analysis. *Atmospheric Environment*, 34(5), pp. 689-698.
- Hu, L. et al., 2014. How can we use MODIS land surface temperature to validate long-term urban model simulations?. *Journal of Geophysical Research: Atmospheres*, Volume 119, pp. 3185-3201.
- Hurley, P., 2005. *CSIRO Atmospheric Research Technical Paper No. 71, 54*, s.l.: s.n.
- Hyndman, R. & Koehler, A., 2006. Another look at measures of forecast accuracy. *International Journal of Forecasting*, 22(4), pp. 679-688.
- Idsoa, C., Idso, S. & Balling, R., 1998. The urban co2 dome of Phoenix, Arizona. *Physical Geography*, 19(2), pp. 95-108.
- IPCC, 1990. *First Assessment Report (FAR) Climate Change: The IPCC Impacts Assessment*, Canberra, Australia: Australian Government Publishing Service.
- IPCC, 1995. *IPCC Second Assessment Report (SAR)*, Cambridge, United Kingdom: Cambridge University Press.
- IPCC, 2001. *IPCC Third Assessment Report (TAR) Impacts, Adaptation and Vulnerability*, Cambridge, United Kingdom: Cambridge University Press.
- IPCC, 2007. *IPCC Fourth Assessment Report (AR4)*, Cambridge, United Kingdom: Cambridge University Press.
- IPCC, 2014. *Human Settlements, Infrastructure and Spatial Planning. In: Climate Change 2014: Mitigation of Climate Change. Contribution of Working Group III to the Fifth*

*Assessment Report of the Intergovernmental Panel on Climate Change*. Cambridge, United Kingdom and New York, NY, USA: Cambridge University Press.

Jackson, L., 2003. The relationship of urban design to human health and condition. *Landscape and Urban Planning*, 64(4), pp. 191-200.

Järvi, L., Grimmond, C. & Christen, A., 2011. The Surface Urban Energy and Water Balance Scheme (SUEWS): Evaluation in Los Angeles and Vancouver. *Journal of Hydrology*, 411(3-4), pp. 219-237.

Järvi, L., Grimmond, C. & Christen, A., 2011. The Surface Urban Energy and Water Balance Scheme (SUEWS): Evaluation in Los Angeles and Vancouver. *Journal of Hydrology*, 411(3-4), pp. 219-237.

Järvi, L. et al., 2014. Development of the Surface Urban Energy and Water Balance Scheme (SUEWS) for cold climate cities. *Geoscientif Model Development*, Volume 7, pp. 1691-1711.

Järvi, L. et al., 2014. Development of the Surface Urban Energy and Water Balance Scheme (SUEWS) for cold climate cities. *Geoscientific Model Development*, 7(4), pp. 1691-1711.

Jorgenson, A. & Rice, J., 2010. Urban Slum Growth and Human Health: A Panel Study of Infant and Child Mortality in Less-Developed Countries, 1990–2005. *Journal of Poverty*, 14(4), pp. 382-402.

Karl, T., Diaz, H. & Kukla, G., 1988. Urbanization: Its Detection and Effect in the United States Climate Record. *Journal of Climate*, 1(11), pp. 1099-1123.

Karppinen, A. et al., 2000. A modelling system for predicting urban air pollution: comparison of model predictions with the data of an urban measurement network in Helsinki. *Atmospheric Environment*, 34(22), pp. 3735-3743.

- Keogh, S., 2015. *Quantifying carbon dioxide concentrations and fluxes for Dublin, Kildare, Ireland*: National University of Ireland Maynooth.
- Keogh, S., Mills, G. & Fealy, R., 2012. The energy budget of the urban surface: two locations in Dublin. *Irish Geography*, 4(1), pp. 1-23.
- Kimura, F. & Takahashi, S., 1991. The Effects of Land-Use and Anthropogenic Heating on the Surface Temperature in the Tokyo Metropolitan Area: A Numerical Experiment. *Atmospheric Environment*, Volume 25B, pp. 155-164.
- Koh, T.-Y., Wang, S. & Bhatt, B., 2012. A diagnostic suite to assess NWP performance. *Journal of Geophysical Research*, 117(9), pp. 1-20.
- Kovács, A. & Németh, Á., 2012. Tendencies and differences in human thermal comfort in distinct urban areas in Budapest, Hungary. *Acta Climatol. Chorol*, Volume 46, pp. 115-124.
- Krayenhoff, E. & Voogt, J., 2007. A microscale three-dimensional urban energy balance model for studying surface temperatures. *Boundary-Layer Meteorology*, 123(3), pp. 433-461.
- Kusaka, H. & Kimura, F., 2004. Coupling a Single-Layer Urban Canopy Model with a Simple Atmospheric Model: Impact on Urban Heat Island Simulation for an Idealized Case. *Journal of the Meteorological Society of Japan*, 82(1), pp. 67-80.
- Kusaka, H., Kondo, H., Kikegawa, Y. & Kimura, F., 2001. A Simple Single-Layer Urban Canopy Model For Atmospheric Models: Comparison With Multi-Layer And Slab Models. *Boundary-Layer Meteorology*, 101(3), pp. 329-358.
- Leconte, F., Bouyer, J., Claverie, R. & Pétrissans, M., 2015. Using Local Climate Zone scheme for UHI assessment: Evaluation of the method using mobile measurements. *Building and Environment*, Volume 83, pp. 39-49.
- Lee, A. & Maheswaran, R., 2011. The health benefits of urban green spaces: a review of the evidence. *Journal of Public Health*, 33(2), pp. 212-222.

- Lee, S. et al., 2011. Evaluation of urban surface parameterizations in the WRF model using measurements during the Texas Air Quality Study 2006 field campaign. *Atmospheric Chemistry and Physics*, 11(5), pp. 2127-2143.
- Lemonsu, A. et al., 2013. Evolution of the Parisian urban climate under a global changing climate. *Climatic Change*, 116(3-4), pp. 679-692.
- Levlovics, E., Gál, T. & Unger, J., 2013. Mapping Local Climate Zones With A Vector-Based GIS Method. *AERPA Conference*, Available at([http://aerapa.conference.ubbcluj.ro/2013/pdf/53%20lelovics%20et%20al%20423\\_430.pdf](http://aerapa.conference.ubbcluj.ro/2013/pdf/53%20lelovics%20et%20al%20423_430.pdf)), pp. 423-230.
- Lin, C.-Y. et al., 2008. Urban Heat Island effect and its impact on boundary layer development and land-sea circulation over northern Taiwan. *Atmospheric Environment*, 42(22), pp. 5635-5649.
- Lindberg, F. & Grimmond, C., 2011. The influence of vegetation and building morphology on shadow patterns and mean radiant temperatures in urban areas: model development and evaluation. *Theoretical and Applied Climatology*, 105(3-4), pp. 311-323.
- Lindberg, F., Grimmond, S., Onomura, S. & Järvi, L., 2015. UMEP - An Integrated tool for urban climatology and climate sensitive planning applications. *ICUC9 - 9th International Conference on Urban Climate jointly with 12th Symposium on the Urban Environment*, Toulouse(France), pp. 1-4.
- Lindberg, F., Holmer, B. & Thorsson, S., 2008. SOLWEIG 1.0 – Modelling spatial variations of 3D radiant fluxes and mean radiant temperature in complex urban settings. *International Journal of Biometeorology*, 52(7), pp. 697-713.
- Liu, H., Feng, J., Järvi, L. & Vesala, T., 2012. Four-year (2006-2009) eddy covariance measurements of CO<sub>2</sub> flux over an urban area in Beijing. *Atmospheric Chemistry and Physics*, Volume 12, pp. 7881-7892.

- Loridan, T. & Grimmond, C., 2012. Multi-site evaluation of an urban land-surface model: intra-urban heterogeneity, seasonality and parameter complexity requirements. *Quarterly Journal of the Royal Meteorological Society*, 138(665), pp. 1094-1113.
- Loridan, T. et al., 2010. Trade-offs and responsiveness of the single-layer urban canopy parametrization in WRF: An offline evaluation using the MOSCEM optimization algorithm and field observations. *Quarterly Journal of the Royal Meteorological Society*, 136(649), pp. 997-1019.
- Lowry, W., 1977. Empirical Estimation of Urban Effects on Climate: A Problem Analysis. *Journal of Applied Meteorology*, 16(2), pp. 129-135.
- Marland, G. et al., 2003. The climatic impacts of land surface change and carbon management, and the implications for climate-change mitigation policy. *Climate Policy*, 3(2), pp. 149-157.
- Martine, G., McGranahan, G., Montgomery, M. & Fernández-Castillia, R., 2008. *The New Global Frontier: Urbanization, Poverty and Environmental in the 21st Century*. 1st ed. London: Earthscan (Routledge).
- Masson, V., 2000. A Physically-Based Scheme For The Urban Energy Budget In Atmospheric Models. *Boundary-Layer Meteorology*, 94(3), pp. 357-397.
- Masson, V. et al., 2014. Adapting cities to climate change: A systemic modelling approach. *Urban Climate*, 10(December 2014), pp. 407-429.
- Mertes, C. et al., 2015. Detecting change in urban areas at continental scales with MODIS data. *Remote Sensing of Environment*, Volume 158, pp. 331-347.
- Middel, A. et al., 2012. Land cover, climate, and the summer surface energy balance in Phoenix, AZ, and Portland, OR.. *International Journal of Climatology*, 32(13), pp. 2020-2032.
- Middel, A., Brazel, A., Kaplan, S. & Myint, S., 2012. Daytime cooling efficiency and diurnal energy balance in Phoenix, Arizona, USA. *Climate Research*, Volume 54, pp. 21-34.

- Middel, A. et al., 2014. Impact of urban form and design on mid-afternoon microclimate in Phoenix Local Climate Zones. *Landscape and Urban Planning*, Volume 122, p. 16–28.
- Mills, G., 2007. Cities as agents of global change. *International Journal of Climatology*, 27(14), pp. 1849-1857.
- Mills, G., 2008. *Urban climatology and its relevance to urban design*. Dublin Ireland, (Accessed 24/04/15) [http://architecture.ucd.ie/Paul/PLEA2008/content/papers/oral/PLEA\\_FinalPaper\\_ref\\_250.pdf](http://architecture.ucd.ie/Paul/PLEA2008/content/papers/oral/PLEA_FinalPaper_ref_250.pdf), pp. 251-256.
- Mills, G. et al., 2015. An Introduction to the WUDAPT project. In: *Proceedings of the ICUC9*. Meteo France, Toulouse, France.
- Mills, G. et al., 2010. Climate Information for Improved Planning and Management of Mega Cities (Needs Perspective),. *Procedia Environmental Sciences*, 1(1), pp. 228-246.
- Moriasi, D. et al., 2007. Model Evaluation Guidelines for Systematic Quantification of Accuracy in Watershed Simulations. *Transactions of the ASABE*, 50(3), pp. 885-900.
- Morris, C. & Simmonds, I., 2000. Association between varying magnitudes of the urban heat island and the synoptic climatology in Melbourne, Australia. *International Journal of Climatology*, 20(3), pp. 1931-1954.
- Moussiopoulos, N., Sahm, P. & Kessler, C., 1995. Numerical simulation of photochemical smog formation in Athens, Greece - A case study. *Atmospheric Environment*, 29(24), pp. 3619-3632.
- Muller, C. et al., 2013. Sensors and the city: a review of urban meteorological networks. *International Journal of Climatology*, 33(7), pp. 1585-1600.
- Muller, C. et al., 2015. Crowdsourcing for climate and atmospheric sciences: current status and future potential. *International Journal of Climatology*, 35(11), pp. 3185-3203.

- Myrup, L., 1969. A Numerical Model of the Urban Heat Island. *Journal of Applied Meteorology*, 8(6), pp. 908-918.
- National Research Council, 2012. *Urban Meteorology: Forecasting, Monitoring, and Meeting Users' Needs*, Washington, D.C.: The National Academies Press.
- Ng, E., 2011. Towards planning and practical understanding of the need for meteorological and climatic information in the design of high-density cities: A case-based study of Hong Kong. *International Journal of Climatology*, 32(4), p. 582–598.
- Offerle, B., Grimmond, C. & Fortuniak, K., 2005. Heat storage and anthropogenic heat flux in relation to the energy balance of a central European city centre. *International Journal of Climatology*, 25(10), pp. 1405-1419.
- Offerle, B., Grimmond, C. & Oke, T., 2003. Parameterization of Net All-Wave Radiation for Urban Areas. *Journal of applied Meteorology*, 42(8), pp. 1157-1173.
- Oke, T., 1982. The energetic basis of the urban heat island. *Quarterly Journal of the Royal Meteorological Society*, 108(455), pp. 1-24.
- Oke, T., 1984. Towards a prescription for the greater use of climatic principles in settlement planning. *Energy and Buildings*, 7(1), pp. 1-10.
- Oke, T., 1984. Towards a prescription for the greater use of climatic principles in settlement planning. *Energy and Buildings*, 7(1), pp. 1-10.
- Oke, T., 1987. *Boundary-Layer Climates*. 3rd ed. London: Routledge.
- Oke, T., 1988. The urban energy balance. *Progress in Physical Geography*, 12(4), pp. 471-508.
- Oke, T., 2004. *Initial guidance to obtain representative meteorological observations at urban sites*, Geneva: World Meteorological Organisation: IOM Report No. 81, WMO/TD No.1250.
- Oke, T., 2006. Towards better scientific communication in urban climate. *Theoretical and Applied Climatology*, Issue 84, pp. 179-190.

- Oleson, K. et al., 2008. An Urban Parameterization for a Global Climate Model. Part I: Formulation and Evaluation for Two Cities. *Journal of Applied Meteorology and Climatology*, 47(4), pp. 1038-1060.
- Onomura, S. et al., 2015. Meteorological forcing data for urban outdoor thermal comfort models from a coupled convective boundary layer and surface energy balance scheme. *Urban Climate*, 11(March 2015), pp. 1-23.
- Ord, J. & Getis, A., 1995. Local Spatial Autocorrelation Statistics: Distributional Issues and an Application. *Geographical Analysis*, 27(4), pp. 286-306.
- Oreskes, N., 1998. Evaluation (Not Validation) of Quantitative Models. *Environmental Health Perspectives*, 106(6), pp. 1453-1460.
- Oreskes, N., Shrader-Frechette, K. & Belitz, K., 1994. Verification, Validation, and Confirmation of Numerical Models in the Earth Sciences. *Science*, 263(1), pp. 641-646.
- Patz, J., Campbell-Lendrum, D., Holloway, T. & Foley, J., 2005. Impact of regional climate change on human health. *Nature*, Issue 438, pp. 310-317.
- Pearlmutter, D., Krüger, E. & Berliner, P., 2008. The role of evaporation in the energy balance of an open-air scaled urban surface. *International Journal of Climatology*, 29(6), pp. 911-920.
- Peng, L. & Jim, C., 2013. Green-Roof Effects on Neighborhood Microclimate and Human Thermal Sensation. *Energies*, 6(2), pp. 598-618.
- Picone, N. & Campo, A., 2015. Preparing urban climate maps using Local Climate Zones (LCZ) methodology to improve communication with urban planners: the case of Tandil city, Argentina. *9th International Conference on Urban Climate (ICUC9) Proceedings*, Volume TUKUP6: Indicators and climate maps II : urban planning, pp. Toulouse, France.

- Pigeon, G., Legain, D., Durand, P. & Masson, V., 2007. Anthropogenic heat release in an old European agglomeration (Toulouse, France). *International Journal of Climatology*, 27(14), pp. 1969-1981.
- Ren, C., Lau, K., Yiu, K. & Ng, E., 2013. The application of urban climatic mapping to the urban planning of high-density cities: The case of Kaohsiung, Taiwan. *Cities*, 31(April), pp. 1-16.
- Ren, C., Ng, E. & Katzschner, L., 2011. Urban climatic map studies: a review. *International Journal of Climatology*, 31(15), pp. 2213-2233.
- Rohan, P., 1983. *The climate of Dublin*, Dublin, Ireland: Irish Meteorological Service.
- Romero, H., Salgado, M. & Smith, P., 2010. Climate Change and Urban Climate: Relations between thermal zones and the socioeconomic conditions of the population of Santiago, Chile. *Revista INVI*, Volume 70, pp. 151-179.
- Sailor, D. & Lu, L., 2004. A top-down methodology for developing diurnal and seasonal anthropogenic heating profiles for urban areas. *Atmospheric Environment*, 38(17), pp. 2737-2748.
- Sailor, D. & Vasireddy, C., 2006. Correcting aggregate energy consumption data to account for variability in local weather. *Environmental Modelling & Software*, 21(5), pp. 733-738.
- Satterthwaite, D., 2007. *Climate Change and Urbanization: Effects and Implications for Urban Governance*, New York: United Nations Expert Group on Population Distribution, Urbanization, Internal Migration and Development.
- Schlünzen, K. et al., 2011. Joint modelling of obstacle induced and mesoscale changes – current limits and challenges. *Journal of Wind Engineering and Industrial Aerodynamics*, Volume 99, pp. 217-225.
- Schlünzen, K. et al., 2003. Flow and Transport in the Obstacle Layer: First Results of the Micro-Scale Model MITRAS. *Journal of Atmospheric Chemistry*, 44(2), pp. 113-130.

- See, L. et al., 2015. *Generating WUDAPT's Specific Scale-dependent Urban Modeling and Activity Parameters: Collection of Level 1 and Level 2 Data*. Toulouse, France, 20-24th July 2015, pp. 1-4.
- Shaviv, E., 1984. Climate and building design - tradition, research and design tools. *Energy and Buildings*, 7(1), pp. 55-69.
- Shir, C. & Shieh, J., 1974. A Generalized Urban Air Pollution Model and Its Application to the Study of SO<sub>2</sub> Distributions in the St. Louis Metropolitan Area.. *Journal of Applied Meteorology*, 13(2), pp. 185-204.
- Spate, O., 1942. Factors in the Development of Capital Cities. *Geographical Review*, 32(4), pp. 622-631.
- Steer, A. & Ishii, N., 2015. *Sustainable Cities and Buildings at COP21: Delivering Our Future Today*. [Online]  
Available at: [http://www.huffingtonpost.com/dr-andrew-steer/sustainable-cities-and-buildings-at-cop21-delivering-our-future-today\\_b\\_8707866.html](http://www.huffingtonpost.com/dr-andrew-steer/sustainable-cities-and-buildings-at-cop21-delivering-our-future-today_b_8707866.html)  
[Accessed 12 December 2015].
- Stewart, I., 2011. A systematic review and scientific critique of methodology in modern urban heat island literature. *International Journal of Climatology*, 31(2), pp. 200-217.
- Stewart, I. & Oke, T., 2012. Local Climate Zones for Urban Temperature Studies. *Bulletin of the American Meteorological Society*, Volume 93, pp. 1879-1900.
- Stewart, I., Oke, T. & Krayenhoff, E., 2014. Evaluation of the 'local climate zone' scheme using temperature observations and model simulations. *International Journal of Climatology*, 34(4), pp. 1062-1080.
- Stewart, I. & Oke, T. R., 2012. Local climate zones for urban temperatures. *Bulletin of the American Meteorological Society*, pp. 1879 - 1900.

- Steyerberg, E. & Vergouew, Y., 2014. Towards better clinical prediction models: seven steps for development and an ABCD for validation. *European Heart Journal*, 35(3), pp. 1925-1931.
- Sunderland, K., Mills, G. & Conlon, M., 2013. Estimating the wind resource in an urban area: A case study of micro-wind generation potential in Dublin, Ireland. *Journal of Wind Engineering and Industrial Aerodynamics*, 118(July), pp. 44-53.
- Susca, T., Gaffin, S. & Dell'Osso, G., 2011. Positive effect of vegetation: Urban heat island and green roofs. *Environmental Pollution*, 159(8-9), pp. 2119-2126.
- Svensson, M. & Eliasson, I., 2002. Diurnal air temperatures in built-up areas in relation to urban planning. *Landscape and Urban Planning*, 61(1), pp. 37-57.
- Sweeney, J., 1987. The Urban Heat Island of Dublin City. *Irish Geography*, 20(1), pp. 1-10.
- Taha, H., 1997. Urban climate and heat islands: albedo, evapotranspiration, and anthropogenic heat. *Energy and Buildings*, 25(2), pp. 99-103.
- Taha, H., Akbari, H., Rosenfeld, A. & Huang, J., 1988. Residential cooling loads and the urban heat island—the effects of albedo. *Building and Environment*, 23(4), pp. 271-283.
- Takano, T., Nakamura, K. & Watanabe, M., 2002. Urban residential environments and senior citizens' longevity in megacity areas: the importance of walkable green spaces. *Journal of Epidemiol Community Health*, 56(9), pp. 913-918.
- Taylor, K., 2001. Summarizing multiple aspects of model performance in a single diagram. *Journal of Geophysical Research*, 106(7), pp. 7183-7192.
- Thorsson, S., Lindqvist, M. & Lindqvist, S., 2004. Thermal bioclimatic conditions and patterns of behaviour in an urban park in Göteborg, Sweden. *International Journal of Biometeorology*, 48(3), pp. 149-156.

- Tomlinson, C., Chapman, L., Thornes, J. & Baker, C., 2011. Remote sensing land surface temperature for meteorology and climatology: a review. *Meteorological Applications*, 18(3), pp. 293-306.
- UN, 2014. *World Urbanization Prospects The 2014 Revision*, New York: United Nations ISBN 978-92-1-151517-6.
- United Nations, 2014. *World Urbanization Prospects: The 2014 Revision, Highlights (ST/ESA/SER.A/352)*, United Nations: Department of Economic and Social Affairs, Population Division.
- Voogt, J. & Oke, T., 1997. Complete urban surface temperatures. *Journal of Applied Meteorology*, Volume 36, pp. 117-1132.
- Walsh, S., 2010. *Monthly Weather Bulletin No. 291, July 2010*, Dublin: Meteorological Service of Ireland, Met Éireann.
- Walsh, S., 2012. *A summary of climate averages for Ireland, 1981-2010 [Report]*, Dublin: Met Éireann, 14, Climatological Note, 2012-05.
- Walsh, S., 2014. *Annual Summary 2014*, Dublin: Climatology and Observations Division.
- Wang, X. et al., 2007. A numerical study of influences of urban land-use change on ozone distribution over the Pearl River Delta Region, China. *Tellus B - Chemical and Physical Meteorology*, 59(3), pp. 633-641.
- Ward, H., Evans, J. & Grimmond, C., 2014. Multi-Scale Sensible Heat Fluxes in the Suburban Environment from Large-Aperture Scintillometry and Eddy Covariance. *Boundary-Layer Meteorology*, 152(1), pp. 65-89.
- Ward, I., 2003. The Usefulness of Climatic Maps of Built-Up Areas in Determining Drivers for the Energy and Environmental Efficiency of Buildings and External Areas. *International Journal of Ventilation*, 2(3), pp. 277-286.

- Whitford, V., Ennos, A. & Handley, J., 2001. City form and natural process – indicators for the ecological performance of urban areas and their application to Merseyside, UK. *Landscape and Urban Planning*, 57(2), pp. 91-103.
- Wilby, R., 2003. Past and projected trends in London's urban heat island. *Weather*, 58(7), pp. 251-260.
- Williams, B. et al., 2012. Utilizing an Urban-Regional Model (MOLAND) for Testing the Planning and Provision of Wastewater Treatment Capacity in the Dublin Region 2006–2026. *Planning Practice & Research*, 27(2), pp. 227-248.
- Willmott, C. & Matsuura, K., 2005. Advantages of the Mean Absolute Error (MAE) over the Root Mean Square Error (RMSE) in assessing average model performance. *Climate Research*, Volume 30, pp. 79-82.
- Wong, N. & Yu, C., 2005. Study of green areas and urban heat island in a tropical city. *Habitat International*, 29(3), pp. 547-558.
- Yaghoobian, N., Kleissl, J. & Krayenhoff, E., 2010. Modeling the Thermal Effects of Artificial Turf on the Urban Environment. *Journal of Applied Meteorology and Climatology*, 49(3), pp. 332-345.

**Appendix 1 Declarations of Co-authorship**

**Paper 1 / Chapter 3**

**PhD by Published Work  
Declaration of Co-authorship**

**This form is to accompany the submission of a PhD that contains research reported in published or unpublished co-authored work.** Please include one copy of this form for each co-authored work.

Thesis Chapter/Pages	Chapter 3 (38-74)
Publication title	<i>Using LCZ data to run an Urban Energy Balance Model</i>
Publication status	<b><i>Published</i></b>
Type of publication and full citation if possible	<b><i>Alexander, P.J., Mills, G., Fealy, R. (2015) Using LCZ data to run an urban energy balance model, Urban Climate, Volume 13, September 2015, Pages 14-37, ISSN 2212-0955, <a href="http://dx.doi.org/10.1016/j.uclim.2015.05.001">http://dx.doi.org/10.1016/j.uclim.2015.05.001</a>.</i></b>

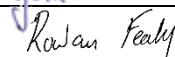
The nature and extent of my contribution to the work detailed above is as follows:

<b>Nature of contribution</b>	<b>Lead author (Tick as appropriate)</b>
For this paper, I developed the research design, carried out the model simulations and analysis of the results and the writing of the paper	<input checked="" type="checkbox"/> Yes <input type="checkbox"/> No

The following co-authors contributed to the work.

<b>Name</b>	<b>Nature of contribution</b>
<b>Gerald Mills</b>	Proof-reading, minor edits to the original text
<b>Rowan Fealy</b>	Proof-reading, minor edits to the original text

The undersigned hereby certify that the above declaration correctly reflects the nature and extent of the student's and co-authors' contributions to this work.

	<b>Name</b>	<b>Signature</b>	<b>Date</b>
<b>Student</b>	Paul Alexander		
<b>Co-author 1</b>	Gerald Mills		
<b>Co-author 2</b>	Rowan Fealy		

**PhD by Published Work  
Declaration of Co-authorship**

**This form is to accompany the submission of a PhD that contains research reported in published or unpublished co-authored work.** Please include one copy of this form for each co-authored work.

Thesis Chapter/Pages	Chapter 4 (75-106)
Publication title	<i>Linking urban climate classification with an urban energy and water budget model: multi-site and multi-seasonal evaluation</i>
Publication status	<i>Submitted (Under Review)</i>
Type of publication and full citation if possible	<i>Alexander, P.J., Bechtel, B., Chow, W., Fealy, R., Mills, G. (2016) Linking urban climate classification with an urban energy and water budget model: multi-site and multi-seasonal evaluation 1-23pp - Urban Climate</i>

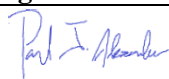
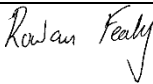
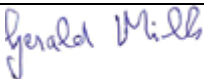
The nature and extent of my contribution to the work detailed above is as follows:

<b>Nature of contribution</b>	<b>Lead author (Tick as appropriate)</b>
For this paper, I developed the research design, carried out the model simulations and analysis of the results and the writing of the paper	<input checked="" type="checkbox"/> Yes <input type="checkbox"/> No

The following co-authors contributed to the work.

Name	Nature of contribution
<b>Benjamin Bechtel</b>	Provision of Hamburg Data, proof-reading, minor edits to the original text
<b>Winston Chow</b>	Provision of Phoenix Data, proof-reading, minor edits to the original text
<b>Gerald Mills</b>	Proof-reading, minor edits to the original text
<b>Rowan Fealy</b>	Proof-reading, minor edits to the original text

The undersigned hereby certify that the above declaration correctly reflects the nature and extent of the student's and co-authors' contributions to this work.

	Name	Signature	Date
<b>Student</b>	Paul Alexander		
<b>Co-author 1</b>	Benjamin Bechtel		
<b>Co-author 2</b>	Winston Chow		
<b>Co-author 3</b>	Rowan Fealy		
<b>Co-author 4</b>	Gerald Mills		

**PhD by Published Work  
Declaration of Co-authorship**

**This form is to accompany the submission of a PhD that contains research reported in published or unpublished co-authored work.** Please include one copy of this form for each co-authored work.

Thesis Chapter/Pages	Chapter 5 (107-128)
Publication title	<i>Spatial validation of an urban energy balance model using multi-temporal remotely sensed surface temperature</i>
Publication status	<b><i>Published</i></b>
Type of publication and full citation if possible	<b><i>Alexander, P.J., Fealy, R., Mills, G. (2015) Spatial validation of an urban energy balance model using multi-temporal remotely sensed surface temperature, in IEEE Urban Remote Sensing Event (JURSE), 2015 Joint, vol., no., pp.1-4, March 30 2015-April 1 2015 doi: 10.1109/JURSE.2015.7120500</i></b>

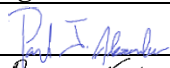
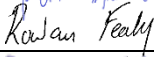
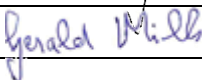
The nature and extent of my contribution to the work detailed above is as follows:

<b>Nature of contribution</b>	<b>Lead author (Tick as appropriate)</b>
For this paper, I developed the research design, collection and processing of LST data, carried out the model simulations and analysis of the results and the writing of the paper	<input checked="" type="checkbox"/> Yes <input type="checkbox"/> No

The following co-authors contributed to the work.

<b>Name</b>	<b>Nature of contribution</b>
<b>Rowan Fealy</b>	Proof-reading, minor edits to the original text
<b>Gerald Mills</b>	Proof-reading, minor edits to the original text

The undersigned hereby certify that the above declaration correctly reflects the nature and extent of the student's and co-authors' contributions to this work.

	<b>Name</b>	<b>Signature</b>	<b>Date</b>
<b>Student</b>	Paul Alexander		
<b>Co-author 1</b>	Rowan Fealy		
<b>Co-author 2</b>	Gerald Mills		

**PhD by Published Work  
Declaration of Co-authorship**

**This form is to accompany the submission of a PhD that contains research reported in published or unpublished co-authored work.** Please include one copy of this form for each co-authored work.

Thesis Chapter/Pages	Chapter 6 (129-162)
Publication title	<i>Simulating the impact of different urban development pathways on the local climate: A scenario-based analysis in the greater Dublin region, Ireland</i>
Publication status	<i>In Press</i>
Type of publication and full citation if possible	<i>Alexander, P.J., Fealy, R., Mills, G. (2016) Simulating the impact of different urban development pathways on the local climate: A scenario-based analysis in the greater Dublin region, Ireland. Landscape and Urban Planning. DOI: 10.1016/j.landurbplan.2016.02.006</i>

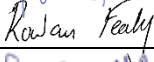
The nature and extent of my contribution to the work detailed above is as follows:

Nature of contribution	Lead author (Tick as appropriate)
For this paper, I developed the research design, carried out the model simulations and analysis of the results and the writing of the paper	<input checked="" type="checkbox"/> Yes <input type="checkbox"/> No

The following co-authors contributed to the work.

Name	Nature of contribution
<b>Rowan Fealy</b>	Proof-reading, minor edits to the original text
<b>Gerald Mills</b>	Proof-reading, minor edits to the original text

The undersigned hereby certify that the above declaration correctly reflects the nature and extent of the student's and co-authors' contributions to this work.

	Name	Signature	Date
<b>Student</b>	Paul Alexander		
<b>Co-author 1</b>	Rowan Fealy		
<b>Co-author 2</b>	Gerald Mills		

---

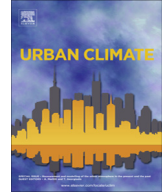
**Appendix 2 Published Words / Authors Pre-Prints**

---



Contents lists available at ScienceDirect

## Urban Climate

journal homepage: [www.elsevier.com/locate/uclim](http://www.elsevier.com/locate/uclim)

# Using LCZ data to run an urban energy balance model



Paul John Alexander<sup>a,\*</sup>, Gerald Mills<sup>b</sup>, Rowan Fealy<sup>c</sup>

<sup>a</sup> Irish Climate Analysis & Research Units (ICARUS), Maynooth University, Kildare, Ireland

<sup>b</sup> School of Geography Planning & Environmental Policy (GPEP), University College Dublin, Belfield, Ireland

<sup>c</sup> Department of Geography, Maynooth University, Kildare, Ireland

## ARTICLE INFO

### Article history:

Received 17 June 2014

Revised 20 April 2015

Accepted 1 May 2015

### Keywords:

LCZ

SUEWS

UEB

Urban

Landcover

## ABSTRACT

In recent years a number of models have been developed that describe the urban surface and simulate its climatic effects. Their great advantage is that they can be applied in environments outside the cities in which they have been developed and evaluated. Thus, they may be applied to cities in the economically developing world, which are growing rapidly, and where the results of such models may have greatest impact with respect to informing planning decisions. However, data requirements, particularly for the more complex urban models, represent a major obstacle to their employment. Here, we examine the potential for running the Surface Urban Energy and Water Balance model (SUEWS) using readily obtained data. SUEWS was designed to simulate energy and water balance terms at a neighbourhood scale ( $\geq 1 \text{ km}^2$ ) and requires site-specific meteorological data and a detailed description of the surface. Here, its simulations are evaluated by comparison with measurements made over a seven month (approximately 3 seasons) period (April–October) at two flux tower sites (representing urban and suburban landscapes) in Dublin, Ireland. However, the main purpose of this work is to test the performance of the model under ‘ideal’ and ‘imperfect’ circumstances in relation to the input data required to run SUEWS. The ideal case uses detailed urban land cover data and meteorological data from the tower sites. The imperfect cases use parameters derived from the Local Climate Zone (LCZ) classification scheme and meteorological data from a standard weather station located beyond the urban area. For the period of record examined, the simulations show good

\* Corresponding author at: ICARUS Room 1.8 Laraghbryan House, North Campus, Maynooth University, Maynooth, Kildare, Ireland. Tel.: +353 1 7083432.

E-mail address: [paul.alexander@nuim.ie](mailto:paul.alexander@nuim.ie) (P.J. Alexander).

agreement with the observations in both ideal and imperfect cases, suggesting that the model can be used with data that is more easily derived. The comparison also shows the importance of including vegetative cover and of the initial moisture state in simulating the urban energy budget.

© 2015 Elsevier B.V. All rights reserved.

---

## 1. Introduction

Within the next four decades the global population is projected to increase by 2.3 billion, within the same period it is expected that urban areas will gain 2.6 billion (UN, 2012), absorbing projected growth and continuing to draw from existing rural populations. While this trend appears globally, there are regional differences. The urban population in more economically developed regions has already reached 78%, whereas in less developed regions it currently stands at 47%. Taking the projections for Asia and Africa together, their urban population will grow by 2.3 billion by the middle of the century. If these projections are realised, most of the urbanisation in the future will occur in the economically developing world (Satterthwaite, 2007). Responding to this challenge will result in large-scale housing and critical infrastructure projects (e.g. energy and water supply, waste removal facilities and transport) that, once in place, create an urban form that is difficult to change; hence, it is important that urban growth is well managed. At least two responses might be expected: horizontal expansion of the urban area and densification of the existing urban fabric (Moonen et al., 2012). If future urban development is to reduce environmental impacts (e.g. air quality, hydrology and thermal effects) that result from conventional urbanisation some guidance on development pathways is needed (Schwela, 2000; Schuster et al., 2005; Arnfield, 2003; Chen and Ng, 2012). One component of this guidance should be physically-based models that can simulate the effect of alternative urban plans and designs and inform decision-making. However, these models only have value if they have been tested, that is, applied to urban places, evaluated against observations and validated. Unfortunately, there are few examples of the application of urban climate models to these types of problems (Oke, 2006).

Although there are an increasing number of diverse urban climate models available, there is little evidence that they are routinely applied. A significant impediment to their route use includes the paucity of relevant information on: the physical character of cities (that is the buildings, materials, layout, etc.) needed to derive model parameters and; the meteorological data needed to ‘force’ the models and evaluate their simulations. In fact, the lack of urban specific data has been recently highlighted in the 5th assessment report (AR5) of the Intergovernmental Panel on Climate Change (IPCC, 2014). Specifically AR5 highlights serious data limitations with respect to geophysical, biological and socio-economic data, as well as inadequate knowledge surrounding the vulnerability of the built environment and building materials to climate change. These issues are particularly acute for the rapidly growing cities of the economically developing world, many of which are outside the mid-latitude climates where the models have been developed and may lack the necessary urban and meteorological information required. Recently, a protocol for collecting urban parameters in an efficient and standardised manner has been proposed to address this problem (Ching, 2013; Bechtel et al., 2015).

This paper examines the issue of information quality and its impact on the performance of an urban energy balance model (UEB). The Surface Urban Energy and Water Balance model (SUEWS) is a moderately complex UEB that requires detailed information on the urban landscape and is usually run using on-site meteorological data. We use SUEWS to simulate the energy budget at two Dublin locations for which we have detailed energy flux stations and detailed spatial information (e.g. individual building footprints, heights) on the surrounding urban landscape. This allows us to run the model and evaluate its simulations of turbulent fluxes over a period of time. We then use readily available standard meteorological data and coarse land-cover data and perform the same evaluation. The

performance of SUEWS is judged against two different urban landscapes – city centre and green suburbs – where eddy-flux towers are located that provide observations of the UEB terms. The results are compared with observations to assess the relative effect of input data quality. Specifically we address two questions, which have implications for the use of UEB models in data-poor settings:

1. How does SUEWS perform in terms of discriminating between different urban environments when run using readily available but coarse land-cover data and standard meteorological data relative to using optimal data?
2. Specific to the Dublin case study, which is more important for running SUEWS; on-site detailed meteorological data or high quality, spatially detailed land-cover?

The answers are based on the application of the SUEWS in Dublin (Ireland), for which we have a range of data suitable for evaluating model performance under ideal and non-ideal circumstances.

## 2. Urban energy budget (UEB) models

A number of urban models have been developed at a variety of spatial and temporal scales with a range of applications, the most common of which are based on the surface energy budget (Oke, 1988),

$$Q^* + Q_F = Q_H + Q_E + \Delta Q_S, \quad [\text{W m}^{-2}] \quad (1)$$

where  $Q^*$  is net radiation,  $Q_F$  is anthropogenic heat flux,  $Q_H$  and  $Q_E$  are the turbulent sensible and latent heat fluxes respectively and  $\Delta Q_S$  is storage heat flux. This equation refers to a representative urban volume that extends from of the surface in which there is no net horizontal transfer (that is, an extensive surface type) and no significant energy exchange across the lower boundary. Hence, assessing each of the terms at the upper surface of the volume, which is located above the canopy layer captures the exchanges between the urban surface and overlying boundary layer. The process of urbanisation results in the replacement of natural surfaces by hard impervious surfaces (e.g. roads, pavements, car parks) and buildings. This greatly alters the surface energy balance by, for example, increasing (decreasing) the sensible (latent) heat flux and increasing heat storage. One of the best known outcomes is the formation of an urban heat island (Oke, 1980; Grimmond and Oke, 2002).

There are three approaches for UEB modelling: deriving empirically based models; modification of existing models designed for non-urban areas and; development of new models with urban specific conceptualisation and physics (Hidalgo et al., 2008). The latter two approaches simulate the urban effect by describing the urban landscape using parameterisations that can range from the very simple e.g. concrete slab approach used by Taha (1999) and Kusaka and Kimura (2004) to more complex schemes that take into account building dimensions, materials, and internal energy use, see for example, Kimura and Takahashi (1991), Mills (1997), Masson (2000), Martilli et al. (2002) and Kanda et al. (2005). Most of these describe urban areas by partitioning the surface into cells each of which has distinct properties related to aspects of urban form (e.g. fraction that is impervious) and function (e.g. anthropogenic heat flux). Evaluating and comparing these models has proved difficult owing to their distinct histories, which reflects different designs that have evolved in response to user needs and data requirements and availability. In fact, there has been a call for the standardisation of how parameters are gathered regardless of which model is being employed (Ching, 2013; Bechtel et al., 2015). This would greatly aid communication among researchers, allow for better comparisons between models and allow the transfer of models (and results) between cities.

Grimmond et al. (2010 and 2011) categorised 33 UEB models into simple, medium and complex based on 12 characteristics and compared their simulations against observations of the UEB made across a range of urban settings (see Table 1). In these tests, each UEB model had distinct merits such that no single model performed best or worst in comparisons; however broad conclusions emerged. First, those models that included information on building facades (that is the walls and roof) and on vegetation had smaller errors when simulating outgoing shortwave radiation ( $K\uparrow$ ), net radiation ( $Q^*$ ) and the turbulent fluxes ( $Q_H$  and  $Q_E$ ). Second, providing additional data on building materials (such as detailed thermal properties and albedo) did not necessarily improve the models performance;

**Table 1**

Aspects of UEB models which are used for classification of model complexity. For example in the case of criteria 1, “simple” would be associated with modelling only one or two fluxes, “complex” would be associated with modelling all fluxes.

Criteria	Characteristic	Typical treatment (Categories)	Levels of complexity
1	Fluxes included	All fluxes/individual fluxes	4
2	Vegetation	Separated/integrated	3
3	$Q_F$	Internal building/modelled	4
4	Temporal $\Delta Q_S$	Fixed/variable	3
5	Urban morphology	Single layer(s)/multiple	7
6	Facet/orientation	Bulk/canyons	4
7	Reflections	Single/multiple/infinite	3
8	Albedo/emissivity	Bulk/multiple facets	3
9	$\Delta Q_S$	Residual/conduction	3
10	Resistance	Single layer/multi-layer	3
11	Surface temperature/moisture	Bulk/single/multiple	4
12	Air temperature/moisture	Forcing height/single/multi-layer	3

for simple models, a net improvement was often observed but this was not the case for complex models. In other work, [Loridan et al. \(2010\)](#) evaluated the single-layer urban climate model (SLUCM), as a component of the mesoscale Weather Forecasting Model (WRF) model, and found that data on vegetative cover was especially important for improved simulations. Similarly, [Loridan and Grimmond \(2012\)](#) using the same model found that using data that described the character of urban neighbourhoods where flux observations are made, rather than using generic urban data, had a marked effect; SLUCM was better able to reproduce the turbulent fluxes at 15 sites across the US, Mexico, Canada, Australia, Finland and Poland.

These studies provide a cautionary tale; while information on the nature of the urban surface is critical for UEB simulations, there is no guarantee that acquiring more detailed information will improve model performance. This has significant implications for the acquisition of urban data suited for a model as it can take a considerable amount of time but might yield little benefit. For example, UEB model evaluations consistently show the value of information on vegetation for simulating the turbulent fluxes but this does not mean that obtaining information on the details of trees (e.g. species, age, health, etc.) will make a difference to simulations. This is important as, from a planning and design perspective, city greening initiatives are a major component of climate-based policies and any UEB model chosen must be able to assess the impact of modifying vegetation cover/type ([Breuste, 2004](#); [Kovács and Németh, 2012](#)). However, it will be important to know what sort of data is needed, as this will guide the type of modelling exercise and help in interpreting the results. Practically then the challenge is to acquire urban data at a sufficient scale and detail to run a validated model suited for a purpose.

For many purposes, it may be possible that model ‘look-up’ tables that link urban landscape types to typical climate-relevant parameters could address the lack of land-cover information. The Local Climate Zone (LCZ) classification scheme for example, partitions the landscape into 10 urban and 7 non-urban classes, permits mixed categories and allows seasonality to be taken into account (see [Table 2](#); [Stewart and Oke, 2012](#)). The advantages of this approach include: LCZ types are purported to be universal in their depiction of landscapes and their climate impacts; it is relatively easy to categorise urban neighbourhoods into an LCZ type from fieldwork and readily available sources (e.g. GoogleEarth) and; each LCZ type is associated with a typical range of parameter values that describe surface cover, building heights and street aspect ratio, etc. ([Table 2](#)). The scheme has been applied most to the study of the Urban Heat Island (UHI), for which it was developed – see [Fenner et al. \(2014\)](#), [Leconte et al. \(2014\)](#), and [Stewart et al. \(2014\)](#). As an example, [Fig. 1](#) shows the LCZ map of Dublin, which was generated for an urban heat island study using available land-cover data, remote sensing and fieldwork ([Alexander and Mills, 2014](#)).

### 3. Methodology

In this work we examine the quality of the input data needed to run a moderately complex UEB model satisfactorily. Our examination is based on data gathered for Dublin, Ireland (53°N, 6°W), which

**Table 2**

Outline of Local Climate Zone Classes and their properties (modified from Stewart and Oke, 2012). Those that are asterisked are present in the Dublin study area.

Local Climate Zone (LCZ)	Building surface fraction (%)	Impervious surface fraction	Pervious surface fraction	Height of roughness elements (m)
Compact high-rise	40–60	40–60	<10	>25
*Compact midrise	40–70	30–50	<20	10–25
*Compact low-rise	40–70	20–50	<30	3–10
Open high-rise	20–40	30–40	30–40	>25
*Open midrise	20–40	30–50	20–40	10–25
*Open low-rise	20–40	20–50	30–60	3–10
Lightweight low-rise	60–90	<20	<30	2–4
*Large low-rise	30–50	40–50	<20	3–10
Sparsely built	10–20	<20	60–80	3–10
*Heavy industry	20–30	20–40	40–50	5–15
*Dense trees	<10	<10	>90	3–30
Scattered trees	<10	<10	>90	3–15
Bush, scrub	<10	<10	>90	<2
*Low plants	<10	<10	>90	<1
*Bare rock or paved	<10	>90	<10	<0.25
Bare soil or sand	<10	<10	>90	<0.25
*Water	<10	<10	>90	–

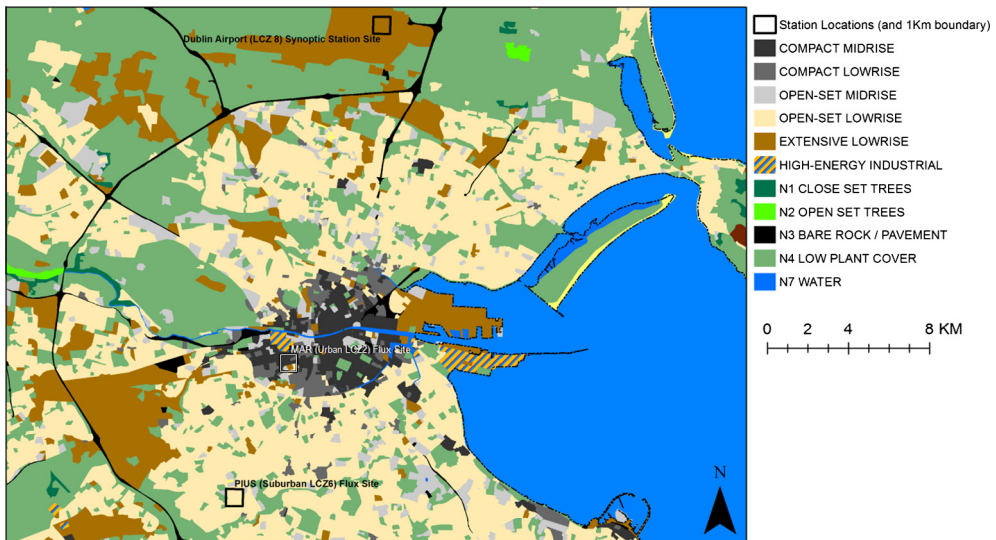


**Fig. 1.** LCZ map of Dublin. Also shown are flux site locations and synoptic station location with a 1 km grid box which represents extent of area used to calculate surface fractions (Modified from Alexander and Mills, 2014).

has a mild, mid-latitude climate (Cfb). It provides an ideal place for this study as it has two observation sites (located in urban and suburban neighbourhoods) where detailed energy flux and meteorological observations have been made since 2009; these data can be used to run the model and compare its simulations with observations. In addition: there is a LCZ description of the city that outlines major neighbourhood types and; a WMO standard weather station at Dublin Airport, which is 5–10 km distant from the flux sites, records hourly observations.

The Surface Urban Energy and Water balance Scheme (SUEWS v.2013b) is used to simulate the UEB (Eq. (1)) of both neighbourhoods. SUEWS requires a relatively low number of input parameters that may include: meteorological data; socio-economic-demographic data and; surface cover and urban

structure data. Some of these inputs are required to run the model, while other inputs are optional. At the very least the model requires standard meteorological data and details on the fractions of the landscape that is occupied by buildings, vegetation, impervious paving, etc. The challenges of operational employment of the earlier stages of model have been documented (Cleugh et al., 2005) and include the parameterisation schemes themselves along with acquiring the necessary forcing data.

Järvi et al. (2011) evaluated SUEWS using flux observations (spanning various time lengths from different years) from sites in Los Angeles (34°N, Köppen climate type, Csb) and Vancouver (49°N, Cfb). The results showed the model to be capable of simulating net radiation, sensible and latent and heat fluxes with RMSE ranges of 25–47 W m<sup>-2</sup>, 30–64 W m<sup>-2</sup> and 20–56 W m<sup>-2</sup>, respectively. Moreover, while the model reproduced the diurnal cycle of the turbulent fluxes, it tends to underestimate  $Q_E$  and overestimate  $Q_H$  in the day time. Here, we compare SUEWS model output with energy flux observations at two flux sites. The initial model runs use detailed site-specific meteorological and land-cover data. Subsequently, SUEWS is run using meteorological data from Dublin Airport and land-cover data representative of the LCZ type in which each flux site is located. In the following sections we describe the SUEWS model, the meteorological/flux data and the urban land-cover data used in this study. We then outline the structure of the experiment.

### 3.1. SUEWS

SUEWS was designed for urban simulations at a neighbourhood-scale, which corresponds to an area of approximately 1 km<sup>2</sup>. It simulates both the urban energy budget (Eq. (1)) and water budget (Grimmond and Oke, 1991),

$$P + I_e + F = E + R + \Delta S \quad [\text{mm h}^{-1}] \quad (2)$$

where  $P$  is precipitation,  $I_e$  is externally piped water,  $F$  is anthropogenic water emission,  $E$  is evaporation (including transpiration),  $R$  is runoff and  $\Delta S$  is change in storage. Eqs. (1) and (2) are connected directly through the evaporative terms ( $Q_E$  and  $E$ ) and indirectly via other terms; for example a precipitation event may result in water storage in soil that will affect its thermal properties. The energy budget (Eq. (1)), which is the focus of this paper describes flux exchanges at a plane that separates the roughness sub-layer (between 2 and 4 times the mean height of the roughness elements) from the remainder of the boundary-layer. The modelled fluxes therefore correspond to the inertial sub-layer, where micro-scale variability driven by individual roughness elements becomes integrated into neighbourhood signals. Moreover, one should note the absence of advective terms in Eq. (1), so that it assumes there is a negligible horizontal energy transfer. Strictly speaking then, this limits the application of SUEWS to extensive neighbourhood types where the landscape may be described as relatively homogenous (Middel et al., 2012). The absence of detailed accounting for radiative transfer within the canyons below the simulated level should also be noted.

The data inputs employed by the model are listed in Table 3 and include hourly meteorological data, land cover parameters and anthropogenic fluxes. SUEWS describes the milieu of different surface types in a neighbourhood in terms of fractional coverage ( $\lambda$ ) of buildings, pavements, water, vegetated areas (both irrigated and non-irrigated) and trees (coniferous and deciduous) and unmanaged land cover such as bare soils or rock. Anthropogenic water and energy use can also be provided; hourly water use can be expressed as a proportion of the daily total and hourly anthropogenic heat fluxes can be estimated from typical daily patterns, divided into weekday and weekend values.

### 3.2. Meteorological and energy flux data

The atmospheric observations used here are of two types. The first is standard meteorological information obtained from Dublin Airport, which is located 5 km from the city centre in an area dominated by warehouses (Fig. 1). Hourly observations are available for a number of elements: air temperature ( $T$ ), precipitation ( $P$ ), pressure ( $Pr$ ), humidity ( $RH$ ), wind-speed ( $V$ ) and direction and solar radiation received ( $K_{\downarrow}$ ). Note that hourly values for  $K_{\downarrow}$  are a required model input.

The second is meteorological and energy flux data that is acquired at two stations (Fig. 1) that are part of the International Urban Flux Network (Keogh et al., 2012). The measurement sites were

**Table 3**  
Summary of inputs required to run SUEWS model.

Variable	Units	Comments
<i>Meteorological</i>		
Air temperature ( $T$ )	°C	
Relative humidity (RH)	%	
Pressure (Pr)	kPa	
Precipitation ( $P$ )	mm h <sup>-1</sup>	
Wind speed ( $V$ )	m s <sup>-1</sup>	
Incoming short wave ( $K\downarrow$ )	W m <sup>-2</sup>	
Incoming long wave ( $L\downarrow$ )	W m <sup>-2</sup>	Optional (otherwise uses $T$ and RH)
Observed sensible heat ( $Q_H$ )	W m <sup>-2</sup>	Optional
Observed latent heat ( $Q_E$ )	W m <sup>-2</sup>	Optional
Observed storage heat ( $\Delta Q_s$ )	W m <sup>-2</sup>	Optional
Cloud fraction	Tenths	Optional
Soil moisture deficit	m <sup>3</sup> m <sup>-3</sup>	Optional
Leaf Area Index (LAI)		Optional
<i>Anthropogenic inputs</i>		
Anthropogenic heat ( $Q_F$ )	W m <sup>-2</sup>	Optional, hourly values (otherwise modelled)
Anthropogenic water use	%	Optional, hourly ratio of total diurnal usage
<i>Surface inputs</i>		
Fractional coverage of surface types ( $\lambda$ )	%	Urban, pavement, soil, grass (irrigated and un-irrigated), trees (coniferous and deciduous) water
Surface area	Ha	
Water usage area	Ha	Optional
Latitude/longitude	°	
Storage capacity of pipes	mm	Optional
Frontal area fractions		Optional, buildings and trees separate
Roughness length for momentum ( $z_0$ )	m	Optional
Zero displacement height ( $z_d$ )	m	Optional
Surface element heights	m	Optional, buildings and trees separate

**Table 4**

A list of the energy budget and meteorological variables and the instruments used at each site; the height of the instruments at urban and suburban sites respectively is shown in the parentheses. The final column lists the equivalent SUEWS parameters (Table 3).

Variable	Instrument	SUEWS parameter
Radiation	Net radiation sensor (15/11)	$K\downarrow$ , $K\uparrow$ , $L\downarrow$ , $L\uparrow$
	Hukseflux (NR01)	
3D wind velocity	Sonic anemometer (17/12)	$V$ , $Q_H$ , $Q_E$
	Campbell Scientific (CSAT3)	
Water vapour density	InfraRed Gas Analyser (17/12)	$Q_E$
	Licor Sciences (LI-7500)	
Air temperature and relative humidity	Temperature and relative humidity probe (17/12)	$T$ , RH
	Vaisala HMP45C	
Precipitation	Campbell Scientific tipping bucket gauge	$P$

selected to represent sites that typify Dublin's urban land-cover. Each has an identical suite of instruments (see Table 4) and radiation and turbulent flux terms are recorded alongside the meteorological variables listed above. The suburban site is located in a residential area consisting of similar two-story houses about 6 m tall and much of the landcover is vegetated (open low-rise or LCZ6). The instruments are positioned on a mast that is located on the roof of a school at a height of 12 m (10 m for the net radiometer). The urban site is located in a mixed-use area closer to the city centre; much of the surrounding landscape is impermeable and the average building height is about 8 m (compact midrise or LCZ2). The support mast is on the roof of a 12 m tall building and the instruments are at a height of 17 m (15 m for net radiometer).

Upward and downward facing radiometers provide  $K\downarrow$ ,  $K\uparrow$ ,  $L\downarrow$  and  $L\uparrow$ . The turbulent fluxes  $Q_H$  and  $Q_E$  heat are obtained using an open-path eddy covariance system that is interrogated at a rate of 10 Hz; the recorded fluxes are based on 30 min averages. These data are then corrected following Webb et al. (1980), which results in increasing  $Q_E$  and decreasing  $Q_H$  and somewhat reducing the residual. The heat storage term ( $\Delta Q_S$ ) is then estimated as a residual of the measured terms,

$$\Delta Q_S \approx Q^* - (Q_H + Q_E) \text{ [W m}^{-2}\text{]} \quad (3)$$

Thus,  $\Delta Q_S$  includes any errors associated with the estimation of the other fluxes. Also, while the anthropogenic heat flux ( $Q_F$ ) is not distinguishable in the observations, it is present in all the measured terms.

Each tower is located well within its LCZ type and the flux instruments are positioned at a level that is approximately twice the height of the surrounding buildings and at about the height of the inertial sub-layer established by that surface type. In other words, we are assuming that advection is negligible and that  $\Delta Q_A$  can be ignored. Finally, it is also assumed that the *makeup* of source regions for the radiation ( $K\uparrow$  and  $L\uparrow$ ) and the turbulent ( $Q_H$  and  $Q_E$ ) fluxes are similar even though the source for the former is fixed and that for the latter changes with wind direction and stability (Oke, 2006). In practice, this means that observations of  $K\uparrow$  and  $L\uparrow$  are strongly dependent on the surfaces directly below the sensors. In the case of the suburban site, which is a located in the grounds of a small school, the underlying surface consists mostly of a dark roof surface and asphalt car park so that these terms are less likely to be representative of the open low-rise suburban setting than the turbulent terms.

For both data types, observations for the period April 08 – October 18 2010 were used. Both the winter period 2009 (i.e. November 2009 – January 2010) and 2010 (November 2010 – January 2011) saw atypical synoptic conditions, specifically widespread snow/ice was present across both Ireland and the UK for most of the period. This resulted in restricted access to on-site data loggers at the flux locations. As such, the period of observations utilised represents a contiguous period of observations without significant data gaps.

### 3.3. Urban land-cover parameters

The required urban land-cover fractions ( $\lambda$ , see Table 5) were derived using GoogleEarth. Values of  $\lambda$  were calculated for a 1 km<sup>2</sup> area around each flux site by digitizing polygons representing roads, buildings and vegetated surfaces and points to represent trees. The total tree canopy coverage was estimated based on the average canopy size for trees in Dublin (Ningal et al., 2010). All trees were classified as deciduous. The total area coverages of buildings, pavements, water, vegetated areas, trees and unmanaged land were computed and then converted to fraction values ( $\lambda$ ) for each site.

**Table 5**

Local Climate Zones (LCZ) in Dublin city with estimated plan area fractions ( $\lambda$ ). These were computed by taking the average of  $n$  randomly sampled areas (1 km<sup>2</sup> in size) within each LCZ type. The equivalent fractions calculated for the area around the urban and suburban observation sites are listed in the final two rows.

LCZ	Built	Impervious	Unmanaged	Trees	Grass	Water	(n)
2 Compact mid	33	55	00	06	06	00	5
3 Compact low	22	61	00	07	10	00	5
5 Open mid	13	48	00	11	28	00	5
6 Open low	14	52	00	11	23	00	10
8 Large low	30	61	00	04	05	00	5
10 Industrial	16	69	00	08	07	00	5
101 Close trees	01	02	04	48	45	00	5
104 Low plant	03	08	03	18	67	00	10
105 Bare rock	09	49	00	14	29	00	2
106 Bare sand	06	20	55	19	00	00	1
107 Water	00	00	00	00	00	100	–
Urban site (LCZ2)	33	66	00	00	00	00	–
Suburban site (LCZ6)	18	48	00	05	29	00	–

The LCZ scheme also provides a range of  $\lambda$  values for each of the 17 types (Table 2) and for the Dublin study area, 11 of these types are present (Fig. 1). Fractional areas were calculated using GIS for each of these by random sampling from within each type; the size of sample varied in proportion to the area that that LCZ type occupied in the city (Grimmond and Souch, 1994). Thus for example, we sampled at 10 locations within the large suburban swath around the city centre (Open low-rise type, LCZ6) and at 5 places in the more densely built city centre (Compact mid-rise, LCZ2). None of the sampled places correspond with the observation site calculations. We treated the LCZ impervious fraction as pavement surface type in SUEWS. The final  $\lambda$  values calculated for each LCZ is the average of the sampled sites (Table 5); a comparison with the LCZ ranges is presented in Table 2.

### 3.4. Model experiment

SUEWS is run in four modes, which are used to represent optimal and suboptimal modes:

Mode	Land cover	Meteorological forcing	Description	Pairing
1	High-resolution	Flux sites	Optimal situation that uses meteorological data and land-cover parameters for the observation sites	Modes 2 and 4
2	High-resolution	Off-site standard weather station	Suboptimal as it uses meteorological data from a standard weather station to represent the city	Modes 1 and 3
3	LCZ	Off-site standard weather station	Suboptimal as it uses meteorological data from a standard weather station and land-cover parameters estimated for the larger LCZ neighbourhood type in which the sites are situated	Modes 4 and 2
4	LCZ	Flux sites	Suboptimal as it uses LCZ land cover parameters and $L\downarrow$ is derived from $T$ and $RH$ (Loridan et al., 2011)	Modes 3 and 1

Simulations were completed for the period April 08 – October 18 2010 (that is, Julian dates 98 through 291), which corresponds with the period for which daily observations of  $Q^*$ ,  $Q_H$ ,  $Q_E$  and  $\Delta Q_S$  are available for both flux sites. Our comparison between different Modes is based on the hourly values and on the average diurnal (daily) profiles calculated for each month. The anthropogenic heat and water fluxes options in SUEWS are not implemented here; this is reasonable in the Irish climate which is mild and wet and the contributions of traffic is likely to be small (perhaps  $\leq 20 \text{ W m}^{-2}$  using Pigeon et al. (2007) as a guide).

At the start of the period (April) the soil moisture status in SUEWS is set at field capacity (150 mm). The recorded precipitation at stations around Dublin in March, 2010 was about 55 mm which represented 110% of the average for that month and resulted in wide spread localised flooding toward the end of the month. At agricultural meteorological stations proximate to Dublin, soil moisture deficit

(SMD) was reported at  $-10$  mm (surplus) at stations. The spring period (February–April) of 2010 was especially cold so it might be expected that vegetation growth was inhibited, even in the city. To account for this, the Leaf Area Index (LAI) at the beginning of April was obtained from MODerate Resolution Imaging Spectroradiometer (MODIS) data (MOD-15), which are available at  $1 \text{ km}^2$  resolution at 8-day intervals.

### 3.5. Model evaluation and sensitivity

The performance of SUEWS run in each of the Modes listed above is evaluated against the observations at the urban and suburban flux sites. A measure of the goodness of fit for each modelled term is provided by the RMSE,

$$\text{RMSE} = \left[ \sum_{i=1}^n \frac{(\hat{y}_i - y_i)^2}{n} \right]^{0.5} \quad (4)$$

where  $(\hat{y}_i - y_i)$  represents the difference between the observed ( $y$ ) and simulated ( $\hat{y}$ ) flux term (e.g.  $Q^*$ ) at each hourly time interval ( $i$ );  $N$  represents the total number of hours. RMSE is commonly used to assess the total error, regardless of its direction. To measure any bias in the simulations the Mean Fractional Bias (MFB) is used,

$$\text{MFB} = \frac{1}{n} \sum_{i=1}^n \frac{(\hat{y}_i - y_i)}{(\hat{y}_i + y_i)/2} \quad (5)$$

where all terms have the same meaning as in the RMSE; this statistic produces a value between  $-2$  and  $+2$  where the sign indicates over (+) or under (–) estimates. Additionally, to examine the relative performance across all months between each Mode we generated Taylor diagrams for each of the simulated flux terms which employ three statistics: the centred RMSE ( $E'$ ), the correlation coefficient ( $R$ ), and the standard deviation ( $\sigma$ ) (Taylor, 2001):

$$E' = \frac{1}{N} \sum_{i=1}^N [(\hat{y}_i - \bar{\hat{y}}) - (y_i - \bar{y})]^2 \quad (6)$$

$$R = \frac{\frac{1}{N} \sum_{i=1}^N (\hat{y}_i - \bar{\hat{y}})(y_i - \bar{y})}{\sigma_{\hat{y}} \sigma_y} \quad (7)$$

where  $\sigma_{\hat{y}}$  and  $\sigma_y$  are the standard deviations of the model and observed variable, respectively. The other terms are the same as Eq. (4) and resulting values are in  $\text{W m}^{-2}$  with the exception of Eqs. (5) and (7). For the period of examination, there are a total 4656 hourly values (194 days) of observed ( $y$ ) and simulated ( $\hat{y}$ ) values for each model run for each site.

To test the sensitivity of SUEWS to differences in meteorological forcing data (for example differences which might arise between off-site and on-site stations) we employed a one-factor-a-time (OFAT) approach (Griensven et al., 2002). First, we generated highly typified data i.e. data derived from a loess curve for a 168 h period for each required meteorological variable (see Table 3). We excluded precipitation from these data. To test SUEWS sensitivity to  $K\downarrow$ ,  $T/\text{RH}$  and  $V$  we perturbed these data  $\pm 10\%$  of the mean state in order to examine the impact on modelled turbulent fluxes ( $\Delta Q_S$ ,  $Q_H$  and  $Q_E$ ). For the purpose of our OFAT analysis we distributed land cover evenly across all land cover types (excluding water), meaning differences in our simulations of  $\Delta Q_S$ ,  $Q_H$  and  $Q_E$  between each perturbation would arise due to the modification of forcing data.

## 4. Results

In the following section the *relative* performance of SUEWS in each Mode is examined by comparing simulated and observed fluxes at each site. Initially, the diurnal performance of SUEWS when run in different Modes is examined based on the hourly simulations for the month of June. In this section

we also present the differences between our forcing data sites. Subsequently, the overall performance of the model based on daily outcomes is presented followed by an examination of the impact of modifying: the land cover and meteorological forcing data.

#### 4.1. Hourly fluxes comparison – June 2010

The meteorological forcing data available for the Dublin Airport (A) site and that available for the urban and suburban sites in June are shown in Tables 6 and 7. Rainfall was recorded on 9 days in June and with two exceptions, all stations recorded rainfall on corresponding days. The total amount of rainfall recorded at the Airport was 53.6 mm (Table 6), which was higher and lower than that recorded at the urban and suburban sites, respectively; this is not surprising given the non-standard exposure of the gauges at the flux sites. Recorded wind-speed at the Airport averaged  $2.17 \text{ ms}^{-1}$ , which was lower than that measured over the ‘rougher’ urban surface at both sites, which may be surprising but mean wind-speed was lower than normal in June 2010 owing to the dominance of high pressure ( $\sim 1018 \text{ hPa}$  for the month). The difference between the sites is clearest when air temperature and solar radiation observations are compared (Table 7): T at the Airport is consistently lower than values in the city, especially at night and;  $K_{\downarrow}$  is higher on average especially in the morning hours. These differences are probably influenced by the local climate at the Airport, which is closer to the coast and may be affected by an afternoon sea-breeze in generally calm conditions. These types of differences might be expected of any station located ‘near’ the site of interest but subject to its own local influences; as such, using the observations from a WMO synoptic station (that might be expected to record the background climate) to force SUEWS is a good test of its robustness.

The hourly observed and simulated fluxes for June 2010 for both sites are presented in Fig. 2. The diurnal cycle at the urban site shows that most of the available energy ( $Q^*$ ) is partitioned into sensible heat, either as storage in the fabric ( $\Delta Q_S$ ) or as turbulent exchange with the atmosphere ( $Q_H$ ); relatively little is expended as evaporation ( $Q_E$ ), about 10% ( $25 \text{ W m}^{-2}$ ) of  $Q^*$  around noon. Before mid-day it is  $\Delta Q_S$  that dominates but  $Q_H$  is the largest non-radiative flux after noon. At the suburban site, the same basic pattern is present but  $Q_E$  is larger, reaching values of  $60 \text{ W m}^{-2}$  in early afternoon about one-third the magnitude of  $Q_H$ . The difference in patterns between the sites reflects their respective vegetated fractions.

Overall, SUEWS reproduces the diurnal cycle and shows good agreement with the observations at both locations, even when the model is run using standard meteorological data and urban parameters derived from the LCZ dataset, rather than the site specific data (Mode 3). Table 8 summarises the relative differences in hourly RMSE and MFB in terms of changing the land cover and meteorological forcing data. The run with optimal model inputs (Mode 1) uses measured values of  $K_{\downarrow}$  and  $L_{\downarrow}$  are provided by the observation platforms so not surprisingly  $Q^*$  is simulated closely at both sites (RMSE  $\approx 10 \text{ W m}^{-2}$  with little bias). The error for  $K_{\uparrow}$  is 3.5 and  $20.2 \text{ W m}^{-2}$  at the urban and suburban sites, respectively. Noticeably the bias and error in the simulation at the suburban site (MFB = 0.55)

**Table 6**

Daily rainfall receipt at Dublin Airport (RA) and the difference recorded at the urban ( $\Delta R_{A-U}$ ) and suburban ( $\Delta R_{A-S}$ ) flux sites.

Day	RA (mm)	$\Delta R_{A-U}$	$\Delta R_{A-S}$
June 1	14.20	−6.20	−8.20
June 7	7.80	−1.80	−6.20
June 8	15.20	7.40	.60
June 9	1.00	−.60	−.60
June 10	.20	.00	.20
June 14	11.80	5.60	1.40
June 27	2.70	1.70	1.10
June 28	.00	−1.60	−.20
June 29	.70	.70	.50
Total	53.6	5.2	−11.4

**Table 7**

Mean hourly wind speed ( $V_A$ ), air temperature ( $T_A$ ), and shortwave radiation receipt ( $K_{\downarrow A}$ ) at Dublin Airport and the differences ( $\Delta$ ) recorded at the urban (u) and suburban (s) flux sites.

Hour	$V_A$	$\Delta V_{A-U}$	$\Delta V_{A-S}$	$T_A$	$\Delta T_{A-U}$	$\Delta T_{A-S}$	$K_{\downarrow A}$	$\Delta K_{\downarrow A-U}$	$\Delta K_{\downarrow A-S}$
0	1.70	-0.40	-0.50	11.37	-4.43	-5.03	.0	.0	.0
1	1.83	-0.31	-0.39	11.20	-4.15	-4.63	.0	.0	.0
2	1.81	-0.29	-0.40	10.70	-4.15	-4.70	.0	.0	.0
3	1.84	-0.33	-0.42	10.46	-4.02	-4.81	.0	.0	.0
4	1.74	-0.25	-0.54	10.61	-3.75	-4.79	2.1	1.7	1.7
5	1.63	-0.35	-0.50	11.32	-3.15	-4.36	38.7	11.6	7.8
6	1.82	-0.18	-0.48	12.36	-2.49	-3.94	108.8	20.7	12.7
7	2.05	-0.21	-0.62	13.59	-1.96	-3.15	194.9	30.1	9.1
8	2.25	-0.33	-0.62	14.58	-1.86	-2.70	311.6	43.1	9.8
9	2.35	-0.42	-0.83	15.35	-1.48	-2.45	385.6	22.4	-3.5
10	2.43	-0.54	-0.76	16.20	-1.30	-2.10	487.4	-2.6	20.78
11	2.49	-0.46	-0.78	16.71	-1.30	-1.83	569.1	60.5	37.8
12	2.57	-0.49	-0.82	17.03	-1.44	-1.84	546.9	32.2	57.9
13	2.58	-0.83	-1.06	17.47	-1.30	-1.53	559.4	27.6	43.8
14	2.55	-0.83	-1.30	17.63	-1.35	-1.59	524.4	-6.7	12.8
15	2.59	-0.79	-1.29	17.73	-1.56	-1.55	460.3	-29.1	28.9
16	2.69	-0.72	-1.17	17.80	-1.56	-1.60	388.2	-30.9	-21.3
17	2.58	-0.69	-1.28	17.64	-1.72	-1.74	332.4	-7.7	-1.7
18	2.45	-0.66	-1.07	17.20	-2.18	-2.12	229.1	-4.0	-17.0
19	2.38	-0.52	-0.94	16.62	-2.54	-2.49	116.8	-16.2	-12.1
20	2.13	-0.42	-0.75	15.61	-3.22	-3.16	40.1	-4.1	-4.8
21	1.92	-0.22	-0.58	14.21	-4.10	-3.94	1.9	-1.1	-1.0
22	1.86	-0.37	-0.53	13.07	-4.17	-4.46	.0	.0	.0
23	1.73	-0.38	-0.51	12.34	-4.28	-4.56	.0	.0	.0
Mean	2.17	-0.46	-0.76	14.53	-2.64	-3.13	220.7	6.1	7.6
St. Dev	0.98	0.79	0.87	3.60	1.64	1.97	255.5	94.6	76.9
Skewness	0.18	-0.15	0.64	-0.18	-0.66	-1.05	1.00	0.20	1.08
Median	2.22	-0.44	-0.79	14.60	-2.40	-2.77	107.0	0	0
Quartile 25	1.39	-0.93	-1.28	12.00	-3.50	-3.80	0	-9.1	-9.5
Quartile 75	2.78	0.01	-0.27	17.40	-1.50	-1.98	378.5	21.8	14.6

indicates persistent overestimation by SUEWS; this is not unexpected given the nature of the urban surface directly below the net radiometer at the suburban site discussed earlier, which results in a lower albedo than expected. The RMSE values for  $L_{\uparrow}$  are 30 and 20  $W m^{-2}$  at the urban and suburban sites but the MFB values are close to zero. The errors in the non-radiative terms are 15 (19), 15 (17), 31 (27)  $W m^{-2}$  for  $Q_H$ ,  $Q_E$  and  $\Delta Q_S$ , respectively for the urban and suburban sites (the latter in parentheses). The  $Q_E$  term is overestimated at both sites (more so at the urban site where little evaporation was measured) but the overestimate in  $\Delta Q_S$  at the suburban site is a distinguishable feature.

Running SUEWS in Mode 2 changes the source of meteorological input data, which are no longer collected *in situ* with the non-radiative flux terms. In addition,  $L_{\downarrow}$  is now estimated from temperature and relative humidity (Loridan et al., 2011). The effect of these changes on the radiative terms is to introduce an error into  $K_{\downarrow}$  of about 23 (25)  $W m^{-2}$  and into  $L_{\downarrow}$  of about 7 (7)  $W m^{-2}$ , but no mean bias. The effect can be seen in the diurnal curve of  $Q^*$  (Fig. 2b), which is lower in the daytime by about 20  $W m^{-2}$  near noon and higher at night-time (less negative). However, change in RMSE is largest for  $Q^*$  at 15 (10)  $W m^{-2}$  but as  $Q^*$  is the largest component in the energy budget, this increase is not substantial. The patterns of the non-radiative terms are broadly consistent with the observations. The changes in the hourly RMSE values for the non-radiative fluxes at both sites are not large ( $\pm 5 W m^{-2}$ );  $\Delta Q_S$  and  $Q_E$  are smaller but  $Q_H$  is larger. However these changes do affect the bias; the MFB generally increases in magnitude and, in the case of  $Q_E$  at the urban site, the sign reverses. However, the magnitude of  $Q_E$  at this site is very small so it is especially sensitive. Running SUEWS in Mode 3 by using the typical LCZ values (Table 5) has a minor additional impact; RMSE values changed from between 2 and 6  $W m^{-2}$  at both sites. The additional error introduced to the non-radiative terms is relatively small, increasing RMSE values by about 6  $W m^{-2}$ .

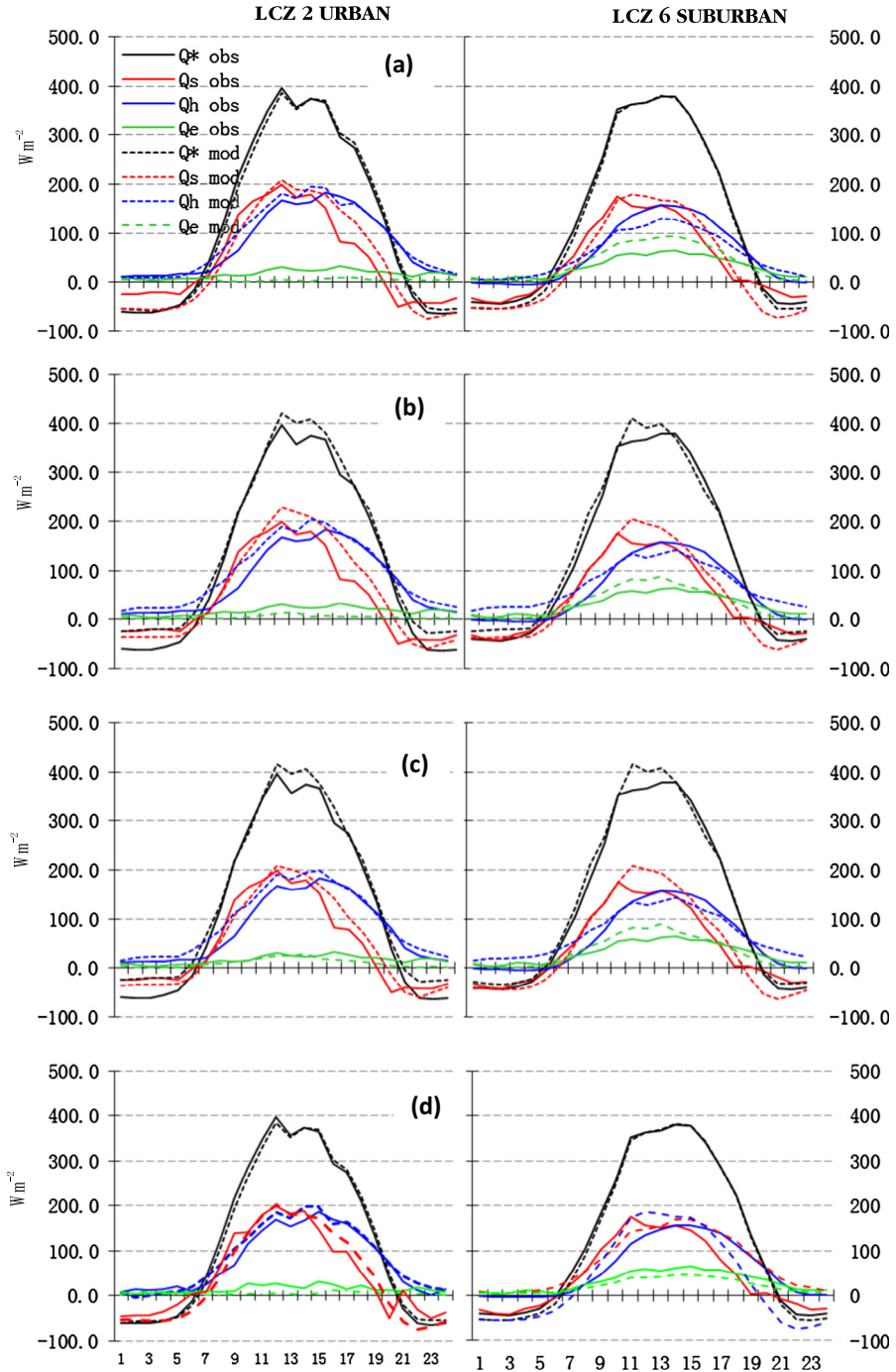


**Fig. 2.** Average hourly energy fluxes (measured and simulated) in  $W m^{-2}$  for June 2010. The graphs on the left refer to the urban site and those on the right refer to the suburban site. The rows (a–d) show simulations when SUEWS is run in different modes (a: Flux Forcing (FF) with Site Specific (SS) land cover (Mode 1), b: Synoptic Forcing (SF) with SS land cover (Mode ...), c: SF with LCZ land cover d: FF with LCZ land cover). See text for details. X-axis is local time.

**Table 8**

Root mean square error (RMSE) and Mean Fractional Bias (MFB) and bias direction change for each energy budget term based on hourly fluxes for June 2010. The top is urban (LCZ2 site) bottom is suburban (LCZ6 site). RMSE values are in  $\text{W m}^{-2}$ . Negative values denote a reduction in RMSE (i.e. model improvement) whereas positive values denote an increase in RMSE. Negative values in MFB denote a decrease in absolute bias, positive denotes an increase in absolute bias. MFB directional changes denote if the model switches (>) from over (+) to under (-) prediction or if the direction of the bias remains the same (=).

	Degrading meteorological forcing			Degrading land cover		
	RMSE	MFB	MFB direction	RMSE	MFB	MFB direction
<i>LCZ2</i>						
$Q^*$	16.5	0.17	=	-0.9	-0.01	=
$K\downarrow$	-	-	-	0	0	=
$K\uparrow$	3	0.03	=	2.2	0.06	=
$L\downarrow$	-	-	-	0	0	=
$L\uparrow$	-11.7	-0.03	=	-0.1	0	=
$\Delta Q_S$	-3.5	0.26	- > +	-6	-0.13	=
$Q_H$	6.1	0.09	=	-1.2	-0.01	=
$Q_E$	-0.3	-0.15	=	-5.6	0.72	=
<i>LCZ6</i>						
$Q^*$	9.7	0.14	- > +	-1.7	-0.01	=
$K\downarrow$	-	-	-	0	0	=
$K\uparrow$	4.7	0.02	=	-1.5	-0.02	=
$L\downarrow$	-	-	-	0	0	=
$L\uparrow$	3.5	-0.03	=	-0.2	0	=
$\Delta Q_S$	-4.1	0.28	- > +	2.5	-0.02	=
$Q_H$	4.4	0.2	- > +	-2.3	-0.01	=
$Q_E$	-4.5	-0.14	=	0.1	0	=

Running the model in Mode 3 has little effect. Similarly the difference between Modes 1 and 4 where the difference is in land cover representation utilising meteorology from the flux sites were negligible; at both sites the radiative RMSE difference was  $<1.0 \text{ W m}^{-2}$  and difference in RMSE for the turbulent fluxes was  $<2.0 \text{ W m}^{-2}$ .

Overall, the difference in the urban environments around each site is captured by the model; this is clearest in the  $Q_E$  differences between sites that correspond with their respective vegetated fractions. Most of the errors associated with using sub-optimum input data is associated with the use of off-site meteorological inputs that affected the incoming radiative terms ( $K\downarrow$  and  $L\downarrow$ ) most directly. However, the suburban site consistent overestimation of  $K\uparrow$  suggests strongly that there is a discrepancy between the site-specific albedo and that of the neighbourhood generally. The diurnal and daily patterns of exchanges are simulated by SUEWS but there are obvious issues with simulating  $Q_E$  at both sites. The difference in running the model in Mode 2 and Mode 3 is small, which suggests that the use of off-site meteorological input data is of greater significance than the use of the LCZ-based evaluation of urban land-cover.

#### 4.2. Daily fluxes comparison

Table 9 shows the average daily RMSE scores for each of the flux terms by month and by Mode for the urban and suburban observation sites. Thus, for example, for the entire period at the urban site, the average RMSE values for SUEWS run in Mode 1 are: 21.7 ( $\text{RMSE}_{Q^*}$ ); 25.3 ( $\text{RMSE}_{\Delta Q_S}$ ); 23.9 ( $\text{RMSE}_{Q_H}$ ) and;  $16.7 \text{ W m}^{-2}$  ( $\text{RMSE}_{Q_E}$ ). The total ( $\Sigma_{\text{RMSE}}$ ) error ( $87.6 \text{ W m}^{-2}$ ) is the sum of the individual flux error terms and is a useful measure of overall model performance. For the optimal case (Mode 1) the  $\Sigma_{\text{RMSE}}$  for the urban site is  $89.1 \text{ W m}^{-2}$  while that for the suburban site is  $83.3 \text{ W m}^{-2}$ . The overall performance is also presented in Fig. 3.

Changing the land-cover and meteorological data input data had little impact on the overall performance of the model. For the urban site,  $\Sigma_{\text{RMSE}}$  values are 90.3, 82.7 and  $92.6 \text{ W m}^{-2}$  for Modes 2, 3 and 4, respectively. Similarly, for the suburban site, the differences compared to Mode 1 are all  $<5.5 \text{ W m}^{-2}$ . The best performance (i.e. the lowest  $\Sigma_{\text{RMSE}}$ ) was found in Mode 1 for the LCZ6 site



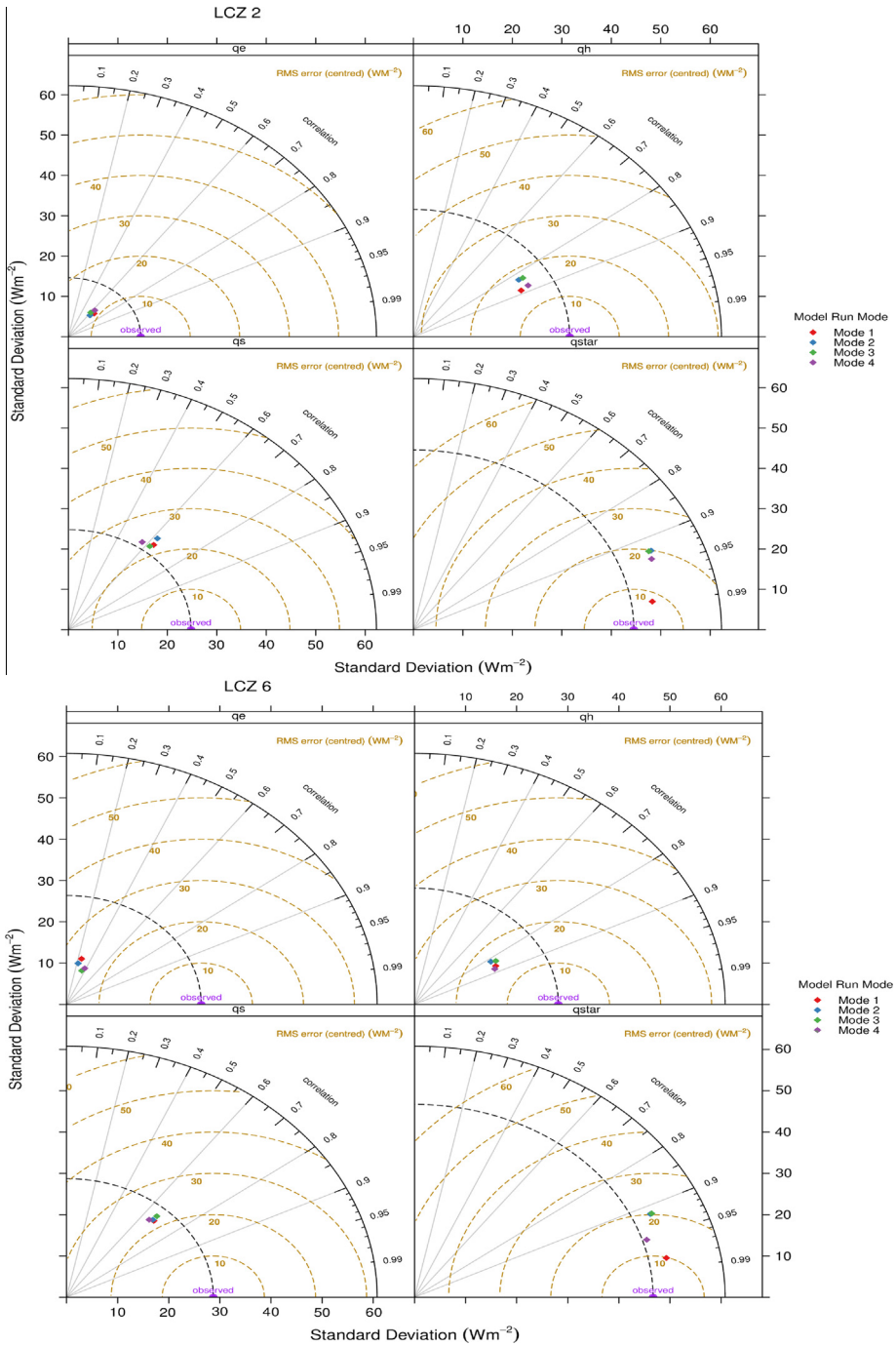


**Fig. 3.** Taylor diagrams for Mode 1–4 based on daily values of  $Q_E$ ,  $Q_H$ ,  $\Delta Q_S$  and  $Q_*$  for LCZ2 (top) and LCZ6 (bottom) Mode 1 uses High-Resolution land cover (HRLC) and forcing data obtained at the flux sites, Mode 2 uses HRLC and forcing data obtained off-site by a standard weather station. Mode 3 uses LCZ derived land cover fractions and off-site forcing data. Finally Mode 4 uses LCZ land cover and forcing data obtained at the flux sites.

and Mode 3 for the LCZ2 site. The worst performance (highest  $\Sigma_{\text{RMSE}}$ ) was found in Mode 3 and Mode 4 for the LCZ6 and LCZ2 site respectively. The difference between the best and worst performances was  $5.5 \text{ W m}^{-2}$  for the LCZ6 site and approximately double this ( $9.9 \text{ W m}^{-2}$ ) for the LCZ2 site. The range of RMSE across all fluxes was  $<30 \text{ W m}^{-2}$  for the LCZ2 site in all Modes and was  $<40 \text{ W m}^{-2}$  for the LCZ6 site in all modes.

Examining the individual flux performance more closely looking firstly at  $Q^*$ ; the lowest mean RMSE value was  $22.1 \text{ W m}^{-2}$  for the LCZ2 site in Mode 1 and  $15.6 \text{ W m}^{-2}$  for the LCZ6 site, also in Mode 1. The highest mean RMSE value for  $Q^*$  was  $29.1 \text{ W m}^{-2}$  in Mode 4 for the LCZ2 site and  $20.1 \text{ W m}^{-2}$  for the LCZ6 site in Mode 3. Given the relatively large magnitude of this flux, this may be regarded as negligible. For the turbulent fluxes ( $Q_H$  and  $Q_E$ ), the lowest mean RMSE value for  $Q_H$  and  $Q_E$  (respectively) was  $23.0 \text{ W m}^{-2}$  (Mode 3) and  $13.9 \text{ W m}^{-2}$  (Mode 4) for the LCZ2 site and  $20.4 \text{ W m}^{-2}$  (Mode 2) and  $23.6 \text{ W m}^{-2}$  (Mode 4) for the LCZ6 site.  $\Delta Q_S$  mean RMSE ranged between a minimum of  $22.3 \text{ W m}^{-2}$  (in Mode 2) and maximum of  $26.0 \text{ W m}^{-2}$  (in Mode 1) for the LCZ2 site and a minimum of  $21.1 \text{ W m}^{-2}$  (in Mode 1) and maximum of  $23.2 \text{ W m}^{-2}$  (in Mode 3) for the LCZ6 site.

In general, the model was consistently biased (MFB) across all months and all Modes. The model exhibited a minor positive bias ( $<0.5$ ) for both  $Q^*$  and  $Q_H$  for both sites in all Modes. For both sites,  $\Delta Q_S$  exhibited a strong negative bias ( $<-1.0$ ) in all Modes, whereas  $Q_E$  varied between a strong negative bias for the LCZ2 site and a minor negative bias for the LCZ6 site (see Table 10).

#### 4.3. Impact of meteorological forcing data on performance

Comparing model performance between Mode 1 to Mode 2 and Mode 4 to Mode 3 reveals an insight into the impact of meteorological forcing data when utilising the same quality of land cover information. This is summarised by Table 11. For the high-resolution land cover cases, utilising off-site meteorological data to force SUEWS decreased the performance (i.e. increase RMSE) of  $Q^*$  by  $1.5 \text{ W m}^{-2}$  for the LCZ2 site and by  $4.2 \text{ W m}^{-2}$  for the LCZ6 site. This decrease in performance did not cascade through all turbulent fluxes, model performance increased (i.e. decreased RMSE) marginally for  $Q_H$  and  $\Delta Q_S$  (by  $0.4$  and  $0.3 \text{ W m}^{-2}$  respectively) for the LCZ2 site whereas RMSE was increased by  $0.7 \text{ W m}^{-2}$  for  $Q_E$ . For the LCZ6 site, RMSE for  $Q_H$  decreased by  $1.8 \text{ W m}^{-2}$  and by  $0.3 \text{ W m}^{-2}$  for  $Q_E$  when utilising off-site meteorology,  $\Delta Q_S$  RMSE increased by  $2.0 \text{ W m}^{-2}$ . Accounting for performance increases and decreases, the mean RMSE difference taken across all the turbulent fluxes for both sites is  $0 \text{ W m}^{-2}$ . By including off-site meteorological data for the Modes which utilised LCZ land cover information, RMSE decreased by  $6.5$ ,  $3.4$  and  $1.6 \text{ W m}^{-2}$  for  $Q^*$ ,  $\Delta Q_S$  and  $Q_H$  respectively for the LCZ2 site. RMSE for  $Q_E$  increased by  $0.8 \text{ W m}^{-2}$ . For the LCZ6 site, RMSE increased by  $2.7$ ,  $1.0$  and  $0.2 \text{ W m}^{-2}$  for  $Q^*$ ,  $\Delta Q_S$  and  $Q_E$  respectively. RMSE for  $Q_H$  decreased by  $1.4 \text{ W m}^{-2}$ . MFB direction did not change between Modes.

The impact of meteorological forcing data had a larger impact on  $\Delta Q_S$  and  $Q_H$  than for  $Q_E$ . This was also borne out during our OFAT analysis over a grid with equal distribution of urban, paved, and vegetated and tree cover. Differences in  $K\downarrow$  had the largest impact on simulated turbulent fluxes, followed by temperature. The model was insensitive to variation in wind speed ( $V$ ) – see Fig. 4. The mean difference in daily RMSE across both sites for all fluxes and all months when using off-site meteorological data in place of on-site was  $\sim 0.7 \text{ W m}^{-2}$ .

#### 4.4. Impact of land cover on performance

Table 11 also presents the impact on relative performance when land cover data are changed. Using on site meteorological forcing data (Mode 1) and subsequently utilising LCZ for land cover (Mode 4) had a larger impact on the performance of  $Q^*$  for both sites. For the LCZ2 site, RMSE increased by  $7.2 \text{ W m}^{-2}$  (to  $28.9 \text{ W m}^{-2}$ ) for  $Q^*$  when employing the LCZ data. Again, given the large magnitude of this flux this is rather small. As for the turbulent fluxes,  $Q_H$  RMSE increased by  $<1 \text{ W m}^{-2}$  ( $0.7 \text{ W m}^{-2}$ ),  $Q_E$  decreased (i.e. improved model performance) by  $3.3 \text{ W m}^{-2}$  and  $\Delta Q_S$  increased by  $0.4 \text{ W m}^{-2}$ . For the LCZ6 site, again comparing Modes which utilised on-site meteorological forcing, RMSE for  $Q^*$  increased by  $1.6 \text{ W m}^{-2}$  when utilising the LCZ, by  $1.5 \text{ W m}^{-2}$  for  $Q_H$ ,  $0.8 \text{ W m}^{-2}$  for  $\Delta Q_S$  and decreased by  $1.2 \text{ W m}^{-2}$  for  $Q_E$ . There was no impact on model bias between Modes 1 and

**Table 10**

Mean Fractional Bias (MFB) results for urban (LCZ2) site and suburban (LCZ6) site April–October. Mode 1 uses High-Resolution land cover (HRLC) and forcing data obtained at the flux sites. Mode 2 uses HRLC and forcing data obtained off-site by a standard weather station. Mode 3 uses LCZ derived land cover fractions and off-site forcing data. Finally Mode 4 uses LCZ land cover and forcing data obtained at the flux sites.

	LCZ2								LCZ6							
	April	May	June	July	August	September	October	Mean	April	May	June	July	August	September	October	Mean
$Q^*$																
Mode1	0.22	0.20	0.20	0.16	0.20	0.26	0.27	0.21	0.12	0.16	0.11	0.11	0.10	0.15	0.02	0.11
Mode2	0.18	0.13	0.17	0.05	0.16	0.15	0.02	0.12	-0.03	0.04	0.08	-0.07	0.05	0.00	-0.02	0.01
Mode3	0.16	0.12	0.16	0.04	0.15	0.14	0.00	0.11	-0.02	0.04	0.08	-0.06	0.05	0.01	-0.02	0.01
Mode4	0.31	0.24	0.19	0.21	0.20	0.28	0.05	0.21	0.02	0.11	0.11	0.05	0.09	0.12	0.25	0.11
$\Delta Q_S$																
Mode1	0.37	0.49	0.47	0.72	0.59	0.24	-1.12	0.25	-0.27	-0.06	-0.09	0.22	0.11	0.18	-3.60	-0.50
Mode2	0.30	0.39	0.43	0.57	0.55	-0.04	-1.63	0.08	-0.55	-0.26	-0.14	-0.08	0.02	-0.35	-3.95	-0.76
Mode3	0.14	0.26	0.31	0.43	0.41	-0.30	-1.41	-0.02	-0.49	-0.20	-0.08	-0.02	0.08	-0.23	-3.82	-0.68
Mode4	0.39	0.44	0.35	0.68	0.49	0.10	-1.97	0.07	-0.40	-0.08	-0.04	0.18	0.14	0.19	-2.16	-0.31
$Q_E$																
Mode1	-1.17	-1.29	-1.32	-1.19	-0.97	-0.88	-1.06	-1.13	0.44	0.04	0.19	-0.26	-0.09	-0.54	-0.18	-0.06
Mode2	-1.21	-1.39	-1.42	-1.21	-1.03	-1.02	-1.22	-1.22	0.35	0.04	0.15	-0.27	-0.13	-0.62	-0.33	-0.12
Mode3	-0.56	-0.85	-0.68	-0.75	-0.55	-0.69	-0.89	-0.71	0.15	-0.15	-0.01	-0.43	-0.29	-0.74	-0.48	-0.28
Mode4	-0.41	-0.76	-0.56	-0.74	-0.47	-0.55	-0.68	-0.59	0.23	-0.14	0.03	-0.47	-0.28	-0.67	-0.52	-0.26
$Q_H$																
Mode1	0.27	0.21	0.19	0.15	0.21	0.47	0.74	0.32	0.22	0.32	0.15	0.23	0.20	0.84	1.17	0.45
Mode2	0.25	0.17	0.18	0.08	0.20	0.44	0.66	0.28	0.14	0.21	0.15	0.07	0.16	0.79	1.18	0.38
Mode3	0.25	0.18	0.17	0.06	0.18	0.41	0.65	0.27	0.20	0.26	0.20	0.13	0.23	0.84	1.23	0.44
Mode4	0.33	0.25	0.18	0.19	0.20	0.46	0.65	0.32	0.20	0.32	0.21	0.25	0.26	0.88	1.29	0.49

**Table 11**

The impact of degrading meteorological forcing data (top Mode 1 versus Mode 2) and land cover (bottom, Mode 1 versus Mode 4) on daily RMSE values for the LCZ2 and LCZ6 site. Values are in  $W m^{-2}$ , negative values denote a reduction in RMSE (i.e. model improvement) whereas positive values denote an increase in RMSE.

	April	May	June	July	August	September	October
<i>Impact of degrading forcing data on daily RMSE values</i>							
LCZ2							
$Q^*$	-1.3	0.9	1.8	-2.7	6.0	-0.4	6.3
$\Delta Q_S$	-3.1	-1.6	-1.2	-4.4	-1.0	0.8	7.9
$Q_H$	-0.1	-0.5	1.8	0.0	2.7	-1.5	-4.5
$Q_E$	0.2	0.9	0.8	0.1	0.3	2.1	0.2
LCZ6							
$Q^*$	-3.0	0.4	8.9	9.1	4.8	1.8	7.7
$\Delta Q_S$	5.4	3.5	4.0	3.3	-1.4	1.1	-1.6
$Q_H$	-3.2	-4.1	0.8	-3.1	-0.6	-2.1	-0.4
$Q_E$	-2.6	-0.9	-0.7	-2.6	1.5	2.6	0.6
<i>Impact of degrading land cover quality on daily RMSE values</i>							
LCZ2							
$Q^*$	-1.0	-1.0	-1.4	-0.5	-0.9	-0.6	-0.2
$\Delta Q_S$	-2.3	-3.3	-5.4	-3.9	-3.9	-0.5	0.8
$Q_H$	0.2	0.1	-0.4	-1.1	-0.6	-1.4	-0.6
$Q_E$	-2.8	-3.1	-4.2	-4.7	-3.8	-2.3	-1.1
LCZ6							
$Q^*$	0.1	-0.3	-0.4	0.1	-0.2	-0.2	0.0
$\Delta Q_S$	1.2	0.6	0.1	-0.1	-0.1	0.1	0.3
$Q_H$	-2.9	-2.3	-2.1	0.0	-2.1	-2.1	-2.7
$Q_E$	3.6	0.6	3.1	-1.3	-0.5	-1.1	0.6

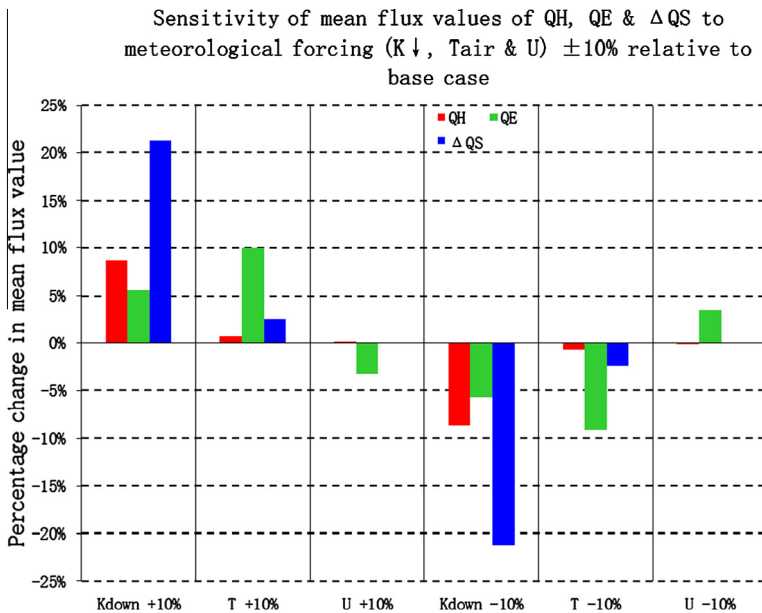


**Fig. 4.** One-Factor-A-Time (OFAT) sensitivity analysis of forcing data impact on SUEWS simulation of turbulent fluxes. A base case (168 h) was established using data derived from loess curve (least square) of required meteorological forcing (see Table 3). We then perturbed  $K \downarrow$ ,  $T$  and  $u \pm 10\%$  of the base case. Presented above is the % difference in the mean value (over the 168 h) of  $Q_H$ ,  $Q_E$  and  $\Delta Q_S$ . It should be noted that RH was not modified when perturbing  $T$ , hence the apparent increase/decrease in  $Q_E$ .

4 and Modes 2 and 3 with the exception of  $\Delta Q_S$  for the LCZ2 site, where the model exhibited a minor positive MFB (over-prediction) of heat storage in Mode 1 (0.25), and a close to zero ( $-0.07$ ) negative MFB in Mode 4.

Examining the impact of land cover input when off-site meteorological forcing data was utilised (i.e. comparing Mode 2 and Mode 3), often a net improvement in model performance was observed when utilising the LCZ data. However as with the performance changes arising between the on-site meteorological Modes, the changes here can be summarised as marginal improvements. Utilising the LCZ for the LCZ2 site improved model performance by  $0.8 \text{ W m}^{-2}$  for  $Q^*$ ,  $2.6 \text{ W m}^{-2}$  for  $\Delta Q_S$ ,  $0.5 \text{ W m}^{-2}$  for  $Q_H$  and  $3.3 \text{ W m}^{-2}$  for  $Q_E$ . For the LCZ6 site, RMSE increased by  $0.1 \text{ W m}^{-2}$  for  $Q^*$  and by  $2.0 \text{ W m}^{-2}$  for  $Q_H$ . RMSE decreased by  $0.3 \text{ W m}^{-2}$  for  $\Delta Q_S$  and  $0.7 \text{ W m}^{-2}$  for  $Q_E$ . As with the on-site Modes, MFB did not change direction when utilising the LCZ for land cover. The mean difference in daily RMSE across both sites for all fluxes and all months when using LCZ land cover in place of high-resolution land cover was  $\sim -1 \text{ W m}^{-2}$ .

## 5. Discussion

### 5.1. SUEWS accuracy and measurement errors

It would be incorrect to attribute the difference between 'best case' (Mode 1) simulations by SUEWS and site observations (i.e. performance) to model errors only. The fractional coverage values used by the model represent the surrounding neighbourhood but the observation site may still be exposed to atypical surface characteristics. This appears to be the case for the suburban site here where  $K\uparrow$  is consistently overestimated owing to the exposure of the radiometer to low albedo surfaces directly below the instrument. As a result, the magnitude of  $\Delta Q_S$  computed from observations (Eq. (3)) for this site is probably an overestimation for the neighbourhood; this partly explains the differences between observations and simulations. In this regard it is interesting to note the simulated values for  $K\uparrow$  at the LCZ6 site is likely more realistic representation for the surrounding area than observed  $K\uparrow$ .

The Objective Hysteresis Model (Grimmond et al., 1991; Grimmond and Oke, 1999) (OHM) which is the sub model within SUEWS that directly relates to  $\Delta Q_S$  in all modes overestimates storage relative to the observational data. It is also important to consider the energy balance closure problem (see for example: Kanda et al., 2004; Kawai and Kanda, 2010; Foken, 2008) which relates to the underestimation of the turbulent fluxes in observational data. The observational data here are corrected following Webb et al. (1980), which results in increasing  $Q_E$  and decreasing  $Q_H$  and somewhat reducing the residual. Nevertheless, as per (Eq. (3)) the likelihood is that  $\Delta Q_S$  is exaggerated by the observational data. This especially important to highlight if examining the nocturnal withdrawal of heat from the substrate leading to (for instance) the UHI effect.

Overall the daily and hourly flux patterns simulated by SUEWS at both urban and suburban sites show good agreement with the observed fluxes. When provided with observed  $K\downarrow$  and  $L\downarrow$ , SUEWS distinguishes between the two sites on the basis of the non-radiative terms: the model results under(over)-estimated  $Q_E$  and over(under)-estimated  $Q_H$  and  $\Delta Q_S$  at the urban (suburban) site. The role of  $Q_E$  appears to be critical as its magnitude is managed by the availability of water and plant growth. The former here is expressed in terms of the soil moisture content, which is set to field capacity. The latter is a function of the vegetative fraction and leaf area fraction. Looking at the daily and hourly simulations of SUEWS (Figs. 2 and Fig. 4) it seems that the description of plant growth (canopy cover, tree species, etc.) may be critical, which is consistent with Grimmond et al. (2011). In addition, the model has difficulty in responding quickly to precipitation events when rapid increases in the magnitude of  $Q_E$  are observed.

### 5.2. Impact of non-local meteorological and LCZ data

Using off-site meteorological observations of  $K\downarrow$  and of temperature and relative humidity to estimate  $L\downarrow$  increases the difference between the observations at the site and SUEWS simulations but nevertheless the model still shows itself capable of discriminating between neighbourhood types. The use

of LCZs to capture information about the type of neighbourhood in which the observation site is located has a marginal effect. The differences in meteorology between the off-site and on-site stations are highlighted in Tables 6 and 7. Such differences may be expected of most cities where off-site meteorological stations conforming to WMO standards will likely record higher wind speeds (due to less friction), colder air temperatures (more evapotranspiration, less heat storage) and higher levels of precipitation. This was not the case for Dublin, where off-site recordings were cooler, but wind speeds were also lower. In order to verify this finding, additional situations comparing off-site and on-site data with respect to model performance are needed; we plan to undertake this in a subsequent paper.

Nevertheless the differences between Modes were relatively minor, moreover the model showed itself to be relatively insensitive to such differences. This suggests that SUEWS may be used to discriminate between different urban neighbourhoods by sampling from within LCZs and obtaining land-cover fractions and forcing the model with off-site meteorology.

To test this proposition, we ran SUEWS in Mode 3 for four additional LCZ types present in the Dublin area to represent other urban and non-urban covers. These include: compact low-rise (LCZ3) for inner-city residential area; large low-rise (LCZ8) for warehouse areas found at the edge of the city; low plant cover (LCZ104) for grass-covered landscape and; closed trees (LCZ101) for forested areas. Each LCZ area was sampled (Table 5) as before and fractional areas were calculated. Fig. 5 shows the mean value for each non-radiative flux for June 2010 for each LCZ, including the urban and suburban LCZs used in the body of this study. The values are presented as a difference from the overall mean calculated for the six LCZs; thus,  $Q_H$  for an LCZ is shown as the difference from the mean  $Q_H$  value for all LCZ. This highlights the partitioning of the UEB across different LCZs. The results make intuitive sense. Note that the LCZs with the highest combined fractions of buildings and impervious surface cover (LCZs 2, 3 and 8) exhibit above average values of  $Q_H$  and  $\Delta Q_S$ ; these areas store more sensible heat (higher surface temperatures) and heat the overlying atmosphere rather than evaporate water. Oppositely, the well vegetated suburbs and the natural land-covers partition available energy into  $Q_E$  rather than  $Q_H + \Delta Q_S$ .

Stewart and Oke (2012) speculate that energy partitioning zones are unlikely to coincide exactly with LCZs because similar flux densities can occur above canopy layers with distinctly different micro-scale structure, land cover, and thermal climate. The profiles for June presented in Fig. 5 illustrates this

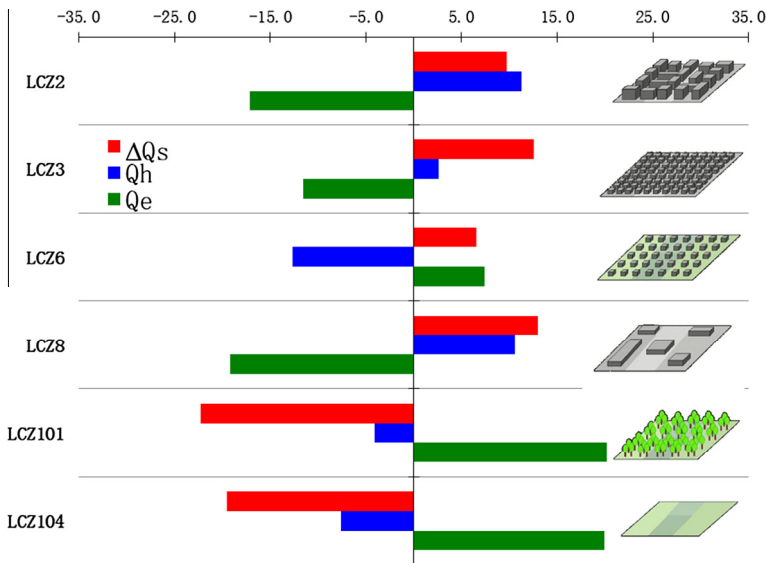


Fig. 5. Relative partitioning of turbulent fluxes at each LCZ site for June (2010) the mean value of  $Q_H$ ,  $Q_E$  and  $\Delta Q_S$  for each LCZ are subtracted from the group mean. X-axis is  $W m^{-2}$ . LCZ images reproduced from Stewart and Oke (2012).

problem, note for instance  $Q_H$  profiles for LCZ2 and LCZ3 vary by  $<10 \text{ W m}^{-2}$ . However, these data have been averaged in order to examine the signal for the entire month of June. Diurnal variations exhibited a higher degree of variation than the mean value for June; moreover energy partitioning for specific boundary layer conditions (for instance high pressure, little wind, no precipitation) maybe of greater importance to one user than other, reinforcing the earlier point on the need for models to undergo extensive validation in differing circumstances and conditions.

Nevertheless the LCZ classification provides a useful sampling framework for the derivation of the land-cover fractions needed to run SUEWS. This proved an efficient and effective means of gathering LCZ data here and provided a means of extending the model to other parts of the city. However, using the LCZ for this, does introduce a degree of subjectivity into data acquisition as there is no objective means of delineating a spatially contiguous LCZ type for individual cities. Ultimately users should avoid simply employing the mid-range of values which are provided for each LCZ type to derive land cover and/or anthropogenic parameters. For example within Dublin, the fractional coverage of buildings for LCZ2 was at the lowest end of the provided LCZ range, while impervious fraction was at the highest end of the range. Meaning the generic LCZ2 mid-range would not accurately describe this LCZ in Dublin.

While the scheme allows for sub-categories within each LCZ category, for example: dense compact midrise/open compact midrise etc. the development of mean values for the objective discrimination between LCZ types (rather than within a single LCZ class) would allow for a more consistent usage and allow comparisons between LCZs across cities and climate types.

## 6. Summary and conclusion

The input needs of urban atmospheric models present a barrier to their application in many places where information on the physical characteristics and urban energy budgets are sparse. Here we examined a means to overcome this obstacle by presenting a modelling framework that draws upon basic descriptions of the characteristics of city (Local Climate Zones) and tested this with a moderately complex urban energy budget model (SUEWS) which was forced with meteorological data obtained from outside the urban area. The use of forcing data obtained from a WMO synoptic station in lieu of data obtained from flux observation platforms in SUEWS resulted in a slight reduction in *relative* model performance against two urban types. The use of parameters that represent LCZ types however had no significant impact in this case study.

Our primary aim was to demonstrate/validate a modelling approach that could apply a moderately complex UEB model utilising readily available data beyond one or two instrumented sites. Based on the results from Dublin, SUEWS appears capable of being run with easily obtainable meteorological and land cover data with no significant impact on model performance across multiple seasons.

## Acknowledgments

We wish to acknowledge the helpful comments of the anonymous reviewers. The authors also wish to acknowledge the kind advice of the SUEWS model developers while carrying out the model runs for all cases. The detailed land cover data for Dublin is provided by the OSI. The Flux sites are funded by the Higher Education Authority of Ireland. This work is funded by the Doctoral Teaching Fellowship, Maynooth University, supported through HEA Ireland.

## References

- Alexander, P.J., Mills, G., 2014. Local climate classification and Dublin's urban heat island. *Atmosphere* 5 (4), 755–777.
- Arnfield, J., 2003. Two decades of urban climate research: a review of turbulence, exchanges of energy and water, and the urban heat island. *Int. J. Climatol.* 23 (1), 1–26.
- Bechtel, B., Alexander, P.J., Böhner, J., Ching, J., Conrad, O., Feddema, J., Mills, G., See, L., Stewart, I., 2015. Mapping local climate zones for a worldwide database of the form and function of cities. *ISPORS Int. J. Geo-Inf.* 4, 199–219.
- Breuste, J., 2004. Decision making, planning and design for the conservation of indigenous vegetation within urban development. *Landscape Urban Plan* 68 (1), 439–452.
- Chen, L., Ng, E., 2012. Outdoor thermal comfort and outdoor activities: a review of research in the past decade. *Cities* 29, 118–125.

- Ching, J., 2013. A perspective on urban canopy layer modeling for weather, climate and air quality applications. *Urban Climate* 3 (1), 13–39.
- Cleugh, H., Bui, E., Mitchell, V., Xu, J., Grimmond, C., Simon, D., 2005. Evapotranspiration in urban water balance models: a methodological framework. Canberra, Australia: International Congress on Modelling and Simulation (MODSIM05).
- Fenner, D., Meier, F., Scherer, D., Polze, A., 2014. Spatial and temporal air temperature variability in Berlin, Germany, during the years 2001–2010. *Urban Climate*.
- Foken, T., 2008. The energy balance closure problem: an overview. *Ecol. Appl.* 18 (6), 1351–1367.
- Griensven, A., Francos, A., Bauwens, W., 2002. Sensitivity analysis and auto-calibration of an integral dynamic model for river water quality. *Water Sci. Technol.* 45 (9), 325–332.
- Grimmond, C., Oke, T., 1991. An evaporation-interception model for urban areas. *Water Resour. Res.* 27 (7), 1739–1755.
- Grimmond, C., Oke, T., 1999. Heat storage in urban areas: local-scale observations and evaluation of a simple model. *J. Appl. Meteorol.* 38 (2), 922–940.
- Grimmond, C., Oke, T., 2002. Turbulent heat fluxes in urban areas: observations and a local-scale urban meteorological parameterization scheme (LUMPS). *J. Appl. Meteorol.* 41 (7), 792–810.
- Grimmond, C., Souch, C., 1994. Surface description for urban climate studies: a GIS based methodology. *Geocarto Int.* 1, 47–59.
- Grimmond, C., Blackett, M., Best, M., Barlow, J., Baik, J., Belcher, S., et al., 2010. The international urban energy balance models comparison project: first results from phase 1. *J. Appl. Meteorol. Climatol.* 49, 1268–1292.
- Grimmond, C., Blackett, M., Best, M., Barlow, J., Baik, J., Belcher, S., et al., 2011. Initial results from Phase 2 of the international urban energy balance model comparison. *Int. J. Climatol.* 31 (2), 244–272.
- Grimmond, C., Cleugh, H., Oke, T., 1991. An objective urban heat storage model and its comparison with other schemes. *Atmos. Environ. Part B: Urban Atmos.* 25 (3), 311–326.
- Hidalgo, J., Masson, V., Baklanov, A., Pigeon, G., Gimeno, L., 2008. Advances in urban climate modeling. *Ann. N. Y. Acad. Sci.* 1146, 354–374.
- IPCC, 2014. Climate change 2014: impacts, adaptation, and vulnerability. Part A: Global and sectoral aspects. In: Field, C.B., Barros, V.R., Dokken, D.J., Mach, K.J., Mastrandrea, M.D., Bilir, T.E., Chatterjee, M., Ebi, K.L., Estrada, Y.O., Genova, R.C., Girma, B., Kissel, E.S., Levy, A.N., MacCracken, S., Mastrandrea, P.R., White, L.L. (Eds.), *Contribution of Working Group II to the Fifth Assessment Report of the Intergovernmental Panel on Climate Change*. Cambridge University Press, Cambridge, United Kingdom and New York, NY, USA, p. 1132.
- Järvi, L., Grimmond, C., Christen, A., 2011. The surface urban energy and water balance scheme (SUEWS): evaluation in Los Angeles and Vancouver. *J. Hydrol.* 411 (3–4), 219–237.
- Kanda, M., Inagaki, A., Letzel, M.O., Raasch, S., Watanabe, T., 2004. LES study of the energy imbalance problem with eddy covariance fluxes. *Bound.-Layer Meteorol.* 110, 381–404.
- Kanda, M., Kawai, T., Kanega, M., Moriwaki, R., Narita, K., Hagishima, A., 2005. Simple energy balance model for regular building arrays. *Bound.-Layer Meteorol.* 116, 423–443.
- Kawai, T., Kanda, M., 2010. Urban energy balance obtained from the comprehensive outdoor scale model experiment. Part I: Basic features of the surface energy balance. *J. Appl. Meteorol. Climatol.* 49, 1360–1376.
- Keogh, S., Fealy, R., Mills, G., 2012. The energy budget of the urban surface: two locations in Dublin. *Irish Geogr.* 45 (1), 1–23.
- Kimura, F., Takahashi, S., 1991. The effects of land-use and anthropogenic heating on the surface temperature in the Tokyo metropolitan area: a numerical experiment. *Atmos. Environ.* 25B, 155–164.
- Kovács, A., Németh, Á., 2012. Tendencis and differences in human thermal comfort in distinct urban areas in Budapest, Hungary. *Acta Climatologica et Chorologica* 46, 115–124.
- Kusaka, H., Kimura, F., 2004. Thermal effects of urban canyon structure on the nocturnal heat island: numerical experiment using a mesoscale model coupled with an urban canopy model. *J. Am. Meteorol. Soc.* 43, 1899–1910.
- Lecante, F., Bouyer, J., Claverie, R., Pétrissans, M., 2014. Using local climate zone scheme for UHI assessment: evaluation of the method using mobile measurements. *Build. Environ.*
- Loridan, T., Grimmond, C., 2012. Multi-site evaluation of an urban land-surface model: intra-urban heterogeneity, seasonality and parameter complexity requirements. *Quart. J. Roy. Meteorol. Soc.* 138 (665), 1094–1113.
- Loridan, T., Grimmond, C., Grossman-Clarke, S., Chen, F., Tewari, M., Manning, K., et al., 2010. Trade-offs and responsiveness of the single-layer urban canopy parameterization in WRF: an offline evaluation using the MOSCEM optimization algorithm and field observations. *J. Roy. Meteorol. Soc.* 136, 997–1019.
- Loridan, T., Grimmond, C., Offerle, B., Young, D., Smith, T., Järvi, L., et al., 2011. Local-scale urban meteorological parameterization scheme (LUMPS): longwave radiation parameterization and seasonality-related developments. *J. Appl. Meteorol. Climatol.* 50 (1), 185–202.
- Martilli, A., Clappier, A., Rotach, M., 2002. An urban surface exchange parameterisation for mesoscale models. *Bound.-Layer Meteorol.* 104, 261–304.
- Masson, V., 2000. A physically-based scheme for the urban energy budget in atmospheric models. *Bound.-Layer Meteorol.* 94, 357–397.
- Middel, A., Brazel, A., Kaplan, S., Myint, S., 2012. Daytime cooling efficiency and diurnal energy balance in Phoenix, Arizona, USA. *Climate Res.* 54, 21–34.
- Mills, G., 1997. An urban canopy-layer climate model. *Theoret. Appl. Climatol.* 57, 229–244.
- Moonen, P., Defraeyne, T., Dores, V., Blocken, B., Carmeliet, J., 2012. Urban physics: effect of micro-climate on comfort, health and energy demand. *J. Front. Archit. Res.* 1 (3), 197–228.
- Ningal, T., Mills, G., Smithwick, P., 2010. An inventory of trees in Dublin city centre. *Irish Geogr.* 43 (2), 161–176.
- Oke, T., 1980. Climatic impacts of urbanization. In: Bach, W., Pankrath, J., Williams, J., (Eds.), *Interactions of Energy and Climate*. Proceedings of International Workshop on Energy and Climate, Münster, Germany, Germany, pp. 339–361.
- Oke, T., 1988. The urban energy balance. *Prog. Phys. Geogr.* 12 (4), 471–508.
- Oke, T., 2006. Towards better scientific communication in urban climate. *Theor. Appl. Climatol.* 84, 179–190.
- Pigeon, G., Legain, D., Durand, P., Masson, V., 2007. Anthropogenic heat release in an old European agglomeration (Toulouse, France). *Int. J. Climatol.* 27 (14), 1969–1981.

- Satterthwaite, D., 2007. Climate change and urbanization: effects and implications for urban governance. United Nations Expert Group on Population Distribution, Urbanization, Internal Migration and Development, New York.
- Schuster, W., Bonta, J., Thurston, H., Warnemuende, E., Smith, D., 2005. Impacts of impervious surface on watershed hydrology: a review. *Urban Water J.* 2 (4), 263–275.
- Schwela, D., 2000. Air pollution and health in urban areas. *Rev. Environ. Health* 15 (1), 13–42.
- Stewart, I., Oke, T., 2012. Local climate zones for urban temperature studies. *Bull. Am. Meteorol. Soc.* 93, 1879–1900.
- Stewart, I.D., Oke, T.R., Krayenhoff, E.S., 2014. Evaluation of the “local climate zone” scheme using temperature observations and model simulations. *Int. J. Climatol.* 34, 1062–1080.
- Taha, H., 1999. Modifying a mesoscale meteorological model to better incorporate urban heat storage: a bulk-parameterization approach. *J. Appl. Meteorol.* 38, 466–473.
- Taylor, K.E., 2001. Summarizing multiple aspects of model performance in a single diagram. *J. Geophys. Res.* 106 (D7), 7183–7192. <http://dx.doi.org/10.1029/2000JD900719>.
- UN, 2012. United Nations Department of Economic and Social Affairs (DESA) Population Division: World Urbanization Prospects, the 2011 Revision. Final Report with Annex Tables, New York.
- Webb, E.K., Pearman, G.I., Leuning, R., 1980. Correction of flux measurements for density effects due to heat and water vapour transfer. *Q.J.R. Meteorol. Soc.* 106, 85–100. <http://dx.doi.org/10.1002/qj.49710644707>.

# Linking urban climate classification with an urban energy and water budget model: multi-site and multi-seasonal evaluation

Alexander, P.J.<sup>1</sup>; Bechtel, B.<sup>2</sup>; Chow, W.<sup>3</sup>; Fealy, R.J.<sup>4</sup>; Mills, G.M.<sup>5</sup>

<sup>1</sup> Irish Climate Analysis & Research Units, Maynooth University, Co. Kildare, Ireland e-mail: [paul.alexander@nuim.ie](mailto:paul.alexander@nuim.ie)

<sup>2</sup> Institute of Geography, University of Hamburg, Hamburg, Germany

<sup>3</sup> Department of Geography, National University of Singapore, Singapore

<sup>4</sup> Department of Geography, Maynooth University, Co. Kildare, Ireland

<sup>5</sup> School of Geography, University College Dublin, Dublin, Ireland

## Abstract

There are a number of models available for examining the interaction between cities and the atmosphere over a range of scales, from small scales - such as individual facades, buildings, neighbourhoods - to the effect of the entire conurbation itself. Many of these models require detailed morphological characteristics and material properties along with relevant meteorological data to be initialised. However, these data are difficult to obtain given the heterogeneity of built forms, particularly in newly emerging cities. Yet, the need for models which can be applied to urban areas (for instance to address planning problems) is increasingly urgent as the global population becomes more urban. In this paper, a modeling approach which derives the required land cover parameters for a mid-complex urban energy budget and water budget model (SUEWS) in a consistent manner is evaluated in four cities (Dublin, Hamburg, Melbourne and Phoenix). The required parameters for the SUEWS model are derived using local climate zones (LCZs) for land cover, and meteorological observations from off-site synoptic stations. More detailed land cover and meteorological data are then added to the model in stages to examine the impact on model performance with respect to observations of turbulent fluxes of sensible ( $Q_H$ ) and latent ( $Q_E$ ) heat. Replacing LCZ land cover with detailed fractional coverages was shown to marginally improve model performance, however the performance of model coupled with 'coarse' LCZ data was within the same range of error (20-40  $Wm^{-2}$  for  $Q_E$  and 40-60  $Wm^{-2}$  for  $Q_H$ ) as high resolution data.

Keywords: UEB, SUEWS, LCZ, urban model evaluation, flux measurements

## 1. Introduction

There has been considerable progress in the representation of urban-scale processes within atmospheric models. A variety of urban-scale models now exist which are capable of simulating the urban heat island either empirically or using physical models (Taha et al., 1988; Myrup, 1969; Atkinson, 2003; Botlyán & Unger, 2003; Kusaka & Kimura, 2004; Hoffmann et al., 2012), urban air quality (Shir & Shieh, 1974; Huang et al., 2000; Karppinen et al., 2000), human thermal comfort in the outdoor urban environment (de Dear & Brager, 1998; Ali-Toudert & Mayer, 2006), energy demand and anthropogenic emissions of heat (Block et al., 2004; Fan & Sailor, 2005; Allen et al., 2011). There are a wide number of surface schemes for modeling fluxes of mass, momentum and energy in urban areas (i.e. the urban energy balance - UEB), which vary in complexity in terms of their parameterisation and hence, their input requirements. More complex UEB schemes have been shown to be very useful in examining, for instance, the detailed hygrothermal impact of different urban forms and functions on the micro-scale climate (Barlow et al., 2004; Harman et al., 2004; Dupont et al., 2004). Such models are invaluable for understanding the processes in operation within urban environments. Moreover, there are some examples of where UEB models have been coupled with meso-scale models (Harman & Belcher, 2006; Bueno et al., 2013; Stewart et al., 2014; Onomura et al., 2015; De Ridder et al., 2015) which would effectively allow for micro-scale meteorological forecasts.

These complex UEB models however are incapable of being run in many data poor settings, or at least routinely, for cities in the economically developing world where the application of such models to planning problems and adaptation to extreme weather conditions would have the largest potential benefit. There is now a clear need to overcome this knowledge gap so as to allow greater integration of urban climate knowledge with the planning and policy communities (Mills et al., 2010; Ching, 2013; Hebbert & Mackillop, 2013; Heaphy, 2015). For instance, a comparison of 33 models by Grimmond *et al.* (2010) highlighted the large number (145) of input parameters required by the group of models considered. Providing such parameters for a single neighbourhood is challenging, and this is before we consider the parameters required for an entire urban area. In order to carry out simulations across an entire urban domain, generalisations will be needed in the interim.

Obtaining the necessary input parameters in data poor settings is only part of the problem, greater rigour in evaluating models in differing background climates and in different cities is also urgently needed. As stated by Oke (2006), without extensive model evaluation exercises the utility of UEB models for planning problems remains dubious. The international urban climate model comparison (Grimmond et al., 2010; Grimmond et al., 2011) went a large way towards discovering the general ability of UEB models in simulating the urban effect on turbulent fluxes and prioritising the most important input parameters. Research on specific model performance in different settings is also beginning to emerge (Loridan & Grimmond, 2012). Despite this there is still a noted lack of integration of urban climate knowledge in the planning process. Very few examples exist of UEB models being applied to real planning problems in collaboration with city planners (Eliasson, 2000). In order to bridge this knowledge gap, more specific evaluation of individual UEB models needs to be undertaken, with clearer links to planning applications, as proposed by Masson *et al.* (2014). It is unlikely that there will emerge a one-model-fits-all scheme that will apply to all situations, however a starting point may be to seek a balance between realistically representing urban processes, ensuring good model accuracy and requiring readily obtained input parameters that are derived in a consistent manner so as to allow inter-city comparisons.

While concerted effort has been placed on model development (Hidalgo et al., 2008) to better represent urban climate processes and move towards operational use in forecasting models, there is a clear need for more general models which are also capable of studying the impacts of urbanisation on the environment with fewer input requirements. One example is the local scale urban meteorological parameterisation scheme (LUMPS – Grimmond & Oke, 2002) which has been shown to accurately simulate the UEB in multiple cities requiring only simple input parameters. The simple treatment of

vegetation and water availability i.e. urban water balance (UWB) within LUMPS limits its application to real planning challenges. Hence a mid-complex scheme, the surface urban energy and water balance scheme (SUEWS – Järvi et al., 2011) was subsequently developed which has a high potential to fill this intermediate space between complex parameterisation, accuracy and ease of implementation.

SUEWS requires more input parameters than LUMPS, however it is still relatively straightforward to carry out simulations and due to its inclusion of the UWB can be applied for planning problems. The model has already been evaluated in Helsinki, Los Angeles (Järvi et al., 2011; Järvi et al., 2014) and Dublin (Alexander et al., 2015) where the necessary inputs to force the model and evaluate its performance were available.

Here we evaluate SUEWS further in three additional background climates and urban configurations. However, our primary aim is to consider the impact of data quality and evaluate model accuracy in a systematic way across multiple sites. In order to derive a means to apply SUEWS in data poor situations we employ a modeling approach which links the local climate zone (LCZ) classification (Stewart & Oke, 2012) with SUEWS. LCZ are linked with SUEWS to derive the necessary land cover parameters easily and in a consistent manner across an entire urban domain. Here, we extend the proof of concept established in a previous paper (Alexander et al., 2015) to include additional background climates and multiple urban environments in order to validate the LCZ-SUEWS approach and answer the following questions:

- 1) Can off-site meteorological data be used to force SUEWS and what is the impact on performance?
- 2) Is the impact of “low quality” (i.e. LCZ) land cover data on SUEWS performance comparable across different cities?

The answer to these questions will have a direct impact on applying the model in data-poor settings such as rapidly expanding urban areas. Prior to outlining the methods employed in this paper, the use of LCZ with the SUEWS model is discussed.

## **2. LCZ-SUEWS approach**

The traditional approach for modeling urban areas involves a number of procedures. Firstly, the urban area is parameterised in terms of fraction coverage ( $\lambda$ ) of buildings, roads and pathways, vegetation, soils and water. Building form (morphology) and vegetation are then derived based either from LiDAR, aerial imagery or field work. From these other parameters are derived for example the sky view factor ( $\psi$ ) and height/width (H/W) ratio. The function (as well building materials) are derived using local expert knowledge. Finally, the derivation of meteorological forcing data, either from observations made on site or through an atmospheric model such as a regional climate model. A number of different methods and data can be employed in each of these stages, a standard does not exist for any scale, and thus inter-site comparisons remain largely elusive. Moreover, in some data starved regions the availability of high-quality data (i.e. multispatial, multitemporal) required by some methods is sparse or simply non-existent.

The basic premise of the linked LCZ-SUEWS approach is address this disparity. Rather than view the urban area as a collection of individual surfaces (walls, rooftops, roads, materials) the approach employs as its starting point the notion that the urban area is a collection of discrete homogenous neighbourhoods of similar characteristics, seeks to identify these neighbourhoods and standardise the approach for deriving parameters for these neighbourhoods required by models.

The thermal differentiation of urban areas using LCZ as a basis has already been demonstrated both empirically and through modeling (Fenner et al., 2014; Stewart et al., 2014; Leconte et al., 2015; Colunga et al., 2015). Moreover, the ability to identify LCZ across entire urban areas i.e. to map LCZ has also been demonstrated (Bechtel et al., 2015). Therefore, LCZ are ideally placed for standardising

the collection of model parameters and for applying the outputs of UEB models across a much larger domain, thus reducing computational expense. There are a number of advantages of the approach:

1. The LCZ scheme itself is defined based on fractional coverages of different land cover types and urban parameters (building height / roughness,  $\psi$  and  $H/W$ ) thus enables a first estimate of these parameters for models
2. The classification of a city into LCZ enables subsequent strategic sampling of the urban area to derive details parameters and characteristics such as building materials, population density and land use
3. LCZ were designed to better describe the site characteristics of urban temperature sensors, hence can aid in the placement of instruments, the interpretation and evaluation of model simulations based on these observations
4. The scheme was designed to be universally understood and since they employ standard building forms are likely to coincide (either in part or entirely) with other land use land cover classifications that have already been established (Alexander & Mills, 2014; Leconte et al., 2015)

Figure 1 illustrates the approach in terms of linking LCZ to a UCM across multiple urban scales, highlighting points 1-4 from above. Methods are currently being tested to create LCZ maps for most cities using readily obtained open source data (Bechtel et al., 2015). Therefore we are assuming for the approach either (i) a LCZ map of the urban area is available or (ii) another LULC map which can be translated into LCZ is available.

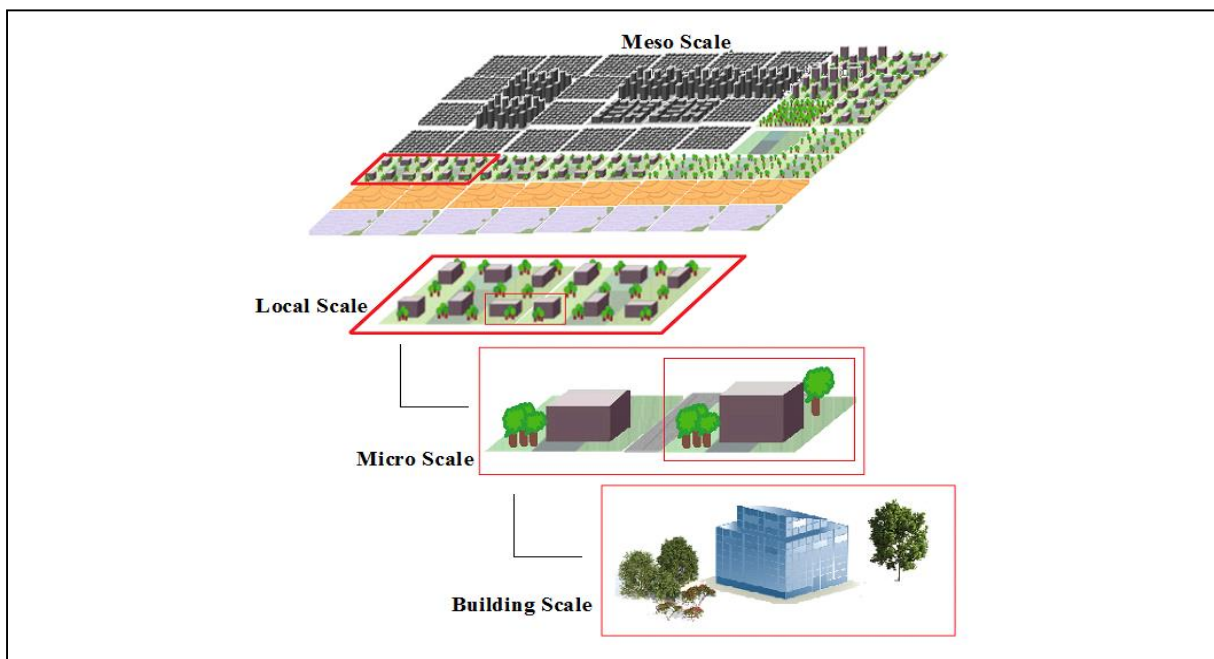


Figure 1 – LCZ-SUEWS approach: At the mesoscale (10s-100s of  $Km^2$ ), model parameters are derived by integrating all LCZ across the entire domain. At the local scale (1-10s of  $Km^2$ ) specific model parameters for *individual* LCZ types are derived. At the microscale and building scale (10s-100s of  $m^2$ ) the approach is as yet untested, but would involve the addition of building dimensions and spacing, individual vegetative species as well as detailed material data.

It should be noted there are only a few examples of where LCZ have been linked to microscale ( $\leq 100$  m) models (see Middel *et al.* (2014) for example) essentially where subsets of a neighbourhood are examined using the LCZ framework. There are currently no examples in literature of linking LCZ to building scale ( $\leq 10$  m) models. This may be possible in some instances where particular forms and functions can be inferred from individual LCZ classes (for instance, it would be unlikely LCZ 10 would ever describe a residential area and more likely to be required to conform to particular design/material

regulations). While examining building scale through the LCZ may seem impractical, it potentially allows for later upscaling to micro, local and meso scale therefore may be useful. However, for this work the approach employs the local scale (500-1000m) to derive model parameters and apply model outputs.

### 3. Experimental outline

We test the effect of using LCZ data which is derived in a consistent way on SUEWS performance by carrying out simulations of the UEB at four locations and compare the results against observations of turbulent fluxes of sensible ( $Q_H$ ) and latent heat ( $Q_E$ ). The SUEWS model (v.2014b) is outlined in detail in (Järvi et al., 2011) and (Järvi et al., 2014). In brief, the model calculates hourly radiative fluxes ( $Q^* = K^* + L^*$ ) using the net all-wave radiation parameterisation (NARP - Offerle et al., 2003) latent heat,  $Q_E$ , using a modified Penman-Monteith equation (Grimmond & Oke, 1991) heat storage,  $\Delta Q_S$ , using the Objective Hysteresis Model (OHM - Grimmond & Oke, 1999) and anthropogenic heat,  $Q_F$ , using the Sailor and Vasireddy approach (Sailor & Vasireddy, 2006). Finally,  $Q_H$  is calculated as the residual from the calculated fluxes i.e.  $Q_H = Q^* - [Q_E + \Delta Q_S + Q_F]$ .

#### 3.1 Experimental setup

In order to evaluate the LCZ-SUEWS approach, we designed a systematic experiment to test the impact of improving data quality on model performance. Our evaluation is carried out in four cities. The locations and data descriptions are outlined in section 3.2 below, here we provide an outline of the experimental procedure – see table 1 for overview.

We adopted a similar approach to the inter-model comparison project (Grimmond et al., 2011) whereby SUEWS was initially run using baseline land cover parameters and off-site meteorology (“low” quality data sampled using LCZ maps). Subsequently more detailed land cover fractions and meteorological data were added in stages. Each step was intended to reveal the importance of information quality on the model output. Due to the uncertainty/assumptions required in relation to  $Q_F$  for several of the sites we opted to exclude this flux from the model runs – though estimates are provided for some of the sites which indicate the magnitude is low ( $\leq 30 \text{ W m}^{-2}$ ).

*Table 1 Outline of systematic experiment used to test the LCZ-SUEWS approach across multiple sites / climates / urban configurations. Each stage subsequent to stage 1 adds additional detail, hence, when interpreting results, the additional effort in providing these data should be considered.*

Stage	Experiment Alias	Land cover data use for model run	Meteorological data used for model run
1	Base-line	Local Climate Zone fractions derived from sampling sites across the urban area	Proximate WMO standard synoptic station (airport sites): T, RH, $K_{\downarrow}$ , Pr, P, U, V
2	Detailed land cover	Fractional values derived from 1 km <sup>2</sup> immediately surrounding flux site	Proximate WMO standard synoptic station (airport sites): T, RH, $K_{\downarrow}$ , Pr, P, U, V
3	Detailed meteorology	Fractional values derived from 1 km <sup>2</sup> immediately surrounding flux site	Meteorological data collected adjacent flux observation platforms: T, RH, $K_{\downarrow}$ , $L_{\downarrow}$ , Pr, P, U, V

Data from urban flux observations sites and proximate WMO standard synoptic stations were obtained by contacting data holders at each of the four sites. Once these data were released and collated for a period of approximately one year for each site, we generated a LCZ classification following the method outlined in Bechtel *et al.* (2015) for each city where data were available. Land cover parameters were then derived by sampling LCZs (excluding the area surrounding the flux sites) and manually computing fractional coverages, this was done in Google Earth Pro similar to the method proposed by See *et al.* (2015). For high-resolution land cover we used the reported meta-data values for the flux sites. Where

this was unavailable, we derived detailed fractional coverages, building heights and vegetation type(s) surrounding each of the sites out to radius of 500m from the flux platforms.

The model was span up prior to each of the experiments using the following approach: for each of the sites, we saturated the surrounding landscape i.e. soil moisture content (SMC) was set to maximum, and the model was span up until SMC reached an equilibrium and appropriate estimates of leaf area index were thus obtained for the initiation period (January 1<sup>st</sup>).

### 3.2 Test locations

Tables 2 and Figure 2 below provides an overview of the four sites included in this work. SUEWS has mostly been applied in temperate climates though the simpler model LUMPS has been applied in arid environments before (Middel et al., 2012). Here we applied SUEWS to a newly (<2 years) instrumented site in Dublin, Ireland; a long term (5-10 years) site in Hamburg; Germany; a long term site in Melbourne, Australia; and an established site (2-4 years) in Phoenix, USA. The latter two sites represent environments with low precipitation and high annual temperatures, whereas the former two represent (i) a cool temperate climate with little annual temperature variation and high precipitation and (ii) a warm humid continental climate respectively. In Table 3, we highlight the required fractional values of land cover types required by SUEWS as computed using high resolution data and the LCZ approach.

Table 2 Meta-data of the sites included in this study. Shown is the year in which observations were obtained, the background climate type, the location of both the flux sites and alternative synoptic stations. Shown also in meters are the instrument height of the flux towers ( $Z_m$ ) the displacement height ( $Z_0$ ) and the mean building height surrounding the site ( $Z_b$ ).

Location	Year	Köppen	Site	LAT	LONG	WMO ID	$Z_m$	$Z_0$	$Z_b$
Dublin, Ireland Site code: DUB	2013	Cfb	Flux	53.34	-6.27	---	37	0.6	16.3
			Synoptic	53.43	-6.25	39690			
Hamburg, Germany Site code: HAM	2014	Dfb	Flux	53.52	10.10	---	50	0.6	8.8
			Synoptic	53.63	10.00	101470			
Melbourne, Australia Site code: MEL	2004	Cfb	Flux	-37.73	145.01	---	40	0.4	6.4
			Synoptic	-37.67	144.83	948660			
Phoenix, USA Site code: PHX	2012	BWh	Flux	33.48	-112.14	---	22.1	0.5	4.5
			Synoptic	33.42	-112.02	722780			

Table 3 Land cover fractions ( $\lambda$ ) used to force the model calculated using the LCZ approach (stage 1) and traditional approach using high resolution (HR) data immediately surrounding the sites (stage 2 and 3)

Location	Land cover	Building	Pavements	Unmanaged	Trees	Grass	Water
Dublin, Ireland [DUB]	LCZ 2 - Compact Midrise	33	55	00	06	06	0
	HR <sup>1</sup>	39	49	00	10	02	0
Hamburg, Germany [HAM]	LCZ 8 - Large low-rise	40	20	10	17	11	2
	LCZ D <sup>2</sup> - Low plants	05	02	07	35	49	2
	HR <sup>1</sup>	27	15	07	22	18	11
Melbourne, Australia [MEL]	LCZ 6 - Openset low-rise	37	16	0	21	26	0
	HR <sup>3</sup>	44	16	0	29	11	0
Phoenix, USA [PHX]	LCZ 6 - Openset low-rise	49	18	27	02	04	0
	HR <sup>4</sup>	26	22	37	05	10	0

<sup>1</sup> Based on 1 km immediately surrounding flux site,  $\lambda$  calculated using 2.5m imagery in GoogleEarth Pro <sup>2</sup> Data not used in this study <sup>3</sup> Based on values reported in Coutts *et al.*, (2007) <sup>4</sup> Based on values reported in Chow *et al.*, (2014)

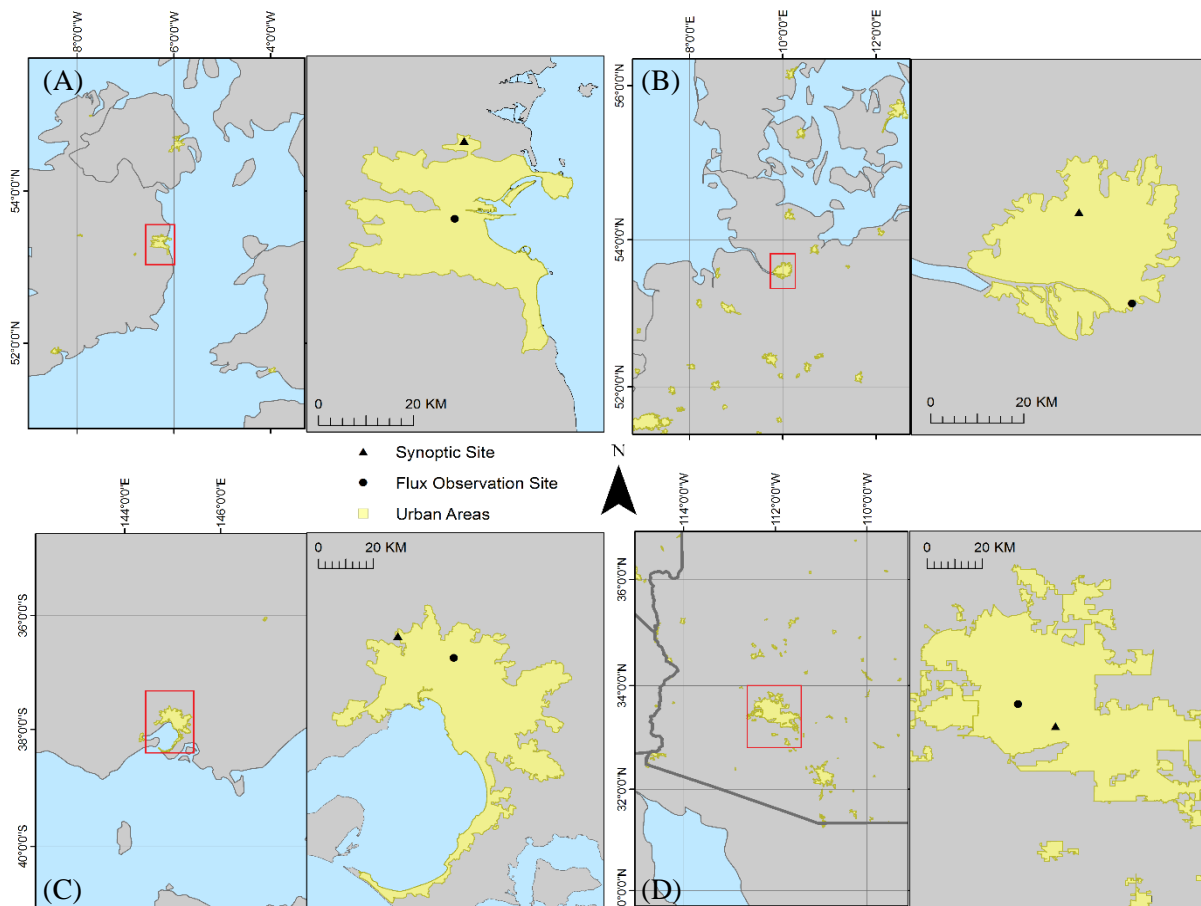


Figure 2 Location of the four sites used in this experiment (A) is Dublin, Ireland (B) is Hamburg, Germany (C) is Melbourne, Australia (D) is Phoenix, USA.. Shown are the locations of the synoptic and flux sites. Urban land cover obtained from Global Rural-Urban Mapping Project, Version 1 (GRUMPv1)

The first site, Dublin Ireland – DUB – the flux observations are made on a mast located in a recently instrumented flat rooftop located on the grounds of a technical institute, just south of the centre of the urban area amidst a mix of dense commercial units and residential apartments (Sunderland et al., 2013; Keogh, 2015). The buildings surrounding the flux site are between 15-20m tall, compact spacing with little vegetation. The site was not present during the initial test case of the LCZ-SUEWS approach in Dublin (Alexander et al., 2015). The synoptic station for DUB is located approximate 15km north of the urban centre adjacent Dublin International Airport conforming to WMO standards; large homogenous fetch of short grass, no tall trees, and no nearby buildings.

The second site, Hamburg Germany – HAM – the flux observations are made at various height levels of a large telecommunications mast located 8km east of the urban centre (Brümmer et al., 2012). This site essentially straddles two differing LCZs, to the west of the flux site, is characterised by large warehousing units <15m tall with little vegetation. To the East of the mast there is largely green vegetation, trees and little building coverage. The synoptic station for HAM is located at Hamburg International Airport approximately 11km north of the urban centre, again conforming to WMO standards.

The third site, Melbourne Australia – MEL – here the flux observations are made in Preston, a suburban area located approximately 10km north of the centre of Melbourne (Coutts et al., 2007). The instruments are located on a mast surrounded by medium density residential houses 5-8m tall, open spacing and an ample amount of vegetation both grass and trees. The accompanying synoptic data were obtained from Melbourne Airport, located 23km north-west of the urban centre.

The final site, Phoenix USA – PHX – for this location, observations are made within a residential area located 7.5km North-West of downtown Phoenix in the suburban area of Maryvale (Chow et al., 2014). The surrounding area is comprised almost entirely of low rise residential housing 5-8m tall with dry xeric landscaping i.e. little green vegetation. The synoptic data for this site were obtained from Phoenix Skyharbor airport which is proximate to the centre of the urban area (approximately 3.5km southeast of downtown Phoenix). Solar radiation data were unavailable at Skyharbor airport, therefore solar radiation data for a nearby Arizona Meteorological network (AZMET) station located 1km northwest of the airport at Encanto were used.

Figure 3 illustrates the LCZ descriptions applicable immediately below and surrounding each of the sites along with satellite imagery and annual wind roses from each location. These LCZ descriptions along with wind direction were used to filter the observational data to ensure the source area for each site was consistent with the LCZ type used for the model runs. For example, for DUB site, this meant including westerly vectors while excluding easterly winds. For HAM, observational data were split into 2 sub datasets corresponding with LCZ 8 (westerly flows) and LCZ D (easterly flows). For the purposes of this study we only considered the LCZ 8 data. For both MEL and PHX the relative homogeneity of the surrounding urban area (along with the low wind speeds) meant no additional filtering was carried out on the provided observational data.

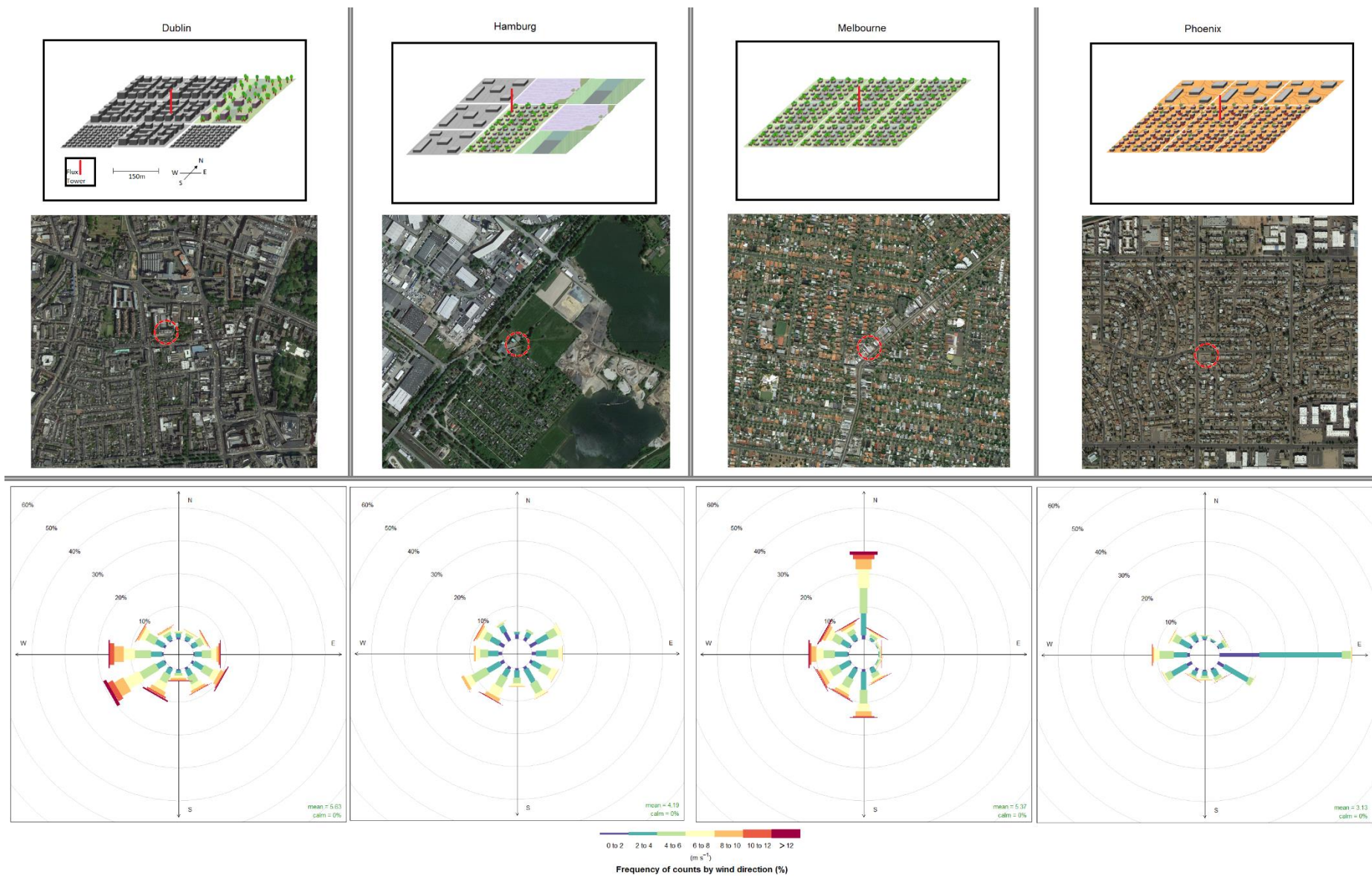


Figure 3 – **Top:** LCZ description of the land cover immediately surrounding each site. **Middle:** Satellite imagery surrounding each of the sites. **Bottom:** Annual wind roses collected at the flux sites, each coloured bar represents a different wind speed ( $m s^{-1}$ ), wind direction was partitioned into 16 compass vectors.

### 3.3 Evaluation of experiments

The performance of SUEWS run in each stage of the experiment is evaluated against the observations at each of the sites. Table 4 highlights the observational data available against which the model is judged, Table 5 highlights the raw data post-processing steps undertaken at each site along with the instruments used at each site. We employed root mean squared error (RMSE) and mean fractional bias (MFB) and Taylor diagrams which further employ the centred RMSE ( $E^*$ ), the correlation coefficient (R), and the standard deviation ( $\sigma$ ) (Taylor, 2001) to assess the model performance in each of the stages highlighted previously. Additionally, regression analysis was carried out between model simulations and observations, for this the coefficient of determination ( $R^2$ ) is reported.

Table 4 Descriptive statistics illustrating the availability of flux data (top rows) as a percentage of the entire year considered. Note: DOY 1 = January 1<sup>st</sup>. Also given are the means ( $\mu$ ) and standard deviations ( $\sigma$ ) of wind speed (u) relative humidity (rh) air temperature (Tair) air pressure (pres) and insolation (kdown) recorded at the synoptic sites.

	Site	DUB	HAM <sub>LCZ8</sub>	MEL	PHX
	Year	2013	2014	2004	2012
	DOY span	1-109, 149-305	1-365	1-70, 87-183, 210-242, 275-333	1-77, 108-110, 121-157, 164-223, 242-366
	N (valid)	3567 (45%)	4536 (57%)	3705 (47%)	6784 (86%)
<b>U</b> <b>ms<sup>-1</sup></b>	$\mu$	5.6	4.2	5.3	1.1
	$\sigma$	2.9	2.1	2.8	0.9
<b>RH</b> <b>%</b>	$\mu$	81.7	80.7	67.5	28.2
	$\sigma$	12.3	15.4	18.8	16.8
<b>Tair</b> <b>°C</b>	$\mu$	9.5	10.8	13.7	25.1
	$\sigma$	5.5	7	5.3	9.3
<b>pres</b> <b>kPa</b>	$\mu$	101.4	101.4	101.6	101.1
	$\sigma$	1.2	0.8	1.7	1.2
<b>rain</b> <b>mm</b>	Max	12.9	14.9	8.5	14.7
	Sum	763.9	679.4	448.6	114.19
<b>kdown</b> <b>W m<sup>-2</sup></b>	$\mu$	115.1	121	164.38	231.49
	$\sigma$	188.2	197.7	253.29	308.92

Table 5 Meta-data illustrating instrumentation at the four flux site along with corrections carried out on flux measurements

Site	DUB	HAM	MEL	PHX
Instruments [ Model ]	<p><u>Tower (48 m AGL)</u></p> <ul style="list-style-type: none"> <li>3D sonic anemometer [WindMaster Pro, Gill]</li> <li>Gas analyser [LI-7200]</li> <li>Temperature-relative humidity sensor [HMP45C]</li> <li>Net radiometer [NR-01] 47 m</li> </ul> <p><u>Roof level (37 m)</u></p> <ul style="list-style-type: none"> <li>Tipping bucket rain gauge [ARG100]</li> </ul>	<p><u>Tower (50 m AGL)</u></p> <ul style="list-style-type: none"> <li>3D sonic anemometer [USA-1]</li> <li>Gas analyser [LI-7500]</li> <li>Thermometer [Pt-100]</li> <li>Humidity sensor [HMP 45] 12 m</li> <li>Pyranometer [Kipp+Zonen]</li> <li>Pyrgometer [Eppley]</li> </ul> <p><u>Ground level</u></p> <ul style="list-style-type: none"> <li>Pressure sensor [PTB 200 A]</li> <li>Tipping bucket rain gauge</li> </ul>	<p><u>Tower (40m AGL)</u></p> <ul style="list-style-type: none"> <li>3D sonic anemometer [CSAT3]</li> <li>Infrared gas analyser [LI-7500]</li> <li>Krypton hygrometer [KH20]</li> <li>Temperature-relative humidity [HMP45C]</li> <li>Net radiometer [Q7.1]</li> <li>Albedometer [CM 7B]</li> <li>Pyrgometer [CG2]</li> </ul>	<p><u>Tower (22m AGL)</u></p> <ul style="list-style-type: none"> <li>3D sonic anemometer [CSAT3]</li> <li>Infrared gas analyser [LI-7500]</li> <li>Temperature-relative humidity sensor [HMP45AC]</li> <li>Net radiometer [NR-01]</li> </ul> <p><u>Ground level</u></p> <ul style="list-style-type: none"> <li>Rain gauge [TB4]</li> </ul>
10/20 Hz data corrections	<ol style="list-style-type: none"> <li>Planar fit rotation (Wilczak et al., 2001)</li> <li>Block averaged (30 min)</li> <li>Offset for sensor lag (co-variance maximization)</li> <li>Signal de-spiking (Vickers and Mahrt, 1997), accepted spikes: 1 %</li> <li>Missing sample allowance 10 %</li> <li>Density effects (Webb et al., 1980)</li> <li>Flagging according Foken 2003, QC &gt;= 7 discarded</li> </ol> <p>Foot print model: Kormann and Meixner 2001</p>	<ol style="list-style-type: none"> <li>Double rotation</li> <li>Block averaged (60 min)</li> <li>Offset for sensor lag (co-variance maximization)</li> <li>Signal de-spiking (Mauder et al. 2013), accepted spikes: 2 %</li> <li>Missing sample allowance 10 %</li> <li>Density effects (Webb et al., 1980)</li> <li>Flagging according Foken 2003, QC &gt;= 7 discarded</li> </ol> <p>Foot print model: Kormann and Meixner 2001</p>	<ol style="list-style-type: none"> <li>Signal de-spiking</li> <li>Oxygen absorption (Tanner et al., 1993)</li> <li>Offset for sensor lag</li> <li>Block averaged (30 min)</li> <li>Density effects (Webb et al., 1980)</li> </ol> <p>Foot print model: None reported</p>	<ol style="list-style-type: none"> <li>Signal de-spiking</li> <li>Aligned into natural wind coordinates (w = 0) (Kimal &amp; Finnigan, 1994)</li> <li>Offset for sensor lag</li> <li>Block averaged (30 min)</li> <li>Frequency response correction</li> <li>Density effects (Webb et al., 1980)</li> </ol> <p>Foot print model: Schmid et al., 1991</p>

## 4. Results

In the following sections the results of the systematic experiment for the four flux sites across each of the stages are presented. The differences in model performance between stages and how these differences related across the four sites is the primary focus. The performance of SUEWS in simulating the radiative fluxes where they have direct bearing on the subsequent estimation of the turbulent fluxes is also highlighted. Our analysis focused on two key temporal scales; (i) hourly / mean diurnal simulations and (ii) daily flux densities. We also examined seasonal performance focusing on two key periods where solar insolation is at a minimum / maximum and where phenological conditions result in different surface processes occurring, namely (i) winter-time, conventionally defined as the months of December January and February (DJF) in the northern hemisphere and (ii) summer-time, defined as June July and August (JJA). When reporting seasonal results, the months of DJF are used for MEL for summer and JJA for winter.

### 4.1 Stage 1: Daily and Hourly Performance Results

The first stage of the experiment established a base-line performance against which the subsequent addition of more detailed meteorological and land cover data is judged. In this stage of the experiment, landcover data are not obtained directly from the area surrounding each of the flux sites, but rather by sampling the LCZ. The performance for each of the sites are highlighted in Table 6.

The ranking from lowest to highest RMSE (values reported in parenthesis) based on the daily estimates of  $Q_E$  - PHX performed best in stage 1 (9.66 W m<sup>-2</sup>), followed by DUB (9.98 W m<sup>-2</sup>), MEL (30.99 W m<sup>-2</sup>) and HAM (37.72 W m<sup>-2</sup>). In terms of model bias, PHX and MEL underestimate  $Q_E$  (-1.02, -0.18 respectively). DUB and HAM both showed negligible negative and positive biases (-0.02 and 0.02) respectively. For  $Q_H$  the ranking from lowest to highest daily RMSE values was DUB (24.65 W m<sup>-2</sup>) HAM (32.07 W m<sup>-2</sup>) MEL (32.31 W m<sup>-2</sup>) and PHX (47.27 W m<sup>-2</sup>) in stage 1.  $Q_H$  was underestimated for the DUB site (-0.16) and overestimated for HAM (0.67), MEL (0.62) and PHX (0.31).

For  $Q_E$  the highest  $R^2$  value achieved in stage 1 was for HAM the lowest value was for PHX followed by MEL and DUB.  $Q_H$  in stage 1 is characterised by relatively high  $R^2$  values compared to  $Q_E$  (ranging from 0.26-0.69).

The calculation of RMSE based on hourly values often includes large isolated errors which can occur between specific hourly flux densities, these errors can arise either due to observational errors which were not filtered correctly or poor model performance. Unsurprisingly for most sites / variables, hourly RMSE was higher than daily RMSE, for instance, for DUB  $Q_E$  RMSE was 37.11 W m<sup>-2</sup> which was approximately 3.5 times higher (i.e. worse) than the daily performance, though this was an extreme example. Generally hourly performance was 1.5 times poorer than daily for  $Q_E$  and  $Q_H$  in stage 1.

Table 6 Root Mean Square Error (RMSE) statistics ( $W m^{-2}$ ) calculated for daily mean flux density and individual hourly flux densities. Also shown are mean fractional bias (MFB) calculated using the daily flux densities (-2 to +2). Also shown are the coefficient of determination ( $R^2$ ). Below presents a colour key summary for highest and lowest daily RMSE scores illustrating the best performance (lowest RMSE) to worse performance (highest RMSE): Lowest RMSE (best performance) = Green, Highest RMSE (worst performance) = Red, intermediate RMSE = Yellow

[DUB]			[HAM]			[MEL]			[PHX]			
$Q_E$												
Stage	$R^2$	RMSE (hourly)	MFB									
1	0.11	9.98	-0.02	0.45	37.72	0.02	0.06	30.99	-0.18	0.01	9.66	-1.02
2	0.10	10.51	0.01	0.48	47.02	0.20	0.07	32.70	-0.35	0.06	13.16	-0.80
3	0.06	19.47	0.67	0.47	51.53	0.17	0.05	32.67	-0.46	0.00	7.99	-1.26
$Q_H$												
Stage	$R^2$	RMSE (hourly)	MFB									
1	0.67	24.65	-0.16	0.56	32.07	0.67	0.26	32.31	0.62	0.69	47.27	0.31
2	0.67	25.48	-0.17	0.54	38.96	0.58	0.25	31.77	0.69	0.67	43.59	0.27
3	0.59	39.89	-0.74	0.57	40.74	0.61	0.31	33.66	0.48	0.79	45.37	0.46
n		128			353			235			291	
		3567			4536			3705			6784	

### *Stage 2 and Stage 3: Performance Results*

In the second stage of the experiment, the land cover types used for the model runs were modified using fractional values calculated out to 1 km<sup>2</sup> surrounding each site. While these fractional values relate to the area directly surrounding the flux site, they require additional effort to compute. The largest difference between stage 1 and 2 in terms of land cover fractions was HAM and PHX which both had significantly lower building fractions than those calculated using the LCZ approach – recall Table 3. This was borne out in the model performance – Table 6. The impact of high resolution land cover was to increase daily RMSE marginally for Q<sub>E</sub> at all sites. The largest RMSE increase was 9.3 W m<sup>-2</sup> compared to stage 1 for HAM, followed by PHX, RMSE increased by 3.5 W m<sup>-2</sup>. The increase was 0.53 W m<sup>-2</sup> and 1.71 W m<sup>-2</sup> for DUB and MEL respectively. The impact on daily Q<sub>H</sub> was less consistent across the sites compared to Q<sub>E</sub>. For MEL and PHX a slight improvement was seen (RMSE decreased by 0.54 and 4.77 W m<sup>-2</sup> respectively) whereas performance decreased slightly for DUB (0.83 Wm<sup>-2</sup>) and HAM (6.89 Wm<sup>-2</sup>).

Model bias did not change direction in stage 2, for HAM the positive bias (i.e. model overestimation) for Q<sub>E</sub> increased by 0.18. For MEL and PHX, which both exhibited negative bias (i.e. model underestimation) in stage 1 also had negative biases in stage 2. The bias increased by 0.17 for MEL but a significant improvement was seen in PHX, bias was reduced by 0.22, though the model still underestimated Q<sub>E</sub>. For DUB, there was no change in bias for Q<sub>E</sub> and Q<sub>H</sub> between stage 1 and 2. Interestingly, the impact on RMSE calculated from the hourly flux densities in stage 2 was an average reduction in RMSE of 2.5 Wm<sup>-2</sup>. The largest improvement in hourly flux calculation was Q<sub>E</sub> for DUB which reduced RMSE by 15.57 Wm<sup>-2</sup>.

For the final stage of the experiment, off-site meteorological forcing data was replaced with measurements made on site. The most significant difference for this stage is the use of observations of the incident radiation (K↓, L↓) made at the four sites. There was little impact on daily RMSE in stage 3 for HAM, MEL and PHX when compared to values for stage 2. For DUB, daily RMSE increased by 8.96 and 14.41 Wm<sup>-2</sup> for Q<sub>E</sub> and Q<sub>H</sub> respectively. For HAM, RMSE increased by 4.51 and 1.78 Wm<sup>-2</sup> for Q<sub>E</sub> and Q<sub>H</sub>, whereas for PHX, RMSE was decreased by 5.17 Wm<sup>-2</sup> for Q<sub>E</sub> and increased by 1.78 Wm<sup>-2</sup> for Q<sub>H</sub>. RMSE for MEL was practically unchanged in terms of Q<sub>E</sub> between stage 2 and 3 (improved model performance by 0.03 Wm<sup>-2</sup>) similarly to HAM and PHX the difference in Q<sub>H</sub> was < 2 Wm<sup>-2</sup> (1.89 Wm<sup>-2</sup>).

A larger impact was seen in the hourly flux density RMSE, particularly for HAM - moving from stage 2 to 3, RMSE increased by a similar amount for both Q<sub>E</sub> (21.03 Wm<sup>-2</sup>) and Q<sub>H</sub> (21.61 Wm<sup>-2</sup>) though the bias remained positive indicating overestimation by the model compared to the observations. For DUB, model RMSE also increased between stage 2 and 3 by 4.25 and 7.27 Wm<sup>-2</sup> for Q<sub>E</sub> and Q<sub>H</sub>. For MEL, hourly performance improved (RMSE decreased) slightly for Q<sub>E</sub> (2.2 Wm<sup>-2</sup>) and Q<sub>H</sub> (10.5 Wm<sup>-2</sup>) between stage 2 and 3. There was no impact on hourly RMSE for PHX between stage 2 and 3 (0.03 and 0.92 Wm<sup>-2</sup>) – though it should be noted hourly Q<sub>H</sub> RMSE was the highest amongst the four sites with a persistent positive bias (model over estimation of Q<sub>H</sub> compared to observations).

#### *4.2 Seasonal and Annual Performance Results*

The seasonal RMSE values are given in Table 7. Model performance tended to be better in winter than summer for all sites during all stages. RMSE for Q<sub>E</sub> was lower than Q<sub>H</sub> for all sites in both seasons. Looking initially at difference between the seasonal RMSE for individual stages, the largest difference in model performance was for Q<sub>H</sub> for PHX, performance in summer was 31.11, 18.83 and 33.57 Wm<sup>-2</sup> worse than winter in stage 1, 2 and 3 respectively. The smallest difference in seasonal performance was for Q<sub>E</sub> for DUB.

Examining the seasonal difference across all stages (i.e. RMSE summed for stage 1-3) reinforces the trend between summer and winter performance. The performance in summer is worse for both Q<sub>H</sub> and

$Q_E$ , the exception was  $Q_E$  for MEL which exhibits higher RMSE in winter and  $Q_H$  for DUB which was slightly higher, though this was due to large wintertime RMSE in stage 3: for stage 1 and 2 RMSE was higher in summer. While there was a clear difference in the seasonal performance for all sites, the difference between stages were small with only some exceptions.

The overall annual performance for each of the sites are presented as Taylor diagrams in Figure 4, which compares the individual stages. Taking the entire annual performance across all sites, the difference between stages 1 and 2 are generally lower than between stages 1 and 3. The centred RMSE for  $Q_H$  tended to be higher for all sites, there was also stronger correlation with observations for  $Q_H$  than for  $Q_E$ . The simulated annual variation ( $\sigma$ ) across the entire period was close with the variation in observations, the clear exceptions were  $Q_E$  for DUB which exhibited significant higher variation in observations compared to the model in all stages. The other exception was  $Q_H$  for MEL which illustrated higher variation in the model compared with the observations. Stage 1 (LCZ derived inputs) and Stage 2 (high-resolution land cover) exhibited similar performances on an annual basis.

Table 7 Seasonal RMSE values calculated for each site. Summer refers to June July and August for DUB, HAM and PHX and December January February for MEL. Winter refers to December January February for DUB, HAM and PHX and June July and August for MEL. Values are in  $Wm^{-2}$ . RMSE values are derived using daily flux densities thus are slightly more conservative than hourly RMSE values. Given also is the sum of the RMSE value across all stages, which provides an overview of seasonal performance

$Q_E$				
Stage	DUB	HAM	MEL	PHX
<i>Summer</i>				
Stage 1	12.13	27.69	16.08	29.27
Stage 2	12.75	26.76	17.05	22.46
Stage 3	18.09	25.98	16.84	31.40
$\Sigma_{RMSE\ 1-3}$	42.98	80.42	49.98	83.12
<i>Winter</i>				
Stage 1	8.28	10.78	20.39	13.32
Stage 2	8.73	12.08	20.38	18.71
Stage 3	21.42	41.36	19.90	13.65
$\Sigma_{RMSE\ 1-3}$	38.42	64.22	60.66	45.67
$Q_H$				
<i>Summer</i>				
Stage 1	25.86	46.86	39.29	48.70
Stage 2	27.39	35.22	40.89	39.65
Stage 3	28.85	31.74	34.37	57.04
$\Sigma_{RMSE\ 1-3}$	82.10	113.82	114.55	145.39
<i>Winter</i>				
Stage 1	23.05	21.93	39.92	17.59
Stage 2	25.40	22.87	44.31	20.82
Stage 3	41.85	48.32	24.44	23.47
$\Sigma_{RMSE\ 1-3}$	90.29	93.12	108.67	61.89

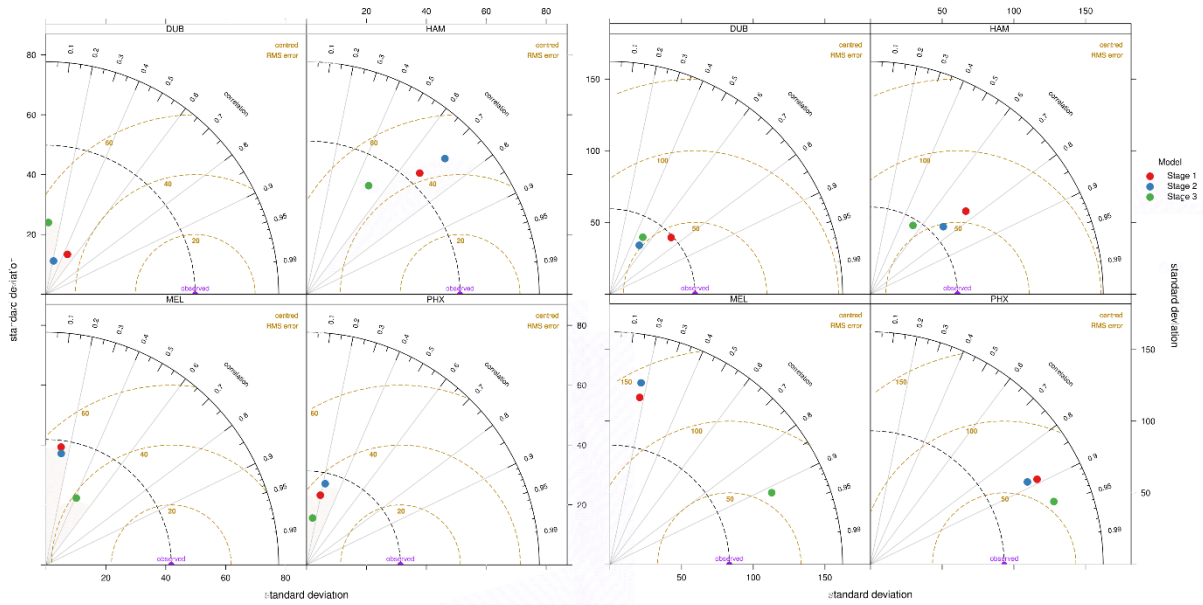


Figure 4 – Taylor diagrams based on all (i.e. hourly) observations for  $Q_E$  (left) and  $Q_H$  (right)

## 5. Discussion

Despite differences in background climate, urban land cover type, building materials, and vegetative species, the performance of SUEWS in simulating the turbulent fluxes  $Q_E$  and  $Q_H$  is broadly consistent between sites. RMSE for  $Q_E$  falls into a range of between 20-30  $Wm^{-2}$  while a RMSE range of 40-60  $Wm^{-2}$  for  $Q_H$  captures all sites, ranges similar to those reported in Järvi *et al.* (2011) for Los Angeles and Vancouver. The improved ability of the model in simulating  $Q_E$  is evident, errors were consistently lower than  $Q_H$  for most of the sites.

The addition of high resolution land cover fractions did not significantly impact on model performance across any of the sites considered, despite large differences between those calculated by the LCZ approach. Given the increased amount of effort required to derive the high resolution fractions, it appears LCZ fractional values can satisfactorily be used in combination with the SUEWS model.

In all stages, the model captures well the relative differences between the four sites when considering both latitude and urban density. For the urban LCZ considered here,  $Q_H > Q_E$  while  $Q_E$  is higher in summer owing to phenological development and higher amount of energy. Both of these factors may explain the seasonal variation in performance whereby performance was better in winter than summer. Vegetation, even small amounts, have been identified as a critical component for most UEB models (Loridan *et al.*, 2010; Grimmond *et al.*, 2011), here single species (i.e. deciduous or coniferous) were used for all sites, it is possible that increased detail on annual phenological development, observed LAI progression for example, along with multiple species will reduce the seasonal differences in model performance.

As different levels of data are added to the model for the experiment, the impact on performance relative to the observation sites was largely consistent across all domains. In terms of hourly simulations of  $Q_H$ , using additional details on surrounding land cover fractions improved the model performance, though the reduction in RMSE was relatively minor (often  $< 15 Wm^{-2}$ ) compared to stage 1 - there was no impact on bias direction. Similar magnitudes were found in previous work.

The impact of adding meteorological data collected adjacent the flux sites is the most difficult finding to explain. Generally, performance was diminished using on-site meteorological data coupled with high resolution land cover in all cases except PHX, though the differences were extremely small. This may be due to observational error whereby the meteorological data collected alongside the towers are unduly

influenced by local effects whereas the flux platforms have a more representative fetch. This would certainly be the case for DUB and HAM which had relatively heterogeneous fetches surrounding the flux sites.

As with previous studies, errors should not be attributed solely to model performance; observations of  $Q_E$  are notoriously difficult and subject to large errors / uncertainty particularly immediately during and after precipitation events. Observations at each of the flux sites included underwent post processing of some kind however some observational errors may have been included despite this and despite the additional filtering carried out using the LCZ approach and wind vectors. For instance, the magnitude of observed  $Q_E$  for DUB [LCZ 2] was larger than would be expected given the sparse amount of vegetation surrounding this site. A similarly instrumented site also classed as LCZ 2 (reported in Alexander *et al.* 2015) exhibited a much lower magnitude and range of  $Q_E$  during summer months, where the maximum observed value was about  $60 \text{ Wm}^{-2}$  and a median value of  $25 \text{ Wm}^{-2}$ . Here, the observed median value for DUB during summer was  $67.57 \text{ Wm}^{-2}$  with a maximum of  $215 \text{ Wm}^{-2}$  around midday. There is nothing that readily accounts for the large magnitude of  $Q_E$  observed at this site, again given the lack of vegetation. The instruments for DUB are located about 5 m lower than the alternative LCZ 2 site, so it is unlikely to be due to measurements being made within the roughness sublayer. However, this only occurred for the diurnal profiles, taking hourly and daily values goes some ways towards filtering out such erroneous observations. In terms of the HAM site, the addition of more detailed land cover data resulted in a decrease in model performance – this is likely attributed to the source area of the observations following the filtering process. Note the fractional values immediately surrounding the site have a higher fraction of vegetation and water coverage however the observational dataset sought to exclude the influence of these land cover types. It is unsurprising the model overestimated the magnitude of  $Q_E$  in this instance.

Another important component for UEB model performance is net radiation. Here, there was a consistent overestimation of  $Q_H$  for PHX, this was due to the model underestimation of albedo ( $\alpha$ ) leading to lower value of  $K\uparrow$  (not shown). The model estimated  $\alpha$  to be 0.15 – however in reality, the building material in PHX are much lighter than the group average, as such,  $\alpha$  based on observations was  $\sim 0.25$ . Therefore, the model retained more energy, leading to overestimation of both  $Q_E$  and  $Q_H$ . This means a subset of LCZ material properties may need to be compiled for applying the model in environments with similar building materials, but it should be noted the partitioning of energy normalised by available energy, that is  $Q_H/Q^*$  and  $Q_E/Q^*$ , was similar between observations and the modelled fluxes.

Nevertheless, SUEWS simulations for both daily and hourly turbulent fluxes agree well with observations using the LCZ approach, with errors well within previously reported ranges. This enables us for the first time to carry out inter-site comparisons in the UEB across similar LCZ types. Figure 5 shows the summer time diurnal flux profiles for three LCZ 6 sites (derived using the setup in stage 1) to illustrate this point. As shown, the partitioning of energy amongst these sites are remarkably similar. Day length (i.e. positive  $Q^*$ ) is shown to be slightly longer in the DUB data with a lower amount of energy at midday as would be expected of this climate. As a consequence,  $Q^*$  at midday was  $457.25 \text{ Wm}^{-2}$ ,  $65 \text{ Wm}^{-2}$  lower than MEL and  $132 \text{ Wm}^{-2}$  lower than PHX. PHX exhibits slightly higher proportion of energy expended towards  $Q_H$  throughout the course of the day compared to both DUB and MEL, as would be expected given the lack of vegetation/water in this environment. The differences in land cover can also be examined e.g. building material and artificial surface extent across all sites can be examined in detail to explore the effect on  $\Delta Q_S$  – a principle component of nocturnal UHI formation.

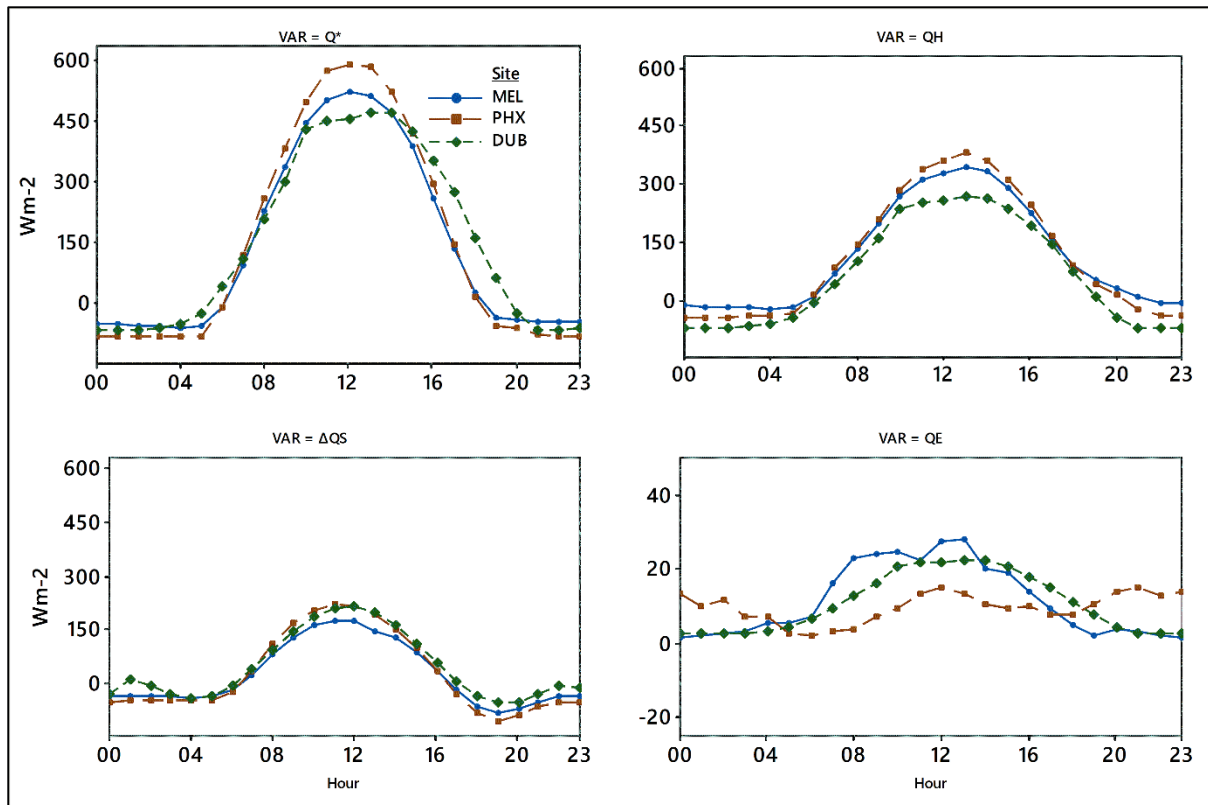


Figure 5 - LCZ 6 summer time Diurnal profile for MEL, PHX and also shown is LCZ 6 site from Alexander et al. (2015) Top left panel is  $Q^*$ , followed by  $Q_H$  (top right),  $\Delta Q_S$  (bottom left) and  $Q_E$  (bottom right)

The use of a standardised method for collecting land cover (LCZ) and meteorological data in order to perform initial assessments of an area’s urban energy and water balance should not discourage the continued establishment of high-quality and long-term flux towers in cities. Here, we considered only three LCZ classes, namely LCZ 2, 6 and 8 as these represented the sites with available data. As additional instrumented sites become available, the approach outlined here should undergo further evaluation.

While the approach has obvious applications in overcoming fiscal/computational limitations in cities with limited resources, the application of the approach needs to be further validated in sparse urban environments, as well as non-urban environments. Different background climates should also be considered. While we requested urban flux data for a range of background climates the four sites included in this study were the only cities for which data were made available. Therefore, eddy-covariance platforms are still an essential investment in any city. Despite the limited sites included here, the extension of the LCZ-SUEWS approach into additional arid / continental type climates undertaken here builds upon the original case study, which further supports the notion that the approach employed with the SUEWS model is capable of realistically simulating the UEB in a variety of circumstances and urban environments.

## 6. Conclusions

In this study we systematically tested a modeling approach which seeks to overcome data scarcity in terms of urban morphology and meteorological observations made within the urban environment. To that end, we coupled the local climate zone (LCZ) scheme of Stewart and Oke (2014) with the surface energy and water balance scheme (SUEWS) v.2014b (Järvi et al., 2014). The approach was tested in four background climates and different urban configurations. Detailed land cover data and meteorological observations were added to the SUEWS model in stages to examine the impact on model

performance relative to the coarse LCZ data and meteorological observations made at airports conforming to WMO standards.

The results show that the addition of detailed data on model performance varied across the sites considered, however root mean squared error (RMSE) consistently fell within a range of between 20-40  $\text{Wm}^{-2}$  for  $Q_E$  and between 40- 60  $\text{Wm}^{-2}$  for  $Q_H$ . The difference between the use of LCZ and detailed land cover was generally small indicating that utilising LCZ data with SUEWS for the initial assessment of the urban energy and water balance is an appropriate approach to take. Furthermore, meteorological observations which are designed to exclude the urban effect are appropriate as forcing data for SUEWS, without impacting significantly on model performance. The results indicate that this modelling approach can be used in data poor settings to rapidly derive in a consistent manner the parameters required by most urban climate models, provided an LCZ map of the city is available.

## Acknowledgements

The authors wish to thank Dr. Andrew Coutts, Monash University and Prof. Sue Grimmond for kindly providing the data for Melbourne. We also wish to thank Prof. Anthony Brazel for providing the synoptic data for Phoenix. The Dublin flux towers are funded by the Higher Education Authority (HEA) of Ireland.

## References

- Alexander, P.J. & Mills, G.M., 2014. Local Climate Classification and Dublin's Urban Heat Island. *Atmosphere*, 5(4), pp.755-74.
- Alexander, P.J., Mills, G.M. & Fealy, R.J., 2015. Using LCZ data to run an Urban Energy Balance Model. *Urban Climate*, 13(3), pp.14-37.
- Ali-Toudert, F. & Mayer, H., 2006. Numerical study on the effects of aspect ratio and orientation of an urban street canyon on outdoor thermal comfort in hot and dry climate. *Building and Environment*, 41(2), pp.94-108.
- Allen, L., Lindberg, F. & Grimmond, C.S.B., 2011. Global to city scale urban anthropogenic heat flux: model and variability. *International Journal of Climatology*, 31(13), pp.1990-2005.
- Arnfield, A.J., 2003. Two decades of urban climate research: A review of turbulence, exchanges of energy and water, and the urban heat island. *International Journal of Climatology*, 23, pp.1-26.
- Atkinson, B.W., 2003. Numerical Modelling of Urban Heat-Island Intensity. *Boundary-Layer Meteorology*, 109(3), pp.285-310.
- Barlow, J., Harman, I. & Belcher, S., 2004. Scalar fluxes from urban street canyons. Part I: laboratory simulation. *Boundary-Layer Meteorology*, 113(3), pp.369-85.
- Bechtel, B. et al., 2015. Mapping Local Climate Zones for a Worldwide Database of the Form and Function of Cities. *ISPRS Int. J. Geo-Inf*, 4(1), pp.199-219.
- Block, A., Keuler, K. & Schaller, E., 2004. Impacts of anthropogenic heat on regional climate patterns. *Geophysical Research Letters*, 31(12).
- Bottayán, Z. & Unger, J., 2003. A multiple linear statistical model for estimating the mean maximum urban heat island. *Theoretical and Applied Climatology*, 75(3), pp.233-43.
- Brümmer, B., Lange, I. & Konow, H., 2012. Atmospheric boundary layer measurements at the 280 m high Hamburg weather mast 1995-2011: mean annual and diurnal cycles. *Meteorologische Zeitschrift*, 21(4), pp.319-35.

- Bueno, B., Norford, L., Hidalgo, J. & Pigeon, G., 2013. The urban weather generator. *Journal of Building Performance Simulation*, 6(4), pp.269-81.
- Ching, J.K.S., 2013. A perspective on urban canopy layer modeling for weather, climate and air quality applications. *Urban Climate*, 3(1), pp.13-39.
- Chow, W.T.L. et al., 2014. Seasonal dynamics of a suburban energy balance in Phoenix, Arizona. *International Journal of Climatology*, 34(15), pp.3863-80.
- Colunga, M.L. et al., 2015. The role of urban vegetation in temperature and heat island effects in Querétaro city, Mexico. *Atmósfera*, 28(3), pp.205-18.
- Coutts, A.M., Beringer, J. & Tapper, N.J., 2007. Impact of Increasing Urban Density on Local Climate: Spatial and Temporal Variations in the Surface Energy Balance in Melbourne, Australia. *Journal of Applied Meteorology and Climatology*, 46(4), pp.477-93.
- de Dear, R. & Brager, G.S., 1998. Developing an adaptive model of thermal comfort and preference. *ASHRAE Transactions. Center for the Built Environment*, 104(1), pp.1-18.
- De Ridder, K., Lauwaet, D. & Maiheu, B., 2015. UrbClim – A fast urban boundary layer climate model. *Urban Climate*, 12(June 2015), pp.21-48.
- Dupont, S., Otte, T.L. & Ching, J.K.S., 2004. Simulation of Meteorological Fields Within and Above Urban and Rural Canopies with a Mesoscale Model. *Boundary-Layer Meteorology*, 113(1), pp.111-58.
- Eliasson, I., 2000. The use of climate knowledge in urban planning. *Landscape and Urban Planning*, 48(1-2), pp.31-44.
- Fan, H. & Sailor, D.J., 2005. Modeling the impacts of anthropogenic heating on the urban climate of Philadelphia: a comparison of implementations in two PBL schemes. *Atmospheric Environment*, 39(1), pp.73-84.
- Fenner, D., Meier, F., Scherer, D. & Polze, A., 2014. Spatial and temporal air temperature variability in Berlin, Germany, during the years 2001–2010. *Urban Climate*, 10(2), pp.308-31.
- Grimmond, C.S.B. et al., 2011. Initial results from Phase 2 of the international urban energy balance model comparison. *International Journal of Climatology*, 31(2), pp.244-72.
- Grimmond, C.S.B. et al., 2010. The International Urban Energy Balance Models Comparison Project: First Results from Phase 1. *Journal of Applied Meteorology and Climatology*, 49(6), pp.1268–92.
- Grimmond, C.S.B. & Oke, T.R., 1991. An evaporation-interception model for urban areas. *Water Resource Research*, 27(7), pp.1739-55.
- Grimmond, C.S.B. & Oke, T.R., 1999. Heat Storage in Urban Areas: Local-Scale Observations and Evaluation of a Simple Model. *Journal of Applied Meteorology*, 38(2), pp.922-40.
- Grimmond, C.S.B. & Oke, T.R., 2002. Turbulent Heat Fluxes in Urban Areas: Observations and a Local-Scale Urban Meteorological Parameterization Scheme (LUMPS). *Journal of Applied Meteorology*, 41(7), pp.792-810.
- Harman, I., Barlow, J. & Belcher, S., 2004. Scalar fluxes from urban street canyons part II: Model. *Boundary-Layer Meteorology*, 113(3), pp.387-410.
- Harman, I.N. & Belcher, S.E., 2006. The surface energy balance and boundary layer over urban street canyons. *Quarterly Journal of the Royal Meteorological Society*, 132(621), pp.2749-68.

- Heaphy, L.J., 2015. The role of climate models in adaptation decision-making: the case of the UK climate projections 2009. *European Journal for Philosophy of Science*, 5(2), pp.233-57.
- Hebbert, M. & Mackillop, F., 2013. Urban climatology applied to urban planning: a postwar knowledge circulation failure. *International Journal of Urban and Regional Research*, 37(5), pp.1542-58.
- Hidalgo, J. et al., 2008. Advances in urban climate modeling. *Annals of the New York Academy of Sciences*, 1146, pp.354-74.
- Hoffmann, P., Krueger, O. & Schlünzen, K.H., 2012. A statistical model for the urban heat island and its application to a climate change scenario. *International Journal of Climatology*, 32(8), pp.1238-48.
- Huang, H., Akutsu, Y., Arai, M. & Tamura, M., 2000. A two-dimensional air quality model in an urban street canyon: evaluation and sensitivity analysis. *Atmospheric Environment*, 34(5), pp.689-98.
- Järvi, L., Grimmond, C.S.B. & Christen, A., 2011. The Surface Urban Energy and Water Balance Scheme (SUEWS): Evaluation in Los Angeles and Vancouver. *Journal of Hydrology*, 411(3-4), pp.219-37.
- Järvi, L. et al., 2014. Development of the Surface Urban Energy and Water Balance Scheme (SUEWS) for cold climate cities. *Geoscientif Model Development*, 7, pp.1691-711.
- Karppinen, A. et al., 2000. A modelling system for predicting urban air pollution: comparison of model predictions with the data of an urban measurement network in Helsinki. *Atmospheric Environment*, 34(22), pp.3735-43.
- Keogh, S., 2015. *Quantifying carbon dioxide concentrations and fluxes for Dublin*. PhD Thesis. Kildare, Ireland: National University of Ireland Maynooth, Irish Climate Analysis & Research Units.
- Keogh, S., Mills, G.M. & Fealy, R.J., 2012. The energy budget of the urban surface: two locations in Dublin. *Irish Geography*, 4(1), pp.1-23.
- Kusaka, H. & Kimura, F., 2004. Coupling a Single-Layer Urban Canopy Model with a Simple Atmospheric Model: Impact on Urban Heat Island Simulation for an Idealized Case. *Journal of the Meteorological Society of Japan*, 82(1), pp.67-80.
- Leconte, F., Bouyer, J., Claverie, R. & Pétrissans, M., 2015. Using Local Climate Zone scheme for UHI assessment: Evaluation of the method using mobile measurements. *Building and Environment*, 83, pp.39-49.
- Loridan, T. & Grimmond, C.S.B., 2012. Multi-site evaluation of an urban land-surface model: intra-urban heterogeneity, seasonality and parameter complexity requirements. *Quarterly Journal of the Royal Meteorological Society*, 138(665), pp.1094-113.
- Loridan, T. et al., 2010. Trade-offs and responsiveness of the single-layer urban canopy parametrization in WRF: An offline evaluation using the MOSCEM optimization algorithm and field observations. *Quarterly Journal of the Royal Meteorological Society*, 136(649), pp.997-1019.
- Masson, V. et al., 2014. Adapting cities to climate change: A systemic modelling approach. *Urban Climate*, 10(December 2014), pp.407-29.
- Middel, A. et al., 2012. Land cover, climate, and the summer surface energy balance in Phoenix, AZ, and Portland, OR. *International Journal of Climatology*, 32(13), pp.2020-32.
- Middel, A. et al., 2014. Impact of urban form and design on mid-afternoon microclimate in Phoenix Local Climate Zones. *Landscape and Urban Planning*, 122, pp.16-28.

- Mills, G.M. et al., 2010. Climate Information for Improved Planning and Management of Mega Cities (Needs Perspective). *Procedia Environmental Sciences*, 1(1), pp.228-46.
- Myrup, L.O., 1969. A Numerical Model of the Urban Heat Island. *Journal of Applied Meteorology*, 8(6), pp.908-18.
- Offerle, B., Grimmond, C.S.B. & Oke, T.R., 2003. Parameterization of Net All-Wave Radiation for Urban Areas. *Journal of applied Meteorology*, 42(8), pp.1157-73.
- Oke, T.R., 2006. Towards better scientific communication in urban climate. *Theoretical and Applied Climatology*, (84), pp.179-90.
- Onomura, S. et al., 2015. Meteorological forcing data for urban outdoor thermal comfort models from a coupled convective boundary layer and surface energy balance scheme. *Urban Climate*, 11(March 2015), pp.1-23.
- Sailor, D.J. & Vasireddy, C., 2006. Correcting aggregate energy consumption data to account for variability in local weather. *Environmental Modelling & Software*, 21(5), pp.733-38.
- See, L. et al., 2015. Generating WUDAPT's Specific Scale-dependent Urban Modeling and Activity Parameters: Collection of Level 1 and Level 2 Data. In *ICUC9 - 9th International Conference on Urban Climate jointly with 12th Symposium on the Urban Environment*. Toulouse, France, 2015. 20-24th July 2015.
- Shir, C.C. & Shieh, J., 1974. A Generalized Urban Air Pollution Model and Its Application to the Study of SO<sub>2</sub> Distributions in the St. Louis Metropolitan Area. *Journal of Applied Meteorology*, 13(2), pp.185-204.
- Stewart, I.D. & Oke, T.R., 2012. Local Climate Zones for Urban Temperature Studies. *Bulletin of the American Meteorological Society*, 93, pp.1879-900.
- Stewart, I.D., Oke, T.R. & Krayenhoff, E.S., 2014. Evaluation of the 'local climate zone' scheme using temperature observations and model simulations. *International Journal of Climatology*, 34(4), pp.1062-80.
- Sunderland, K.M., Mills, G. & Conlon, M.F., 2013. Estimating the wind resource in an urban area: A case study of micro-wind generation potential in Dublin, Ireland. *Journal of Wind Engineering and Industrial Aerodynamics*, 118(July), pp.44-53.
- Taha, H., Akbari, H., Rosenfeld, A. & Huang, J., 1988. Residential cooling loads and the urban heat island—the effects of albedo. *Building and Environment*, 23(4), pp.271-83.

# Spatial validation of an urban energy balance model using multi-temporal RS surface temperature

Paul J. Alexander and Rowan Fealy  
Irish Climate Analysis & Research Units  
Department of Geography,  
Maynooth University  
Kildare, Ireland  
paul.alexander@nuim.ie

Gerald Mills  
School of Geography, Planning & Environmental Policy  
University College Dublin,  
Dublin, Ireland

**Abstract**— Despite a growing number of urban energy balance (UEB) model applications being undertaken within urban climate literature, the number of independent validation exercises remains very limited. This in turn has raised questions as to the value of model applications without due consideration to the models performance in space and time. The PILPS-URBAN project went some ways towards understanding the general performance of 33 UEB models and highlighted the need for careful treatment of urban and non-urban land surfaces within model parameterization and also the derivation of input parameters. Nevertheless the need for independent external validation of specific models is now evident. Here we undertake an external validation of the SUEWS model in Dublin (Ireland). We present a method for spatially validating the model across the entire Dublin area by employing remotely sensed surface temperatures obtained through the MODIS satellite platform.

## I. INTRODUCTION

Urban areas are the most significant biome for human habitation with over half of the world's population residing within cities across the globe [1]. The introduction of hard, impervious surfaces results in a significantly modified land surface which in turn modifies the energetics at the interface between the surface and the atmosphere [2,3]. Understanding this modification both historically and into the future is now critical as continued urbanization and demographic changes means more urban residents will become at risk to heat-related stresses especially as cities come to realise global climate change [4]. In order to assess whether responses seeking to mitigate risk to urban dwellers are appropriate and cost effective requires detailed meteorological forecasting prior to their implementation. Atmospheric models are useful in this regard.

Broadly speaking, this requires two primary considerations in order to effectively aid decision making; 1) how urban areas are described in terms of their morphology and 2) the accuracy/ability of models to capture the key processes that impact on the urban population [5]. In terms of the former, much work has gone into extracting detailed urban parameters for use in urban canopy models (UCMs) both from field work [6,7] and remotely sensed data [8,9]. Whereas the latter has received much less attention, generally UCMs are only validated by developers themselves. Moreover, it is typical that urban models are validated against in-situ measurements made

within distinctive urban landscapes. This approach assumes that the area in which observations are made can be reproduced across the entire urban area, however in light of the difficulty in placing observational platforms (both in terms of urban heterogeneity and identifying a location that is safe and secure) often it is the case that this assumption cannot be upheld except in very specific circumstances.

Employing a modelling and observational approach which deliberately generalises an urban area into its key components which yield the most significant impact on land-atmosphere exchanges can go some ways towards alleviating this problem. However as more UCMs move toward including advective terms i.e. the horizontal transfer of energy and/or mass, there is now an urgent need to assess how models performance spatially. Reformulating observational approaches can achieve this, but will inevitably encounter the same issues highlighted above when brought to bear on a real urban situation. Recently it has been proposed to utilise remotely sensed (RS) observations for model validation which have an obvious spatial advantage over in-situ platforms.

Here we undertake a spatial validation of the Surface Energy and Water Balance Scheme (SUEWS) model in Dublin, Ireland. We employ standard metrics to evaluate the models performance at two flux observation platforms, providing an estimate of its performance at 2 points. Subsequently we employ RS land surface temperature (LST) data from the MODIS platform to assess how the model performs across Dublin city during conditions that are conducive to strong urban modification of the atmosphere.

## II. URBAN ENERGY BALANCE MODELS

A number of urban models have been developed at a variety of spatial and temporal scales with a range of applications, the most common of which are based on the urban energy budget (UEB):

$$Q^* + Q_F = Q_H + Q_E + \Delta Q_S \quad [W \text{ m}^{-2}] \quad (1)$$

where  $Q^*$  is net radiation,  $Q_F$  is anthropogenic heat flux,  $Q_H$  and  $Q_E$  are the turbulent sensible and latent heat fluxes, respectively and  $\Delta Q_S$  is storage heat flux. This equation refers to a representative urban volume that extends from of the surface in which there is no net horizontal transfer (that is, an

extensive surface type) and no significant energy exchange across the lower boundary. Hence, assessing each of the terms at the upper surface of the volume, which is located above the canopy layer captures the exchanges between the urban surface and overlying boundary layer. The process of urbanization results in the replacement of natural surfaces by hard impervious surfaces (e.g. roads, pavements, car parks) and buildings. This greatly alters the surface energy balance by, for example, increasing (decreasing) the sensible (latent) heat flux and increasing heat storage. One of the best known outcomes is the formation of an urban heat island.

The UEB model used here is the Surface Urban Energy and Water balance Scheme (SUEWS v.2013b). SUEWS is able to simulate both the UEB (Eqn. 1) and urban surface water balance of an urban neighborhood and requires a relatively low number of input requirements that may include: meteorological data; population-economy related data and; surface cover and urban structure data. Some of these inputs are required to run the model, while other inputs are optional. At the very least the model requires standard meteorological data and details on the fractions of the landscape that is occupied by buildings, vegetation, impervious paving, etc. Järvia, et al. [10] evaluated SUEWS using flux observations (spanning various time lengths from different years) from sites in Los Angeles (34°N, Köppen climate type, Csb) and Vancouver (49°N, Cfb). The results showed the model to be capable of simulating net radiation, sensible and latent and heat fluxes with root mean squared error (RMSE) ranges of 25-47 Wm<sup>-2</sup>, 30-64 Wm<sup>-2</sup> and 20-56 Wm<sup>-2</sup>, respectively.

We examine the performance of the SUEWS model at both individual points (flux sites) and across a wider space. Our examination is based on data gathered for Dublin, Ireland (53° N, 6° W), which has a mild, mid-latitude climate (Cfb). It provides an ideal place for this study as it has two observation sites (located in urban and suburban landscapes) where detailed energy flux and meteorological observations have been made since 2009; these data can be used to run the model and compare its simulations with observations. In addition, there is a local climate zone (LCZ) description of the city that outlines major neighborhood types and standard weather station observations available at Dublin Airport, which is between 5 and 10km distant from the urban and suburban flux sites, respectively.

### III. METHODS

#### A. SUEWS model

The SUEWS model (V.2013b) was designed for urban simulations at a neighbourhood-scale, which corresponds to an area of approximately 1km<sup>2</sup>. It simulates both the urban energy budget (Eqn. 1) and water budget:

$$P + I_e + F = E + R + \Delta S \text{ [mm h}^{-1}\text{]} \quad (2)$$

Where P is precipitation, I<sub>e</sub> is externally piped water, F is anthropogenic water emission, E is evaporation (including transpiration) R is runoff and ΔS is change in storage. Eqns. 1 and 2 are connected directly through the evaporative terms (Q<sub>E</sub>

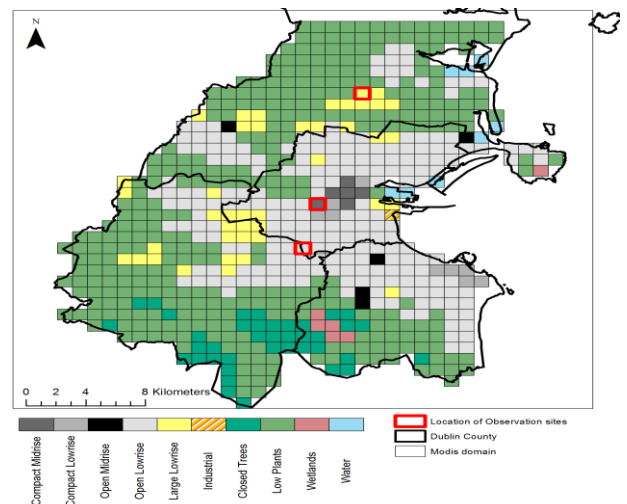
and E) and indirectly via other terms; for example a precipitation event may result in water storage in soil that will affect its thermal properties. The energy budget (Eqn. 1), describes flux exchanges at a plane that separates the roughness sub-layer (between 2 to 4 times the mean height of the roughness elements) from the boundary-layer above. The modelled fluxes therefore correspond to the inertial sub-layer, where micro-scale variability driven by individual roughness elements becomes integrated into neighbourhood signals. This corresponds with the spatial resolution of the MODIS satellite platform (1km). One should note the absence of explicit advective terms in Eqn. 1, so that it assumes there is a negligible horizontal energy transfer. Strictly speaking then, this limits the application of SUEWS to extensive neighbourhood types where the landscape may be described as relatively homogenous.

#### B. Forcing data and observation platforms

The atmospheric observations used here come from standard meteorological information obtained for Dublin airport, which is located 5km from the city centre in an area dominated by warehouses (Figure 1). Hourly observations are available for a number of elements: air temperature (T), precipitation (P), pressure (Pr), humidity (RH), wind-speed (V) and direction and solar radiation receipt (K↓). Note that hourly values for K↓ are a required model input. These data are used to drive the model.

SUEWS also requires fractional coverage of land cover types. The model was furnished with land cover fractions (i.e. % building, pavements, grass, trees, water and soil) for Dublin based on typologies generated from the LCZ classes present in Dublin. We employ LCZ as the basis for examining the correlation between MODIS LST and modelled LST. The model is evaluated against flux data that is acquired at two stations (Fig 1) that are part of the International Urban Flux Network.

Fig. 1. Study area of Dublin city. The grids below correspond with MODIS LST pixels and modelled areas. The grids outlined in red show the observation platform locations



The measurement sites were selected to represent sites that typify Dublin's urban land-cover. The suburban site is located in a residential area consisting of similar two-story houses about 6 m tall; much of the landcover is vegetated (open lowrise or LCZ6). Each has an identical suite of instruments and radiation and turbulent flux terms are recorded alongside the meteorological variables listed above. The instruments are positioned on a mast that is situated on the roof of a school at a height of 12 m (10 m for the net radiometer). The urban site is located in a mixed-use area closer to the city centre; much of the surrounding landscape is impermeable and the average building height is about 8 m (compact midrise or LCZ2). The support mast is on the roof of a 12 m tall building and the instruments are at a height of 17 m (15 m for net radiometer).

Upward and downward facing radiometers provide  $K\downarrow$ ,  $K\uparrow$ ,  $L\downarrow$  and  $L\uparrow$ . The turbulent fluxes  $Q_H$  and  $Q_E$  heat are obtained using an open-path eddy covariance system that is interrogated at a rate of 10Hz; the recorded fluxes are based on 30 minute averages. The heat storage term ( $\Delta Q_S$ ) is estimated as a residual of the measured terms:

$$\Delta Q_S \approx Q^* - (Q_H + Q_E) \text{ [W m}^{-2}\text{]} \quad (3)$$

Each tower is located well within its LCZ type and the flux instruments are positioned at a level that is approximately twice the height of the surrounding buildings and at about the height of the inertial sub-layer established by that surface type. In other words, we are assuming that advection is negligible and that  $\Delta Q_A$  can be ignored.

A measure of the goodness of fit is provided by the RMSE,

$$\text{RMSE} = \left[ \sum_{i=1}^n \frac{(\hat{y}_i - y_i)^2}{n} \right]^{0.5} \quad (4)$$

Where  $(\hat{y}_i - y_i)$  represents the difference between the observed ( $y_i$ ) and simulated ( $\hat{y}_i$ ) flux term (e.g.  $Q^*$ ) at each hourly time interval ( $i$ );  $N$  represents the total number of hours. RMSE is commonly used to assess the total error, regardless of its direction.

Our spatial evaluation is based on data obtained by the MODIS sensor on board the Terra and Aqua Platforms. This provides LST obtained four times per day sampled at a 1km resolution. We obtained 1km daytime LST for Dublin during a period of fine weather in April 2010. The limited temporal scope reflects the number of scenes that were cloud free over Dublin city. However in our judgement while this covers a limited period to evaluate SUEWS spatially, it corresponds with conditions where the model may be expected to perform well i.e. clear-skies, little wind, no precipitation, therefore provides a best-case estimate of its performance across space.

To evaluate simulated LST with observations from MODIS we generated our model grid to align with the LST pixels for each scene. Thus, each grid contained LST from MODIS for each of the days considered, as well as hourly modelled output from SUEWS. We plotted MODIS LST against SUEWS at the corresponding overpass time ( $t$ ) by first calculating the mean LST for each LCZ class and subtracting this from the overall group mean for both the modelled (mod) and observed (obs) LST:

$$LST'_{mod,obs(i)} = \overline{LST}_{mod,obs(i)} - \sum_{i=1}^7 \overline{LST}_{mod,obs(i)} \quad (5)$$

#### IV. RESULTS

We ran the SUEWS model during a period of fine weather in April (April 11-18) 2010. Initially, we present the model evaluation at our flux locations, followed by the results of the spatial evaluation.

##### A. Point Performance

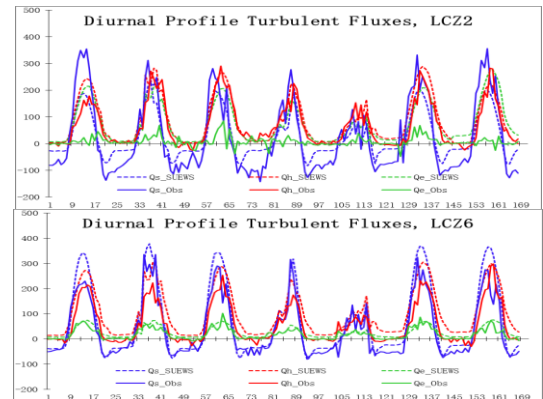
The model performance at the flux sites for the one week period is summarized in Table 1. Generally SUEWS reproduced the turbulent fluxes ( $Q_H$ ,  $Q_E$  and  $\Delta Q_S$ ) well. The performance at the suburban flux site, LCZ 6, was slightly better than the urban flux site (LCZ 2) based on the SUM of the RMSE. RMSE (for LCZ 2 shown in parenthesis) scores for the LCZ 6 site were as follows:  $Q_H$  44.4 (15.6)  $Q_E$  7.2 (65.8) and  $\Delta Q_S$  27.2 (1.3)  $\text{W m}^{-2}$ .

Though  $Q_E$  is a relatively minor term at the LCZ 2 site, SUEWS reproduces the diurnal trend poorly (Fig 2), however there is a noted improvement at the LCZ 6 site. The worst flux in terms of high RMSE at the LCZ 6 site was  $Q_H$  which was routinely overestimated by the model; conversely  $\Delta Q_S$  was underestimated around this site. The simulation of  $Q_H$  and  $\Delta Q_S$  at the LCZ 2 site was remarkably similar to the observation tower though  $Q_E$  was underestimated routinely by a large amount hence the relatively large RMSE for this term. It is worth remembering that the model was forced with off-site data obtained at Dublin airport, which perhaps is closer in morphological characteristics to the LCZ 2 site. Nevertheless, the model performs well over the week simulated with respect to following a logical diurnal pattern.

TABLE I. SUEWS PERFORMANCE AT FLUX SITES

April 11-17 2010	RMSE ( $\text{Wm}^{-2}$ )		
	Turbulent Flux	LCZ 2 site (Urban)	LCZ 6 site (Sub.urb)
	$Q_H$	44.688	15.602
	$Q_E$	7.251	65.862
	$\Delta Q_S$	27.199	1.318

Fig. 2. Diurnal profiles from SUEWS compared to observation platforms. X-axis is hour of model simulation, Y-axis is the flux density given in  $\text{Wm}^{-2}$

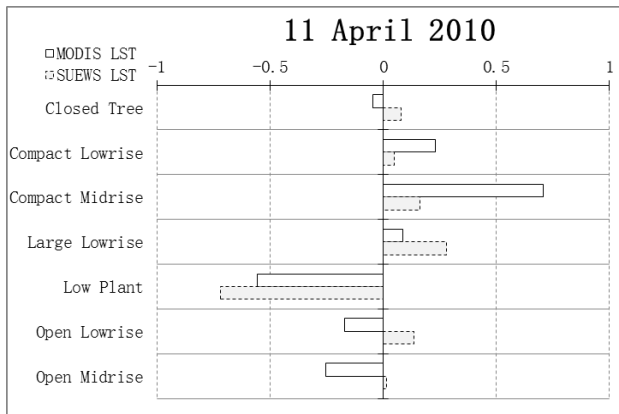


### B. Spatial Performance

The main goal of the present study was to evaluate how SUEWS performs spatially, without the need for a dense observational network. We compared SUEWS LST which is an integration of various surface LST across each grid with MODIS LST. SUEWS provides LST for each hour of simulation, thus, we obtained LST values which correspond with the overpass / acquisition time of Terra and Aqua platforms (approximately 11am local time). Rather than giving a raw comparison pixel by pixel, we first derived typologies of LST based on LCZ land cover (eqn. 5). This is deemed to be a better measure of the spatial performance of SUEWS in terms of the LST relationships it simulates e.g. more built-up areas are expected to exhibit higher LST than extensively vegetated areas etc.

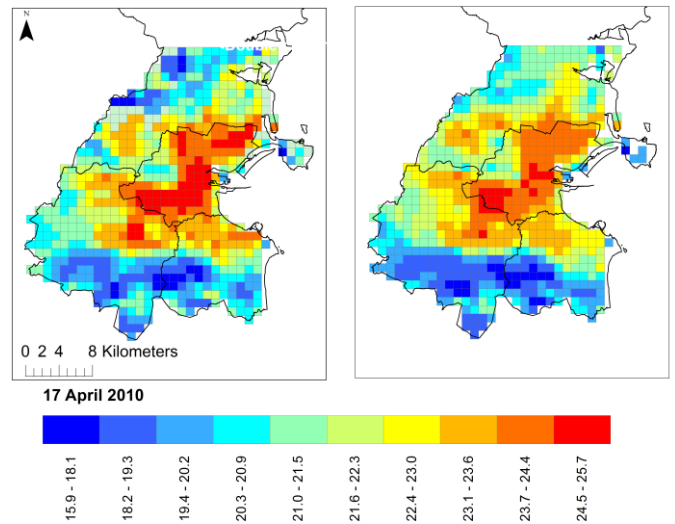
Generally, simulated LST from SUEWS was routinely lower than the observations obtained by MODIS (Fig 3). However, the relationship between LST both from observations and the model are consistent with one another. LST in LCZ 2 was  $\sim 1^\circ\text{C}$  warmer than the group mean based on the MODIS data, whereas SUEWS LST was almost half this value ( $\sim 0.6^\circ\text{C}$ ). The next clearest signal was Low Plants LCZ which exhibited lower than average LST, again as would be expected *a priori*. This LCZ was  $1.2^\circ\text{C}$  lower than the group mean based on MODIS observations, whereas this value was  $0.9^\circ\text{C}$  based on SUEWS.

Fig. 3. LCZ-LST relationship as derived from MODIS and SUEWS simulations. Shown is the start of the period (April 11) which represents a typical profile



The most promising result appears in the spatial patterns of LST revealed by both MODIS and SUEWS, from which clear land cover patterns can be seen (Fig 4). For instance, the warmest LST correspond with the compact inner city of Dublin based on both LST values, whereas the surrounding rural areas are clearly demarcated based on lower LST.

Fig. 4. Spatial correspondence between SUEWS LCZ-LST (right) and MODIS LCZ-LST (left) for April 17 2010, values are in  $^\circ\text{C}$

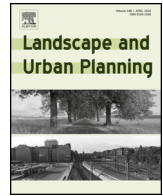


### V. CONCLUSION

In this study we sought to spatially validate the SUEWS model by employing remotely sensed (RS) land surface temperatures (LST). SUEWS was validated at 2 point locations, to ensure good agreement with observations of the urban energy balance (UEB). We generated LST typologies based on land cover and data obtained through MODIS. The SUEWS model performed well at the point locations. LST was generally underestimated by SUEWS when compared to observations.

### References

- [1] Satterthwaite, D. "Climate Change and Urbanization: Effects and Implications for Urban Governance". New York: United Nations Expert Group on Population Distribution, Urbanization, Internal Migration and Development, **2007**.
- [2] Oke, T.R. "The urban energy balance". *Progress in Physical Geography*, **1988**,12(4), p. 471-508.
- [3] Kimura, F., & Takahashi, S. "The Effects of Land-Use and Anthropogenic Heating on the Surface Temperature in the Tokyo Metropolitan Area: A Numerical Experiment". *Atmospheric Environment*, **1991**, 25(2), p. 155-164.
- [4] National Research Council. "Urban Meteorology: Forecasting, Monitoring, and Meeting Users' Needs". Washington, D.C: The National Academies Press, **2012**.
- [5] Arnfield, J. "Two decades of urban climate research: a review of turbulence, exchanges of energy and water, and the urban heat island." *International Journal of Climatology*, **2003**, 23(1), p. 1-26.
- [6] Cleugh, H., Bui, E., Mitchell, V., Xu, J., Grimmond, C., & Simon, D. "Evapotranspiration in Urban Water Balance Models: A Methodological Framework". Canberra, Australia: International Congress on Modelling and Simulation (MODSIM05). **2005**.
- [7] Grimmond, C., & Oke, T. "An evaporation-interception model for urban areas". *Water Resource Research*, **1991**, 27(7), p. 1739-1755.
- [8] Grimmond, C., & Souch, C. "Surface description for urban climate studies: a GIS based methodology". *Geocarto International*, **1994**, 1, p. 47-59.
- [9] Middel, A., Brazel, A., Kaplan, S., & Myint, S. "Daytime cooling efficiency and diurnal energy balance in Phoenix, Arizona, USA". *Climate Research*, **2012**, 54, p.21-34.
- [10] Järvia, L., Grimmond, C., & Christen, A. "The Surface Urban Energy and Water Balance Scheme (SUEWS): Evaluation in Los Angeles and Vancouver". *Journal of Hydrology*, **2011**, 411(3-4), p. 219-237.



# Simulating the impact of urban development pathways on the local climate: A scenario-based analysis in the greater Dublin region, Ireland



P.J. Alexander<sup>a,\*</sup>, R. Fealy<sup>b</sup>, G.M. Mills<sup>c</sup>

<sup>a</sup> Irish Climate Analysis & Research Units, National University of Ireland, Maynooth, County Kildare, Ireland

<sup>b</sup> Department of Geography, National University of Ireland, Maynooth, County Kildare, Ireland

<sup>c</sup> School of Geography, Planning & Environmental Policy, University College Dublin, Dublin 4, Ireland

## HIGHLIGHTS

- The impact of different future development pathways on local climate are simulated.
- Sprawling scenarios increased sensible/stored heat across 7.7–14.9% of the domain.
- Greening rooftops resulted in the lowering the impact on local scale climate.

## ARTICLE INFO

### Article history:

Received 8 August 2015

Received in revised form 2 February 2016

Accepted 4 February 2016

### Keywords:

Neighbourhood climate  
Urban planning  
SUEWS modelling  
Surface energy balance  
Low impact development  
Local climate zones

## ABSTRACT

In this study, the impact of different urban development scenarios on neighbourhood climate are examined. The investigation considers the relative impact differing policy/planning choices will have on the local-scale climate across a city during a typical climatological year (TCY). The aim is to demonstrate a modelling approach which couples a climate-based land classification and simple urban climate model and how this can be used to examine the impact differing urban forms and design strategies have on neighbourhood scale partitioning of energy and resulting consequences. Utilising the Surface Urban Energy and Water Balance (SUEWS) model (Järvi et al., 2011) hourly fluxes of sensible, latent and stored heat are simulated for an entire year under four different urban development scenarios. The land cover scenarios are based on those obtained by the MOLAND model for 2026 (Brennan et al., 2009) in our case study city Dublin (Ireland). MOLAND LULC are translated into local climate zones (Stewart and Oke, 2012) for examination. Subsequently, the types of building forms, vegetation type and coverage are modified based on realistic examples currently found across Dublin city. Our results focused on 2 principle aspects: the seasonality of energy partitioning with respect to vegetation and average diurnal partitioning of energy. Our analysis illustrates that compact scenarios are suitable form of future urban development in terms of reducing the spatial impact on the existing surface energy budget in Dublin. Design interventions which maintain the level of vegetation at a ratio  $\geq 9:16$  to artificial surfaces reduces the impact.

© 2016 Elsevier B.V. All rights reserved.

## 1. Introduction

Globally, city planners face significant pressures to accommodate a rapidly growing urban population. In the past 60 years, the urban population has increased by 3.154 billion and more than 50%

\* Corresponding author at: Irish Climate Analysis & Research Units, Maynooth University, Room 1.8, Laraghbryan House, North Campus, Maynooth, County Kildare, Ireland.

E-mail addresses: [paul.alexander@nuim.ie](mailto:paul.alexander@nuim.ie), [paul.j.alexander@outlook.com](mailto:paul.j.alexander@outlook.com) (P.J. Alexander), [rowan.fealy@nuim.ie](mailto:rowan.fealy@nuim.ie) (R. Fealy), [gerald.mills@ucd.ie](mailto:gerald.mills@ucd.ie) (G.M. Mills).

of the global population are now urban; by 2050, it is projected that this proportion will exceed 66% (UN, 2014). Urban areas are a focus of human activity, energy consumption and greenhouse gas emissions and consequently are major drivers of global climate change; moreover, their locations at low altitude, along rivers and close to coasts exposes them to hazards (such as coastal flooding) that are likely to be exacerbated in under various climate change scenarios (IPCC, 2014). Urban areas also modify the local climate profoundly, producing well known climatic phenomena such as the urban heat island (UHI) (Karl, Diaz, & Kukla, 1988; Patz, Campbell-Lendrum, Holloway, & Foley, 2005), CO<sub>2</sub> dome (Balling, Cerveny, & Idso, 2001; Idso, Idso, & Balling, 1998) and photochemical smog (Gray &

Finster, 2000; Moussiopoulos, Sahm, & Kessler, 1995). These local to global climate effects are caused by two different, but related, aspects of cities. Urban form describes the surface cover (e.g. impervious fraction), the construction materials (e.g. asphalt) and the built geometry (e.g. the building dimensions and their juxtaposition). Urban function describes the activities in cities that require water, energy, materials etc.; the waste heat, vapour and materials are deposited into the atmosphere, hydrosphere and lithosphere. Urban form and function are strongly related so that, for example, more compact and densely occupied cities have lower per capita fuel use for transportation (Bramley & Power, 2009; Breheny, 1991; Elkin, McLaren, & Hillman, 1991; Mills, 2007).

As the world continues to urbanise, the global sustainable development challenges (and opportunities) will increasingly be concentrated in cities. Urban policies that address these must manage aspects of urban form and functions to mitigate (and adapt to) climate changes at different scales. This is especially true for economically developing countries where the rates of urbanisation are greatest and population growth outstrips the pace of planned development (Jorgenson & Rice, 2010; Martine, McGranahan, Montgomery, & Fernández-Castillia, 2008). The emerging layout of these fast-growing cities (e.g. urban extent, population and building density) will have long-term implications as once constructed, cities have proved difficult to alter. Incorporating climate knowledge into urban decision-making will be an important component in urban planning and creating more sustainable cities. In this respect, urban climate models (UCMs) are a potentially valuable tool for evaluating the impacts of different urban designs, land use, population densities and activities on the surface energy and water balances and the consequent effects on the local atmosphere and hydrology, respectively. Addressing local climate conditions (such as the UHI) can help reduce the contribution of individual cities to global climate change. In fact a variety of UCMs have been applied for precisely this purpose (see Table 1), yet there is little evidence that they have been used to inform spatial decision making (Eliasson, 2000; Hebbert & Mackillop, 2013; Mills, 2008; Oke, 1984). By comparison, climatic considerations are routinely employed to assist building design (Brager & de Dear, 1998; Givoni, 1992; Shaviv, 1984).

This 'knowledge circulation failure' (Hebbert & MacKillop, 2013) has been attributed to many causes, including a mismatch between urban climate knowledge and planning/design concerns. For example, while climate research has examined the nocturnal UHI in considerable detail, architects and planners are most interested in daytime conditions when people occupy outdoor spaces and building energy demands are highest (Svensson & Eliasson, 2002). To overcome this failure, existing research should be codified for planning use (Alcoforado, Andrade, Lopes, & Vasconcelos, 2009; Mills et al., 2010) but also new research needs to be undertaken that meets urban planning needs (Gál & Unger, 2009; Marland et al., 2003; Ward, 2003).

The use of land cover scenarios as one component of a planning support system is well established as a means of exploring factors which can be controlled by practitioners, and how they might be used to improve planning decisions and outcomes (Couclelis, 2005; Xiang & Clarke, 2003). They are valuable tools for exploring the spatial impact of decisions on future land cover (Van de Voorde et al., 2016) and for testing particular policy priorities on future land use and land cover change (Veldkamp & Fresco, 1997) or for exploring the impact of land cover on physical processes and risks, such as precipitation runoff (Niehoff, Fritsch, & Bronstert, 2002). In this respect, while a scenario should be viewed as a possibility or projection rather than as a prediction, scenario-sets can be extremely useful for examining bio-physical impacts of urbanisation, and thus help reduce any inadvertent consequences associated with urban development when combined UCMs which have been evaluated

in many circumstances and have demonstrated their potential for planning applications (Grimmond et al., 2010, 2011).

Previous research has demonstrated how available meteorological data can be used to run mid-to-complex urban energy balance models, which would allow the urban climate effect to be included in the planning process (Alexander, Mills, & Fealy, 2015; Grimmond & Oke, 2002). However, there has been little guidance on how to run UCMs using inputs from land cover scenarios, interpret their findings and integrate their projections to inform policy.

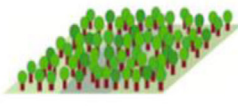
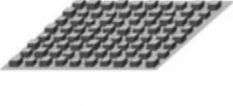
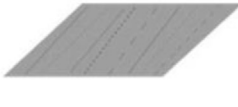
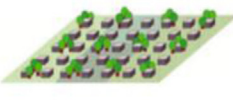
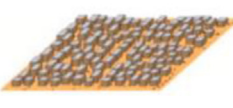
In this study, we demonstrate the utility of the surface urban energy and water balance scheme (SUEWS v.2013b) for evaluating the climatic impact of different scenarios of urban development. SUEWS is parameterised using values obtained from the Local Climate Zone (LCZ) scheme that describes neighbourhood types and is run using available meteorological data. This approach is applied to a case study city (Dublin, Ireland, 53.3° N, 6.3° W) where the pathways for future growth are based on scenarios generated by the MOLAND model to 2026. These scenarios generate distinct land use and land cover (LULC) outcomes, which are translated into LCZ types to provide required parameter values. The output of the model illustrates the impacts of the different development pathways. Before discussing the methodology in detail, the potential value of the SUEWS model – linked with the LCZ scheme – for planning purposes is presented.

## 2. Integrating LCZ and SUEWS to support planning decisions

The LCZ scheme categorises landscapes into types based on their impact on the near-surface air temperature (Stewart & Oke, 2012); it consists of 17 standard types, 10 of which are urban, 7 are non-urban (Fig. 1) but it can also accommodate mixed types. The scheme is properly applied at the local or neighbourhood-scale (areas greater than about 1 km<sup>2</sup>) where each type is differentiated from another based on a range of variables, such as, the fractional impervious cover, mean building height, building materials, sky view factor and anthropogenic heat generation. The net effect of these properties is to modulate the thermal response of the overlying atmosphere and create the urban heat island (UHI) phenomenon; this link has been validated in published work (Levlovics, Gál, & Unger, 2013; Stewart, Oke, & Krayenhoff, 2014). The value of the LCZ scheme extends beyond the UHI however, and could provide a platform for incorporating much urban climate knowledge into planning practice for a number of reasons:

- First, the UHI may be regarded as an indicator of urban climate effects generally, so mitigating it addresses other effects such as the lack of greenspaces and of available water. So a map of LCZ types in a city identifies where the urban effect is greatest.
- Second, LCZ types are designed to be culturally neutral (applicable internationally) and intuitive (user-friendly). As such they can clarify communication between climate scientists and planners e.g. Picone & Campo (2015) see Fig. 2. Moreover, they can facilitate knowledge transfer between cities.
- Third, LCZs are useful for both observational and modelling studies of the local scale climate. A LCZ map of a city can be used to sample the urban landscape to measure climate variables and to gather more detailed information on surface characteristics to run UCMs. Even the current variables in the LCZ scheme correspond with the many UCM parameters.

Here, we link the LCZ scheme with the SUEWS climate model v.2013b (Järvi, Grimmond, & Christen, 2011) to explore the impacts of urban development scenarios on neighbourhood scale climate. By integrating LCZ with SUEWS, urban form is accounted as either

Built types	Definition	Land cover types	Definition
1. Compact high-rise 	Dense mix of tall buildings to tens of stories. Few or no trees. Land cover mostly paved. Concrete, steel, stone, and glass construction materials.	A. Dense trees 	Heavily wooded landscape of deciduous and/or evergreen trees. Land cover mostly pervious (low plants). Zone function is natural forest, tree cultivation, or urban park.
2. Compact midrise 	Dense mix of midrise buildings (3–9 stories). Few or no trees. Land cover mostly paved. Stone, brick, tile, and concrete construction materials.	B. Scattered trees 	Lightly wooded landscape of deciduous and/or evergreen trees. Land cover mostly pervious (low plants). Zone function is natural forest, tree cultivation, or urban park.
3. Compact low-rise 	Dense mix of low-rise buildings (1–3 stories). Few or no trees. Land cover mostly paved. Stone, brick, tile, and concrete construction materials.	C. Bush, scrub 	Open arrangement of bushes, shrubs, and short, woody trees. Land cover mostly pervious (bare soil or sand). Zone function is natural scrubland or agriculture.
4. Open high-rise 	Open arrangement of tall buildings to tens of stories. Abundance of pervious land cover (low plants, scattered trees). Concrete, steel, stone, and glass construction materials.	D. Low plants 	Featureless landscape of grass or herbaceous plants/crops. Few or no trees. Zone function is natural grassland, agriculture, or urban park.
5. Open midrise 	Open arrangement of midrise buildings (3–9 stories). Abundance of pervious land cover (low plants, scattered trees). Concrete, steel, stone, and glass construction materials.	E. Bare rock or paved 	Featureless landscape of rock or paved cover. Few or no trees or plants. Zone function is natural desert (rock) or urban transportation.
6. Open low-rise 	Open arrangement of low-rise buildings (1–3 stories). Abundance of pervious land cover (low plants, scattered trees). Wood, brick, stone, tile, and concrete construction materials.	F. Bare soil or sand 	Featureless landscape of soil or sand cover. Few or no trees or plants. Zone function is natural desert or agriculture.
7. Lightweight low-rise 	Dense mix of single-story buildings. Few or no trees. Land cover mostly hard-packed. Lightweight construction materials (e.g., wood, thatch, corrugated metal).	G. Water 	Large, open water bodies such as seas and lakes, or small bodies such as rivers, reservoirs, and lagoons.
8. Large low-rise 	Open arrangement of large low-rise buildings (1–3 stories). Few or no trees. Land cover mostly paved. Steel, concrete, metal, and stone construction materials.	<b>VARIABLE LAND COVER PROPERTIES</b>	
9. Sparsely built 	Sparse arrangement of small or medium-sized buildings in a natural setting. Abundance of pervious land cover (low plants, scattered trees).	<i>b. bare trees</i>	Leafless deciduous trees (e.g., winter). Increased sky view factor. Reduced albedo.
10. Heavy industry 	Low-rise and midrise industrial structures (towers, tanks, stacks). Few or no trees. Land cover mostly paved or hard-packed. Metal, steel, and concrete construction materials.	<i>s. snow cover</i>	Snow cover >10 cm in depth. Low admittance. High albedo.
		<i>d. dry ground</i>	Parched soil. Low admittance. Large Bowen ratio. Increased albedo.
		<i>w. wet ground</i>	Waterlogged soil. High admittance. Small Bowen ratio. Reduced albedo.

**Fig. 1.** Local climate zone scheme for universally describing neighbourhood morphology and thermal climate (Stewart and Oke, 2012). Each zone is defined on the basis of parameters which impact on the hydrothermal properties such as the % imperviousness, sky-view factor, building materials, waste heat, building and vegetation height and so forth.

**Table 1**

Overview of a selection of urban climate models (UCMs) for planning and research applications. The list below is non-exhaustive and based on non-proprietary models. The list also excludes building-scale energy models. Scale refers to the resolution of the model output, where  $\mu$  = micro (1–100 m)  $\alpha$  = local (1–2 km)  $\beta$  = meso (>2 km) scale.

Model name	Model reference	Scale	Reviewed exemplar applications
ENVI-met	Bruse (1999)	$\mu$ - $\alpha$	Building form impacts on microclimate (Middel, Häb, Brazel, Martin, & Guhathakurta) Green-roof strategies and HTC (Peng and Jim, 2013)
MITRAS	Schlünzen et al. (2003)	$\mu$	Wind flow patterns, dispersion (Schlünzen, Grawe, Bohnenstengel, Schlüter, & Koppmann)
SOLWEIG	Lindberg et al. (2008)	$\mu$ - $\alpha$	Vegetation and building form impacts on shadow patterns, mean radiant temperatures (Lindberg and Grimmond, 2011) Impact of urban planning on HTC (Goldberg, Kurbjuhn, & Bernhofer, 2013)
SLUCM (WRF)	Kusaka et al. (2001)	$\alpha$ - $\beta$	Simulating urban expansion impacts on temperature, wind speed and surface ozone concentrations (Wang, Lin, Yang, Deng, & Lin) Land-Sea breeze and UHI development (Lin et al., 2008)
SUEWS	Järvi et al. (2011)	$\alpha$ - $\beta$	BRIDGE project, ensembles modelling for urban hydrology (Chrysoulakis et al., 2013)
TUF-3D	Krayenhoff and Voogt, (2007)	$\mu$	Use of artificial turf to reduce surface and air temperature (Yaghoobian et al., 2010)
TEB	Masson (2000)	$\mu$ - $\beta$	Impact of climate change on temperature and cooling demands in Paris (Lemonsu, Kounkou-Arnaud, Desplat, Salagnac, & Masson)

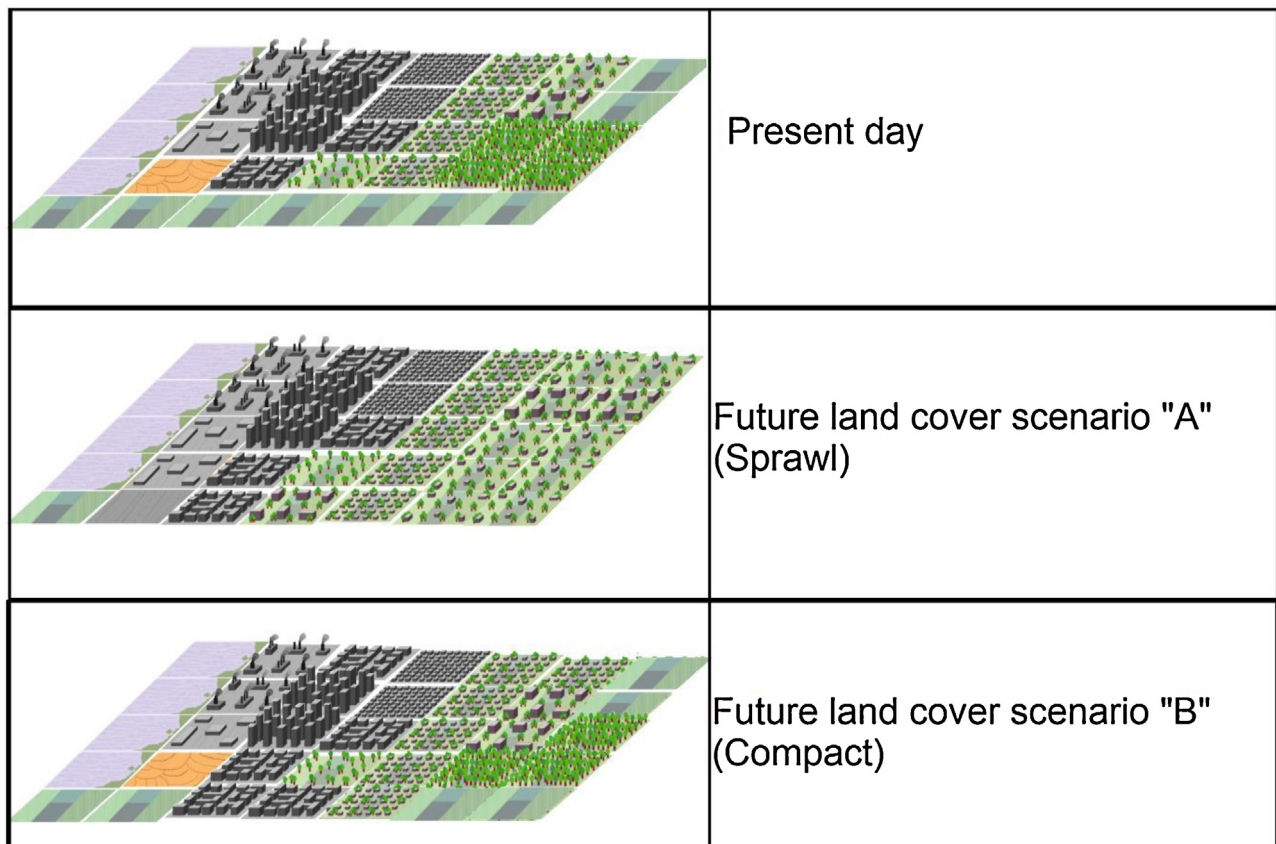


**Fig. 2.** A hypothetical city comprised of different neighbourhood types (LCZ—Fig. 1), with future land cover scenarios classified into LCZ, thus allowing for initial assessment and modelling of climatic impacts of policy/planning decisions at the neighbourhood scale (see for instance Fig. 12/13 in Ching, 2013).

sparse, open or compact neighbourhood areas as well as lowrise, midrise or highrise building elements. While SUEWS cannot explicitly account for building configurations (unlike for example, the ENVI-MET model) it employs several parameters that are determined by the extent of open spaces, buildings and vegetation height and coverage. These choices of form will impact on the local scale partitioning of energy—Eq. (1) below.

SUEWS simulates the effect of urbanisation on the processes responsible for local-scale changes in the climate. These processes are encapsulated in the urban energy budget (UEB), which states

$$Q^* + Q_F = Q_H + Q_E + \Delta Q_S + \Delta Q_A, \quad [W m^{-2}] \quad (1)$$

$Q^*$  is net radiation,  $Q_F$  is anthropogenic heat,  $Q_H$  and  $Q_E$  are the turbulent sensible and latent heat respectively and  $\Delta Q_S$  is storage heat and  $\Delta Q_A$  is advection (i.e. the horizontal transfer of energy). Each term is expressed as a flux density ( $Wm^{-2}$ ) across the sides of an imaginary volume that encloses a section of urban landscape. The volume encloses the urban surface features (buildings, trees, etc.) and extends to a depth within the substrate where energy exchanges are close to zero; in other words,  $Q^*$ ,  $Q_F$ ,  $Q_H$ ,  $Q_E$  and  $\Delta Q_S$  can each be assessed at the top of the volume. SUEWS does not account for advection which is significant at the boundary between surface types, and so is limited to ‘homogenous’ land-

**Table 2**  
Link between urban development/features, impact on energy balance terms and resulting impact on local scale climate/urban heat island relevant for planners particularly in warm climates.

Urban feature	Urban effect	Energy balance term (Relative to non-urban areas)
Canyon geometry	Increased surface area and trapping of radiation	Increased $K^*$
Air pollution	Greater absorption and re-emission	Increased $L_{\downarrow}$
Canyon geometry	Reduced sky view factor (less nocturnal loss to atmosphere)	Decreased $L^*$
Buildings and traffic	Direct addition of heat	Addition of $Q_F$
Construction materials	Increased thermal admittance at night	Increased $\Delta Q_S$
Absence of water bodies/vegetation	Increased surface/air heating	Increased $Q_H$
Construction materials	Increased water-proofing/increase runoff	Decreased $Q_E$
Canyon geometry	Reduces wind speed	Decreased $Q_A$

scapes (both urban and non-urban) where  $\Delta Q_A \approx 0$ . Moreover, the lack of explicit accounting for advection (strictly speaking) further limits the model to synoptic conditions conducive to a strong urban effect i.e. low winds, clear sky, high pressure. Thus, the UEB simulates the total amount of energy available at the urban surface ( $Q^* + Q_F$ ) and its use for heating the air ( $Q_H$ ), evaporating water ( $Q_E$ ) and heating the substrate ( $\Delta Q_S$ ). The partitioning of available energy will govern the urban impact on the substrate, surface and air temperatures and atmospheric humidity; it will also affect the UHI, building energy management and the partitioning of precipitation into runoff and storage (Table 2).

SUEWS is well suited to this study as it requires a relatively low number of input parameters including: meteorological data; socio-economic-demographic data and; surface cover and urban structure data, which is provided by the LCZ scheme.

We simulated neighbourhood/local scale ( $\sim 1 \text{ km}^2$ ) turbulent fluxes in order to examine the impact of different development pathway scenarios on neighbourhood scale climate across a typical climatological year (TCY). We simulated hourly sensible, latent and stored heat using the Surface Urban Energy and Water balance (SUEWS v.2013b) model (Järvi et al., 2011). We forced the model with meteorological data obtained from a WMO standard station located approximately 5 km outside of the metropolitan area. These data are based on 10-year hourly averages, thus represent a TCY, but for clarity, the 10-year period runs from 2005–2014 which contained 3 of the warmest years on record for the region (Walsh, 2014). Hence while the TCY simulations are intended to be a-temporal, they are based on the present climate regime. The model has already been evaluated under a number of different circumstances i.e. background climates and different cities (Alexander et al., 2015; Järvi et al., 2011, 2014) and its potential utility for urban planning has been discussed elsewhere (Chrysoulakis, Anselmo, de Castro, & Moors, 2014).

### 3. Methods

#### 3.1. Case study area

Our case study area is the Greater Dublin Region (GDR) which covers Dublin city (Ireland) and parts of the surrounding counties containing several large satellite towns. Dublin is the capital city of Ireland and located on the east coast, flanked by the Irish Sea to the East, and the Dublin/Wicklow mountains to the South. With the exception of the mountainous southern part, most of the city occupies a flat and low-lying basin ( $< 100 \text{ m}$  above sea level.) and is bisected by the Liffey River—Fig. 3. Despite its latitude, it has a mild climate with little temperature variation through the year (Köppen type *Cfb*) although day-length is significantly longer in summer (16 h in June) than in winter (8 h in December). The urban area under investigation extends to  $\sim 700 \text{ km}^2$  as the city has expanded outside its administrative boundaries over the last three decades. The population of the defined model extent is  $\sim 1.4$  million. Dublin provides an optimum location for undertaking this

case study as it has two flux observation sites (located in urban and suburban neighbourhoods) where detailed energy flux and meteorological observations have been made since 2009 (Keogh, Mills, & Fealy, 2012) which has allowed for model calibration and evaluation as outlined in previous studies (Alexander et al., 2015). In addition there is a LCZ description of the city that outlines major neighbourhood types (Alexander & Mills, 2014) and a WMO standard meteorological station located outside the urban area. The LCZ map of Dublin and the meteorological data are sufficient for running SUEWS.

#### 3.2. Data

SUEWS requires hourly meteorological data, land cover parameters and estimates of anthropogenic fluxes—see Table 3. In terms of land cover, the model describes different surface types in a neighbourhood in terms of fractional coverage of buildings, pavements, water, vegetated areas (both irrigated and non-irrigated) and trees (coniferous and deciduous) and unmanaged land cover such as bare soils or rock. Anthropogenic water and energy use can also be provided. In the following sections, the various input data utilised are described.

##### 3.2.1. Forcing data

We obtained hourly values for temperature, relative humidity, precipitation, pressure, wind speed and incoming solar radiation for the period from 2005 to 2014 from a meteorological station located close to Dublin airport, approximately 5 km north of the inner city. We averaged the hourly values for each day of the year in order to derive a typical climatological year (TCY). The resulting hourly dataset was used to force the model in each of the four MOLAND scenario runs and an additional run for the base line case (BLC) to examine the impact on the urban energy budget (UEB). This allowed for an evaluation of the model simulated turbulent fluxes ( $Q_H$ ,  $Q_E$  and  $\Delta Q_S$ ) against observations made at two flux sites; one urban and one suburban. Each of the flux sites carries the same suite of instruments and measures  $Q^*$ ,  $Q_H$  and  $Q_E$  using an open path eddy-covariance method (see Keogh et al., 2012 for details).  $\Delta Q_S$  is estimated as the residual of the observations (i.e.  $\Delta Q_S \approx Q^* - [Q_H + Q_E]$ ) The instruments are located at approximately twice the height of their surrounding roughness elements, within relatively homogenous land cover fetches (extending outwards to approximately  $\geq 1 \text{ km}^2$  radius from the flux towers); thus are assumed to be making observations within the inertial sub-layer and are representative of the neighbourhood type in which they are located. The flux data are provided as half-hourly averages for each of the flux terms, and have been shown to correspond well with SUEWS simulations forced with off-site meteorological data previously run for Dublin (Alexander et al., 2015).

##### 3.2.2. Land cover scenarios

The land cover data used here are based MOLAND scenarios for Dublin up to 2026 (see Brennan et al., 2009 and Williams,

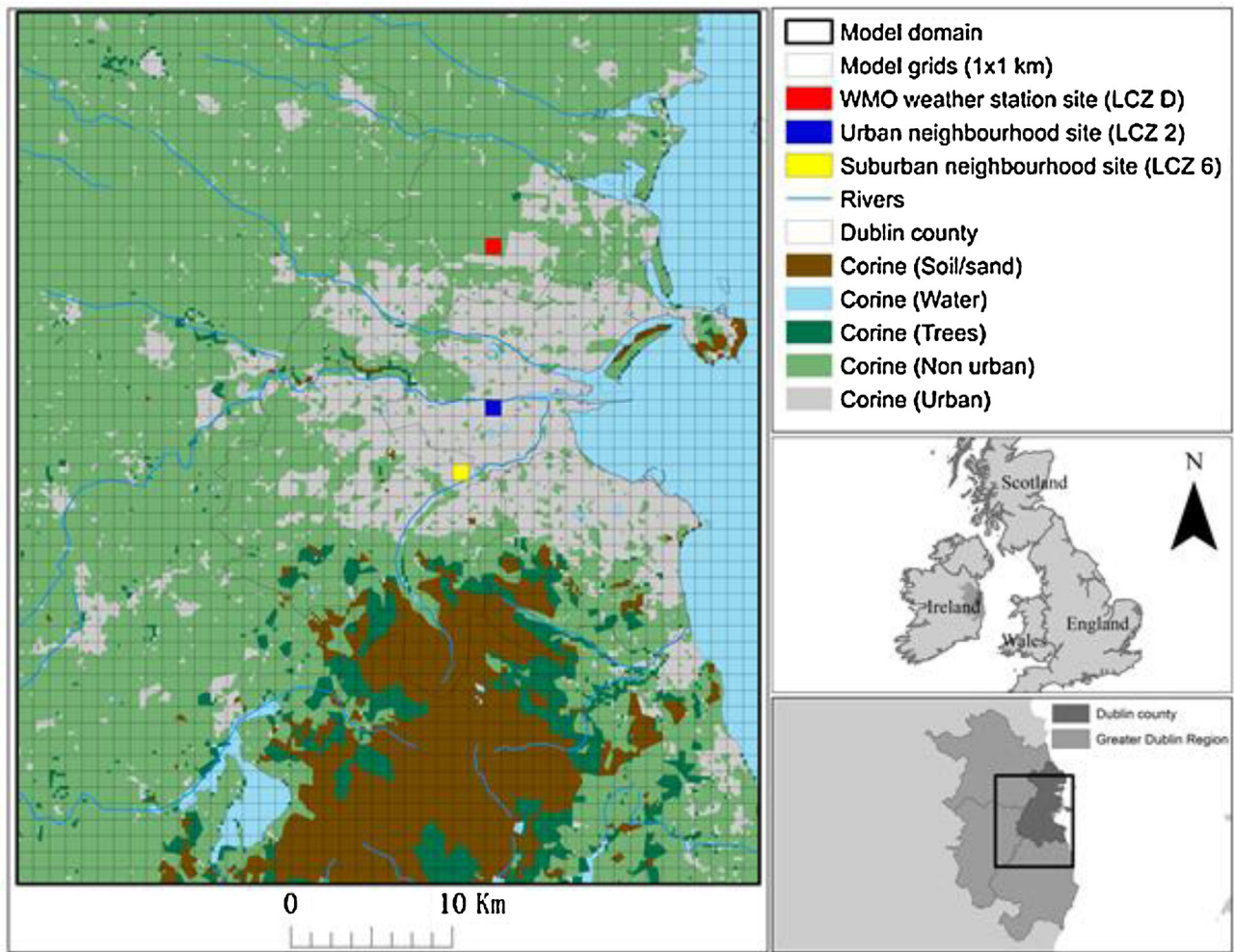


**Fig. 3.** Study area overview. Main image shows the model domain and grids. LULC classes from CORINE were combined to show urban -v- non urban extent. The grids highlighted in blue and yellow represent the two neighbourhoods (inner city and southern suburb respectively) used to evaluate the models' accuracy in previous studies, and the red grid shows the location of the synoptic station used to force all model simulations. (For interpretation of the references to colour in this figure legend, the reader is referred to the web version of this article.)

Shahumyan, Boyle, Convery, & White, 2012 for further details). The MOLAND cellular automata model is discussed in detail by Barredo, Kasanko, and Lavalle, 2013 however, a summary of the scenarios utilised in this study and how these were converted into land cover parameters required by SUEWS are given below.

The development scenarios used in this study are illustrated in Fig. 4. In total four scenarios were examined which are differentiated by different policy priorities and hence, development pathways pursued in order to adhere to the policy chosen. The policies informing the scenarios can be divided into two broad categories; (1) those based on current regional planning guidelines which emphasise strategic green belts between the Dublin metropolitan area and surrounding satellite towns, we refer to this development pathway as urban-densification; (2) consolidation of the metropolitan footprint (MF) with surrounding urban areas by expansion along transport corridors, we refer to this development pathway as urban-expansion (sprawl). Table 4 provides additional details on each of the four development pathway (DP) scenarios, to summarise;

- (i) DP-1; business as usual development based on recent trends.
- (ii) DP-2; urban-expansion along transport corridors.
- (iii) DP-3; urban-consolidation with strategic satellite towns.
- (iv) DP-4; urban-densification of existing MF and satellite towns.

The majority of all planned development in each DP are residential areas, which reflects the increasing demand for housing within the case study area and the density of urban coverage is determined by the population projections. Local planning regulations place restrictions on high-rise development, hence these land cover types are not included in the projections by MOLAND. In order to translate the different land cover classes utilised in the scenarios to a format usable by SUEWS (fractional coverages of buildings/pavements/vegetation/trees/water/unmanaged soils) we took the following approach:

1. The MOLAND land-use land-cover (LULC) classes were spatially correlated with a pre-existing LCZ map for Dublin. After we established a link between MOLAND and LCZ LULC we converted each MOLAND LULC between 2006 and 2026 into a corresponding LCZ code.
2. Model grids (1 km<sup>2</sup>) were then coded into LCZ based on a majority rule (see Fig. 5) and assigned fractional coverage based on the values given in Table 5. These values, obtained from Alexander et al. (2015), were generated by randomly sampling LCZ across Dublin and deriving a more precise fractional value for each cover type per LCZ.
3. To incorporate densification as a development policy into the model's land cover based on DP-4, the land cover fractions and

**Table 3**  
INPUT requirements of SUEWS model (\*) indicates inputs which were used in this study.

Variable	Units	Used in this study marked with*	Comments
<b>Meteorological</b>			
Air temperature ( $T$ )	°C	*	
Relative humidity (RH)	%	*	
Pressure ( $P_r$ )	kPa	*	
Precipitation ( $P$ )	mm h <sup>-1</sup>	*	
Wind speed ( $V$ )	m s <sup>-1</sup>	*	
Incoming short wave ( $K_{\downarrow}$ )	W m <sup>-2</sup>	*	
Incoming long wave ( $L_{\downarrow}$ )	W m <sup>-2</sup>		Optional (otherwise uses $T$ and RH)
Observed sensible heat ( $Q_H$ )	W m <sup>-2</sup>		Optional
Observed latent heat ( $Q_E$ )	W m <sup>-2</sup>		Optional
Observed storage heat ( $\Delta Q_S$ )	W m <sup>-2</sup>		Optional
Cloud fraction	Tenths	*	Optional
Soil moisture deficit (SMD)	m <sup>3</sup> m <sup>-3</sup>	*	Optional
Leaf area index (LAI)		*	Optional
<b>Anthropogenic inputs</b>			
Anthropogenic heat ( $Q_F$ )	W m <sup>-2</sup>	*	Optional, hourly values (otherwise modelled)
Anthropogenic water use	%		Optional, hourly ratio of total diurnal usage
<b>Surface inputs</b>			
Fractional coverage of surface types ( $\lambda$ )	%	*	Urban, pavement, soil, grass (irrigated and un-irrigated), trees (coniferous and deciduous) water
Surface area	Ha	*	
Water usage area	Ha		Optional
Latitude/longitude	°	*	
Storage capacity of pipes	mm		Optional
Frontal area fractions			Optional, buildings and trees separate
Roughness length for momentum ( $z_0$ )	m		Optional
Zero displacement height ( $z_d$ )	m		Optional
Surface element heights	m	*	Optional, buildings and trees separate

building heights for several urban LCZ were modified for the DP-4 model run.

While high-rise development (and very sparse urban development) are excluded from this case study, in other domains where local regulations do not prohibit this type of urban land cover a wider range of LCZ could be tested using this approach.

### 3.2.3. Anthropogenic Data

SUEWS is capable of simulating the addition of local scale anthropogenic heat ( $Q_F$ ) utilising specified population density per grid and a daily mean  $Q_F$  value, which is adjusted based on a diurnal energy use profile. The population density per grid was obtained from the national census of Ireland (C.S.O., 2012). Population density extrapolated for 2026 was based on the population growth trends from previous census statistics—see Table 5. For the model simulations, weekday and weekends are differentiated with two separate hourly  $Q_F$  profiles. The weekday profile assumes an increase in  $Q_F$  from 05:00 h (local time) through to 09:00 h associated with typical commuting patterns and business activity hours. A second peak occurs between 17:00 h and 18:00 h associated with traffic flows leaving the city, with a gradual-steady decline thereafter. The weekend profile is similar, but has no peak around the

so-called rush hours, rather a steady increase and consistent  $Q_F$  throughout the day,  $Q_F$  declines at 22:00 h rather than 17:00 h which is the case for the weekday profile. An estimate of annual  $Q_F$  was obtained from a lookup Table (Flanner, 2009) and was then weighted for each month.  $Q_F$  was set to be slightly lower in summer months (May–September) than the winter months to reflect reduced space heating demand in summer/increased heating in winter and increased car usage etc. as would be expected for a middle-latitude city (Offerle, Grimmond, & Fortuniak, 2005).

## 4. Results

In the following sections, an analysis of the SUEWS simulations of local scale turbulent fluxes across each neighbourhood is given, focusing on how form (openset verses compact) and function impacts the local climate. Firstly, the impact of the four MOLAND development pathways (DPs) relative to the base line case (BLC) is analysed with respect to the annual and seasonal partitioning of available energy into sensible, latent and stored heat and the spatial distribution across the study area in each DP. To highlight the impact of each DP, we derived the sensible heat index ( $\chi$ :  $Q_H/Q^*$ ), the evaporation index ( $\gamma$ :  $Q_E/Q^*$ ), the storage index ( $\Lambda$ :  $\Delta Q_S/Q^*$ ) and the Bowen ratio ( $\beta$ :  $Q_H/Q_E$ ) since these have direct impact on

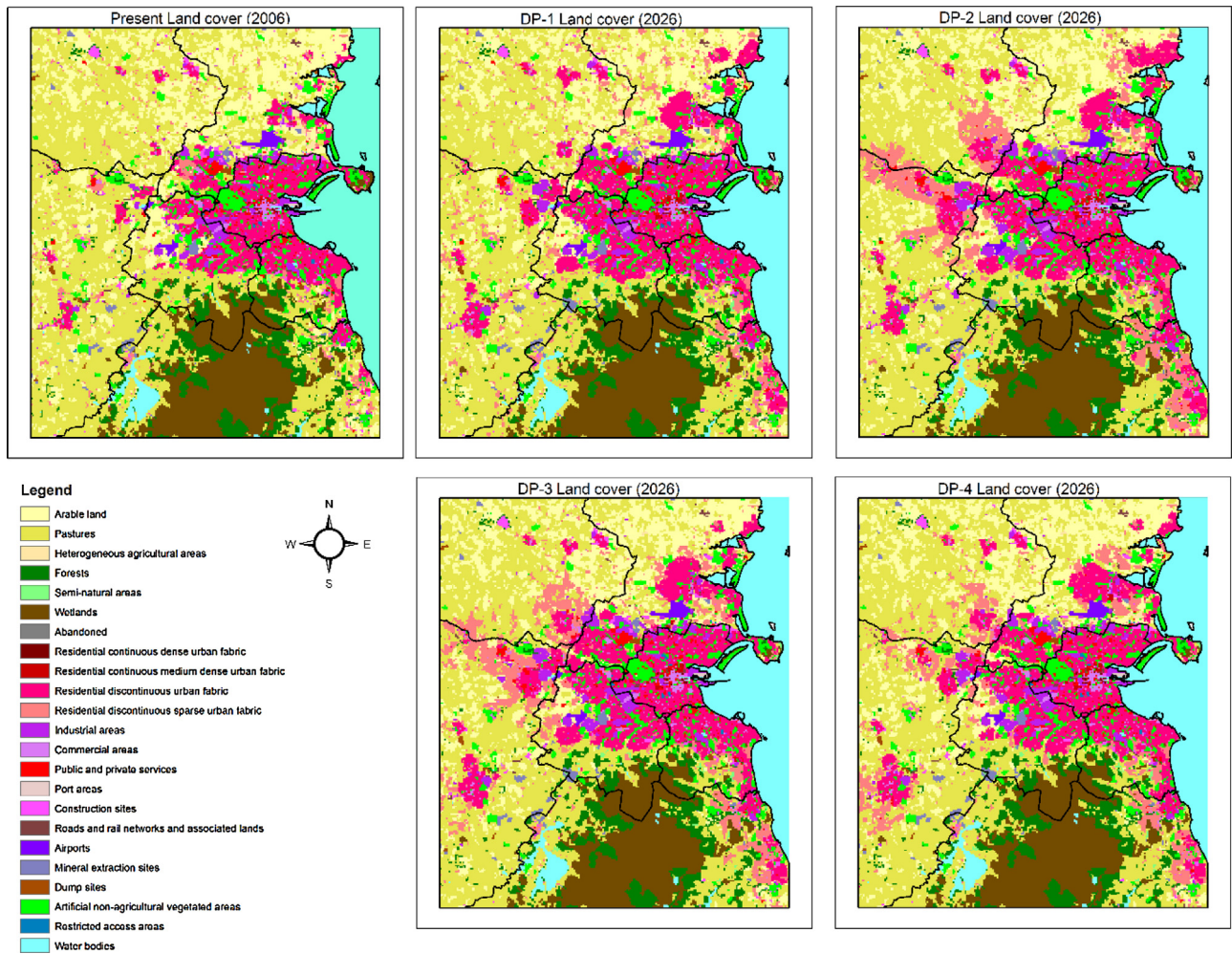


Fig. 4. Overview of present day CORINE land cover classes for study area (top left panel) with development pathway scenarios 1–4—see text/ Table 4 for more details.

Table 4

Outline of the development pathway (DP) scenarios utilised in this study. Further details are provided in Brennan et al. (2009). Urban extent is defined as % of modelled grids that are classed as urban Local Climate Zones (LCZ) the % in parenthesis is the increase in urban LCZ from the 2006 base line case—see Table 4 and Fig. 3.

Scenario short name	Alias	Description	Urban extent
DP-1	Business as usual	As the alias suggests, this scenario explores a continuation of the current, dispersed settlement patterns. Therefore, this pathway simulates a “business as usual” future, whereby implementation of pre-existing development policies has been weak. Reflecting the current economic climate, several transportation projects are delayed in this scenario until 2020. With the divergence of policy and practice concerning Green Belts in mind, this scenario does not contain a greenbelt layer as outlined in Brennan et al. (2009)	19.8% (+6.1%)
DP-2	Undirected sprawl	In this scenario development is strongly directed toward an expanded metropolitan footprint (MF), which is extended along key transport corridors. Strictly enforced Strategic Green Belts are used to discourage excessive development in rural areas and link protected areas together. Two types of Green Belts were created; large Outer Green Belts designed to designate areas where development should be kept to a minimum; and smaller Connector Green Belts, designed to preserve links between urban green space and rural areas	25.8% (+12.1%)
DP-3	Directed Sprawl	This scenario explores a strong consolidation policy, whereby growth was focused within the existing envelope of the MF and towards a limited number of key towns in the Hinterland. Increased densities were delivered by infilling areas within the MF and in the main towns of the Hinterland. Green Belts were more extensive and strategically placed than DP-2	25.4% (+11.7%)
DP-4	Densification	In this scenario, consolidation is promoted; development is focused within the existing MF and development centres. Growth in the Mid-East at public transport nodes within the MF and in designated towns on high quality public transport routes. Although densification within the existing MF was a focus of this scenario, there was a drive to keep towns distinct from one another	23.2% (+9.5%)

**Table 5**  
MOLAND LULC classes converted into corresponding Local climate zones (LCZ) in the study area, the parenthesis in the LCZ column contains the number of grids (*n*) that are coded to that LCZ class for the BLC. Plan area fractions (given in % below) were obtained from Alexander et al. (2015). Population are given as persons per km<sup>2</sup>, the values in parenthesis in this column represent population in 2026. The final row illustrates % changes for 2026 for LCZ 2 DP-4 only.

MOLAND LULC	LCZ Name "Code"	Built	Impervious	Unmanaged	Trees	Grass	Water	Population
			Urban LCZ ( <i>n</i> = 342)					
Residential continuous medium dense urban fabric; Commercial areas; Public and private services	2 Compact midrise "LCZ 2" (12)	33	55	00	06	06	00	10130.2 (11981.0)
Residential continuous dense urban fabric	3 Compact lowrise "LCZ 3" (1)	22	61	00	07	10	00	3867.6 (4574.2)
Port areas; Roads and rail networks and associated lands	5 Open midrise "LCZ 5" (1)	13	48	00	11	28	00	2335.2 (2761.8)
Residential discontinuous urban fabric; Residential discontinuous sparse urban fabric	6 Open lowrise "LCZ 6" (270)	14	52	00	11	23	00	3887.9 (4598.2)
Industrial areas; Construction sites; Airports; Mineral extraction sites	8 Large lowrise "LCZ 8" (58)	30	61	00	04	05	00	1380.7 (1633.0)
			Non-Urban LCZ ( <i>n</i> = 2142)					
Forests; Semi-natural areas	A Dense trees "LCZ 101" (104)	01	02	04	48	45	00	48.3 (57.1)
Arable land; Pastures; Heterogeneous agricultural areas; Dump sites; Artificial non-agricultural vegetated areas; Restricted access areas	D low plant "LCZ 104" (1492)	03	08	03	18	67	00	185.5 (219.4)
Wetlands	F bare soil/sand "LCZ 105" (245)	06	20	55	19	00	00	0.0
Water bodies	G water "LCZ 107" (301)	00	00	00	00	00	100	0.0
	2 compact midrise (DP4)	+11	-5	-	-3	-3	-	

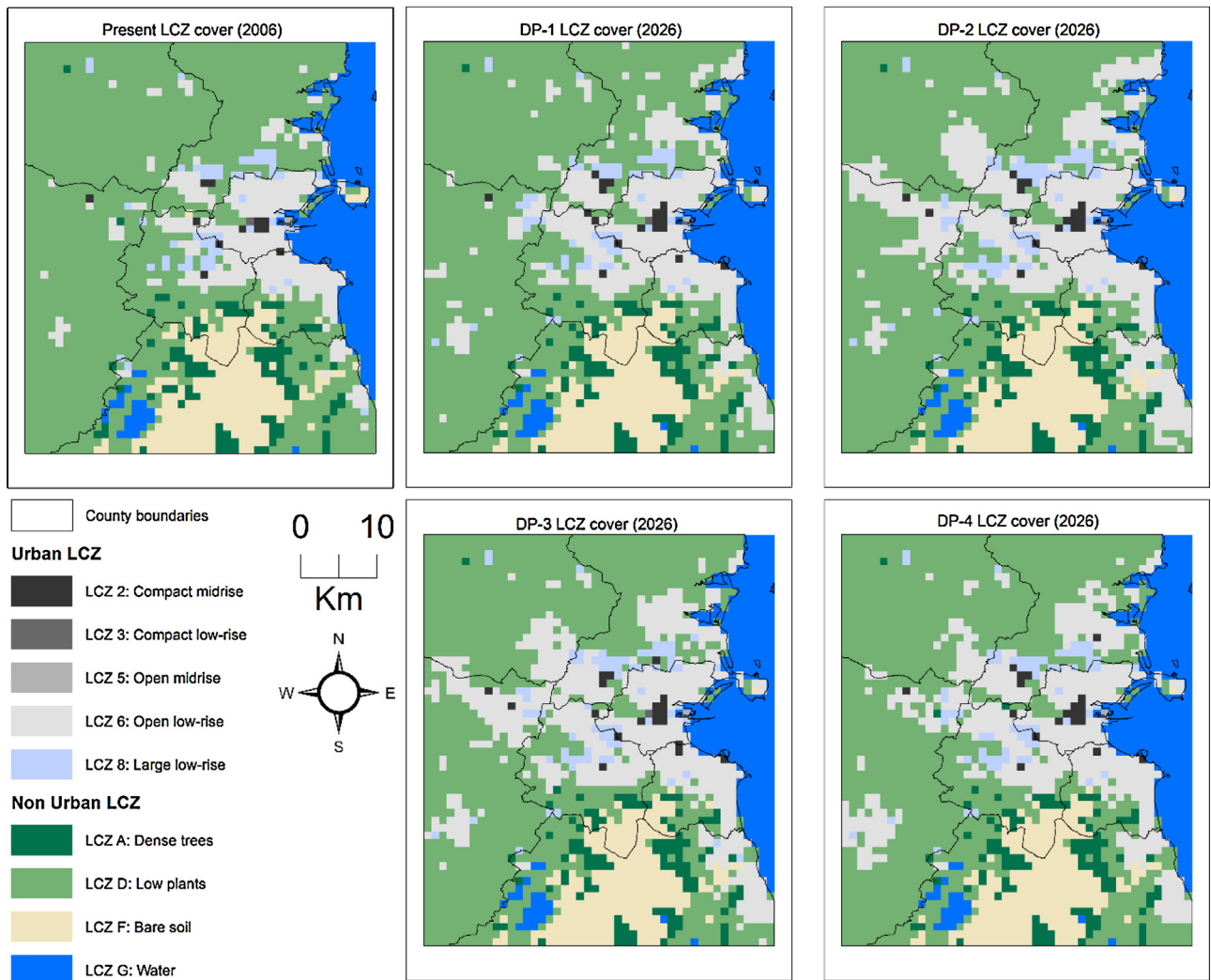


**Fig. 5.** Overview of model treatment of development pathway scenarios. Development pathways (DP-1 to DP-4) are detailed in Table 4 and in text. LCZ fractional coverages are given in Table 5. Each grid is coded into LCZ based on majority rule.

the local climate (Table 2). The diurnal profiles of each local climate zone (LCZ) class are then discussed in relation to areas which undergo urban development in each of the four DPs. An assessment of urban design interventions designed to reduce the amount of energy challenged into sensible and stored heat are then presented.

#### 4.1. Annual and seasonal flux variation

The annual magnitude of sensible heating for LCZ 2 was 60.52% compared to 55.82% and 53.98% for LCZ 6 and LCZ D respectively in the BLC. The impact of DP1-3 was to increase sensible heating by 2.7% and by 7.0% in DP4 for LCZ 2 areas. The increase in LCZ 6 and LCZ D was the same for all DPs, 1.2% and 0.1% respectively. Mean heat storage for non-urban LCZ in the BLC was 16.04–19.03% excluding water bodies which as expected were a significant store of energy (for water bodies, LCZ F, 26.54% of incoming energy was stored on average). LCZ 2 had an annual value of 53.02% which was higher than the most abundant non-urban LCZ class (LCZ D) value which only stored 19.03% of available energy. For LCZ 6, which is spatially related to residential areas, heat storage was 31.95%. This ranking (highest to lowest energy store) was maintained across all DPs, though there was a slight difference. In DP1-3 LCZ heat storage increased by ~3% for LCZ 2 (inner city areas) and by 1% for LCZ 6 (residential suburban areas) whereas for DP4, storage was decreased

by ~2% from the BLC, the increase for LCZ 6 was the same as DP1-3. This LCZ relationship relates to the urban heat island, leading to warmer air temperatures in compact areas of the city compared to vegetated areas and has been demonstrated previously (Alexander & Mills, 2014; Graham, 1993; Sweeney, 1987). The differences in the annual mean values in terms of the amount of energy for surface/air heating and evapotranspiration in each LCZ type are illustrated in Fig. 6a. In all DP scenarios, the presence of water and vegetated LCZ reduced the annual magnitude of sensible heating and heat storage and increased the annual magnitude of evapotranspiration thus decreasing daytime and nighttime temperatures and reducing surface runoff as more energy was used for evaporation.

The seasonal differences between LCZ in each DP was similar to the annual partitioning of energy, although there was a greater distinction during the summer and winter period in terms of differences in mean  $Q_H$  and  $Q_E$  respectively—Fig. 6b. During the summer period, mean  $Q_H$  was 82.7, 70.2 and 66.9  $W m^{-2}$  for LCZ 2, 6 and D respectively. In winter, mean  $Q_H$  was 34.4, 22.3 and 11.2  $W m^{-2}$  for the same three classes. Hence, there was a larger difference in sensible heat in winter between LCZ 2 and D than in summer. The opposite relationship existed between these LCZ for evapotranspiration, where the difference in summer was greater compared to winter as expected.

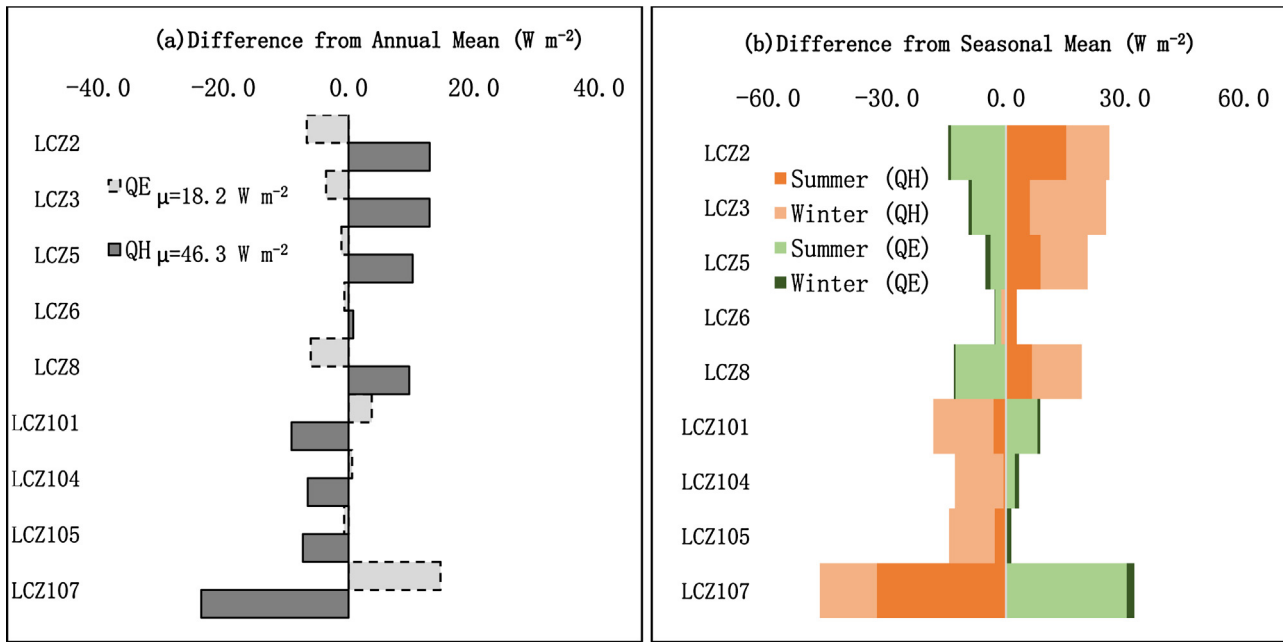


**Fig. 6.** (a) Difference from annual mean  $Q_H$  and  $Q_E$ , this is the mean value taken across all LCZ types, positive values indicate above average annual flux magnitude, in the case of sensible heat, this indicates higher surface/air heating. Negative values indicate below average annual flux magnitude. (b) Differences as with (a) however the values are further divided into seasonal  $Q_H$  (orange shades) and  $Q_E$  (green shades). Note the width of the individual color bars indicates the value above (+) or below (-) average for each season. For example,  $Q_H$  for LCZ 101 in summer is  $-3.2 \text{ W m}^{-2}$  and  $-15.2 \text{ W m}^{-2}$  in winter. (For interpretation of the references to colour in this figure legend, the reader is referred to the web version of this article.)

**Table 6**

Proportioning of  $Q^*$  ( $\chi, \gamma, \Lambda$ ) and the Bowen ratio ( $\beta$ ) when  $Q^* \geq 0 \text{ W m}^{-2}$ . Presented are unit-less flux ratios for annual and seasonal partitioning.

LCZ Code	$\chi(Q_H/Q^*)$			$\gamma(Q_E/Q^*)$			$\Lambda(\Delta Q_S/Q^*)$			$\beta(Q_H/Q_E)$		
	Ann	Sum	Win	Ann	Sum	Win	Ann	Sum	Win	Ann	Sum	Win
LCZ2	0.675	0.572	1.024	0.115	0.103	0.178	0.507	0.465	0.634	5.884	5.541	5.764
LCZ3	0.568	0.449	0.953	0.139	0.133	0.195	0.323	0.397	0.042	4.098	3.368	4.882
LCZ5	0.591	0.499	0.896	0.168	0.166	0.215	0.265	0.346	-0.038	3.522	3.001	4.160
LCZ6	0.573	0.507	0.771	0.192	0.196	0.227	0.330	0.357	0.226	2.976	2.586	3.401
LCZ8	0.563	0.468	0.873	0.115	0.107	0.171	0.236	0.332	-0.115	4.901	4.387	5.102
LCZ101	0.515	0.504	0.512	0.268	0.282	0.255	0.158	0.211	-0.033	1.921	1.787	2.005
LCZ104	0.544	0.519	0.593	0.228	0.239	0.236	0.187	0.237	0.014	2.383	2.176	2.515
LCZ105	0.516	0.489	0.573	0.205	0.216	0.213	0.223	0.277	0.036	2.513	2.262	2.688
LCZ107	0.241	0.214	0.308	0.339	0.396	0.249	0.264	0.338	0.002	0.713	0.541	1.239

The annual and seasonal differences in energy partitioning between LCZ are summarised in Table 6. Generally the ratio of turbulent fluxes to available energy is consistent with previous work (Grimmond & Oke, 1995; Keogh et al., 2012; Ward, Evans, & Grimmond, 2014). For urban LCZ, the available energy was predominantly channelled into surface/air heating and heat storage (annual sensible heat ranged from 56 to 68%; evapotranspiration ranged from 10 to 19% and heat storage ranged from 24 to 50%) whereas for the non-urban LCZ a higher fraction of the available energy was partitioned into evapotranspiration (annual sensible heat ranged from 24 to 50%; evapotranspiration ranged from 20 to 34% and heat storage ranged from 16 to 26%). There was also a seasonal pattern to the Bowen ratio (the relationship between  $Q_H$  and  $Q_E$ ) found in all LCZ. All areas showed lower  $\beta$  values in summer relative to winter, meaning a slightly higher proportion of turbulent exchange was channelled into evapotranspiration during summer months.

4.2. Spatial differences between different development pathways

To examine the spatial variation between DPs impact on the BLC, the annual average of each of the indices were calculated in each

grid cell (Fig. 7) based on hourly values across the entire TCY. To assess the impact relative to the BLC, differences on a grid-by-grid basis were calculated by subtracting the annual mean of the BLC from each of the DPs. To examine significant spatial clustering of differences from the BLC, Getis-Ord  $G_i^*$  (Getis & Ord, 1992; Ord & Getis, 1995) was employed which compares local averages to the global averages. In this case,  $G_i^*$  illustrates where there are spatial clustering of increases and decreases in the turbulent fluxes relative to the BLC—see Fig. 7. This reveals the geographical impact of each DP and identifies specific areas ideal for planning interventions. The partitioning of the annual fluxes for the LCZ classes follows what would be expected in each of the DP scenarios, grids which contain highly urbanised land cover (for instance the compact LCZ 2 and 3) exhibited the highest annual value of sensible heating and heat storage and the lowest annual magnitude of evapotranspiration concentrated around the inner city, whereas grids containing a higher vegetative fraction exhibited comparatively lower values of sensible heating and heat storage and higher evapotranspiration.

As expected, the sprawling scenarios (DP2 and DP3) exhibited the largest spatial increase (that is, the number of areas with higher annual values compared to the BLC) in sensible heating and heat storage coupled with the largest decrease in evapotranspi-

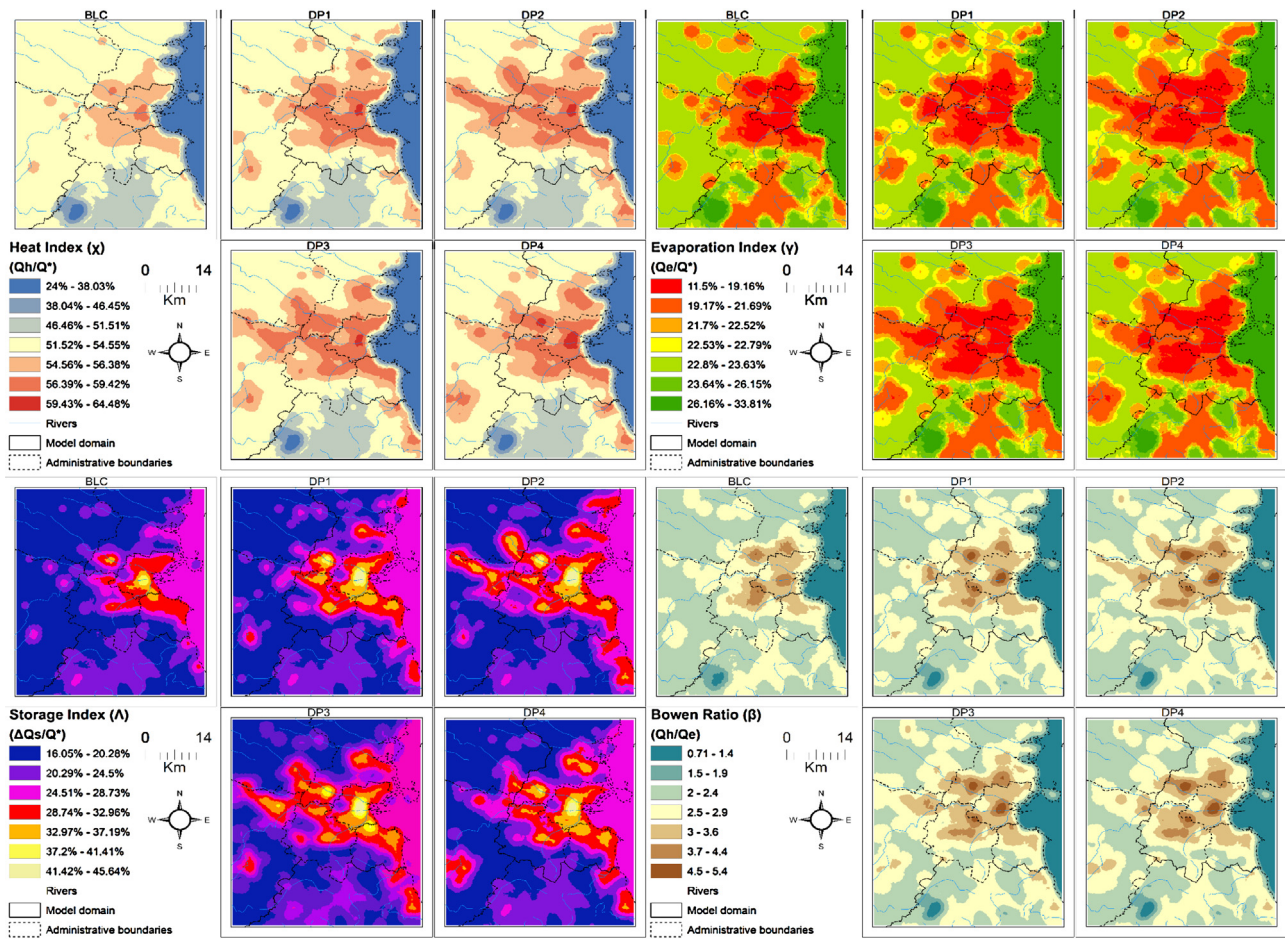


**Fig. 7.** Impact indices for BLC and DPs 1–4. Top left is the heat index ( $\chi$ ) which is the proportion of available energy used for surface/air heating. Top right is the evaporation index ( $\gamma$ ) which is the proportion of energy used for evapotranspiration. Bottom left is the storage index ( $\Lambda$ ) which shows the proportion of available energy stored in the substrate (buildings/pavements/soils), this effectively shows the potential UHI extent. Bottom right is the Bowen ratio ( $\beta$ ) which is the relationship between the heat and evaporative index, a higher number indicates more energy is used for surface/air heating meaning less water is evaporated hence is available for runoff.

**Table 7**

The number of areas (as % of total model domain) with higher/lower annual values of  $\chi$ ,  $\gamma$  and  $\Lambda$  relative to BLC broken down into each DP. Note DP4 has the lowest net spatial impact meaning increases in one part of the city are offset by decreases in other parts.

Development pathway	Net spatial increase/decrease compared to BLC ( $\Sigma_{\text{Increase}} - \text{Decrease}$ )	Significance level					
		+99%	+95%	+90%	−90%	−95%	−99%
<b>DP1</b>							
Heat index $\chi$ ( $Q_H/Q^*$ )	8.9%	4.8%	4.9%	0.2%	0.0%	0.0%	1.0%
Evaporation index $\gamma$ ( $Q_E/Q^*$ )	−2.2%	1.3%	0.3%	0.7%	0.9%	1.7%	1.9%
Storage index $\Lambda$ ( $\Delta Q_S/Q^*$ )	7.7%	7.9%	0.4%	0.7%	0.8%	0.1%	0.4%
<b>DP2</b>							
Heat index $\chi$ ( $Q_H/Q^*$ )	12.1%	7.8%	3.4%	2.1%	0.0%	0.1%	1.1%
Evaporation index $\gamma$ ( $Q_E/Q^*$ )	−4.4%	1.5%	0.3%	0.7%	2.0%	2.4%	2.5%
Storage index $\Lambda$ ( $\Delta Q_S/Q^*$ )	14.9%	9.2%	2.1%	4.3%	0.1%	0.5%	0.1%
<b>DP3</b>							
Heat index $\chi$ ( $Q_H/Q^*$ )	12.9%	8.5%	2.7%	2.9%	0.0%	0.0%	1.2%
Evaporation index $\gamma$ ( $Q_E/Q^*$ )	−4.0%	1.4%	0.3%	0.6%	0.8%	2.5%	3.0%
Storage index $\Lambda$ ( $\Delta Q_S/Q^*$ )	14.9%	9.0%	2.8%	3.7%	0.5%	0.1%	0.0%
<b>DP4</b>							
Heat index $\chi$ ( $Q_H/Q^*$ )	0.1%	6.1%	0.1%	0.2%	3.1%	0.5%	2.7%
Evaporation index $\gamma$ ( $Q_E/Q^*$ )	0.0%	1.9%	0.3%	1.2%	0.2%	1.1%	2.1%
Storage index $\Lambda$ ( $\Delta Q_S/Q^*$ )	0.7%	5.6%	0.4%	0.4%	2.9%	0.2%	2.6%

ration (see Table 7). Taking the number of areas with increased sensible heating relative to the BLC; DP3 exhibited the largest spatial increase (increasing in 14.1% of the modelled area) followed by DP2 (13.3% increase in area), DP1 (9.9% increase in area) and finally DP4 (6.4% increase in area). When the number of grids with

decreases relative to the BLC were also taken into account, the ranking remained the same. The ranking for the number of areas with decreases in evapotranspiration were similar, however the number of areas in DP2 relative to the BLC was marginally higher than DP3 (6.9% and 6.3% respectively). Decreases in evapotranspiration were

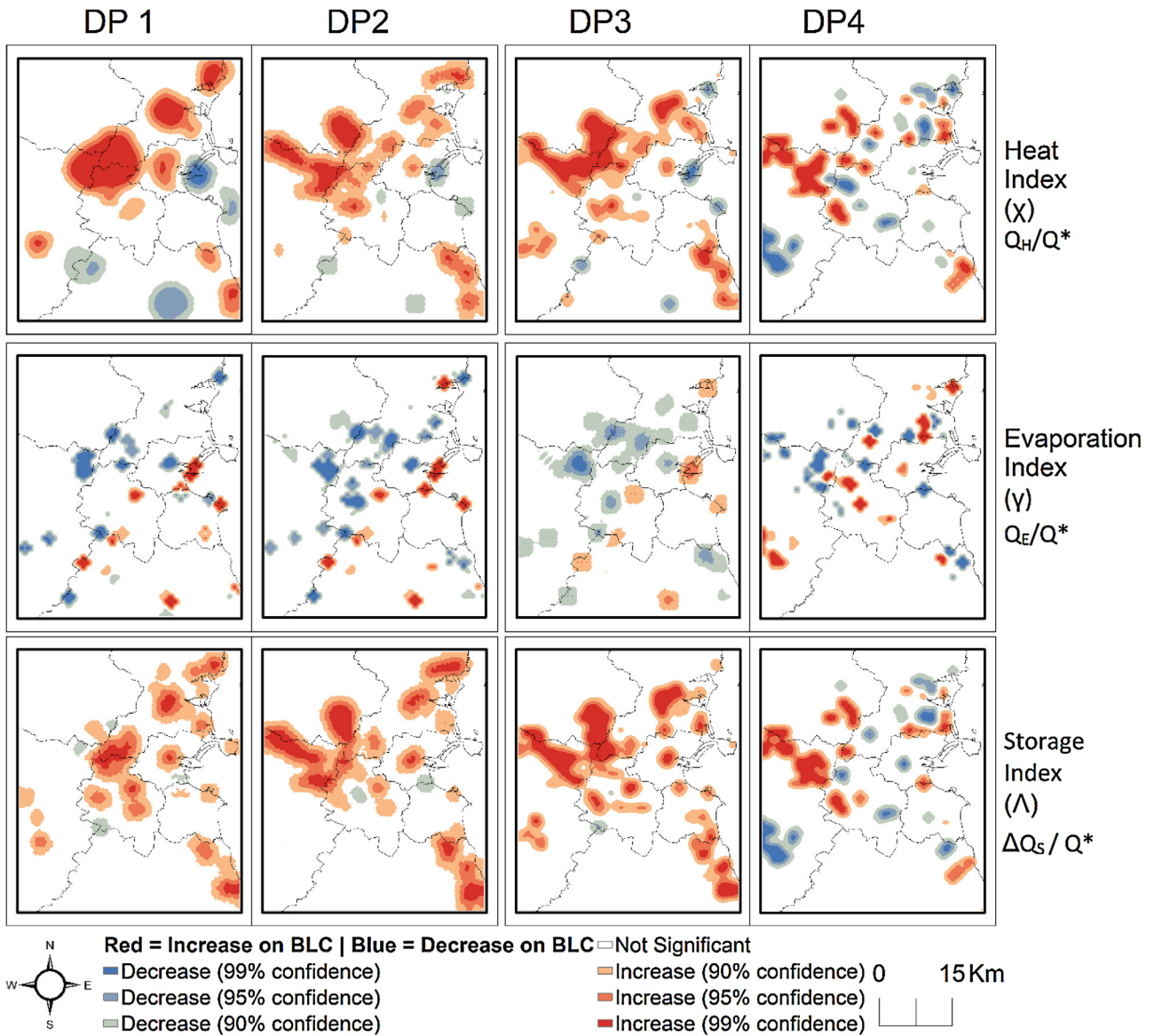


Fig. 8. Spatial distribution of increases/decreases in impact indices compared to BLC for each DP (columns). The differences are based on annual mean values.

greater in DP1 than DP4. For storage, which illustrates the potential of the UHI, the ranking was DP2 (15.6%) followed closely by DP3 (15.5%) then DP1 (9%) and DP4 (6.4%). Out of the four scenarios DP4 had the least impact in respect to the number of areas with surface/air temperature increases, evapotranspiration decreases and heat storage increases (Fig. 8).

To further investigate the spatial differences between DP scenarios, 3 subsets of the model domain were examined based on these impact hotspots (see Fig. 9) located around the inner city and 2 non-urban areas which became urbanised in each DP scenario. These were also used for examination of the diurnal energy profiles (Section 4.3). Within these subset areas, the type of development in each DP controlled the impact relative to the BLC. The replacement of LCZ D with LCZ 6 in the case of DP1–3 had the largest impact relative to BLC sensible heating. There were marginal increases in sensible heating and heat storage in the inner city where LCZ 3 was replaced with LCZ 2 in DP1–4. The impact on evapotranspiration was lower in LCZ 6 areas owing to their higher level of vegetation compared to LCZ 2/3. In the suburban subsets, DP4 was again identified as having the least impact compared to DP1, 2 and 3.

In a study by Demuzere, Oleson, Coutts, Pigeon, and van Lipzig (2013) which simulated the impact of different urban environments on the surface energy balance, a similar energetic-hierarchy was found between compact and open-set residential thermal climate zones, which are an earlier iteration of the LCZ 2 and LCZ 6 classes respectively. The reduction in vegetation fraction leads to a minor decrease in evapotranspiration though the larger impact is found in terms of heat storage as the heat capacity of these areas significantly increases due to the additional buildings and pavements. Work by Stewart et al. (2014) which examines the impact of this hierarchy on air temperatures differences across LCZ, highlights the impact of this on the UHI and diurnal temperature range across different LCZ.

4.3. Impact of development on seasonal diurnal fluxes

Fig. 10 illustrates the findings related to seasonal differences in energy budgets within the subset areas due to land cover change. For the inner-city subset, compact low-rise areas (LCZ 3—Fig. 10c) in the BLC were replaced with compact mid-rise areas (LCZ 2—Fig. 10a)

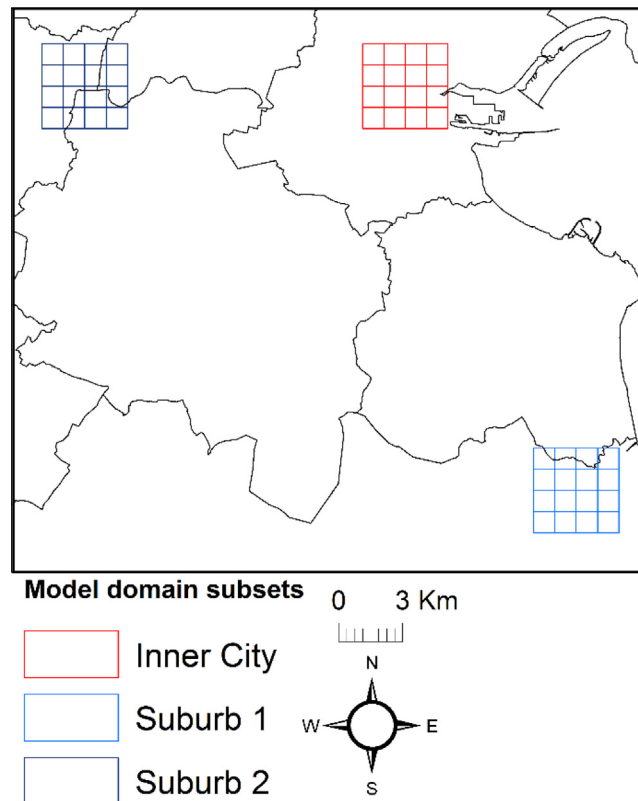


Fig. 9. Illustration of the domain subsets for detailed analysis of change in each DP and diurnal analysis (Section 4.2).

in each of the four DP scenarios. The most distinguishable effect of this was to increase heat storage during both winter and summer and introduce significant hysteresis into the energy budget around these areas. Note for instance, LCZ 3 (BLC) the close temporal correspondence between available energy and heat storage in terms of the diurnal profile, whereas for LCZ 2 (DPs) a lag of 6 h between the time available energy and heat storage both reach a minima value. We hypothesise that due to decreased Sky View Factor ( $\Psi$ ), increased height to width ratio (H/W) and decreased effective albedo, which are parameterised in the LCZ concept, heat withdrawal became less efficient across the inner-city urban subset in each DP scenario relative to the BLC. This applied for both winter and summer.

For the suburban subsets, vegetated areas with low plant cover (LCZ D—Fig. 10d) were replaced with residential areas (LCZ 6—Fig. 10b) in each of the DP scenarios, though the number of areas in the subset varied between DP1–4. In cases where LCZ D was replaced with LCZ 6, the impact during winter was an increase in surface/air heating during all hours, though the increase was slightly higher during daylight hours. Heat storage was increased by during daylight hours. There was little distinction in evapotranspiration though it was marginally higher for LCZ 6.

During the summer, daytime surface/air heating in the urban subset increased significantly at midday. Evaporation during the day was reduced. In the suburban subsets, the largest impacts were on heat storage, which increased significantly at midday, and a reduction in evapotranspiration for all daylight? hours similar to winter, though there was a tenfold increase in the difference during summer.

#### 4.4. Design interventions for low impact development

Based on the previous sections, DP4 had the least impact on the annual, seasonal and spatial fluxes across the model domain

across all scenarios considered. Therefore, we define this as the optimum growth pathway in terms of reducing the spatial impact on the local climate. To examine how sustainable design might be coupled with this type of growth to further reduce the impact on the UEB, several design interventions were tested using DP4 as the growth scenario—see Table 8. The first design intervention was simply to rebalance the ratio of vegetated to paved areas and modify the type of tree species. The second design intervention was to reduce the overall building footprint by instead promoting upward development. Therefore, building heights were modified and expansive green spaces encouraged, as with the first intervention, tree species were modified however an equal mix of deciduous and coniferous trees were used. The third intervention was an extension of this, however additionally roof tops for all buildings were greened. The aim was to reduce the seasonality in evapotranspiration i.e. increase energy partitioning into evapotranspiration during winter and decrease annual fluxes of surface/air heating and heat storage relative to LCZ D areas in the BLC.

The first design intervention is the most modest, in that it simply controls the type and level of vegetation in future developments, specifically, the replacement of LCZ D with LCZ 6. The result was to reduce the impact of urban development on summertime evapotranspiration by 34.0%. Both the second and third design interventions which further modified the coverage and type of buildings reduced the impact further. The second design reduced the impact on summertime evapotranspiration by 47.7%, the third design reduced the impact by 52.2%.

The impact of urban development on the annual magnitude of surface/air heating was reduced by 30.1%, 37.5% and 38.6% in design 1, 2 and 3 respectively, the impact on heat storage was reduced by 7.9%, 15.8% and 21.7%, meaning the green roof design reduced the impact of urban development the most.

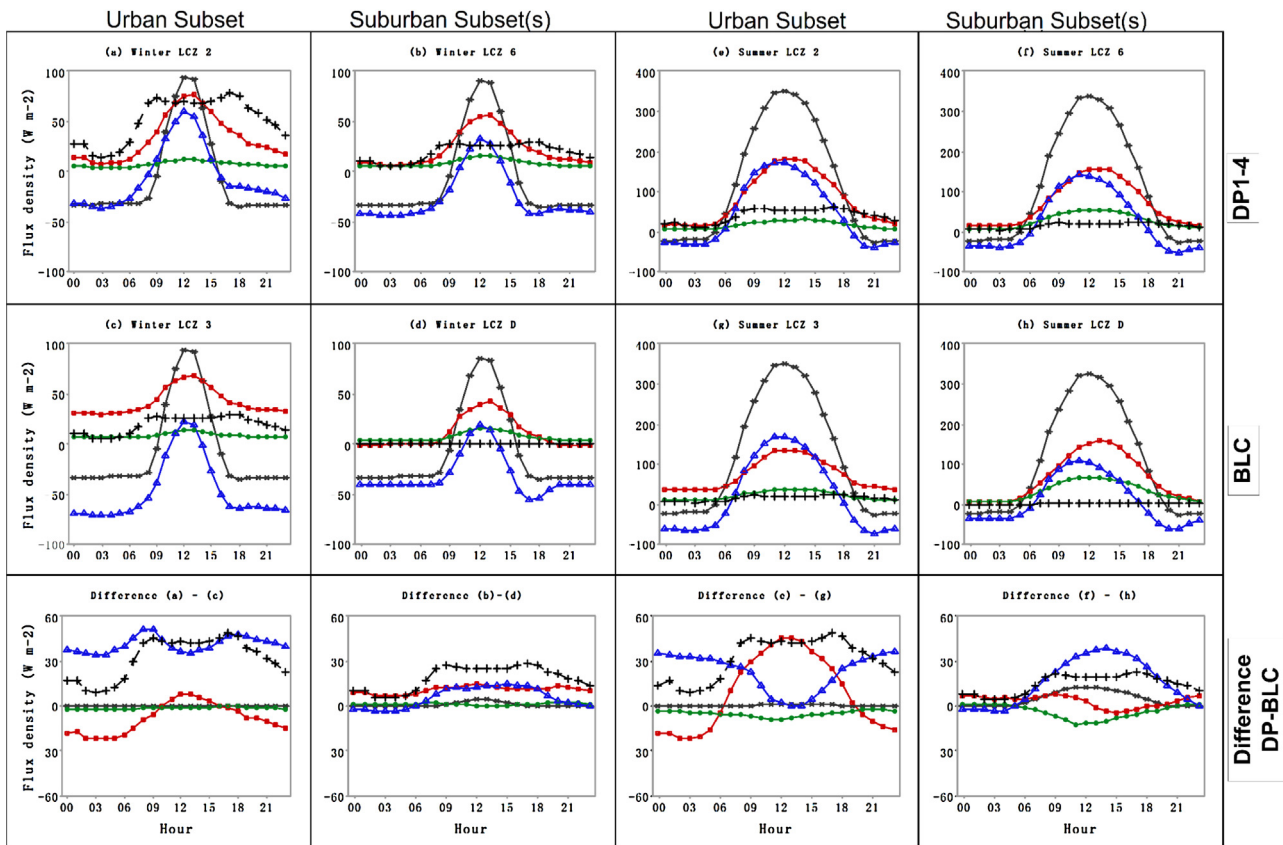


**Fig. 10.** Seasonal diurnal profiles for dominant LCZ in BLC (2nd row) and DP scenarios (1st row). The first 2 columns show winter diurnal profiles; the last 2 columns show summer profiles. The 3rd row illustrates the difference in the first 2 rows in each column. Stars (\*) show  $Q^*$ , squares (□) show  $Q_H$ , circles (○) show  $Q_E$ , triangles (Δ) show  $\Delta Q_S$  and crosses (+) show  $Q_r$ . The impact (final row) from left to right can be interpreted as follows: (1) increased heat storage in the inner city and higher anthropogenic heat source in winter (2) in the suburbs, increased heat storage (UHI) and surface/air heating day and night in winter (3) increased surface/air heating during the daytime hours in the inner city during summer (4) increased heat storage and surface/air heating in summer in suburbs during summer.

## 5. Discussion

The impact of neighbourhood form and development on the urban energy budget (UEB) was examined under 4 distinct development scenarios in order to examine the optimum development pathway for Dublin city. The UEB was examined in terms of spatial changes due to urbanisation (primarily on the existing urban fringes), the seasonal differences in sensible, latent and stored heat and the impact on the diurnal profiles in different areas. Employing the local climate zone (LCZ) scheme allowed for this examination and provides useful guidance (Stewart & Oke, 2012). However as with most urban areas, individual areas though similar in form and function will differ (i.e. intra-LCZ differences) somewhat in terms of specific fractional coverages of vegetation, buildings and pavements. The use of very high resolution data, for example individual building footprints, heights, trees derived from a LIDAR system, would have allowed for examination of the UEB in greater detail and address the limitation of treating all LCZ areas equally. However, in data starved settings for example, cities in the economically developing countries, such an approach is not feasible, therefore this approach was not employed here. Moreover, there has been a recent call for standardisation in how urban areas are described in order to allow for more robust inter-city comparisons with respect to climate, impacts on human comfort, pollution and urban development (Ching, 2013; Bechtel et al., 2015).

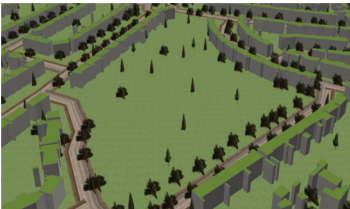
While the replacement of natural, vegetated landscapes with artificial materials associated with urban areas will inevitably impact upon the surface energy budget the results here illustrate that the type of urban development plays a significant role on this

impact at the local scale, moreover seasonal considerations should be taken into account. The densification (i.e. upward development) of existing urban plots was shown to increase winter time storage of heat, thus reducing the level of temperature changes within these areas (sensible heat). However, this will lead to increased levels of heat released back into the atmosphere at night, which serves to enhance the urban heat island effect under the right synoptic conditions. During the summer months, daytime surface/air heat increased in these areas due to multiple reflectance (i.e. increased net radiation) which has major implications for daytime cooling requirements and human thermal comfort. Urban sprawl was shown to increase surface/air heating and heat storage significantly in both winter and summer, and decrease evapotranspiration in summer months. Again this has implications for energy use and human comfort thus strengthens the case for including such information in planning decisions. Moreover, since most of the projected development will occur along river basins, the decrease in evapotranspiration and increase in impermeability will increase runoff levels in these areas, creating a potential flood hazard. This strengthens the case for DP4 as being the DP with the lowest potential impact in terms of local climate.

The design interventions tested here focused on local scale mitigation of the impact on the UEB, undoubtedly such interventions will have a larger impact on the micro-to-building scale climate. The inclusion of coniferous vegetation in mid-latitude city such as Dublin (design intervention 1) served to reduce the seasonality of evapotranspiration which is lower in winter for deciduous vegetation (Lindberg & Grimmond, 2011; Peng & Jim, 2013) this in turn reduces the amplitude of surface/air heating during both win-

**Table 8**

Design interventions tested here. LCZ 6 areas in DP4 were modified as per description and the model re-run. Exemplar images in the first three rows are all existing locations for Dublin city.

GIS model of example area	Exemplar image of existing area	Description
		<b>BLC area (LCZ 6)</b> Area comprises Lowrise buildings ( $\mu = 2.45\text{m}$ ) 15% building cover 10% tree cover (all deciduous) and remainder split between pavements and unirrigated grasses
		<b>Design intervention 1</b> Buildings as with BLC area (above). Tree cover and unirrigated grasses are increased (5% each) replacing paved areas. Tree species are modified to be predominantly coniferous (80:20 split between coniferous and deciduous)
		<b>Design intervention 2</b> Building coverage is reduced by 5% height increased by 2.45m. Tree cover and unirrigated grasses are increased (2.5% each) replacing building areas. Trees are modified to be a mix of species (50:50 split between coniferous and deciduous)
		<b>Design intervention 3</b> As with design intervention 2, however additionally green roof design is introduced to all buildings. Unirrigated vegetation type used to modify OHM coefficients for storage. Albedo and emissivity values ( $\alpha$ , $\epsilon$ ) for building roof tops also modified

ter and summer months. The inclusion of green roof tops (design intervention 3) served to further reduce local scale partitioning of energy into both surface/air heating and heat storage which was the intended outcome. However, the decrease was similar in magnitude to the first design intervention. As such the justification for including this design feature into future planning may appear weak, however the multiple benefits of natural roofing material at different scales should also be considered and will be part of future work.

Overall the SUEWS model proved to be capable of reproducing the expected differences between urban and non-urban UEB when linked with LCZ and forced with off-site meteorological data,

thus enabling background climate data to be translated into urban specific data for identifying specific areas for planning/policy interventions.

## 6. Conclusion

The aim of this study was to investigate the optimum development pathway for a mid-latitude city with respect to reducing the spatial and temporal impact on the surface energy budget. Different policy priorities informing distinct development scenarios were examined. The MOLAND cellular-automata model was linked

with the SUEWS urban energy and water budget model, the local climate zone classification and meteorological data from outside the urban area.

Drawing from the results of this study, we conclude that the optimum development scenario is one which preserves a higher overall proportion of vegetated land cover. Such development inevitably leads to an increased proportion of energy channelled into sensible heating of the near surface atmosphere and additionally heat storage within the urban fabric across the domain.

Therefore, design interventions which aimed to reduce this impact locally were investigated. An effective solution is the inclusion of vegetation that is photosynthetically active throughout the summer months and remains active during the winter months which serves to promote energy uptake by vegetation and thus increase latent heating. We conclude that incorporating urban climate data into development and design processes where meteorological observations are otherwise absent is possible and allows for a range of development pathways and local scale impacts to be examined. Such applications serve to increase the incorporation of urban climate knowledge into the planning and design process which can ameliorate environmental conditions for the urban population and reduce the negative impacts of development.

## References

- Alcoforado, M. J., Andrade, H., Lopes, A., & Vasconcelos, J. (2009). Application of climatic guidelines to urban planning: the example of Lisbon (Portugal). *Landscape and Urban Planning*, 90(1–2), 56–65.
- Alexander, P. J., & Mills, G. M. (2014). Local climate classification and Dublin's urban heat island. *Atmosphere*, 5(4), 755–774.
- Alexander, P. J., Mills, G. M., & Fealy, R. J. (2015). Using LCZ data to run an urban energy balance model. *Urban Climate*, 13(3), 14–37.
- Balling, R. C., Cerverny, R. S., & Idso, C. D. (2001). Does the urban CO<sub>2</sub> dome of phoenix, arizona contribute to its heat island? *Geophysical Research Letters*, 28(24), 4599–4601.
- Barredo, J. I., Kasanko, M. M. N., & Lavallo, C. (2003). Modelling dynamic spatial processes: simulation of future scenarios through cellular automata. *Landscape and Urban Planning*, 6(3), 145–160.
- Bechtel, B., Alexander, Böhner, J., Ching, J., Conrad, O., Feddema, J., et al. (2015). Mapping local climate zones for a worldwide database of the form and function of cities. *ISPRS Int. J. Geo-Inf.*, 4(1), 199–219. <http://dx.doi.org/10.3390/ijgi4010199>
- Brager, G. S., & de Dear, R. J. (1998). Thermal adaptation in the built environment: a literature review. *Energy and Buildings*, 27(1), 83–96.
- Bramley, G., & Power, S. (2009). Urban form and social sustainability: the role of density and housing type. *Environment and Planning B: Planning and Design*, 36, 30–48.
- Breheny, M. J. (1991). Sustainable development and urban form. In *22nd Annual Conference of the British Section of the Regional Science Association at Mansfield College*.
- Brennan, M., Shahumyan, H., Walsh, C., Carty, J., Williams, B., Convery, S., et al. (2009). *Regional planning guideline review: using MOLAND as part Urban Institute Ireland Working Papers Series*; 09/07. pp. 1–23. Available at: <http://www.uep.ie/pdfs/WP%200907%20WV.pdf>
- Bruse, M. (1999). *The influences of local environmental design on microclimate-development of a prognostic numerical Model ENVI-met for the simulation of wind, temperature and humidity distribution in urban structures. PhD thesis: temperature and humidity distribution in urban structures*. Germany: Institute of Geography, University of Bochum (in German).
- CSO. (2011). *Census of Ireland*. Dublin: CSO Central Statistics Office of Ireland. Available online: <http://www.cso.ie/en/census/> Accessed on 18.04.15
- Ching, J. K. S. (2013). A perspective on urban canopy layer modeling for weather, climate and air quality applications. *Urban Climate*, 3(1), 13–39.
- Chrysoulakis, N., Anselmo de Castro, E., & Moors, E. (2014). *Understanding urban metabolism: a tool for urban planning*. London, United Kingdom: Routledge (Taylor and Francis).
- Chrysoulakis, N., et al. (2013). Sustainable urban metabolism as a link between bio-physical sciences and urban planning: The BRIDGE project. *Landscape and Urban Planning*, 112(0), 100–117.
- Couclelis, H. (2005). Where has the future gone? Rethinking the role of integrated land-use models in spatial planning. *Environment and Planning A*, 37(8), 1353–1371.
- Demuzere, M., Oleson, K., Coutts, A. M., Pigeon, G., & van Lipzig, N. P. M. (2013). Simulating the surface energy balance over two contrasting urban environments using the community land model urban. *International Journal of Climatology*, 33(15), 3182–3205.
- Eliasson, I. (2000). The use of climate knowledge in urban planning. *Landscape and Urban Planning*, 48(1–2), 31–44.
- Elkin, T., McLaren, D., & Hillman, M. (1991). *Reviving the city: towards sustainable urban environment*. London: Friends of the Earth.
- Flanner, M. G. (2009). Integrating anthropogenic heat flux with global climate models. *Geophysical Research Letters*, 36(2).
- Gál, T., & Unger, J. (2009). Detection of ventilation paths using high-resolution roughness parameter mapping in a large urban area. *Building and Environment*, 44(1), 198–206.
- Getis, A., & Ord, J. K. (1992). The analysis of spatial association by use of distance statistics. *Geographical Analysis*, 24(3), 189–206.
- Givoni, B. (1992). Comfort, climate analysis and building design guidelines. *Energy and Buildings*, 18(1), 11–23.
- Goldberg, V., Kurbjuhn, C., & Bernhofer, C. (2013). How relevant is urban planning for the thermal comfort of pedestrians? Numerical case studies in two districts of the City of Dresden (Saxony/Germany). *Meteorologische Zeitschrift*, 22(6), 739–751.
- Graham, E. (1993). The urban heat Island of Dublin City during the summer months. *Irish Geography*, 26(1), 45–57.
- Gray, K. A., & Finster, M. E. (2000). *The urban heat island, photochemical smog, and Chicago: local features and the problem and solution*. Evanston, IL: Northeastern University.
- Grimmond, C. S. B., Blackett, M., Best, M. J., Baik, J.-J., Belcher, S. E., Beringer, J., et al. (2011). Initial results from Phase 2 of the international urban energy balance model comparison. *International Journal of Climatology*, 31(2), 244–272.
- Grimmond, C. S. B., Blackett, M., Best, M. J., Barlow, J., Baik, J.-J., Belcher, S. E., et al. (2010). The international urban energy balance models comparison project: first results from Phase 1. *Journal of Applied Meteorology and Climatology*, 49(6), 1268–1292.
- Grimmond, C. S. B., & Oke, T. R. (1995). Comparison of heat fluxes from summertime observations in the suburbs of four North American Cities. *Journal of Applied Meteorology*, 34(4), 873–889.
- Grimmond, C. S. B., & Oke, T. R. (2002). Turbulent heat fluxes in urban areas: observations and a local-scale urban meteorological parameterization scheme (LUMPS). *Journal of Applied Meteorology*, 41(7), 792–810.
- Hebbert, M., & Mackillop, F. (2013). Urban climatology applied to urban planning: a postwar knowledge circulation failure. *International Journal of Urban and Regional Research*, 37(5), 1542–1558.
- Idso, C. D., Idso, S. B., & Balling, R. C. (1998). The urban CO<sub>2</sub> dome of Phoenix, Arizona. *Physical Geography*, 19(2), 95–108.
- IPCC. (2014). Human settlements, infrastructure and spatial planning. In *Climate change 2014: mitigation of climate change. contribution of working group III to the fifth assessment report of the intergovernmental panel on climate change*. Cambridge, United Kingdom and New York, NY, USA: Cambridge University Press.
- Järvi, L., Grimmond, C. S. B., Taka, M., Nordbo, A., Setälä, H., & Strachan, I. B. (2014). Development of the surface urban energy and water balance scheme (SUEWS) for cold climate cities. *Geoscientific Model Development*, 7(4), 1691–1711.
- Järvi, L., Grimmond, C. S. B., & Christen, A. (2011). The surface urban energy and water balance scheme (SUEWS): evaluation in Los Angeles and Vancouver. *Journal of Hydrology*, 411(3–4), 219–237.
- Jorgenson, A. K., & Rice, J. (2010). Urban slum growth and human health: a panel study of infant and child mortality in less-developed countries 1990–2005. *Journal of Poverty*, 14(4), 382–402.
- Karl, T. R., Diaz, H. F., & Kukla, G. (1988). Urbanization: its detection and effect in the United States climate record. *Journal of Climate*, 1(11), 1099–1123.
- Keogh, S., Mills, G. M., & Fealy, R. J. (2012). The energy budget of the urban surface: two locations in Dublin. *Irish Geography*, 4(1), 1–23.
- Krayenhoff, E. S., & Voogt, J. A. (2007). A microscale three-dimensional urban energy balance model for studying surface temperatures. *Boundary-Layer Meteorology*, 123(3), 433–461.
- Kusaka, H., Kondo, H., Kikegawa, Y., & Kimura, F. (2001). A simple single-layer urban canopy model for atmospheric models: comparison with multi-layer and slab models. *Boundary-Layer Meteorology*, 101(3), 329–358.
- Lemonsu, A., Kounkou-Arnaud, R., Desplat, J., Salagnac, J. L., & Masson, V. (2013). Evolution of the Parisian urban climate under a global changing climate. *Climatic Change*, 116(3–4), 679–692.
- Levlovics, E., Gál, T., & Unger, J. (2013). Mapping local climate zones with a vector-based GIS method. *AERPA Conference*, 230–423. Available at (<http://aerapa.conference.ubbcluj.ro/2013/pdf/53%20lelovics%20et%20al%20423.430.pdf>)
- Lin, C.-Y., Chen, F., Huang, J. C., Chen, W.-C., Liou, Y.-A., Chen, W.-N., et al. (2008). Urban Heat Island effect and its impact on boundary layer development and land-sea circulation over northern Taiwan. *Atmospheric Environment*, 42(22), 5635–5649.
- Lindberg, F., & Grimmond, C. S. B. (2011). The influence of vegetation and building morphology on shadow patterns and mean radiant temperatures in urban areas: model development and evaluation. *Theoretical and Applied Climatology*, 105(3–4), 311–323.
- Lindberg, F., Holmer, B., & Thorsson, S. (2008). SOLWEIG 1.0—modelling spatial variations of 3D radiant fluxes and mean radiant temperature in complex urban settings. *International Journal of Biometeorology*, 52(7), 697–713.
- Marland, G., et al. (2003). The climatic impacts of land surface change and carbon management, and the implications for climate-change mitigation policy. *Climate Policy*, 3(2), 149–157.
- Martine, G., McGranahan, G., Montgomery, M., & Fernández-Castilla, R. (2008). *The new global frontier: urbanization, poverty and environmental in the 21st century (1st ed.)*. London: Earthscan (Routledge).

- Masson, V. (2000). A physically-based scheme for the urban energy budget in atmospheric models. *Boundary-Layer Meteorology*, 94(3), 357–397.
- Middel, A., Häb, K., Brazel, A. J., Martin, C. A., & Guhathakurta, S. (2014). Impact of urban form and design on mid-afternoon microclimate in Phoenix local climate zones. *Landscape and Urban Planning*, 122, 16–28.
- Mills, G. M. (2007). Cities as agents of global change. *International Journal of Climatology*, 27(14), 1849–1857.
- Mills, G. M. (2008). Urban climatology and its relevance to urban design. In *PLEA 2008 25th Conference on Passive and Low Energy Architecture*. [http://architecture.ucd.ie/Paul/PLEA2008/content/papers/oral/PLEA.FinalPaper\\_ref\\_250.pdf](http://architecture.ucd.ie/Paul/PLEA2008/content/papers/oral/PLEA.FinalPaper_ref_250.pdf), Accessed 24.04.15
- Mills, G. M., Cleugh, H., Emmanuel, R., Endlicher, W., Erell, E., McGranahan, G., et al. (2010). Climate information for improved planning and management of mega cities (needs perspective). *Procedia Environmental Sciences*, 1(1), 228–246.
- Moussiopoulos, N., Sahm, P., & Kessler, C. H. (1995). Numerical simulation of photochemical smog formation in Athens, Greece—a case study. *Atmospheric Environment*, 29(24), 3619–3632.
- Niehoff, D., Fritsch, U., & Bronstert, A. (2002). Land-use impacts on storm-runoff generation: scenarios of land-use change and simulation of hydrological response in a meso-scale catchment in SW-Germany. *Journal of Hydrology*, 267(1–2), 80–93.
- Offerle, B., Grimmond, C. S. B., & Fortuniak, K. (2005). Heat storage and anthropogenic heat flux in relation to the energy balance of a central European city centre. *International Journal of Climatology*, 25(10), 1405–1419.
- Oke, T. R. (1984). Towards a prescription for the greater use of climatic principles in settlement planning. *Energy and Buildings*, 7(1), 1–10.
- Ord, J. K., & Getis, A. (1995). Local spatial autocorrelation statistics: distributional issues and an application. *Geographical Analysis*, 27(4), 286–306.
- Patz, J., Campbell-Lendrum, D., Holloway, T., & Foley, J. A. (2005). Impact of regional climate change on human health. *Nature*, 438, 310–317.
- Peng, L. L. H., & Jim, C. Y. (2013). Green-roof effects on neighborhood microclimate and human thermal sensation. *Energies*, 6(2), 598–618.
- Picone, N., & Campo, A. M. (2015). Preparing urban climate maps using Local Climate Zones (LCZ) methodology to improve communication with urban planners: the case of Tandil city, Argentina. In *9th International Conference on Urban Climate (ICUC9) Proceedings, TUKUP6: Indicators and climate maps II: urban planning*.
- Schlünzen, K. H., Grawe, D., Bohnenstengel, S. I., Schlüter, I., Koppmann, R., et al. (2011). Joint modelling of obstacle induced and mesoscale changes—current limits and challenges. *Journal of Wind Engineering and Industrial Aerodynamics*, 99, 217–225.
- Schlünzen, K. H., Hinneburg, D., Knoth, O., Lambrecht, M., Leitl, B., López, S., et al. (2003). Flow and transport in the obstacle layer: first results of the micro-scale model MITRAS. *Journal of Atmospheric Chemistry*, 44(2), 113–130.
- Shaviv, E. (1984). Climate and building design—tradition, research and design tools. *Energy and Buildings*, 7(1), 55–69.
- Stewart, I. D., & Oke, T. R. (2012). Local climate zones for urban temperatures. *Bulletin of the American Meteorological Society*, 1879–1900.
- Stewart, I. D., Oke, T. R., & Krayenhoff, E. S. (2014). Evaluation of the 'local climate zone' scheme using temperature observations and model simulations. *International Journal of Climatology*, 34(4), 1062–1080.
- Svensson, M. K., & Eliasson, I. (2002). Diurnal air temperatures in built-up areas in relation to urban planning. *Landscape and Urban Planning*, 61(1), 37–57.
- Sweeney, J. (1987). The urban heat island of Dublin City. *Irish Geography*, 20(1), 1–10.
- UN. (2014). *World urbanization prospects the 2014 revision*. New York: United Nations. ISBN 978-92-1-151517-6.
- Van de Voorde, T., van der Kwast, J., Poelmans, L., Canters, F., Binard, M., Cornet, Y., et al. (2016). Projecting alternative urban growth patterns: the development and application of a remote sensing assisted calibration framework for the Greater Dublin Area. *Ecological Indicators*, 60, 1056–1069.
- Veldkamp, A., & Fresco, L. O. (1997). Exploring land use scenarios, an alternative approach based on actual land use. *Agricultural Systems*, 55(1), 1–17.
- Walsh, S. (2014). *Annual summary 2014. Climate report*. Dublin: Climatology and Observations Division Met Éireann—Irish Meteorological Service.
- Wang, X. M., Lin, W. S., Yang, L. M., Deng, R. R., & Lin, H. (2007). A numerical study of influences of urban land-use change on ozone distribution over the Pearl River Delta Region, China. *Tellus B: Chemical and Physical Meteorology*, 59(3), 633–641.
- Ward, I. C. (2003). The usefulness of climatic maps of built-up areas in determining drivers for the energy and environmental efficiency of buildings and external areas. *International Journal of Ventilation*, 2(3), 277–286.
- Ward, H. C., Evans, J. G., & Grimmond, C. S. B. (2014). Multi-scale sensible heat fluxes in the suburban environment from large-aperture scintillometry and eddy covariance. *Boundary-Layer Meteorology*, 152(1), 65–89.
- Williams, B., Shahumyan, H., Boyle, I., Convery, S., & White, R. (2012). Utilizing an urban-regional model (MOLAND) for testing the planning and provision of wastewater treatment capacity in the Dublin Region 2006–2026. *Planning Practice & Research*, 27(2), 227–248.
- Xiang, W.-N., & Clarke, K. C. (2003). The use of scenarios in land-use planning. *Environment and Planning B: Planning and Design*, 30, 885–909.
- Yaghoobian, N., Kleissl, J., & Krayenhoff, E. S. (2010). Modeling the thermal effects of artificial turf on the urban environment. *Journal of Applied Meteorology and Climatology*, 49(3), 332–345.